The Role of Metabolites and Bioreactor Operating Conditions on T Cell Manufacturing

by

Arman Amini

Department of Biochemical Engineering

University College London

A thesis submitted for the degree of

Doctor of Philosophy (PhD)

2020

Declaration

I, Arman Amini confirm that the work in this thesis is my own, except when indicated. The work presented in this thesis was carried out under the supervision of Dr. Farlan Veraitch and Professor Chris Mason at the Department of Biochemical Engineering, University College London between October of 2016 and September of 2019. This thesis has not been submitted, either in whole or in part, for another degree or another qualification at any other university.

Arman Amini

London, December 2020

Abstract

Chimeric Antigen Receptor (CAR) T cell therapy has emerged as a treatment for haematological malignancies with currently two products approved by the FDA in the USA and EMA in Europe (Kymriah™ and Yescarta™). Recent clinical studies demonstrated that the presence of less differentiated and long-lasting subsets such, as T Central Memory (T_{CM}) cells in the CAR-T products is required to improve their clinical efficacy. Most manufacturing protocols use media containing high glucose concentration when expanding CAR-T cells *ex vivo*. Effector subsets primarily utilise glucose and glycolysis as a primary metabolic pathway, therefore, the hypothesis was that culturing T cells in a glucose-deprived environment would limit T cell differentiation and effector subsets growth, producing T_{CM} enriched products. It was demonstrated that a 2-stage feeding strategy, where CAR-T cells are activated and transduced in the presence of glucose and fed with a glucose-free medium during the expansion phase, would consistently produce a T_{CM} enriched CAR-T product. Improved *in vitro* functionality and proliferation capability was demonstrated using T_{CM} enriched CAR-T therapy compared to the CD19-specific CAR-T cells generated using a standard protocol where a high glucose medium was used throughout the *ex vivo* expansion. The impact of different bioreactor operating conditions on T cells growth and phenotypic composition was further investigated. Two different levels of Dissolved Oxygen (dO_2; 25% and 90%), pH (6.9 and 7.4), and shaking speeds (100 rpm and 200 rpm), as well as the interaction

between them were assessed. The results demonstrated that the optimal culture condition for generating a high number of CD8+ T_{CM} cells is a combination of 200 rpm, 25% dO_2, and pH of 7.4. This thesis highlights the importance of investigating the impact of metabolites in the medium and bioreactor parameters during the T cell therapies manufacturing in order to improve the quality and quantity of the final product.

Impact statement

With the successful approval and commercialisation of CAR-T therapies, the focus of cell and gene therapy industry has turned into characterising and optimising the manufacturing to improve the final product quality and to reduce the high cost of CAR-T therapies ($\sim$ £300,000 per dose). This doctoral thesis aimed to improve the understanding of the *ex vivo* manufacturing by investigating how different metabolites in the medium (i.e. glucose) and bioreactor conditions (i.e. dissolved oxygen and pH) affect the quality and quantity of T cell therapies such as CAR-T cells.

This thesis showed how altering the medium glucose concentration in a novel 2-stage feeding strategy, can be used to improve the quality of CAR-T therapy. Different therapeutic manufacturers or academic institutes can use this novel 2-stage feeding regime to improve the CAR-T product by producing a high content of favourable less differentiated subsets. Other key advantages of the proposed feeding regime are that less volume of medium, cytokines and a smaller size bioreactor will be required for the manufacturing, which ultimately reduces the cost of manufacturing. The presented results also showed the importance of the concentration of glucose in the cell culture medium, which can be used to develop a new cell culture medium suitable for CAR-T cells manufacturing.

Bioreactor conditions were also investigated in this thesis. It was shown that T cells could be expanded in an agitated condition without adversely affecting their quality.

This means that already available and characterised stirred bioreactors can be used to produce various T cell therapies, hence increasing the available expansion platforms for CAR-T therapy manufacturers. Furthermore, this thesis demonstrated the importance of studying the interactions between multiple parameters, rather than studying each parameter individually during process development. Studying the interactions early during the process development would reduce the number of experiments required to characterisation and optimisation, which in turn would accelerate the research and lower the development costs.

Screening multiple parameters using the micro-Matrix system showed the potential application of this platform for research and development. Each well in the micro-Matrix system is an individual bioreactor with a low working volume of 1-7mL. Therefore, this small scale high throughout platform can be used by commercial companies or academic institutes for screening different manufacturing parameters to accelerate their research and to decrease the time to market for under development products.

Acknowledgement

First and foremost, I would like to thank my family, Amir, Nafiseh, Azin and Maedeh for their endless support during my academic life.

I would like to thank my supervisor Dr. Farlan Veraitch for his mentorship and support through my PhD. I could not have asked for a better mentor. I would like to thank Prof. Chris Mason, who motivated and inspired me to pursue a research career in cell and gene therapy, Dr. Sara Ghorashian, for her guidance and advises, and Prof. Gary Lye for his unconditional support through the difficulties. Special thanks go to Ms. Ludmila Ruban for training and supporting me in this doctoral thesis.

This journey would not have been possible without Elena and her support and motivation. Thank you for your help and patience. I would also like to thank all my friends Vaques, Ana, Gerry, Abeer, Becci, Marco, Vincent, Rana, Pedro and Theano. It was a pleasure working with you all.

Finally, I would like to acknowledge the Engineering and Physical Sciences Research Council (EPSRC) for funding this research.

List of Publications

Publications

Amini, A, Wiegmann, V, Patel, H, Veraitch, FS, Baganz, F. Bioprocess considerations for T-cell therapy: Investigating the impact of agitation, dissolved oxygen, and pH on T-cell expansion and differentiation. *Biotechnology and Bioengineering. 2020; 117: 3018– 3028. https://doi.org/10.1002/bit.27468*

Conference Presentations

26th ESACT EU Meeting, Copenhagen, Denmark; held 5th - 8th May 2019: **Poster Presentation and Oral presentation** - *The Use of a Micro-Bioreactor Cultivation System as a High-Throughput Screening Tool for manufacturing of T-cell therapies*

International Society Cell and Gene Therapy (ISCT), Melbourne, Australia; held 29th May - 1st June 2019; **Poster Presentation** - *Glucose Deprivation Enriches For Central Memory T Cells During Chimeric Antigen Receptor-T Cell Expansion*

ESACT UK Conference, Tamworth, UK; held 9th - 10th January 2019: **Poster Presentation and Oral presentation** - *The Use of a Microbioreactor as a High-Throughput Screening Tool for Immunotherapy Applications*

BioProcess UK Conference, Edinburgh, UK; held 20th - 22nd November 2018: **Poster Presentation** - *Bioprocessing of T-cell Therapy Manufacture in a Single-Use High-Throughput Stirred-Tank Bioreactor*

BioProcess UK Conference, Cardiff, UK; held 29th - 30nd November 2017: **Poster Presentation** - *Impact of medium metabolites on T cell differentiation and expansion*

Contents

List of Figures

List of Tables

List of Abbreviations

2DG	2-Deoxy-D-glucose
ACT	Adoptive cell therapy
ALL	Acute lymphoblastic leukemia
AML	Acute myeloid leukemia
AMPK	AMP-activated protein kinase
AMPK	Adenosine monophosphate-activated protein kinase
ANOVA	Analysis of variance
APCs	Antigen presenting cells
ATP	Adenosine Triphosphate
BCMA	B-cell maturation antigen
CAR	Chimeric Antigen Receptor
CGTs	Cell and Gene Therapies
CHO	Chinese hamster ovary
CLL	Chronic lymphocytic leukemia

CPT1a Carnitine palmitoyltransferase I

CRS Cytokine release syndrome

DMEM Dulbecco's modified Eagle's medium

DOE Design of Experiments

EDTA Ethylenediaminetetraacetic acid

EGFR Epidermal growth factor receptor

FAO Fatty Acid Oxidation

FAS Fatty Acid Synthesis

FBS Fetal Bovine Serum

FDA Food and Drug Administration

G6P Glucose 6-phosphate

GD2 Disialoganglioside

GMP Good manufacturing practices

GvHD Graft versus host disease

Her2 Human epidermal growth factor receptor 2

HLA Human leukocyte antigen

HPLC High Performance Liquid Chromatography

IL Interleukin

IL13R Interleukin-13 receptor

LAG-3 Lymphocyte-activation gene 3

LAL	Lysosomal acid lipase
LB	Luria-Bertani
MFI	Median Fluorescence Intensity
MHC	Major histocompatibility complex
MSC	Microbiological safety cabinet
MSCs	Mesenchymal stem cells
mTOR	Mammalian target of rapamycin
NADH	Nicotinamide adenine dinucleotide
NK cells	Natural killer cells
NKT cells	Natural killer T cells
OXPHOS	Oxidative phosphorylation
PD-1	Programmed death protein 1
PEP	phosphoenolpyruvate
PI3K	Phosphoinositide 3-kinases
PMA	Phorbol 12-myristate 13-acetate
RPMI	Roswell Park Memorial Institute
SD	Standard Deviation
TAA	Tumor associated antigens
TCA	Tricarboxylic acid cycle
T_{CM}	T central memory

TCR T cell receptor

T_{EM} T effector memory

TIL tumor-infiltrating lymphocyte

T_N T naïve

T_{SCM} T stem cell memory

VEGF Vascular endothelial growth factor

Chapter 1

Introduction

Rapid advances in Adoptive T cell therapy (ACT) and protein engineering have led to different therapeutic products aiming to treat several previously incurable diseases. The recent success story of Chimeric Antigen Receptor T (CAR-T) therapies for curing blood malignancies is a great example of how patients' immune system can be harnessed to fight cancer cells. There are currently more than one hundred companies developing different CAR-T therapies for different types of diseases. As different products move from the first phase of the clinical trial to later stages, the focus of CAR-T companies is turning toward the manufacturing of these treatments.

In this thesis, the focus was to characterise different aspects of CAR-T therapy manufacturing process, including the impact of medium metabolites and manufacturing process parameters such as dissolved oxygen and pH on the quality of CAR-T cells. The

following will offer a general introduction to Adoptive T cell therapy approaches, with the primary focus directed toward Chimeric Antigen Receptor (CAR)- T therapy.

1.1 Adoptive T cell therapies

Adoptive T cell therapy is a type of treatment, where patients' immune cells are genetically modified to gain specificity for a specific cell surface protein. There have been reports citing clinical efficacy of adoptive T cell therapies for different categories of diseases mainly including blood malignancies. Based on the type of gene modification and T cells used in ACTs, this field can be divided into three categories (Steven A. Rosenberg et al., 2015):

1. Tumour-infiltrating lymphocytes (TILs)

2. Genetically engineered T cell receptor (TCR) T cells

3. Chimeric antigen receptor (CAR) T cells

1.1.1 Tumour-infiltrating lymphocytes

TIL therapy consists of the administration of *ex vivo* expanded TILs that were isolated from tumours. Earliest work on TILs goes back to 1980s, where Steven A. Rosenberg et al. (1986) pioneering pre-clinical work showed that lymphocytes infiltrating and growing in tumours are a great source of lymphocytes capable of recognising and re-

gressing the tumour. This study was followed by clinical investigations which showed the potential therapeutic application of TILs for treating metastatic melanoma (Steven A. Rosenberg et al., 1986; S A Rosenberg et al., 1988). The manufacturing of TIL therapies starts with the isolation of tumour mass containing tumour resident T cells through a surgical procedure. Tumour mass and tumour resident T cells are then processed to smaller fragments and seeded in a suitable medium containing Interleukin-2 (IL-2). During expansion, tumour resident T cells overgrow and kill the tumour cells. TILs expanded from different tumour fragments are then assessed for their specific reactivity against tumour cells. The TILs that are reactive against tumour cells, are then further expanded with IL-2 and feeder cells and a T cell activating reagent such as OKT3 to stimulate T cells growth (Steven A. Rosenberg et al., 2015; Wolf et al., 2019). The TILs are then re-infused back to the patient following a lymphodepletion chemotherapy to achieve tumour remission. This therapy has so far showed successful remissions of metastatic melanoma (Steven A. Rosenberg et al., 2011), ovarian cancer (Fujita et al., 1995) and colorectal cancer (Fabbri et al., n.d.) in different clinical studies. TIL therapy is currently the most effective approach to induce complete remission in metastatic melanoma patients (Steven A. Rosenberg et al., 2015).

1.1.2 Genetically modified peripheral blood T cells

TCR gene therapy and CART therapy, unlike TIL therapy, involve genetically modification and *ex vivo* expansion of T cells that were isolated from peripheral blood. These genetically modified T cell therapies were developed to overcome and bypass peripheral immune tolerance. An effective immune response to cancer cells consists of processing and presentation of tumour-associated antigens by dendritic cells, activation and expansion of T cells (Mellman et al., 2011; Makkouk et al., 2015). The disruption or suppression at any point of this process is called peripheral immune tolerance. The main causes of peripheral immune tolerance are:

- Cancer immunoediting from immune surveillance (Kim et al., 2007): the interaction between tumour cells and the immune system, which ultimately leads to cancer immunoediting is categorised to three phases: elimination, equilibrium and escape. Initially, innate immune cells such as Natural Killer (NK) cells, Natural Killer T (NKT) cells and $\gamma\delta$ T cells are activated by inflammatory cytokines and consequently start to target cancer cells. The second wave of response is produced by antigen-specific T cells, where tumour cell variants that lack major histocompatibility complex class I and II antigens, survive and ultimately reduce the tumour antigens in the equilibrium phase. Finally in the escape phase, tumour-derived soluble factors such as vascular endothelial growth factor (VEGF) (Gabrilovich et al., 1998), Fas and FasL (Erdogan et al., 2005) create a local im-

munosuppressive environment, which leads to tumour growth and metastasis.

- Lack of effective costimulatory signals to activate tumour specific T cells (Driessens et al., 2009): TCR activation without costimulation can result in T cells anergy rather than activation. Many tumour cells lack the costimulatory molecules. These molecules such as B7 and 4-1BBL, which are found on antigen-presenting cells (APC), pair with T cells surface proteins such as CD28 and 4-1BB, resulting in strong T cell activation, proliferation and persistence (Driessens et al., 2009). Therefore, the inclusion of these costimulatory receptors such as CD28 and 4-1BB on genetically modified T cells is considered as a strategy to improve T cell therapies anti-tumour efficacy (Weinkove et al., 2019).

- Lack of trafficking and accumulation of immune cells at the tumour site (Bellone et al., 2013): Exhaustion and immunosuppression due to the extreme tumour microenvironment is another key contributor to peripheral immune tolerance, particularly in solid tumours. The tumour microenvironment is normally associated with low pH, lack of oxygen and an imbalance of free radicals and antioxidants and lack of nutrients such as arginine and cysteine. These conditions result in the inhibition of T cell activation and expansion and induce lymphocyte apoptosis, which leads to an impaired immune response to tumour cells (Rabinovich et al., 2007).

1.1.2.1 TCR gene therapy

T cell receptor (TCR) drives the antigen specificity of T cells to a peptide in the major histocompatibility complex (MHC). Modification and changes in two main arms of TCR, α and β chains, could therefore be used to redirect T cells toward tumour associated antigens (TAA's). TCR gene therapy consists of administration of *ex vivo* expanded T cells that were isolated from peripheral blood and genetically modified to express TAA specific TCR. The common issue with this approach is the downregulation of MHC-I expression as an immune escape mechanism by cancer cells (Romero et al., 2005), and off-tumour on-target toxicity due to recognition of peptide on MHC expressed on normal tissue (Raman et al., 2016; Wolf et al., 2019).

1.1.2.2 CAR-T cell therapy

Chimeric Antigen Receptors are recombinant protein receptors that have been designed to have specificity for a particular antigen through their extracellular domain coupled with an intracellular domain, which enables T cell activation and costimulation (Eshhar et al., 1993). The use of a CAR protein for immunotherapy was first suggested in the 1990s when Eshhar et al. (1993) and Kuwana et al. (1987) demonstrated that these chimeric proteins could be used to redirect the specificity of T cells and result in a cell-mediated immune response in a MHC independent manner (Eshhar et al., 1993; Kuwana et al., 1987).

1.2 CAR-T therapy: the current landscape

CD19-specific CAR-T therapies have recently shown promising clinical responses recently, which was followed by the first approval of two commerical products, Kymriah (Novartis) and Yescarta (Gilead) by U.S. Food and Drug Administration (FDA) for treating B-cell precursor Acute Lymphoblastic Leukaemia (ALL) and non-Hodgkin lymphoma. In this section, the structure, different generations of CAR protein and the most recent advances and applications of CAR-T therapies will be reviewed.

1.2.1 CAR structure

The recombinant protein structure of a CAR consists of three regions;

1. An extracellular domain that binds to a specific antigen: the extracellular domain typically comprises of a single-chain variable fragment (scFV) from variable domains of a monoclonal antibody or a fragment antigen-binding structure from already available libraries or a natural ligand (Sadelain et al., 2013; Gilham et al., 2017). This part of the CAR structure determines CAR specificity and affinity.

2. A transmembrane domain anchoring the CAR structure on the cell: The transmembrane domain is attached to the extracellular domain via a spacer. There are suggestions that the transmembrane domain and CAR length could affect the binding and function of the CAR-T cells (Sadelain et al., 2013).

3. An intracellular signalling domain: This is typically made of one or more signalling domain required for activation and proliferation of T cells.

1.2.2 CAR generations

First-generation CARs were made from the fusion of a CD3ζ chain to an extracellular domain, which is similar to the structure of TCR-CD3 complex. The addition of a CD3ζ chain allowed to achieve an efficient activation of T cells (Irving et al., 1991) in the first-generation CARs. However, limited immune response and anti-tumour efficacy were observed when using the first-generation CARs (Brocker et al., 1995; Brocker, 2000).

In second-generation CARs, a costimulatory signalling domain was added to the CAR structure. This costimulatory component could be derived from different proteins such as CD28, CD27, CD137 (4-1BB) (Kershaw et al., 2013). The presence of costimulatory signalling domain enhanced the *in vivo* survival, IL-2 secretion and proliferation of T cells (Krause et al., 1998; Hombach et al., 2001; Maher et al., 2002). Improved *in vivo* persistence of CAR-T cells consequently enhanced the clinical efficacy of CD19-specific CAR-T cells in ALL and B-cell malignancies patients (Shannon L. Maude et al., 2014; Kochenderfer et al., 2013; Cameron J Turtle et al., 2016). The summary of success rates and different second-generation CAR clinical trials are reviewed comprehensively by Sadelain et al. (2017). Currently, the most commonly used costimulatory

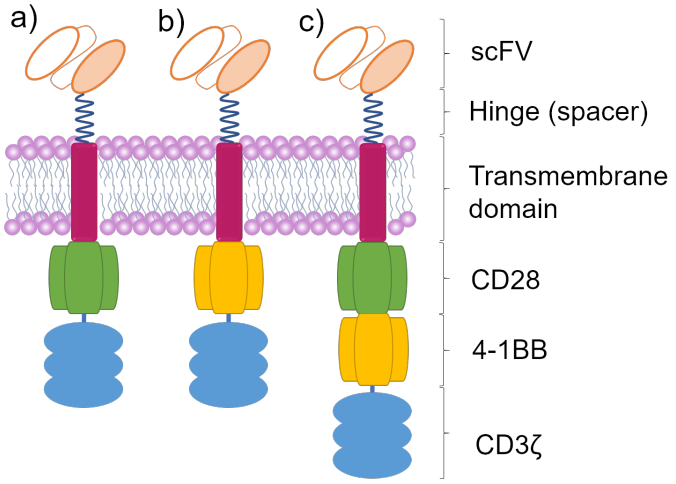

Figure 1.1: Examples of second and third-generation Chimeric Antigen Receptor constructs: a) Second-generation CAR with CD28 costimulatory domain, b) Second-generation CAR with the 4-1BB costimulatory domain, c) Third-generation CAR with 4-1BB and CD28 costimulatory domains.

domains are CD28 and 4-1BB (Sadelain et al., 2017). CD28 costimulation causes fast proliferation and induces glycolytic metabolism in CAR-T cells. The rapid high peak expansion persists for 1-2 months (D. W. Lee et al., 2015; Park et al., 2018). In contrast, CAR-T cells activated via 4-1BB domain showed to adopt lipid oxidation and to favour CAR-T cells persistence rather than rapid activation (H. Zhang et al., 2007; Majzner et al., 2019). The CAR-T cells expansion *in vivo* with 4-1BB domain is slower and has lower but wider expansion peak, which often goes beyond months or years (Shannon L. Maude et al., 2014; S. L. Maude et al., 2018; Gardner et al., 2017). The longer persistence poses a significant advantage for the 4-1BB domain as CAR-T cells continue the immunosurveillance after the initial elimination of CD19+ cancer cells and potentially reduce the relapse in treated patients.

There are limited studies directly comparing the 4-1BB domain with the CD28 domain in clinical trials. Clinical studies using CD19-targeted CART cells with either

the 4-1BB or the CD28 protein has been performed in parallel for treating B cell non-Hodgkin's Lymphoma. Severe adverse events such as neurotoxicity and cytokine release syndrome were observed in CD19-targeted CAR-T cells with CD28 costimulatory domain. On the contrary, CAR-T therapy with 4-1BB was well-tolerated (Ying et al., 2019). CAR-T therapies using the 4-1BB domain have produced better clinical outcomes in children or young adults with ALL, where it appears that persistence of CAR-T cells is an important requirement for complete remission (Shannon L. Maude et al., 2014; S. L. Maude et al., 2018; Gardner et al., 2017). In contrast, CD28 domain in CD19-specific CAR-T therapies for paediatric ALL often results in disease relapse (Jacoby et al., 2018; Majzner et al., 2019). The persistence requirement for CAR-T therapies to treat ALL in older adults has not been proved yet, and there is no clinical evidence suggesting the superiority of 4-1BB domains compared to CD28 domains to cure ALL in older adults. As for treating non-Hodgkin lymphoma, CAR-T therapies using 4-1BB or CD28 domain have shown similar complete response rates (Majzner et al., 2019), suggesting an equivalence in the efficacy of the two domains.

1.2.3 CAR-T applications and advances

The majority of pre-clinical and clinical studies using CAR-T therapies have been focusing on targeting CD19+ cells for treating B cell malignancies. The success story of CAR-T for treating B cell malignancies has inspired researchers and scientists to

explore CAR-T applications beyond the CD19 target antigen.

1.2.3.1 B cell malignancies

There are currently two major antigen targets for CAR-T therapies to treat B cell malignancies; CD19-specific CAR with 60-93% complete response rates in various studies (Majzner et al., 2019). CD22-specific CAR-T cells also demonstrated successful clinical outcomes in paediatric ALL patients (Majzner et al., 2019). On the other hand, the success rates of CD19-specific CAR-T therapies were not as good for Chronic Lymphoblastic Leukaemia (CLL), where complete response rates were only 15-30% (Cameron J. Turtle et al., 2017; Geyer et al., 2018). A recent study showed that CAR-T cells from non-responders CLL patients have phenotypic and metabolic profiles of exhausted cells, whereas, partial or complete responders CAR-T cells have memory phenotypes (Fraietta et al., 2018). Other two B cell malignancies that are being studied extensively are B cell Non-Hodgkin Lymphoma (C. J. Turtle et al., 2016; Schuster et al., 2019; Neelapu et al., 2017; Schuster et al., 2017; Kochenderfer et al., 2017) and multiple myeloma (Brudno et al., 2018; Ali et al., 2016; Raje et al., 2019), where CD19 and B cell maturation antigen (BCMA) are used as targets, respectively.

Another white blood cell cancer that is being investigated is acute myeloid leukaemia (AML), where different targets such as CD123, CD38, and CD33 are being tested (Mardiana et al., 2020). Treating AML is inherently more difficult due to the lack of unique antigens on the surface of AML cells that would allow CAR-T cells to target malignant

myeloid cells without killing the hematopoietic stem cells or progenitor cells.

1.2.3.2 Solid tumours

Multiple clinical trials are currently going on for various types of solid tumours. The solid tumours currently being investigated are neuroblastoma, colon cancer, sarcomas, glioblastoma, prostate cancer and breast cancer (Majzner et al., 2019). The main hurdle for solid tumour treatment with CAR-T cells is finding the appropriate target antigens specific to tumour cells. Target antigens currently being trialled are disialoganglioside (GD2), human epidermal growth factor receptor 2 (Her2), Epidermal growth factor receptor (EGFR) and Interleukin-13 receptor (IL13R). These proteins are also expressed on healthy tissues. Therefore, there is a high chance of observing on-target, off-tumour toxicity in treated patients. To overcome this challenge, various bispecific CARs have been designed to target two specific target antigens. This would reduce on-target, off-tumour toxicity, since bispecific CAR-T cells only recognise cancer cells that co-express both target antigens (Roybal et al., 2016; Fedorov et al., 2013). Another challenge with solid tumours is their hostile microenvironment, where extremely low pH, hypoxia, lack of nutrients and high level of tumour secreted inhibitory cytokines create a challenging environment for CAR-T cells to function and survive (DeRenzo et al., 2019).

1.2.3.3 Viral infections

CAR-T therapies are also currently being explored for the treatment of chronic viral infections. CAR-T therapies for treating HIV infections have been developed to simultaneously target two or three HIV envelope domains (Anthony-Gonda et al., 2019). These gene-modified T cells showed *in vitro* potency against HIV infected cells (Anthony-Gonda et al., 2019). Currently, at least two clinical trials are assessing anti-HIV CAR-T cells (Seif et al., 2019). The key challenges for anti-HIV CAR-T therapies are overcoming HIV escape mechanism and protecting CAR-T cells from being infected themselves (Seif et al., 2019). Other viral infections such as Hepatitis B and C are also being explored in pre-clinical studies (Krebs et al., 2013; Festag et al., 2019).

1.2.3.4 Autoimmune diseases

Another promising field in adoptive cell therapy is CAR-T_{reg} therapies for treating autoimmune diseases. Immunosuppressive property of T_{reg} combined with CAR specificity creates an opportunity to tackle autoimmune diseases such as Graft-versus-host disease (GvHD), transplant rejection and multiple sclerosis (Q. Zhang et al., 2018). Majority of the studies in this field are at a preclinical or early clinical stage. For instance, Boardman et al. (2017) study demonstrated that human leukocyte antigen (HLA)-specific (class I molecule A2) CAR-T_{reg} cells successfully prevented rejection of skin transplant in an animal model. Colitis is another autoimmune disease where car-

cinoembryonic antigen-specific CAR-T_{reg} cells demonstrated promising potential (Blat et al., 2014).

1.3 CAR-T cell therapy manufacturing

Standard CAR-T cell therapy manufacturing process consists of multiple steps including, apheresis, enrichment, activation, expansion and cryopreservation. Although each manufacturing step alone is relatively simple and well-known, there are risks and complexities associated with the whole manufacturing process. Some of the risks and challenges associated with manufacturing include:

1. High variability in raw materials such as donors' cells.
2. Absence of standardisation in each step.
3. Lack of in-process controls, monitoring and automation.
4. High manual intervention between and within each step.
5. Limited understanding of critical process parameters and their impacts on quality of CAR-T cells.
6. Large clean rooms and GMP space requirement for manufacturing.
7. Highly trained GMP technicians are needed for manufacturing.

Collectively, these manufacturing challenges lead to expensive, inconsistent and suboptimal manufacturing. Currently, both Kymriah and Yescarta cost around £300,000 per patient. Here, the main steps of CAR-T therapy manufacturing and available options for each step is reviewed.

1.3.1 Selection

1.3.1.1 Apheresis

CAR-T cell manufacturing starts with a cell collection step from the patient, which occurs at point of care. Leukapheresis process is a gold standard procedure for this step. The purpose of this step is to separate peripheral blood mononuclear cells (PBMC) from the blood and to return all other cell types such as red blood cell to the patient. Leukapheresis is commonly performed via counterflow centrifugal elutriation. Counterflow centrifugal elutriation is a density gradient separation method in which cells are separated based on size and density. Although this method works well for separating red blood cells from PBMCs, it cannot discriminate between different populations of PBMCs. Therefore, the PBMC fraction collected after leukapheresis step from cancer patients contains lymphocytes, monocytes, NK cells and leukaemia cells (Stroncek et al., 2014). Currently, there are different automated systems available that use this technique; these include the Sepax II (GE healthcare) and Elutra (Terumo BCT) (Stroncek et al., 2014).

1.3.1.2 Selection and enrichment

The next step after leukapheresis is an enrichment step in which non-T cell contaminants are removed. Non-T cells contaminants in PBMCs include monocytes, granulocytes, platelets and macrophages. It is well known that non-T cell contaminants such as monocytes, granulocytes, circulating blasts and myeloid-derived suppressor cells negatively impact activation and expansion of T cells (Munn et al., 1996; Munder et al., 2006; Chiao et al., 1986; Gohil et al., 2019). The composition of PBMCs varies from patient-to-patient. This step ensures that the starting cells for CAR-T manufacturing are less variable between different patients, minimising the patient-to-patient variability in the process.

Magnetic bead isolation is currently the most commonly used procedure to isolate CD3+ T cells from the other cells in clinical manufacturing of T cells (Vormittag et al., 2018). In this method, antibodies that either target T cells (positive isolation) or target non-T cells (negative isolation) are conjugated to magnetic beads. The main advantages of magnetic cell sorting compared to other antibody-based sorting techniques such as Fluorescence-Activated Cell Sorting (FACS) are higher speed and better scalability (Plouffe et al., 2015).

1.3.2 Activation

The activation of T cells, a critical step in the T cell manufacturing process, induces the proliferation of T cells. Activation is also pre-requisite for the gene-modification when using retroviruses since retroviral vectors transduce only diving cells. In the human body, T cells are activated by antigen-presenting cells (APCs). APCs such as dendritic cells and macrophages activate T cells via interaction of their major histocompatibility complex with TCR. APCs are currently used for the activation of Tumour Infiltrating Lymphocytes (TILs) (Dudley et al., 2003) and viral-specific T cells such as CMV-specific Cytotoxic T cells (Peggs et al., 2001; Szmania et al., 2001). Other approaches currently used for T cell activation can be divided into: 1) monoclonal antibodies and IL-2, 2) micro-size particles with superparamagnetic properties coated with anti-CD3/anti-CD28 monoclonal antibodies, 3) nano-size particles coated with anti-CD3/anti-CD28 monoclonal antibodies, 4) artificial antigen-presenting cells.

1.3.2.1 Monoclonal antibodies and IL-2

The combination of Anti-CD3 mAb and IL-2 is commonly used for activation of T cells for immunotherapy applications. This method has been extensively used in different clinical trials (Vormittag et al., 2018). Anti-CD3 antibodies provide an initial activation signal to the TCR-CD3 complex. However, TCR-CD3 stimulation is often not enough to stimulate T cell proliferation (Walker et al., 1987). The anti-CD3 antibody does not

provide cross-linking between TCR-CD3 complex and other costimulatory molecules such as CD28. The importance of costimulation and cross-linking of costimulatory molecules to the TCR-CD3 complex for activation and proliferation of T cells has been extensively reviewed by Kenneth A. Frauwirth et al. (2002a). Free soluble antibodies frequently showed to provide limited cross-linking between CD28 and CD3 complex, hence impairing T cell proliferation. In contrast, anti-CD3/anti-C28 mAbs immobilised on beads or a solid surface efficiently expanded T cells (Levine et al., 1996) and could reverse CD3 unresponsiveness in patient T cells that did not respond to anti-CD3 antibody (Shibuya et al., 2000).

1.3.2.2 Anti-CD3/anti-CD28 coated beads

Bead-based activation is the most common activation method for the manufacturing of CAR-T cell therapies used in clinical trials (Vormittag et al., 2018). Cell-sized (4.5 μm) magnetic beads, Dynabead (ThermoFisher) coated with anti-CD3 and anti-CD28 have been used for the two commercially available CAR-T therapies (Kymriah and Yescarta). The small size and high density of the Dynabeads poses a significant mixing challenge when trying to completely suspend the Dynabeads in the medium. Another process challenge attributed to Dynabeads is the additional bead removal step that is required in the manufacturing process to remove the magnetic beads from the final product.

Nano-sized particles, TransAct (Miltenyi Biotec) coated with anti-CD3, and anti-CD28 antibodies have been developed as an activation reagent to minimise the com-

plexity of the manufacturing process. The biodegradable polymeric nano matrix beads are a soluble colloidal reagent; Therefore, they can be removed from the final product via cell culture wash methods such as centrifugation or LOVO cell processing system (Mock et al., 2016).

1.3.2.3 Artificial antigen presenting cells

Activation with artificial Antigen Presenting Cells (aAPCs) is another approach for clinical manufacturing of T cells. Cell lines such as K562 cells need to be modified to express the desired antibodies and stimulating protein and then need to be γ-irradiated (100 Gγ) to make them non-viable aAPCs. This approach was used to selectively activate and expand CD19-specific T cells to treat B cell malignancies (H. Singh et al., 2011; H. Singh et al., 2013). Although aAPCs can be produced under current GMP guidelines and this method is compliant with the clinical manufacturing of T cells, the idea of infusing T cell therapies with malignant cells into cancer patients is considered inappropriate (Neal et al., 2017). Furthermore, generating non-viable aAPC adds another step to the already complex manufacturing process.

1.3.3 Genetic-modification

Gene delivery to produce CAR-T therapies can be categorised to viral and non-viral methods.

1.3.3.1 Viral vectors

Retroviral vectors have been used for transduction of T cells to achieve high transduction efficiencies. Viral transduction works optimally when the cells are activated and proliferating (Merten et al., 2016). Therefore, transduction with viral vectors normally occurs within three days after the activation step. Viral gene delivery is more expensive than other methods due to the costly GMP manufacturing of viral vectors. Viral vectors are commonly produced through transient transfection of cell lines such as HEK293T, where a large amount of different plasmids is used. The current manufacturing process of viral vectors is still highly costly, labour intensive and lacks batch-to-batch consistency and scalability. To mitigate the challenges associated with transient transfection, stable packaging cell lines have been developed (Sanber et al., 2015; Merten et al., 2016). Stable packaging cell lines continuously produce lentiviral vectors and do not require the costly transient transfection and continuous supply of GMP-grade plasmids (Milone et al., 2018).

1.3.3.2 Non-viral vectors

Non-viral vectors mainly rely on the transfer of DNA plasmids directly into T cells. However, naked DNA plasmid delivery into T cells often results in low transfection efficiency due to transgene expression silencing (Bestor, 2000). Alternatively, Sleeping Beauty, a Transposon/transposase system, relies on inserting the CAR transgene into

a transposon sequence within a plasmid and the transponase on another plasmid. The plasmids are then directly transferred into T cells, commonly via electroporation (H. Singh et al., 2013). After translation, the transponase enzyme will insert the CAR sequence into the T cell genome (H. Singh et al., 2014). This approach has been successfully tested in CAR-T clinical trials (H. Singh et al., 2014). The limitations associated with the Sleeping Beauty system are that efficiency of gene delivery is inversely proportional to the size of the transgene and this method relies on electroporation devices such Nucleofector (Lonza) integrated to the T cell manufacturing process.

1.3.4 Expansion

Cell expansion is the longest step for CAR-T cell therapy manufacturing and is required to achieve enough cells for the final product. During expansion, the cell culture volume is adjusted and increased to allow the cells to grow without the limitation of nutrients and space. This is achieved either by building up the culture volume in one vessel or scaling out to a higher number of cell culture vessels. For T cell expansion, there are different expansion platforms available and used in clinical trials including, static T-flask, gas permeable bags, G-Rex bioreactors, the Miltenyi Prodigy system and rocking motion bioreactor (Vormittag et al., 2018).

1.3.4.1 Static culture platforms

T-flasks are the most commonly used cell culture vessel in the life sciences field. However, fluid handling to and from T-flasks is limited to manual open-handling and working in biosafety cabinets (Cleanroom Grade A). Alternatively, gas-permeable bags offer a static platform designed to achieve a high rate of gas transfer to the cell culture media. Sterile tubings can be welded directly to gas-permeable bags, which allows some of the steps to be undertaken in lower clean room environment grades (Grades C and D) for GMP manufacturing of T cell therapies (Tumaini et al., 2013b; Vormittag et al., 2018). The main challenge associated with gas-permeable bags is that the majority of the operations such as medium addition and sampling must be done manually through tube welding. Additionally, gas-permeable bags lack in-line sensing capabilities and process controls. The G-Rex vessel (Wilson Wolf) is another type of gas permeable vessel. The base of the G-Rex bioreactor is made of a thin silicon layer, which allows a high gas exchange. The G-Rex large culture medium capacity allows users to fill the cell culture chamber only once during the beginning of the expansion without an additional feed required for 8-14 days (Bajgain et al., 2014). G-Rex single medium addition also decreases labour intensiveness and the contamination risk associated with continuous manual feeding. Similar to gas-permeable bags, the G-Rex bioreactor lacks in-line sensing capabilities. Another limitation when using G-Rex bioreactor is the sampling; due to the lack of mechanical agitation in G-Rex system, prior to sampling the vessel

needs to be manually mixed in order to resuspend cells in the medium to achieve a representative sample.

1.3.4.2 Rocking motion bioreactor

Rocking motion bioreactors such as WAVE bioreactor (GE healthcare) offers a great alternative option to gas-permeable bags. The WAVE bioreactor is a low-shear agitated cell culture platform (V. Singh, 1999). It can be operated under active continuous media perfusion in a semi-automated manner and hence less manual handling is involved. Continuous perfusion removes waste metabolites and supplements T cells with fresh medium, allowing expansion and maintenance of highly viable cell concentrations, up to 35 million T cells per millilitre (Hollyman et al., 2009). The standard expansion workflow before inoculating the WAVE bioreactor is activation, transduction and pre-expansion for 3-5 days in gas-permeable bags and then transferring the cells to a WAVE bag (Hollyman et al., 2009; Ghassemi et al., 2018). The pre-expansion is necessary due to the large minimum working volume of the current rocking motion bags available (300 mL minimum working volume for a Xuri 1L bag). Furthermore, single-use disposable sensors such as DO, pH and biomass can be integrated for process monitoring and control.

1.3.4.3 Novel all-in-one bioreactors

The CliniMACS Prodigy (Miltenyi Biotec) and the Cocoon Bioreactor (Lonza) are currently the only commercially available all-in-one bioreactors. These platforms are capable of performing isolation, gene modification, cell expansion and cell wash all in one device (Mock et al., 2016). The all-in-one approach minimises the manufacturing cleanroom footprint per patient and decreases the manual transfer between each step. The main limitation associated with all-in-one bioreactors is the lack of flexibility within the device and its function. For instance, the CliniMACS Prodigy activation method is limited to TransAct (Miltenyi Biotec).

1.3.4.4 Summary of expansion platforms

Various manufacturing platforms are available for the manufacturing of CAR-T therapies. The main characteristics of each platform is summarised in Table 1.1:

	Clinical manufacturing of CAR-T platforms						
Platform	**T-flask**	**Gas-permeable bags**	**G-Rex**	**WAVE Bioreactor**	**Prodigy**	**Quantum**	**Cocoon**
Technology	Monolayer cell culture	gas-permeable walls	Gas-permeable base	Rocking motion bioreactor	Rotating wall bioreactor	Hollow fibre bioreactor	Compact rocking motion
Mixing	Static	Static	Static	Rocking motion	Rotating wall	Static	Static & rocking motion
Feeding strategy	Fed-batch	Fed-batch	Batch	Continuous perfusion	Fed-batch & semi-perfusion	Continuous perfusion	Fed-batch & perfusion
In-line monitoring	No	No	No	Dissolved Oxygen & pH	No	No	Dissolved Oxygen & pH
Automated Platform	No	No	No	Semi-automated	Automated	Semi-automated	Automated
Cleanroom space requirement	Low	Low	Low	High	High	High	Medium
Labour intensiveness	High	High	High	Medium	Medium	Medium	Medium
Suitable for scale out and multiplexing	No	No	No	No	No	No	Yes
Suitable for scale up	No	No	No	Yes	No	Yes	No

Table 1.1: The table shows the comparison of currently available technologies for clinical manufacturing of CAR-T therapies.

1.3.5 Strategies for optimising CAR-T therapy manufacturing

CAR-T therapy manufacturing process consists of multiples stages with various variables and inputs in each step. To achieve an optimal CAR-T cell manufacturing in regards to cell yield and quality, critical process parameters in each step need to be identified and optimised. Critical process parameters are parameters that have an impact on the critical quality attributes (CQAs). Critical quality attributes for CAR-T therapy are characteristics of the cell products that need to be maintained within a certain range to ensure the desired product quality. Cell number (or Growth rate), viability, transduction efficiency and phenotypic composition are some of the key and common CQAs between different CAR-T therapies (Levine et al., 2016). In this section, different approaches currently being used to improve the quality and yield of T cell products are reviewed.

1.3.5.1 Supplemented cytokines

Exogenous cytokine addition during T cell manufacturing process provides stimulatory and priming signals for T cells activation and growth and ultimately affects T cells ability to mediate immune response when infused back to the patients. Understanding how different cytokine types and concentrations affect T cell functions is therefore crucial for the manufacturing of CAR-T therapies.

IL-2 was the first cytokine used for adoptive cell therapy (Steven A. Rosenberg et al.,

1986). As explained in section 1.3.2.1, IL-2 can activate T cells and currently is used for *ex vivo* expansion of T cell therapies. According to Vormittag et al. (2018), IL-2 is the most commonly used cytokine for CAR-T manufacturing. There are limitations associated with the use of IL-2 for *ex vivo* expansion of T cells; IL-2 promotes the development and growth of the immunosuppressive subset of T cells, T_{reg}. This is due to the high expression level of IL-2 receptor α chain on the T_{reg} subset (H. Zhang et al., 2005). Additionally, T cells expanded with IL-2 are predominantly composed of effector cells.

Recently, there were suggestions that the use of other cytokines such as IL-7, IL-15 and IL-21 could result in a higher percentage of memory T cells and consequently improve the persistence of CAR-T therapies *in vivo* (Barrett et al., 2014; Xu et al., 2013; Xu et al., 2014; Ghassemi et al., 2016). IL-15 is similar to IL-2 in regards to its receptor subunits since it engages the same β and γ chains as the IL-2 receptor. The specificity of IL-2 and IL-15 receptors is determined by an α chain subunit in their receptors IL2Rα (CD25) or IL15Rα (CD215), respectively (Giri et al., 1995). Despite the similarity in IL-2 and IL-15 receptors, Christopher A Klebanoff et al. (2003) compared *in vivo* functionality of T cells cultured in IL-2 and IL-15 and showed that IL-2 could induce apoptosis and limit CD8+ memory survival, whereas IL-15 improved *in vivo* anti-tumour efficacy. IL-7 is another cytokine that plays a key role in the development, maturation and homeostasis of T cells (Sprent et al., 2011). Several groups, including

Cieri et al. (2013) and Cha et al. (2010) suggested that the combination of IL-7 and IL-15 as supplemental cytokines resulted in a better *in vivo* anti-tumour activity compared to IL-2. The combination of IL-7 and IL-15 also showed to generate and preserve T memory stem cells, which are associated with superior *in vivo* self-renewal, longevity and anti-tumour response (Gattinoni et al., 2011; Cieri et al., 2013).

IL-21 is another cytokine that belongs to γ chain family and structurally is very similar to IL-2 (Spolski et al., 2008). Hinrichs et al. (2008) reported that priming T cells with IL-21 compared to IL-2 limited the effector differentiation of CD8+ T cells and enhanced the *in vivo* anti-tumour efficacy of CD8+ T cells after adoptive cell transfer. The combination of IL-7 and IL-21 as medium supplements was also suggested by Sabatino et al. (2016) to generate a CD19-specific CAR-T therapy enriched in CD8+ memory stem cell, which showed to have enhanced anti-tumour responses.

These studies laid down the foundations of a new group of studies, in which IL-7, IL-15 and IL-21 were used in different combinations and concentrations during CAR-T cells expansion. The optimal combination of these cytokines and their concentrations for CAR-T therapy manufacturing is still unknown. There is no direct comparison to assess and compare them and their clinical efficacy. Therefore this is one area of the manufacturing, where further optimisation is required.

1.3.5.2 Culture media

During CAR-T therapy manufacturing, T cells are activated, genetically modified and expanded over 7-14 days. One of the key challenges for the manufacturing of CAR-T therapies is that human serum is used as a supplement to the medium (Brindley et al., 2012). There are different challenges associated with adding the human serum to the medium;

1. Human serum is very expensive and increases the Cost of Goods for the manufacturing.

2. GMP-grade human serum must go through an extensive testing to ensure the absence of infectious agents

3. Inherently human serum is acquired from different donors; therefore it has high lot-to-lot variability, which in turn increases variability in the manufacturing process.

4. Current supply chain of human serum would not be able to meet the demand if multiple commercial CAR-T products come to market, and therefore it would pose a further bottleneck in the manufacturing process.

5. Human serum often needs to be added to the media at the manufacturing site, adding an extra step and manual handling to the already labour intensive process of manufacturing.

Having serum-free media for expanding CAR-T cells is one of the key requirements for successful commercialisation and manufacturing of CAR-T therapies. Other serum-like supplements such as human growth factor concentrate (Physiologix™ XF SR) (Ghassemi et al., 2020) or human platelet lysate (hPL) (Thieme et al., 2018; Canestrari et al., 2019) have been developed to tackle this challenge. Although newly developed supplements address some of the above-mentioned issues, the challenge around supply chain still persists.

Currently, the most commonly used medium for T cell culture and expansion is RPMI 1640 medium supplemented with 10% fetal bovine serum. In the cancer immunotherapy industry, there is no consensus on which media is the most suitable for manufacturing CAR-T cells. However, X-VIVO15 (Hollyman et al., 2009; David L. Porter et al., 2011; Shannon L. Maude et al., 2014; Grupp et al., 2013; Brentjens et al., n.d.[a]; Davila et al., 2014), TexMACS (Mock et al., 2016; Lu et al., 2016; Lock et al., 2017; Vedvyas et al., 2019) and AIM V (Johnson et al., 2009; Tumaini et al., 2013b; D. W. Lee et al., 2015; Kochenderfer et al., 2010) are currently the most common media used in clinical manufacturing of T cells. Although these media are commercialised as "serum-free media", in most of the clinical manufacturing processes reviewed, typically between 1-5% human AB serum is added to the medium. This is largely due to suboptimal growth and reduced transduction efficiency, when using patient T cells compared to healthy donor T cells (Medvec et al., 2018).

An overlooked aspect of T cell media is the composition of the medium and how the presence or absence of different nutrients or medium components affect the quality and function of CAR-T cells. T cells metabolism is well established and studied (reviewed below in Section 1.4). However, how exogenous nutrients in the media can be used to optimise the CAR-T cell function, *in vivo* persistence and ultimately clinical outcome of cancer treatment is still unknown.

The feeding strategy used to deliver the nutrients to T cells is another important aspect of the manufacturing process for CAR-T therapies. Currently, different expansion platforms use different feeding regimes to supply nutrients to the cells; For instance, the WAVE bioreactor and the Quantum hollow fibre bioreactor use continuous perfusion (up to 1000 mL per day) throughout the expansion period (Ludwig et al., 2020). This means cells are continuously fed with high levels of nutrients available in the medium, and the spent medium is continuously removed regardless of levels of waste metabolites. Continuous feeding strategy has its own advantages such as the ability of the system to produce extremely high density ($< 15 \times 10^6$ cells/mL) and to prevent waste metabolites build up in the medium. On the other hand, a much larger volume of medium and cytokines will be required to continuously run a perfusion system, which in turn increases the cost of goods. Also, continuous exposure of T cells to high levels of supplemental cytokines could have a negative impact on CAR-T cell quality and functions. For instance, continuous exposure to IL-2 could result in a CAR-T product predominantly

made of effector cells (Hinrichs et al., 2008; Cha et al., 2010).

For fed-batch systems, CAR-T cells require to be fed frequently (e.g. every two or three days). However, the feeding volume varies between different manufacturing batches and processes and depends on the growth rate. The disadvantages of this type of feeding are: 1) during 2-3 days feeding interval, cells might experience certain nutrients limitation or high level of waste metabolites, 2) because the amount of feeding volume varies from batch-to-batch, process standardisation will be difficult. However, fed-batch feeding potentially requires less amount of medium and cytokines compared to continuous perfusion.

Batch feeding is currently only being used in the G-Rex protocol. The main challenge for batch protocols is that amount of nutrients and media added at the beginning of the process would determine the length of the process and how much cells can grow. For instance, if the patient's cells grow faster than expected, the manufacturing process must be terminated and harvested earlier than scheduled, or medium exchange must be performed.

1.3.5.3 Reprogramming T cell differentiation in culture

CAR-T product quality is assessed by the phenotypic composition of T cells and the percentage of CAR-positive cells in the final product. Therefore, understanding how T cells differentiate and proliferate both during *in vitro* expansion and *in vivo* tumour mediated response, is critical in order to improve T cell quality during the CAR-T manufacturing.

On one side of the differentiation spectrum (Figure 1.2) there is the least differentiated subset of T cells, Naïve T cells (T_N), that have not been exposed to antigen-presenting cells or stimulatory signals. Upon polyclonal activation or antigen-specific activation, T cells start to proliferate and differentiate to different subsets, gaining or losing phenotypic characteristics and functional properties through progressive epigenetic changes (Luca Gattinoni et al., 2012; Busch et al., 2016). During activation, highly differentiated effector cells known as terminally differentiated T effector (T_{TE}) and memory cells are formed. After cancer cells are eliminated in the body, effector T cells die, and a small subset of long-lived memory cells remains in the body to provide long-term immunity. Currently, there are different ways to categorise memory cells and T cell subsets based on their traits and functions (Jameson et al., 2018). In this thesis, memory cells are categorised in different groups, including T memory stem cells (T_{SCM}), T central memory (T_{CM}), and T effector memory (T_{EM}) cells. The markers used to characterise each subset are described in Section 2.5.3.

The optimal composition of T cells for adoptive cell therapy in regards to CD8+

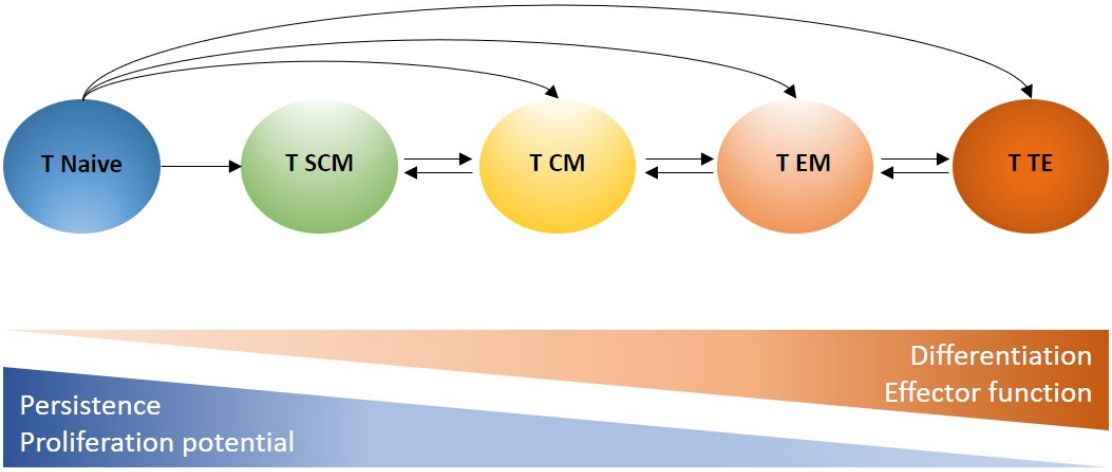

Figure 1.2: Different subsets of T cells; T Naive T_N, T Stem Cell Memory (T_{SCM}), T Cell Memory (T_{CM}), T Effector Memory (T_{EM}), T Terminally differentiated Effector (T_{TE})
.

subsets and the ratio of CD4 to CD8 subsets is still undefined and unknown. There have been suggestions that CAR-T products enriched in less differentiated cells, such as T_{SCM} or T_{CM} cells produce a superior anti-cancer response upon injection as they have greater *in vivo* proliferation capability and persistence (Lipp et al., 1999; Gattinoni et al., 2005; Louis et al., 2011; Kochenderfer et al., 2017; Fraietta et al., 2018). Therefore, new approaches to improve the quality of T cell therapies via generating less-differentiated T cells have been emerged.

One recent novel approach is limiting the differentiation of T cells by reducing the length of expansion. Ghassemi et al. (2018) reported that reducing the duration of cell culture from 9 to 3 days, produce less number of cells but with a higher proportion of memory phenotypes with improved anti-tumour efficacy and potency (Ghassemi et al., 2018). The shorter manufacturing process is also more desirable as the length of

manufacturing impacts the number of patients that can be treated in a year and the costs associated with the quantity of reagent, consumables and labour needed for the manufacturing. Moreover, Lu et al. (2016) developed a rapid expansion protocol by optimising multiple manufacturing steps. The rapid expansion protocol reduced the length of manufacturing from 10 days to 6 days with no impact on functionality and quality of the cells (Lu et al., 2016).

Other strategies to produce less-differentiated T cells mainly targets specific metabolic pathways, involved in the differentiation and development of T cells. These methods are reviewed in the next section (Section 1.4).

1.4 T cell metabolism: a potential target to improve immunotherapy

1.4.1 T cell metabolism: General overview

T cell metabolism is tightly linked with differentiation and their phenotypic fate. In this section, the main metabolic pathways used by different T cell subsets and how different metabolite constituents could affect T cell fates are discussed. During T cell development, haemopoietic stem cell progenitors move from the bone marrow to the thymus, where they acquire a functional TCR. Mature naive T cells then enter the blood circulation and are primarily dependent on oxidation of pyruvate and fatty acid through oxidative phosphorylation (OXPHOS) to generate ATP (Fauci et al., 2005; Heiden et al., 2009).

Naive T cells circulate between the peripheral vascular system and the secondary lymphoid tissues. Once stimulated by TCR ligation and growth factors, T cells undergo metabolic reprogramming to achieve an anabolic metabolism profile. The key regulator of this metabolic programming and switch to glycolysis is the Phosphoinositide 3-kinase (PI3K)/AKT/mammalian target of rapamycin (mTOR) pathway (Kenneth A Frauwirth et al., 2002b; Wieman et al., 2007). Although there is enough oxygen for the cells to support tricarboxylic acid cycle (TCA) and OXPHOS cycle, the cells increase the rate of aerobic glycolysis in response to stimulation by TCR ligation, a phenomenon

termed " the Warburg effect" (Heiden et al., 2009). Aerobic glycolysis is less efficient than OXPHOS in terms of generating ATP per one molecule of glucose. However, aerobic glycolysis occurs much faster than OXPHOS and can generate intermediates needed for biosynthetic pathways to support cell growth and proliferation and to balance NAD+/NADH ratio in the cell (Heiden et al., 2009; MacIver et al., 2013).

It is established that different T cell subsets acquire metabolic reprogramming to support specific function (MacIver et al., 2013). For instance, effector T cells are highly glycolytic to support their pro-inflammatory cytokine production (R. Wang et al., 2011; Michalek et al., 2011). In contrast, memory cells and T_{reg} cells utilise fatty acid oxidation as a primary metabolic pathway to support their long-term persistence (Michalek et al., 2011; Pearce et al., 2009).

1.4.2 Key metabolites and their roles in T cell metabolic pathways

In the following section, the importance of some of the key metabolites for T cell activation, proliferation and function are briefly reviewed.

1.4.2.1 Glucose

Glucose provides energy for T cells by providing the input to glycolysis. ATP molecules will be generated either through glycolysis (Warburg phenomenon) or through TCA cycle and OXPHOS. To generate ATP through OXPHOS, glucose molecules first enter the cells via glucose transporter 1 (Glut1) (Wieman et al., 2007) and then converted to

pyruvate through glycolysis. Pyruvate is then converted to acetyl-CoA, which is used in the TCA cycle to form citrate from oxaloacetate. Citrate can then move to the cytosol to generate acetyl-CoA (via ATP citrate lyase). The cytosolic acetyl-CoA can be utilised for lipid synthesis, and it is essential for cell proliferation (Bauer et al., 2005). The TCA cycle generates the reduced coenzyme NADH, which donates electrons to the electron transport chain and results in ATP generation through OXPHOS. Alternatively, glucose-6-phosphate, an intermediate substrate from glycolysis, can be used in the pentose phosphate pathway.The pentose phosphate pathway can generate building blocks such as ribose sugar for the synthesis of nucleotides and amino acids. NADPH can also be produced through this pathway in T cells (R. Wang et al., 2011).

Glucogenesis, the reversal of glucose catabolism, is a pathway used by mammalian cells to generate glucose from pyruvate. This pathway requires the conversion of pyruvate to oxaloacetate through TCA cycle and then to phosphoenolpyruvate (PEP) via phosphoenolpyruvate carboxykinase (PCK) (J. M. Berg et al., 2012). In further downstream of glucogenesis, glucose-6-phosphate (G6P) generated from PEP is converted to glucose or glycogen (J. M. Berg et al., 2012). Results reported by Ma et al. (2018) suggested that memory T cells shift glucogenesis towards glycogen synthesis. The stored glycogen is converted to produce a stockpile of G6P through the glycogenolysis pathway. This so-called gluconeogenesis–glycogenolysis cycle, which is fuelled by multiple metabolites including glucose, glutamine, pyruvate and acetate was shown to be critical

for memory T cell differentiation and maintenance both *in vitro* and in animal models. Interestingly, pyruvate or non-carbohydrates such as lactate, amino acids and glycerol can be used to fuel gluconeogenesis–glycogenolysis cycle (J. Berg et al., 2002).

1.4.2.2 Amino acids

The amino acid consumption profile of T cells before and after activation differs significantly. One of the crucial amino acids for activation of T cells is glutamine. Upon TCR ligation and activation, T cells increase the expression of glutamine transporters (Carr et al., 2010). Additionally, there are studies suggesting that CD4+ and CD8+ T cells deprived of leucine due to lack of amino acid transporter, Slc7a5, have dysfunctional effector function and impaired clonal expansion (Sinclair et al., 2013). This is due to impaired mTORC1 activation and possibly other key activation-associated mechanisms (Sinclair et al., 2013). Upon activation, alanine serine and cysteine transporter system (ASCT2/SIc1a5) expression also increases on CD4+ T cells (Levring et al., 2012). Impairing this transport system, which also transports glutamine, resulted in decreased OXPHOS (Nakaya et al., 2014). The increasing intracellular level of glutamine can increase leucine uptake as the result of glutamine export and concomitant import of leucine by Slc7a5 (Nicklin et al., 2009). T cells growing in arginine free medium have shown impaired proliferation, aerobic glycolysis and effector function but normal OXPHOS (Fletcher et al., 2015). However, T cells can uptake citrulline and synthesise arginine *de novo*, through arginino-succinate pathway (Qualls et al., 2012).

1.4.2.3 Fatty acids

Fatty acids are another source of energy for T cells. Upon TCR ligation, within the first 24h, the balance between fatty acid oxidation (FAO) and fatty acid synthesis (FAS) changes such that FAO is decreased while FAS is increased. This results in an accumulation of fatty acids necessary for membrane synthesis and proliferation (R. Wang et al., 2011). Although activated T cells continue to uptake extracellular fatty acids, it appears that either fatty acid uptake is not sufficient to cover the cellular needs or that there is an essential requirement for *de novo*-synthesized fatty acids (Berod et al., 2014; J. Lee et al., 2014). Additionally, it was shown that after inhibition of FAS, T cells can function normally if provided with high levels of fatty acids in the medium (Berod et al., 2014; J. Lee et al., 2014). The balance of FAS to FAO differs significantly between different T cell subsets (Berod et al., 2014). In effector T cells, this balance favours FAS, but effector T cells still use FAO to satisfy their high energy demand or to compensate for a low level of glucose (Byersdorfer et al., 2013). This balance shifts toward FAO in CD8+ memory T cells for their development and long-term persistence (Pearce et al., 2009; Windt et al., 2012; Windt et al., 2013). Windt et al. (2013) reported that increasing FAO in memory T cells through increased expression of carnitine palmitoyl-transferase 1a (CPT1a), the rate limiting enzyme for the transport of long-chain fatty acids, enhances CD8+ memory T cell generation upon TCR ligation. O'Sullivan et al. (2014a) discovered that CD8+ memory T cells preferentially use *de novo* FAS to fuel FAO rather than

simply uptaking extracellular fatty acids. CD8+ memory T cells use glucose to produce triacylglycerides (TAGs) which are subsequently hydrolysed by lysosomal acid lipase (LAL) to support mitochondrial FAO (O'Sullivan et al., 2014a). *de novo* FAS requirement in CD8+ memory T cells is further supported by a study by G. Cui et al. (2015), which showed that glycerol, a molecular backbone for TAGs, is required for memory T cell formation and survival after activation (G. Cui et al., 2015).

1.4.3 Targeting metabolism in immunotherapy design

Targeting the metabolism of T cells to enhance their function and persistence is an emerging area in the optimisation of CAR-T product quality. These strategies can be divided into two categories; 1) targeting inhibitory receptors or administration of metabolism modulators *in vivo*, 2) metabolic alterations during *in vitro* expansion of T cell products manufacturing,

Administration of metabolic modulators such as mTOR inhibitor during cancer has promoted and inhibited effector T cells in two different models (Y. Wang et al., 2011; Chaoul et al., 2015). For instance, systemic PD-1 antibody administration has become a viable cancer treatment option for non–small-cell lung cancer (Topalian et al., 2012; McGowan et al., 2020). This is as the result of the metabolic switch of effector cells from glycolysis to FAO, which diminish their effector function and enhance their persistence (Patsoukis et al., 2015).

Targeting T cell metabolism during manufacturing falls under the second category, where several different clinical and non-clinical protocols and strategies currently exist to achieve a T cell therapy product with fewer differentiated T cells. These strategies often include supplementing T cell expansion media with a metabolic inhibitor and are listed below:

- Disruption of metabolic balance: this category includes small molecule inhibitors that targets PI3K/AKT/mTOR pathways. Christopher A Klebanoff et al. (2017) created a clinical protocol using AKT Inhibitor VIII as an additional supplement to the medium in order to preserve minimally differentiated memory cells while allowing T cell expansion and transduction (Christopher A Klebanoff et al., 2017). A similar protocol was also used by Urak et al. (2017) to produce T cells with higher levels of CD62L and CD28. CD19 CAR-T cells produced using these protocols exhibited an improved clinical outcome and superior anti-tumour activity.

- Disrupting T cell development: this group includes a small molecule inhibitor that induces Wnt-β signalling pathways. Gattinoni et al. (2009) used TWS119, a potent pyrrolopyrimidine inhibitor of glycogen synthase kinase 3 beta (GSK-3β), to induce Wnt signalling through triggering the accumulation of β-catenin. The consequence of Wnt signalling is the upregulation of T cell factor-1 (Tcf-7) and lymphoid enhance-binding factor-1 (Lef-1), which decreases differentiation of CD8+ T cells from naive to central and effector memory cells in humans (Will-

inger et al., 2006). Based on this approach, Sabatino et al. (2016) developed a clinical manufacturing protocol for producing CD19-specific CAR-T therapy enriched with memory stem cells. This protocol includes activation of isolated of naive CD8+ T cells in the presence of IL-7, IL-21, and TWS119. In this protocol, limited T cell expansion (5-fold less of total CAR-T cells) was achieved with this protocol but with high purity of T_{SCM} was achieved compared to the standard CAR-T manufacturing protocol, suggesting that the quality of the final CAR-T product is as critical as the cell number.

1.5 Project aims

The main hypothesis of this thesis is to target metabolic pathways associated with different T cell subsets by modulating the provision of critical metabolites in culture media. This novel strategy can be applied to improve CAR-T therapy quality by producing a high content of favourable less differentiated subsets, without the need to supplement the medium with chemical inhibitors. Furthermore, the impact of bioreactor process parameters, including dissolved oxygen and pH, on the growth and the quality of CAR-T cells were investigated. To achieve the aim of this doctoral thesis, the following objectives have been formulated:

1. Investigate the impact of different medium components, including glucose, sodium pyruvate, and fatty acids on T cells phenotype and growth.

2. Establish a new feeding strategy and medium composition suitable for CAR-T expansion in gas-permeable bags, based on previous data.

3. Demonstrate that the produced CAR-T cells using the selected conditions exhibit the desired phenotypic profile, retain their potency and have enhanced proliferation capability.

4. Investigate other process parameters including shaking speed, dissolved oxygen and pH and their impact on T cells growth and phenotype. This will facilitate the translation of the process into bioreactors for clinical manufacturing.

Chapter 2

Materials and Methods

2.1 Materials

2.1.1 Cell lines

Table 2.1: Cell lines used in this doctoral thesis.

Cell line/Type	Vendor	Catalogue Number
HEK293T	Takara Bio	632180
Raji	DSMZ	ACC 319
NALM6	DSMZ	ACC 128
NEB® Stable Competent E.coli	New England BioLabs	C3040I

2.1.2 Tissue culture plasticware

Table 2.2: General plastic ware used in the experiments.

Item	Vendor	Catalogue Number
10 µL sterile pipette tips	Sardstedt	70.1130.210
1000 µL sterile pipette tip	Sardstedt	70.762.211
12 well plate	Thermo Fisher	150628
150mm Petri dish (TC-treated)	Corning	430599
20 µL sterile pipette tips	Sardstedt	70.760.213
200 µL sterile pipette tips	Sardstedt	70.760.211
24 well plate	Thermo Fisher	142475
25 mL yellow centrifuge tubes	Sardstedt	60.9922.243
6 well plate	Thermo Fisher	140675
96 well plate	Thermo Fisher	167008
CoolCell LX Freezing container	Corning	432001
Cryogenic vial	Thermo Fisher	5000-0012
Falcon 15 mL tube	Fisher Scientific	10773501
Falcon 50 mL tube	Fisher Scientific	10788561
Serological pipette 10 mL	Sardstedt	86.1254.001
Serological pipette 25 mL	Sardstedt	86.1685.001
Serological pipette 50 mL	Sardstedt	86.1256.001
Serological pipette 5 mL	Sardstedt	86.1253.001
Stericup-GP Sterile Vacuum Filtration (500 mL)	Merck	SCGPU05RE
T-175 flasks	Thermo Fisher	159910
T-25 flasks	Thermo Fisher	156367
T-75 flasks	Thermo Fisher	156499

2.1.3 Media, buffers and supplements

Table 2.3: General reagents, buffers, media used in the experiments.

Item	Vendor	Catalogue Number
Pan T Cell Isolation Kit	Miltenyi Biotec	130-096-535
CD34 MicroBead Kit, human	Miltenyi Biotec	130-046-702
Cell dissociation medium	Sigma-Aldrich	C5914
CryoStor® CS10	Stemcell Technologies	7930
Dynabeads CD3/CD28	Gibco	11132D
FBS	Gibco	10270106
Lymphoprep	Stemcell Technologies	7861
SepMate-50 (IVD)	Stemcell Technologies	85460
Genejuice	Merck Chemicals Ltd	70967
L-Glutamine (200mM)	Gibco	25030081
IL-7	Miltenyi Biotec	130-095-367
IL-15	Miltenyi Biotec	130-095-760
Ionomycin	Sigma-Aldrich	I0634-1MG
PHA	Sigma-Aldrich	L9017
Retronectin	Takara Bio	T100B
RPMI 1640 Medium, no glutamine	Gibco	21870076
RPMI 1640 Medium, no glucose	Gibco	11879020
DMEM	Gibco	11995073
DMEM Advanced serum-free medium	Gibco	12491023
Linoleic acid-Oleic acid- Albumin	Sigma-Aldrich	L9655-5mL
Bovine Serum Albumin	Sigma-Aldrich	A7906
EDTA (0.5 M)	Thermofisher	AM9260G
PBS	Lonza	BE17-516F/12
PFA	Sigma-Aldrich	P6148
Brilliant Stain Buffer Plus	BD Biosciences	566385
Stain Buffer	BD Biosciences	554656
Geneticin™ (G418 Sulfate)	Thermofisher	10131035
Ampicilin	Sigma-Aldrich	A5354
PES membrane filter	Thermofisher	721-1345
Trypsin-EDTA (0.05%)	Gibco	25300054

2.1.4 Antibodies, staining reagents and kits

Table 2.4: The list of antibodies used flow cytometry analysis.

Staining Antibodies					
Marker	**Colour/Format**	**Isotype**	**Clone**	**Catalogue**	**Vendor**
CD3	BUV395	IgG2a	SK7	564001	BD Biosciences
CD8	BUV737	IgG1	SK1	564629	BD Biosciences
CD4	BUV805	IgG1	SK3	564910	BD Biosciences
CCR7	BV421	IgG2a	150503	562555	BD Biosciences
CD27	BV786	IgG1	L128	563327	BD Biosciences
CD45RA	FITC	IgG2b	HI100	555488	BD Biosciences
CD95	PE	IgG1	DX2	555674	BD Biosciences
CD45RO	PE-Cy7	IgG2a	UCHL-1	337168	BD Biosciences
CD62L	APC	IgG1	Dreg-56	559772	BD Biosciences
LAG-3	AF647	IgG1	T47-530	565717	BD Biosciences
PD-1	PE	IgG1	MIH4	560908	BD Biosciences
CD34	PE	IgG1	QBEND/10	MA5-16927	Invitrogen
TNF–α	AF488	IgG1	MAb11	557722	BD Biosciences
CD107a	BV786	IgG1	H4A3	563869	BD Biosciences
IL-2	PE	IgG2a	MQ1-17H12	554566	BD Biosciences
IFN–γ	APC	IgG1	B27	554702	BD Biosciences

Table 2.5: The list of different kits used in this doctoral thesis.

Item	Vendor	Catalogue Number
Pan T Cell Isolation Kit (human)	Miltenyi Biotec	130-096-535
LS columns	Miltenyi Biotec	130-042-401
CD3 microBead Kit	Miltenyi Biotec	130-050-101
CD34 microBead Kit	Miltenyi Biotec	130-046-702
QIAGEN Plasmid Maxi Kit	Qiagen	12163
QIAGEN Plasmid Mini Kit	Qiagen	12125
Fixation/permeabilisation Solution Kit	BD Biosciences	554714
Human Th1/Th2/Th17 Kit	BD Biosciences	560484
SYTOX™ Red Dead Cell Stain	Thermo Fisher	S34859
CountBright™ Absolute Counting Beads	Thermo Fisher	C36950

2.1.5 Equipment and Software

Table 2.6: Equipment and software used in this doctoral thesis.

Equipment and Software	Vendor
BD Fortessa X20 (UV)	BD Biosciences
Bioprofile FLEX	Nova Biomedical
Cubian HT270	
Dynabead Removal Magent	IBA Life Sciences
Eppendorf 5810R	Eppendorf
FACS Verse	BD Biosciences
FCAP Array Software V3	BD Biosciences
FlowJo V10	BD Biosciences
Nucleocounter NC-3000	Chemometec
Prism V7	Graph Pad

2.2 Primary T cells processing

2.2.1 PBMCs isolation

Fresh blood samples from different healthy donors were purchased from Cambridge Bioscience. All samples were collected from healthy, paid volunteers under informed consent that explicitly permits the use of blood samples and derivatives in a wide range of research applications. The 495 mL of fresh whole blood was collected in the morning and dispatched to the UCL biochemical engineering department at ambient temperature. The freshly collected blood was processed straight after delivery.

Two to four hours before the blood sample was delivered, 33 SepMate-50 tubes were filled with 15 mL of Lymphoprep solution, while avoiding making bubbles under the SepMate-50 membrane. Upon fresh blood delivery, all blood samples were pooled from their containers (50 mL Falcon tubes) to a 2L sterile bottle. The whole blood was then diluted 1:1 with RPMI 1640 medium supplemented with 2% FBS, which was warmed up to room temperature. The whole blood was then gently mixed with the medium by gently pipetting up and down. 30 mL of the diluted whole blood was then added to each SepMate tube while avoid disturbing the Lymphoprep layer.

SepMate tubes were then centrifuged at 1200g for 15 minutes with centrifuge brake on 3. Following the centrifuging, approximately 20 mL of plasma was aspirated without disturbing the PBMC layer, using the pipette gun and 50 mL serological pipette. After plasma aspiration, the PBMCs from all SepMate tubes were pooled together by pouring

the liquid cell layer on top of SepMate tubes membrane in a 1L sterile bottle. The majority of red blood cells and the Lymphoprep solution remain below the SepMate tube membrane, which were then discarded. The pooled PBMCs were then diluted 1:3 with RPMI 1640 containing 2% FBS. The aim of this step was to remove the remnant of Lymphoprep to avoid losing recovery yield.

The diluted PBMCs were then transferred into multiple non-skirted Falcon tubes (40 mL in each tube) using 50 mL serological pipette. All Falcon tubes were then centrifuged at 500g for 10 minutes at room temperature. After centrifuging, the supernatant from each tube was removed by pouring it into a waste bottle. The cell pellet in each tube was then resuspended in 20 mL of RPMI 1640 containing 2% FBS. The resuspended cells from two Falcon tubes (20 mL each) were then pooled into one Falcon tube (40 mL). The Falcon tubes were then centrifuged at 400g for 10 minutes with the centrifuge brake on. After centrifuging, the supernatant was poured off, and the cell pellets were resuspended in RPMI 1640 containing 2% FBS. The cell suspension was then centrifuged again at 150g for 10 minutes with brake off. This step was crucial to reduce the number of platelets in the PBMCs before the isolation step or cryopreservation.

Following the centrifugation step, the supernatant was removed. The pellets were resuspended and pooled together in 50 mL of isolation buffer. The isolation buffer was prepared in PBS solution with the addition of 0.5% bovine serum albumin and 2mM EDTA. A sample was taken at this point to calculate the density of PBMCs or the purity

of CD3+ T cells.

2.2.2 Pan T cell isolation

Lyophilised IL-7 and IL-15 cytokines were reconstituted in deionized sterile- filtered water at a final concentration of 0.1 mg/mL and stored at -20°C. Further dilutions were made, when needed, by thawing an aliquot of frozen cytokine and diluting it with PBS containing 1% BSA. The combination and concentrations of cytokines used during T cell activation, transduction and expansion were 25 ng/mL of IL-7 and 10 ng/mL of IL-15. After the cell count at the end of PBMCs isolation step, the cells were centrifuged at 400g for 5 minutes, and resuspended in 40 µL of isolation buffer at 4°C per 10 million cells. Then 10 µL of Pan T cell Biotin-Antibody cocktail was added per 10 million cells. The solutions were mixed by pipetting gently up and down multiple times. The mixture was then incubated for 5 minutes at 4°C in the fridge. 30 µL of the isolation buffer was added per 10 million cells. In the next step, 20 µL pf Pan T cell microbead cocktail was added per 10 million cells and mixed well by pipetting up and down gently. The mixture was then incubated for 10 minutes at 4°C in the fridge. During the incubation, the LS columns were placed inside the magnet. One LS column was used for 500 million cells. Each column was rinsed with 3 mL of isolation buffer. After the incubation step, the cells and beads mixture was gently added with a P1000 pipette to the LS columns, while avoiding making any bubbles or foam. The flow-through containing CD3+ T cells was

collected in a Falcon tube. Each LS column was washed with 3 mL of the isolation buffer and the flow-through unlabelled cells were added to the rest of the CD3+ cells collected in the previous step. A sample was taken at this step to assess the purity of CD3+ cells, cell density and viability. The cell suspension was then centrifuged at 400g for 5 minutes to remove microbeads and the isolation buffer. The cell pellets were then resuspended either in the desired medium or in cryopreservation medium for freezing.

2.2.3 Cytokine and Media Preparation

Lyophilised IL-7 and IL-15 cytokines were reconstituted in deionised sterile- filtered water at a final concentration of 0.1 mg/mL and stored in -20°C. Further dilutions were made by thawing an aliquot of frozen cytokine and diluting it with PBS containing 1% BSA. The combination and concentrations of cytokines used during T cell activation, transduction and activation are 25 ng/mL of IL-7 and 10 ng/mL of IL-15. Complete RPMI 1640 (cRPMI 1640) medium was made by supplementing 10% FBS, 2mM L-glutamine and 1% Antibiotic-Antimycotic solution.

2.2.4 Activation with Dynabeads

Primary T cells were seeded between $0.4-1.0\times10^{6}$ cells per mL. Primary T cells were activated with Dynabeads at 3 beads to 1 T cell ratio. Dynabeads were washed twice with at least 10 mL of complete medium each time, before adding them to the T cells.

After mixing cells and beads, the cell culture plate, flask or bag was placed inside a humidified incubator at 5% CO_2 and 37°C.

2.2.5 Transduction

Twenty-four hours before the transduction step, a 6-well plate was coated with Retronectin as per manufacturer's instructions. The concentration of Retronectin used was 18 $\mu g/mL$, where 2 mL was used to coat each well (6-well plate). The plate was incubated and coated overnight at 4°C in the fridge. After overnight incubation, the Retronectin solution was aspirated from each well and each well was washed once with PBS (2 mL per well). A lentiviral vector aliquot was thawed from -80°C on ice. 1 mL of lentivirus was added to each well. The 6-well plate was incubated at 4°C in the fridge for 30 minutes. The lentivirus was then aspirated from all wells and discarded. 5 mL of fresh lentivirus was then added to each well and kept at room temperature until the T cells were prepared for transduction.

At this stage, a sample from activated T cells was taken for cell counting. T cells were then moved to a Falcon tube and centrifuged for 5 minutes (400g). The pellet was resuspended in cRPMI 1640 medium supplemented with the cytokines in order to achieve a cell density of 3×10^6 cells per mL. Then, 0.5 mL of T cells containing 1.5×10^6 T cells was added to each well of the 6-well plate already containing lentivirus. The plate was centrifuged for 40 minutes at 1000g at room temperature. After spinoc-

ulation, the well plate was placed inside a humidified incubator at 37°C and 5% CO_2 for 24 hours. After 24 hours, the cells were removed from each well, pooled together and centrifuged in a Falcon tube. The cells were then resuspended in the appropriate amount of medium supplemented with the cytokines. The earliest time point at which transduction efficiency was assessed was five days post-transduction.

2.2.6 Cryopreservation and Thawing

For cryopreservation of isolated T cells, after centrifuging and washing the cell pellet, the cell pellets were resuspended in the desired volume of cold (4°C) CryoStor CS10. The cell pellet was resuspended thoroughly in Cryostor medium using a P1000 pipette. The freezing density used was between $10-50\times10^6$ cells per mL. The cells in the freezing medium were then gently transferred to 1.2 mL or 2 mL cryogenic tubes. The closed vials were then labelled at placed in CoolCell LX freezing container and placed in the -80°C freezer for at least 24 hours. The cryopreserved cells were then moved from -80°C freezer into a liquid nitrogen tank for long-term storage.

For the cryopreservation of expanded T cells, firstly Dynabeads were removed by placing a 50 mL Falcon tube containing the cell suspension and beads inside a magnet. After one minute, the cells were carefully removed from the centre of the Falcon tube using a 25 mL serological pipette without disturbing the Dynabeads attached to the wall of the Falcon tubes. The cells were then counted and centrifuged at 400g for 5 minutes

before proceeding to the freezing step as described above.

For the thawing of cryopreserved T cells, one vial was removed from -80°C or liquid nitrogen and was placed in 37°C water bath for 2 minutes. The cryovial was then moved into a microbiological Safety Cabinets (MSC) hood and the cell suspension contained in the vial was transferred to a 50 mL Falcon tube using a P1000 pipette. Then by using 25 mL serological pipette, 19 mL of pre-warmed complete medium was slowly added to the cell suspension while gently swirling the tube. The Falcon tube was then centrifuged at 400g for 5 minutes. The supernatant was removed by pouring and the cell pellet was gently resuspended. Finally, the pre-warmed complete medium was added to the cells and mixed gently by pipetting up and down. A sample was then taken for cell counting and phenotyping.

2.2.7 Feeding

Before feeding, the complete medium used for the feeding was warmed up to 37°C in the water bath. At the same time, the cytokines were thawed at room temperature. The cytokines were then added to the medium to achieve desired concentration, and the medium was used for feeding.

2.2.7.1 Fed-batch: T-flask, Well plate and Bag

Medium additions in T-flasks and well plates, were performed using a serological pipette inside a MSC hood. For gas-permeable bags, a syringe was used; first, the plunger was

removed in MSC hood and a syringe was attached to the gas-permeable bag through the Luer lock port. The desired amount of medium was then added via a serological pipette to the syringe. The plunger was used to push the medium to the bag. The syringe was then removed, and the Luer lock port was closed with its lid.

2.2.7.2 Pseudo-perfusion: micro-Matrix

The micro-Matrix microbioreactor plate was removed from the bioreactor and placed in MSC hood. The plate lid and its clamps were removed and replaced with a temporary sterile plastic lid from a 24 well-plate lid. This was necessary in order to fit the plate inside the centrifuge. The temporary lid was taped to the plate, and the plate was placed in the centrifuge plate holder. The plate was centrifuged at 150g for 10 minutes (24°C). After centrifuging, the plate was carefully removed from the plate holder and transferred into a MSC hood. The temporary lid was removed, and the plate was held at a 45-degree angle. The desired amount of supernatant was then carefully removed from each well using a P1000 pipette without disturbing the cell layer formed at the bottom of each well. Warm complete medium with the cytokines was then added to each well. The microbioreactor plate lid was finally placed back on and attached to the micro-Matrix control system. Further details on how the micro-Matrix system works and its setup can found in Chapter 5.

2.3 Lentivirus Production

2.3.1 Plasmid Preparation

CD19-CAR plasmid was kindly given by Dr Martin Pule (Cancer Institute, UCL). The CD19-CAR consist of the FMC63 scFV, CD8 alpha stalk, RQR8 site with 4-1BB endodomain as described in Philip et al. (2014) and Stavrou et al. (2018). RQR8 has the CD34 epitope and is recognised by QBEND/10 anti-CD34 mAb, which is used in CD34 isolation kit (Miltenyi Biotec). RQR8 site can also be stained with CD34-PE mAb (QBEND/10), and therefore the expression of CAR on T cells and transduction efficiency can be measured via staining with CD34-PE mAb (QBEND/10).

2.3.1.1 Transformation

A tube of NEB E.Coli cells was thawed on ice. The cells were then gently mixed, and 50 μL of cells was moved to the transformation tube on ice. 1 μL of CAR plasmid DNA equivalent to approximately 100ng was added to the transformation tube. The cells and DNA plasmid were mixed by flicking the tube. The mixture was kept on ice for 30 minutes. Meanwhile, the water bath was warmed up to 42°C. After 30 minutes on ice, the mixture was placed in the water bath for 30 seconds and then moved back on ice for 5 minutes. 950 μL of NEB-10 beta medium was added to the mixture, and the tube was placed inside the 32°C incubator shaker (300rpm) for one hour. The day before, a selection Agar-Lysogeny broth (LB) plate was prepared with Geneticin (G-418 Sulfate)

at the concentration of 50 $\mu g/mL$ and kept in the fridge. The plate was warmed up to 32°C during one-hour incubation of transformed bacteria. 100 μL of cells was then added to a selection plate, and the plate was incubated at 37°C overnight.

2.3.1.2 Small scale plasmid preparation

Following the transformation and overnight incubation, a single colony was picked from the selection plate and added to 10 mL of LB supplemented with an appropriate antibiotic in a Falcon tube. For the CAR plasmid, 50 $\mu g/mL$ of Geneticin was used, whereas, for the lentivirus packaging plasmids, 100 $\mu g/mL$ of Ampicillin was used. The Falcon tube was placed on an incubator shaker (37°C) overnight. After overnight culture, the Qiagen miniprep kit was used to verify the plasmid with restrictive digest enzymes. After verification, the transformed bacteria were frozen by mixing 500 μL of the overnight culture with 500 μL of 50% glycerol in a 2 mL cryovial. The cryovial was frozen at -80°C.

2.3.1.3 Large scale plasmid preparation

A selection Agar-LB plate was prepared with an antibiotic (as explained above). The cryovial of transformed CAR bacteria or packaging plasmid bacteria was thawed overnight. 100 μL of cells was added to a selection plate, and the plate was incubated for 16 hours at 37°C overnight. After overnight incubation, a single colony was picked from the selection plate and added to 10 mL of LB supplemented with an appropriate antibiotic

in a Falcon tube. The Falcon tube was placed in 37°C shaker incubator (250rpm) for 8 hours to prepare the inoculum. 500-1000 mL of LB broth was autoclaved and added to 1-2L shaker flask. After, 8 hours incubation the inoculum was added to the shaker flask and placed 37°C shaker incubator (250rpm) overnight. The Qiagen maxiprep kit was used to isolate the plasmid DNA as per the manufacturer's instructions. After plasmid isolation, the DNA concentration was measured by absorbance of light at 260nm wavelength with a Nanodrop spectrophotometer. The ratio of absorbance at 260nm:280nm was used to establish purity, where 1.8 indicates a high degree of purity with no/little protein contamination. The DNA was frozen at the concentration of 500 $\mathrm{ng}/\mu\mathrm{L}$ in -20°C freezer.

2.3.2 Lentiviral vector production

2.3.2.1 Lentivirus system

The 2nd generation lentivirus system (Didier Trono Lab) was used to produce CAR-lentiviral vector. This system consists of one transfer plasmid (CD19-CAR), one envelope plasmid (pMD2.G for VSV-G) and one packaging plasmid (pCMVR8.74 for gag, pol, tat and rev). The packaging and envelope plasmids were delivered as agar stab. The plasmids were produced initially at small scale and verified with restrictive digest enzymes, before producing them in large scale. Both pMD2.G and pCMVR8.74 were purchased from Addgene with catalogue numbers 1225 and 22036, respectively.

2.3.2.2 HEK293T culture

HEK293T were thawed and passaged at least two times in T-175 flask before being used for lentiviral vector production. 40 mL of high glucose DMEM containing sodium pyruvate and Glutamax supplemented with 10% FBS was used for culturing HEK293T cells in T-175 flasks. For passaging, the medium was aspirated from the T-flask, and the cells were washed once with PBS. Then, 15 mL of Trypsin-EDTA (0.05%) was added and incubated for 5 minutes at 37°C. The T-flask was then tapped to detach the cells from the surface. 15 mL of DMEM supplemented with 10% FBS was added to the cells to inactivate the Trypsin-EDTA. The cell suspension was then transferred into a Falcon tube and centrifuged at 300g for 10 minutes. The supernatant was then aspirated, and the cell pellet was resuspended in the appropriate amount of the DMEM medium. The HEK293T cells were split at a ratio of 1:10 dilution when they reached 90% confluency.

2.3.2.3 Transient transfection

4×10^6 HEK293T cells were seeded in a 15cm TC-treated culture dish in DMEM supplemented with 10% FBS. When approximately 70% was achieved, normally after two days, the transfection protocol was performed. Initially, the serum-containing medium the cells were cultured in was removed, and the cells were carefully washed once with PBS solution using a 25 mL serological pipette to remove serum residues. 20 mL of pre-warmed advance serum-free (SF) DMEM medium was then added to each plate. The

HEK293T cells were then placed inside a 37°C and 5% CO_2 incubator, while preparing the transfection reagent. To prepare the transfection reagent, 30 μL of Gene Juice was added dropwise to 470 μL of SF DMEM for each plate. The mixture was vortexed and incubated at room temperature for 5 minutes. Then, the following amounts of DNA were added to make the transfection mixture: 5.4 μg of pCMVR8.74, 2.9 μg of pMDG.2, and 4.2 μg of CD19-CAR DNA. The mixture was gently mixed by pipetting and incubated for 15 minutes at room temperature. The mixture was added dropwise to the HEK293T cells. The plate was then gently rocked before placing it inside the 37°C and 5% CO_2 incubator. After 2 hours incubation, the medium was aspirated without disturbing the cells using a 25 mL serological pipette. Pre-warmed fresh DMEM medium supplemented with 10% FBS was added (20 mL per plate). The plate was then transferred back to the 37°C and 5% CO_2 incubator for 48 hours. After 48 hours, the supernatant containing lentiviral particles was collected from each plate. The supernatant was filtered using a 0.45 μm PES filter and a 50 mL syringe. A quality control sample was then taken for characterisation, and the rest of the supernatant was frozen in -80c freezer in 25 mL and 50 mL aliquots.

2.3.2.4 FACS titration of lentivirus

HEK293T cells were seeded at 3×10^5 cells per well in 1 mL of DMEM medium supplemented with 10% FBS in 12-well plates. After 24 hours, one well was sacrificed for cell count. The medium was aspirated from the other 11 wells and replaced with the

volume of lentivirus as shown in Figure 2.1. Subsequently, each well was topped up using DMEM supplemented with 10% FBS to reach the final volume of 500 μL. For the non-transduced control, 500 μL of DMEM supplemented with 10% FBS was added. The plate was then returned to 37°C and 5% CO_2 incubator for 24 hours. After 24 hours, 1 mL of DMEM supplemented with 10% FBS was added to each well to feed the cells. 72 hours after transduction, the supernatant was removed and Trypsin-EDTA (0.05%) solution was added to each. The cells were incubated with Trypsin-EDTA (0.05%) solution for 5 minutes in a 37°C and 5% CO_2 incubator. The cells were then removed from each well and placed in a Falcon tube and centrifuged at 300g for 10 minutes. The cell pellets were washed once with PBS and stained with anti-CD34 PE antibody. The cells were then fixed with 1% PFA for 15 minutes and washed twice prior to resuspending them in PBS and running them on the flow cytometer.

For analysis, CD34 positive cells were gated using Flowjo software. The percentage of the positive population for each dilution was calculated based on two technical replicates. The value between 1% to 20% positive population was then selected. The following formula (Equation2.1) was used to calculate the titre. The average of titre for each dilution was calculated and used as an infectious titre.

$$\text{Titre(TU/mL)} = \frac{\text{Number of cells on day one} \times (\frac{\text{Percentage of positive cells}}{100})}{\text{Volume of viral supernatant (mL)}} \tag{2.1}$$

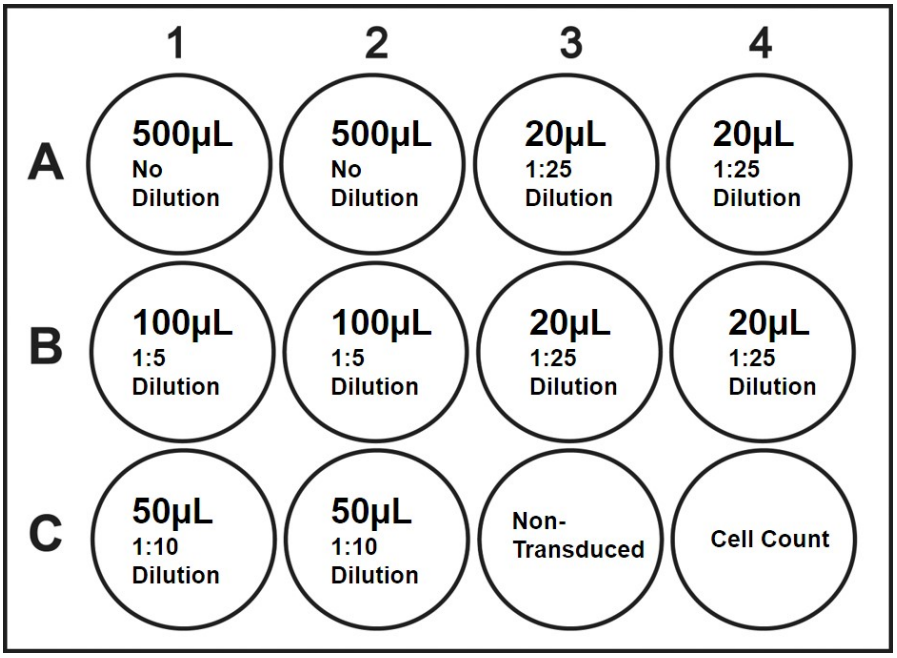

Figure 2.1: The plate layout used to perform the infectivity assay for lentivirus. The dilution ratio indicates how diluted the lentivirus supernatant was in each well. The volume value written on each well indicates how much of lentivirus supernatant was added.

2.4 *In vitro* assays

2.4.1 CD34 magnetic bead isolation

On the day of harvest, Dynabeads from expanded CAR-T cells were removed using a magnet as explained in Section 2.2.6. The transduced T cells with the CD19-specific RQR8 CAR construct were isolated using CD34 positive isolation beads with LS columns (Miltenyi Biotec) as per manufacturer's instructions. Isolated CAR-T cells from all conditions were then rested overnight in RPMI 1640 supplemented with 10% FBS and 2 mM L-glutamine and used in the killing assay or proliferation assay or cytokine release assay.

2.4.2 FACS killing assay

The killing assay was performed using CD19-positive NALM6 and Raji as target cells. To ensure healthy cells were being used for the killing assay, both cell lines were cultured for at least seven days after thawing. The medium used for culturing NALM6 and Raji cells was RPMI 1640 supplemented with 10% FBS and 2mM L-glutamine.

The killing assay was performed in three technical replicates for each donor. 50 µL of isolated CAR-T cells containing 50,000 cells were added in a flat bottom 96-well plate. 50 µL of either NALM6 or Raji cells containing 50,000 cells were added to each well to achieve 1:1 effector to target ratio. Non transduced T-cells and target cells alone were seeded in separate wells as controls. The plate was then placed in a 37°C and 5% CO_2 incubator for 48 hours.

After 48 hours, using a multi-channel pipette, the whole plate containing all the conditions was transferred from the flat bottom 96-well plate to a V bottom 96-well plate. The flat bottom 96-well plate was washed with 100 µL of PBS which were then added to the V bottom plate. The plate was centrifuged at 300g for 5 minutes. The supernatant was removed by flicking the plate carefully. The pellets were then resuspended and washed in 100 µL of PBS and centrifuged again. In the meantime, a staining solution with CD3 antibody was prepared by mixing 1 mL of PBS with 6.25 µL of CD3 BUV395 antibody. After centrifuging and removing the supernatant, the pellets were resuspended in 100 µL of the staining solution using a multi-channel pipette. The plate

was incubated on ice for 30 minutes. After the incubation, 100 μL of PBS was added to each well, and the plate was centrifuged at 300g for 5 minutes. After centrifuging, the cells were washed once and resuspended in 200 μL 0.1% SYTOX red solution for live/dead staining. The content of the well plate was then transferred to multiple FACS tubes. 25 μL of CountBright absolute counting beads were added to each FACS tube.

The samples were analysed using the BD Fortessa X20 (with a UV laser). On the flow cytometer, first the FSC-H and SSC-H were adjusted to capture all Countbeads. Then, 2000 events were recorded on Countbead gate. The following equations were used to calculate the total number of viable target cells (VTCs) and the remaining target viable cell (%). The example of gating strategy is shown in Figure 2.2.

$$\text{Total number of VTCs} = \frac{\text{number of VTC events}}{\text{Number of bead events}} \times \text{number of beads in 25 } \mu\text{L of Countbead} \tag{2.2}$$

$$\text{Remaining target viable cell (\%)} = \frac{\text{Total number of VTCs (in CAR-T wells)}}{\text{Total number of VTCs (in Non-transduced well)}} \times 100 \tag{2.3}$$

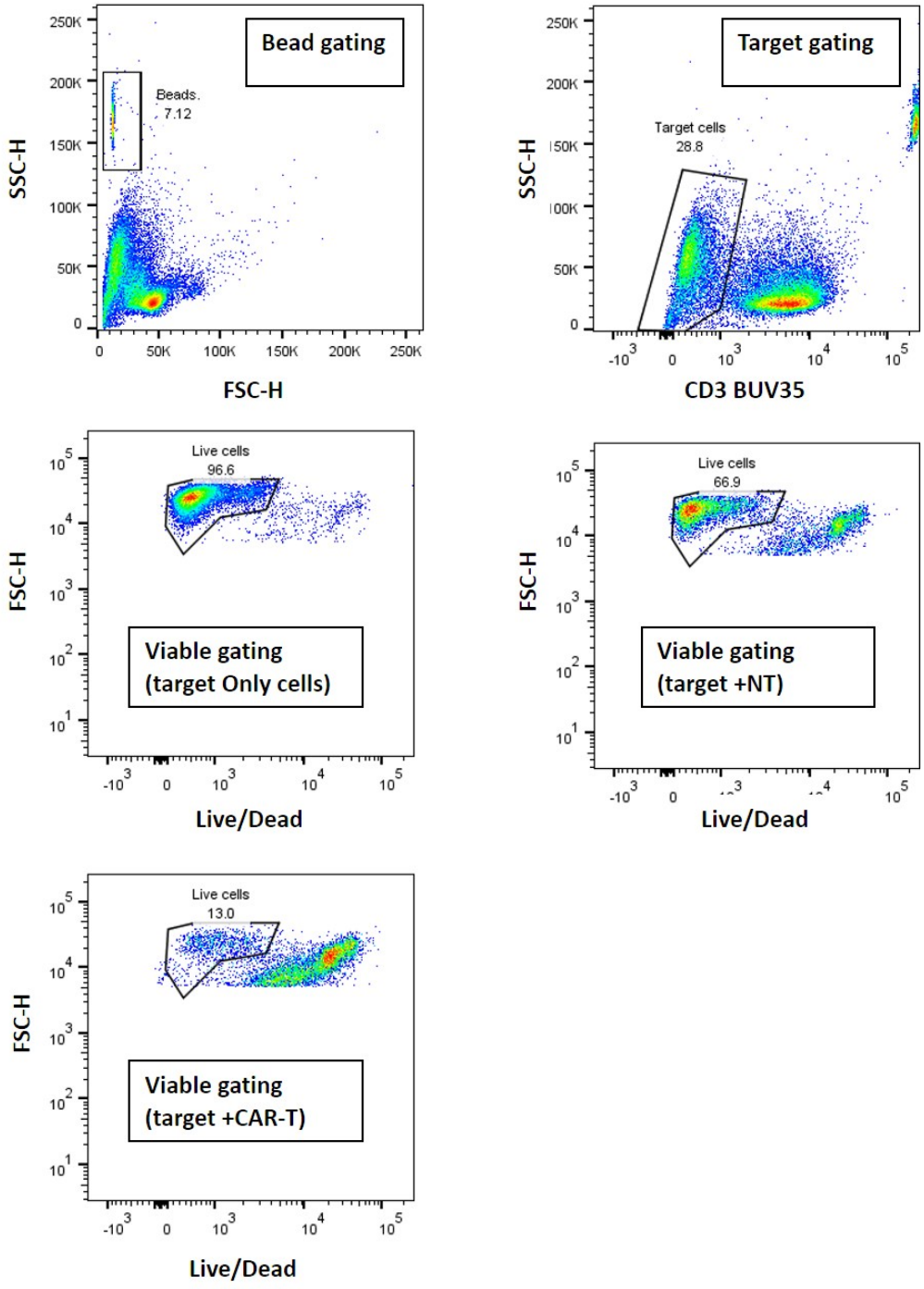

Figure 2.2: Gating strategy for target only, non-transduced T cells with target cells and CAR-T cells with target cells are shown. Target only sample was used to set live/dead gating for other samples.

2.4.3 Soluble Cytokine Analysis

To assess the soluble cytokine secreted by CAR-T cells, the same experimental setup, as explained in Section 2.4.2 was used. 50 μL of isolated CAR-T cells containing 50,000 cells were added to 50 μL of NALM6 cells containing 50,000 cells in a 96 well plate to achieve 1:1 effector to target ratio. The plate was then placed in 5% CO_2 incubator for 24 hours. After incubation, the plate was centrifuged at 300g for 5 minutes, and 50 μL of supernatant was removed using a multi-channel pipette. The samples were transferred to another 96-well plate and stored in -80°C until ready to be processed and analysed. Once the samples were thawed, the analysis of cytokines in the supernatant was performed using the BD Cytometric Bead Array (CBA) Human Th1/Th2/Th17 Cytokine Kit as per the manufacturer's instructions. The samples were analysed using BD FACSVerse, and the data were analysed using FCAP Array™ software.

2.4.4 Proliferation assay

The proliferation assay was designed to assess the proliferation capability of CD19-specific CAR-T cells after repeated exposure to CD19-positive NALM6 cells. The isolated CAR-T cells from each donor were mixed with NALM6 cells in a 6-well plate at a 1:1 ratio, using 2×10^6 CAR-T cells and 2×10^6 NALM6 cells in each well. The plate was placed in a 37°C and 5% CO_2 incubator . After 72 hours of co-culture, a 200 μL sample was taken from each well for flow cytometry analysis. The sample was stained

with CD3 BUV395 and SYTOX Red to distinguish the live CD3+ cells from the cancer target cells. The Countbright beads were also used to calculate the absolute number of live CD3+ cells.

After the 72 hours sample was taken, the co-culture was fed with fresh cRPMI 1640 at 1:1 dilution. The plate was incubated in a 37°C and 5% CO_2 incubator for further 72 hours. After 144 hours (6 days) of co-culture and 72 hours after the last sample was taken, another 200 μL sample was taken from each well in order to assess the absolute number of live CD3+ cells via flow cytometry assay as described above.

After flow cytometry analysis, the co-cultured cells were harvested and washed once in PBS to remove debris. Then, CD3+ cells were isolated from any remaining target cells using CD3+ positive isolation kit with LS columns (Miltenyi Biotec). The isolated CAR-T cells (CD3+ T cells) were then rested overnight in the incubator, prior to starting the second round of co-culture. For the second and third runs of co-culture, the experimental procedure explained above was repeated two times.

2.5 Analytical Techniques

2.5.1 Cell density and viability

Total cell count, viable cell count and viability were determined using NucleoCounter NC-3000 cell counter. Before taking the cell count, the cell suspension was mixed gently either by pipetting up and down in T-flasks and well plates or by gently massaging the bag in gas-permeable bags. To perform the cell count, 200 μL of the sample was taken after mixing the cell suspension and transferred to a 1.5 mL Eppendorf tube. The sample was then immediately taken for analysis, where Via-1 Cassette containing acridine orange and DAPI was used with the NucleoCounter to determine the cell count and viability. The automated cell counter calculated the number of cells and viability based on captured images. After the cell count, the images were checked to ensure the absence of bubbles in the sample. If a bubble was observed, another sample was taken with a new Via-1 Cassette.

The fold expansion was calculated using the equation below:

$$\text{Fold Expansion} = \frac{\mathrm{VCC_i} \times \mathrm{V_i}}{\mathrm{VCC_0} \times \mathrm{V_0}} \tag{2.4}$$

where $\mathrm{VCC_i}$ and $\mathrm{V_i}$ are the viable cell concentration and volume of cell culture at $\mathrm{t_i}$, respectively. where $\mathrm{VCC_0}$ and $\mathrm{V_0}$ are the viable cell concentration and volume of cell culture at $\mathrm{t_0}$, respectively.

2.5.2 Metabolite Analysis

To analyse different metabolites such as glucose, lactate, ammonia and glutamine, 0.5 mL of spent medium was taken throughout the cell culture. The samples were stored at -20°C for a maximum of two months. Before analysing the metabolites, the samples were thawed in room temperature and vortexed to ensure well-mixed samples were loaded into the Cubian HT270 medium analyser. After media analysis, the specific consumption rate or production rate for each metabolite was calculated using the following equations:

$$q_{Met}\ (\text{g/cell.h}) = \frac{c_{i-1} - c_i}{IVCC_i} \tag{2.5}$$

Where c_i is the concentration of the metabolite in the cell culture sample at t_i and c_{i-1} is the concentration of the metabolite in the cell culture sample at t_{i-1}. The IVCC was calculated as below:

$$\text{IVCC (cells/mL/h)} = \frac{x_i + x_{i-1}}{2} \times (t_i - t_{i-1}) \tag{2.6}$$

Where x_i is the viable cell concentration at t_i and x_{i-1} is the viable cell concentration at t_{i-1}.

The lactate yield from glucose was calculated as below:

$$\mathrm{Y_{Lac/Gluc}} = \frac{\mathrm{q_{Lac}}}{\mathrm{q_{Gluc}}} \tag{2.7}$$

Where $\mathrm{q_{Gluc}}$ is the specific consumption rate of glucose, $\mathrm{q_{Lac}}$ is the specific production rate of lactate.

2.5.3 Phenotypic characterisation

Different flow cytometry panels were designed and used to characterise T cells. All flow cytometry data were analysed using FlowJo v10 software.

2.5.3.1 Extracellular marker staining protocol

For antibodies cocktail preparation, 50 μL of BD Horizon Brilliant stain buffer was added to an Eppendorf tube. Each fluorescent reagent at the recommended volume per test as determined in titration was added and mixed well with Briliant stain buffer. BD stain buffer was added to make up the volume of antibody cocktail to 90 μL per test. To stain a sample of cells, $0.5-1.0 \times 10^6$ cells were transferred to an Eppendorf tube. The sample volume was centrifuged at 400 g for 5 minutes at room temperature. The pellet was then resuspended in 1 mL BD stain buffer and centrifuged again. Following the last wash, the supernatant was removed, and the pellet was resuspended in 50 μL of BD stain buffer. 2.5 μg of Human BD Fc Block was added to each sample and incubated at

room temperature for 10 minutes. Following the FC blocking step, 90 μL of antibody cocktail prepared previously (as explained above) was added to each tube. The mixture was then incubated over ice for 30 minutes. After incubation, the sample was washed twice with minimum 1 mL of BD stain buffer. The sample was kept at +4°C in the fridge and analysed within the next 2 hours. If the sample had to be analysed after 24 hours or overnight, fixing procedure was performed. Following, two washes, the stained cells were resuspended in the 2% paraformaldehyde solution and incubated on ice for 15 minutes, Following the fixation, the cells were washed once, resuspended in BD stain buffer and stored at +4°C until analysed.

2.5.3.2 Memory panel

To characterise memory cells, two panels were designed; The first 9 markers panel was designed to characterise T naive cells (T_N), T memory stem cells (T_{SCM}), T central memory cells (T_{CM}), T effector memory cells (T_{EM}) and T terminally effector cells (T_{TE}). The second panel was a reduced version of the first panel with only 5 markers, and was used when T memory stem cells characterisation was not needed.

2.5.3.3 Exhaustion panels

In order to measure the expression of different exhaustion markers, including PD-1 and LAG-3, two panels were designed. Exhaustion Panel 1 consists of CD3 BUV395, CD8+ BUV737, CD4 BUV805, LAG-3 AF647, whereas exhaustion panel 2 consists of CD3

Table 2.7: 9-colour flow cytometry panel to characterise different CD8+ phenotypes, including T Memory Stem Cell.

Memory Panel 1			CD8+ Characterisation				
Marker	Colour/Format	Clone	T_N	T_{SCM}	T_{CM}	T_{EM}	T_{TE}
CD3	BUV395	SK7	+	+	+	+	+
CD8	BUV737	SK1	+	+	+	+	+
CD4	BUV805	SK3	-	-	-	-	-
CCR7	BV421	150503	+	+	+	-	-
CD45RO	PE-Cy7	UCHL-1	-	-	+	+	-
CD27	BV786	L128		+			
CD45RA	FITC	HI100		-			
CD95	PE	DX2		+			
CD62L	APC	Dreg-56		+			

Table 2.8: 5-colour Flow cytometry panel to characterise different CD8+ phenotypes.

Memory Panel 2			CD8+ Characterisation			
Marker	Colour/Format	Clone	T_N	T_{CM}	T_{EM}	T_{TE}
CD3	BUV395	SK7	+	+	+	+
CD8	BUV737	SK1	+	+	+	+
CD4	BUV805	SK3	-	-	-	-
CCR7	BV421	150503	+	+	-	-
CD45RO	PE-Cy7	UCHL-1	-	+	+	-

BUV395, CD8+ BUV737, CD4 BUV805 and PD-1 PE.

2.5.3.4 Transduction efficiency

In order to measure the transduction efficiency on CD4+ and CD8+ T cells, the following panel was used: CD3 BUV395, CD8+ BUV737, CD4 BUV805, CD34 (QBEND/10) PE. The CAR construct used in this thesis has RQR8, which is recognised by QBEND/10 anti-CD34 mAb.The level of CD34 expression was therefore used to measure the level of CAR expression on T cells.

2.5.4 Intracellular staining

In order to measure the intracellular cytokine level of T cells, non-specific stimulation protocol with PMA and Ionomycin was used. First of all, a blocking solution was prepared; 1 μL of Golgi plug and 0.7 μL of Golgi stop was mixed in 198.3 μL of PBS to make a blocking solution. 20 μL of this solution was added to each well in a 96-well plate. For samples preparation, T cells were centrifuged at 400g for 5 minutes and resuspended in the cRPMI 1640 medium to achieve 10^7 cells/mL. 100 μL of the cells containing 10^6 cells were added to each well. In order to activate the T cells, appropriate amount of PMA and Ionomycin were added to achieve the final concentration of 10 ng/mL and 1.0 μg/mL, respectively in 200 μL in each well. 10 μL of anti-human CD107a PE antibody was added to each well, and the volume of each well was adjusted to 200 μL with PBS. The mixture was incubated for 5 hours in a 5% CO_2 and 37°C incubator.

2.5.4.1 Intracellular staining protocol

Following the incubation step at the end of the stimulation protocol, the samples were washed and stained with extracellular staining protocol. The following extracellular antibodies were used extracellular staining: CD3 BUV395, CD8+ BUV737, CCR7 BV421. After the extracellular staining, the following steps were taken for intracellular staining. First of all, the cells were resuspended in 250 μL of BD Fixation/permeabilisation solution for 20 minutes at +4°C. The cells were then washed twice in 1x BD Perm/Wash buffer (1 mL minimum per sample). The cells were then resuspended in 50 μL of BD Perm/Wash buffer containing a predetermined concentration of fluorochrome-conjugated anti-cytokine antibodies as per vendor's instructions. The following intracellular antibodies were used: TNF–α AF488, IL-2 PE, IFN–γ APC. The mixture was incubated on ice for 30 minutes. The samples were washed twice with BD Perm/Wash buffer (1 mL minimum per sample). The cells were then resuspended in BD staining buffer and analysed on the flow cytometer.

2.6 Statistical analyses

Data analysis was performed using GraphPad Prism 7. All results are presented as Mean $\pm$ Standard Deviation. One-way analysis of variance (ANOVA) was used to analyse whether there is a significant difference between the means of three or more unrelated groups. One-way ANOVA was only used where the effect of one factor was assessed between different groups. t-test was used to compare the mean of two different group to assess whether there is significant difference. A two-way ANOVA was used to assess whether there are interactions between two independent factors. For further analysis and to compare different groups, Tukey's multiple comparison tests was used following two-way ANOVA test. The confidence interval used for all the data, unless otherwise stated in the figure legend, was 95% ($\mathrm{P} < 0.05$) for *, 99% ($\mathrm{P} < 0.01$) for ** and 99.9% ($\mathrm{P} < 0.001$) for ***. Normal distribution and homogeneity of variances between groups, the two key assumptions for ANOVA tests, were performed before analysing data using Shapiro-Wilk normality test and Levene's test.

Chapter 3

Effect of Glucose, Pyruvate and Fatty Acids on T cells

3.1 Introduction

With CAR-T therapy emerging as a successful treatment for different kinds of cancers, a wide range of serum-free media were developed to accommodate the need for clinical manufacturing of T cell therapies. A successful CAR-T cell manufacturing process requires medium formulations that produce enough cells for a therapeutic dose without sacrificing the quality of the end product. The quality of CAR-T cells could be characterised by the phenotypic composition of T cells. Several researchers have found that the number of CAR-T cells with memory phenotype in the end product is highly correlated

with improved clinical outcome (Lipp et al., 1999; Gattinoni et al., 2005; Louis et al., 2011; Kochenderfer et al., 2017; Fraietta et al., 2018). Therefore, different strategies were developed to maintain or increase the number of memory cells in CAR-T products (explained in Section 1.4.3).

T cell metabolism is coupled with T cell function and differentiation. Also, different T cell subsets preferentially use different pathways; memory subsets rely preferentially on OXPHOS, whereas effector cells primarily utilise glycolysis (R. Wang et al., 2011; Michalek et al., 2011; Pearce et al., 2009). Therefore, the availability of essential nutrients required for different metabolic pathways would have an impact on T cell expansion, differentiation and the final phenotypic composition. In this chapter, it was assessed how by modulating the provision of key metabolites in the culture medium, the phenotypic composition of T cells could be manipulated and skewed toward central memory subset. The metabolites assessed in this section are glucose, pyruvate and fatty acids. These metabolites are considered essential for T cell expansion and are some of the critical inputs into the major metabolic pathways, including glycolysis and OXPHOS (as explained in Section 1.4). Understanding the effect of these metabolites on T cell quality will allow designing new medium formulations or adjusting feeding strategy to improve the manufacturing of T cell therapies.

3.2 Experimental procedure

Different RPMI 1640 media with various concentrations of glucose, sodium pyruvate and fatty acids were prepared and tested in this chapter. The detailed compositions of the media used in this chapter were provided at the beginning of each experiment.

The following T cell activation and expansion protocol was used in this chapter. T cells were seeded at a density of 500,000 cells/mL in 1 mL of different media in 12-well plate and placed in a 37°C and 5% CO_2 incubator. T cells were stimulated with anti-CD3/anti-CD28 Dynabeads at three beads to one cell ratio as suggested by different manufacturing protocols (David L Porter et al., 2006; Brentjens et al., n.d.[b]; Tumaini et al., 2013a; Cameron J Turtle et al., 2016; N. Singh et al., 2016). Regarding cytokine, the combination of IL-7 (25 ng/mL) and IL-15 (10 ng/mL) was used to supplement the media as suggested by N. Singh et al. (2016), Cha et al. (2010), Cieri et al. (2013), and Xu et al. (2014). For feeding, unless otherwise stated, the fresh medium containing the cytokines was added on day 3, 6 and 7. The dilution ratio of 1:1 was used for feeding, which means the volume of the cell culture was doubled with fresh medium on feeding days. The cells were harvested on day 8. The fold expansion and viability were assessed by using the NC-3000 cell counter. The composition of T cells was assessed by flow cytometry using either flow cytometry panel 1 or 2 (Section 2.5.3). For more detailed procedure for analytical assays, please refer to Section 2.5.

3.3 Results: effect of media metabolites on T cells

This first experiment was designed to: 1) investigate the effect of glucose, sodium pyruvate and fatty acids on T cells and 2) to assess whether it is possible to redirect T cell differentiation through targeting metabolism via nutrient availability in the medium.

3.3.1 Glucose & pyruvate

Glucose is the main input to the glycolysis pathway, whereas pyruvate is one of the products of glycolysis and one of the inputs to the TCA cycle (J. M. Berg et al., 2012). Here, it was hypothesised that by limiting glucose but providing pyruvate, T cells would not have key metabolites to carry out glycolysis but can use the exogenous sodium pyruvate to fuel the TCA cycle, OXPHOS and glucogenesis. Glycolysis is the primary pathway used by effector T cells, whereas, memory cells preferentially use OXPHOS (Windt et al., 2012; Pearce et al., 2013a; Chang et al., 2013; O'Sullivan et al., 2014a). Using this approach, the level of differentiated effector cells or memory cells can be altered. To test this hypothesis and to elucidate the role of glucose and sodium pyruvate in the activation and expansion of T cells, four different combinations of glucose and sodium pyruvate were tested (Table 3.1). To create these combinations, RPMI 1640 medium without glucose was used. The medium was first supplemented with 10% FBS, 2mM of L-glutamine and 1% Antibiotic-Antimycotic solution and then different concentrations of glucose and sodium pyruvate were added (Table 3.1).

Table 3.1: The table shows four conditions with different combinations of glucose and sodium pyruvate tested in this section.

Condition	Glucose (11mM)	Sodium pyruvate (2mM)
1	+	+
2	-	+
3	+	-
4	-	-

3.3.1.1 Growth kinetics

T cells from four healthy donors were activated and expanded in 4 different media conditions (Table 3.1. The fold expansions achieved after eight days are shown in Figure 3.1 (a). Similar fold expansions were achieved in the conditions where glucose were present, regardless of sodium pyruvate presence. Lack of glucose in the medium had a significant impact on the fold expansion; The fold expansion of T cells cultured in the media with no glucose but with sodium pyruvate (4.3 $\pm$ 0.6) was significantly lower ($\mathrm{P} < 0.05$) than T cells cultured in the media with both glucose and sodium pyruvate (19.4 $\pm$ 4.2). Similarly, the absence of glucose in the medium without sodium pyruvate resulted in a significantly lower ($\mathrm{P} < 0.05$) fold expansion of 2.8 $\pm$ 0.6.

Figure 3.1 (b) shows the viability of T cells post eight days of expansion in different media. High viability ($> 90\%$) was achieved in glucose-containing media, regardless of sodium pyruvate presence. Lower viability of 80.6% $\pm$ 3.6 and 79.7% $\pm$ 4.6 were achieved by glucose-deprived T cells in the presence and absence of sodium pyruvate, respectively. This result indicates that the presence of glucose in the medium is the main contributing factor to the viability achieved after expansion.

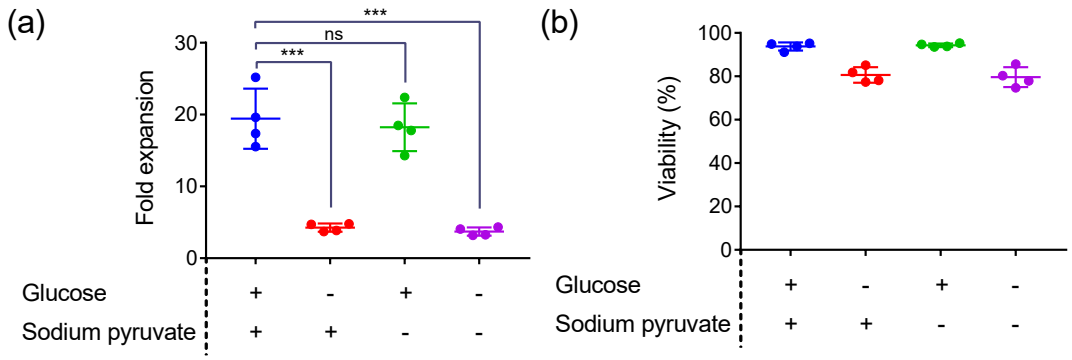

Figure 3.1: Fold expansion (a) and viability (b) of primary T cells after eight days of expansion in different media with different combinations of glucose and sodium pyruvate concentrations. Glucose (+) media contains 11mM of glucose, whereas sodium pyruvate (+) media contain 2mM of sodium pyruvate. Glucose (-) and sodium pyruvate (-) media contain no glucose and sodium pyruvate, respectively. Mean $\pm$ SD, 4 healthy donors are shown. Statistical comparisons were performed using one-way ANOVA followed by Tukey's multiple comparison tests.

3.3.1.2 Immunophenotypic Analysis

Figure 3.2 shows the ratio of CD4+ to CD8+ T cells at the end of eight days of expansion in different media. The CD4:CD8 ratio achieved in glucose-deprived T cells in presence and absence of sodium pyruvate were 3.6 $\pm$ 0.7 and 3.2 $\pm$ 0.5, which is significantly higher ($P < 0.05$) than the control condition (1.8 $\pm$ 0.8) where both glucose and sodium pyruvate were present. From this result, it is evident that the lack of glucose in the media increases CD4:CD8 ratio, whereas sodium pyruvate had no significant impact of CD4:CD8 ratio.

Furthermore, subsets of cytotoxic T cells were assessed by flow cytometry in order to compare the subsets of CD8+ T cells. Figure 3.3 shows the percentages of T Stem Cell Memory cells (T_{SCM}), T central memory (T_{CM}), T effector memory (T_{EM})

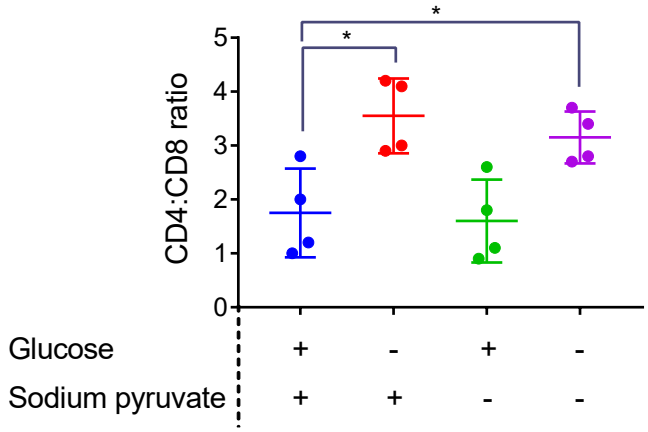

Figure 3.2: CD4:CD8 ratio of T cells at the end of eight days expansion in different media with different combinations of glucose and sodium pyruvate concentrations. Mean $\pm$ SD, 4healthy donors are shown. Statistical comparisons were performed using one-way ANOVA followed by Tukey's multiple comparison tests.

and T terminally differentiated effector (T_{TE}) cells, based on expression of CCR7+ and CD45RO+ markers. Interestingly, the phenotypic analysis showed that the composition of T cells cultured in glucose-free medium was made of significantly high T_{CM} and low T_{EM} percentages. T_{CM} percentages were 80.3% $\pm$ 6.6 and 80.7 % $\pm$ 5.2 for T cells expanded in glucose-free medium with and without sodium pyruvate, respectively. These results were significantly higher compared to the T cells grown in medium containing both glucose and sodium pyruvate (30.4% $\pm$ 9.4). Figure 3.3 (e) and (f) shows memory markers CD27 and CD62L median fluorescence intensity (MFI) on CD3+ T cells. The results showed similar CD27 MFI was observed across the different conditions. In contrast significantly lower ($P < 0.001$) MFI was observed for CD62L, when T cells were expanded in glucose deprivation conditions compared to the T cells expanded in the medium containing glucose.

Collectively, these data suggest that the glucose deprivation conditions produced T cells enriched with T_{CM} population at the cost of lower fold expansion. The presence of

sodium pyruvate had no impact on growth and phenotypic data. Although, CD27 MFI were similar in all conditions, CD62L MFI was decreased in the glucose deprivation conditions.

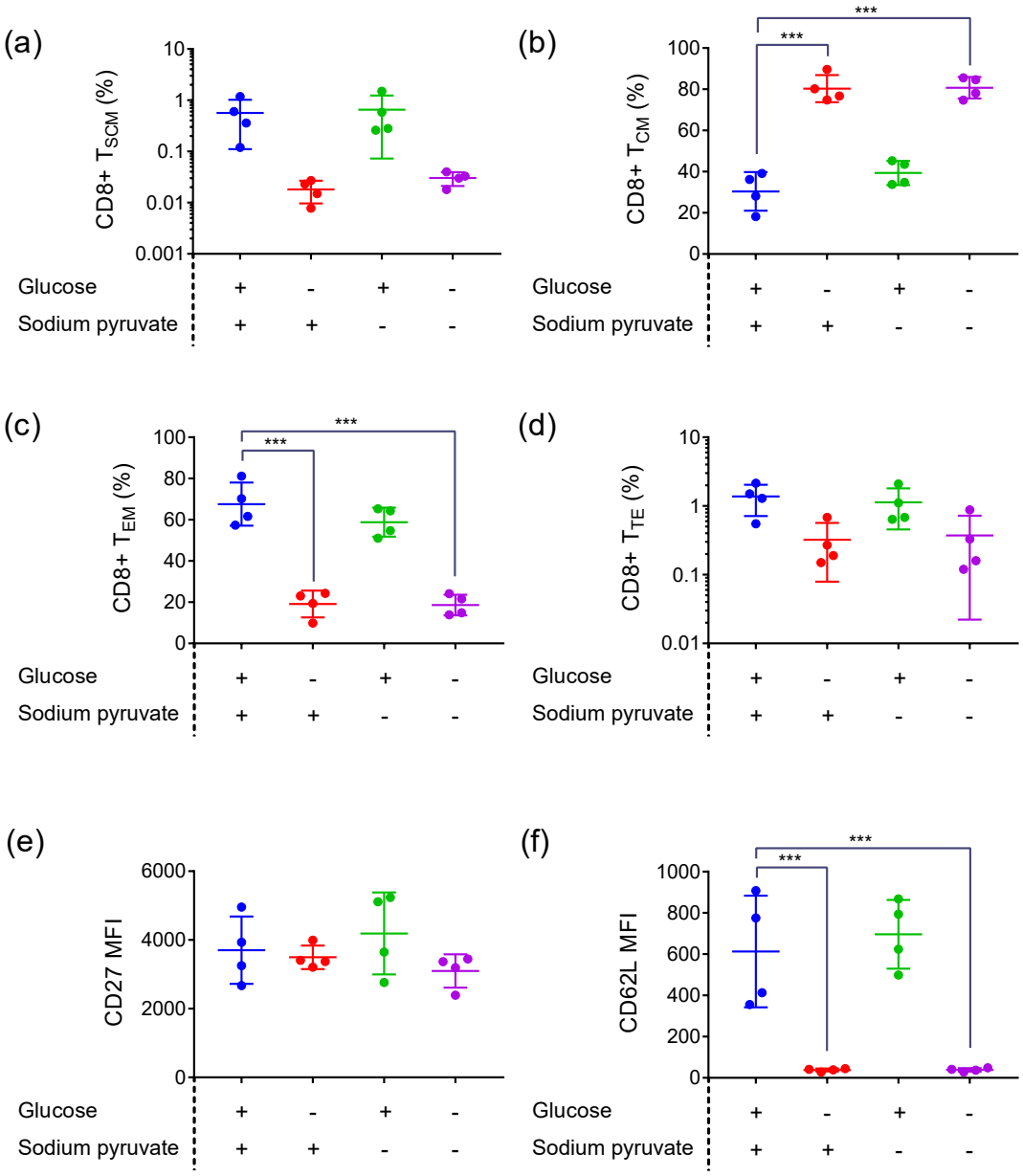

Figure 3.3: Flow cytometry characterisation of CD8+ T cells after eight days expansion. Percentages of CD8+ a) T stem cell memory, b) T central memory, c) T effector memory and d) T terminally differentiated cells. Expression of CD27 (e) and CD62L (f) markers on CD3+ cells are indicated with MFI. Mean $\pm$ SD, 4 healthy donors are shown. Statistical comparisons were performed using one-way ANOVA followed by Tukey's multiple comparison tests.

3.3.2 Fatty Acids

T cell cellular metabolism of fatty acids in two major pathways of fatty acid oxidation (FAO) and de novo fatty acid synthesis (FAS) is critical for their differentiation and proliferation (as explained in Section 1.4.2.3). Additionally, Ecker et al. (2018) showed that T cells uptake exogenous fatty acids in the medium to fuel the OXPHOS. It is also established that FAO is the preferential metabolic pathway for CD8+ memory T cells for development and long-term persistence (Pearce et al., 2009; Windt et al., 2012; Windt et al., 2013). Here, it was assessed whether supplementing the medium with two different fatty acids, linoleic acid and oleic acid, has an impact on differentiation and proliferation. For this experiment, the medium for each condition (shown in Table 3.2) was prepared by supplementing cRPMI 1640 with either 1% linoleic acid (30 μM) or 1% oleic acid (30 μM). The control condition was cRPMI 1640 with no fatty acids.

Table 3.2: The table shows three conditions with different combinations of linoleic acid and oleic acid tested in this section.

Condition	Linoleic acid (30μM)	Oleic acid (30μM)
+ Linoleic acid	+	-
+ Oleic acid	-	+
Control	-	-

3.3.2.1 Growth kinetics

Figure 3.4 shows T cell fold expansion achieved over eight days in cRPMI 1640 medium supplemeted either with linoleic acid or oleic acid. The fold expansion in the medium

containing linoleic acid (24.8 $\pm$ 3.9) or oleic acid (23.7 $\pm$ 3.2) was higher than the control condition (19.4 $\pm$ 4.2) but failed to meet statistical significance ($P > 0.05$). High viabilities ($> 90\%$) were observed in all the conditions.

The data presented in this section suggests

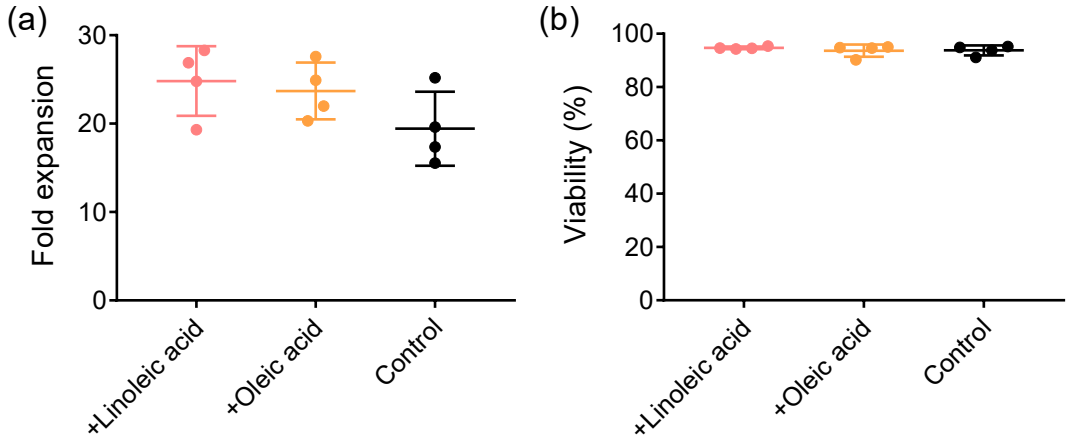

Figure 3.4: Fold expansion (a) and viability (b) of primary T cells after eight days expansion in different media. Control media is cRPMI 1640. +Linoleic acid condition is made of the control media with 1% linoleic acid, +Oleic acid condition is made of the control medium with 1% oleic acid. Mean $\pm$ SD, 4 healthy donors are shown. Statistical comparisons were performed using one-way ANOVA followed by Tukey's multiple comparison tests.

3.3.2.2 Immunophenotypic Analysis

The CD4:CD8 ratio following the eight days culture in different media can be seen in Figure 3.5. Higher CD4:CD8 ratio was achieved, when linoleic acid was present in the medium compared to the control (3.0 $\pm$ 0.8 vs 1.8 $\pm$ 0.8). Supplementing the medium with oleic acid did not affect CD4:CD8 ratio. Flow cytometry analysis of subsets of CD8+ T cells on day eight is presented in Figure 3.6 (a-d). No significant

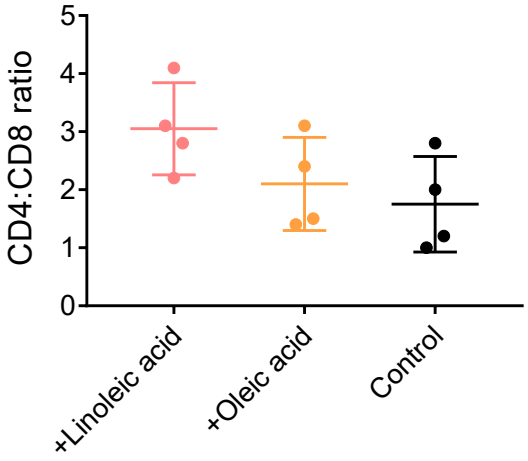

Figure 3.5: CD4:CD8 ratios of T cells at the end of 8 days expansion in presence of either linoleic acid or oleic acid or glycerol. Mean ± SD, 4 healthy donors are shown. Statistical comparisons were performed using one-way ANOVA followed by Tukey's multiple comparison tests.

difference was observed on CD8+ T $_{SCM}$ population percentage in different media. The percentage of T $_{CM}$ subset of cytotoxic T cells was significantly higher ($P < 0.05$) in media supplemented with either linoleic acid (47.1 % ± 2.9) or oleic acid (47.4 % ± 2.7) compared to the control medium (30.4 % ± 9.4). On the other hand, the percentage of CD8+ T $_{EM}$ was significantly lower ($P < 0.05$) in presence of linoleic acid (49.9 % ± 4.3) and oleic acid (50.0 ± 3.9). No significant difference was observed in CD8+ T $_{EM}$ (%) across different media. MFI of CD27 and CD62L markers are presented in Figure 3.6 (e,f). No significant difference was observed comparing CD27 and CD62L MFI. These findings suggest that supplementing the medium with linoleic acid or oleic acid improved the growth of T cells and increase the T_{CM} population in the final product.

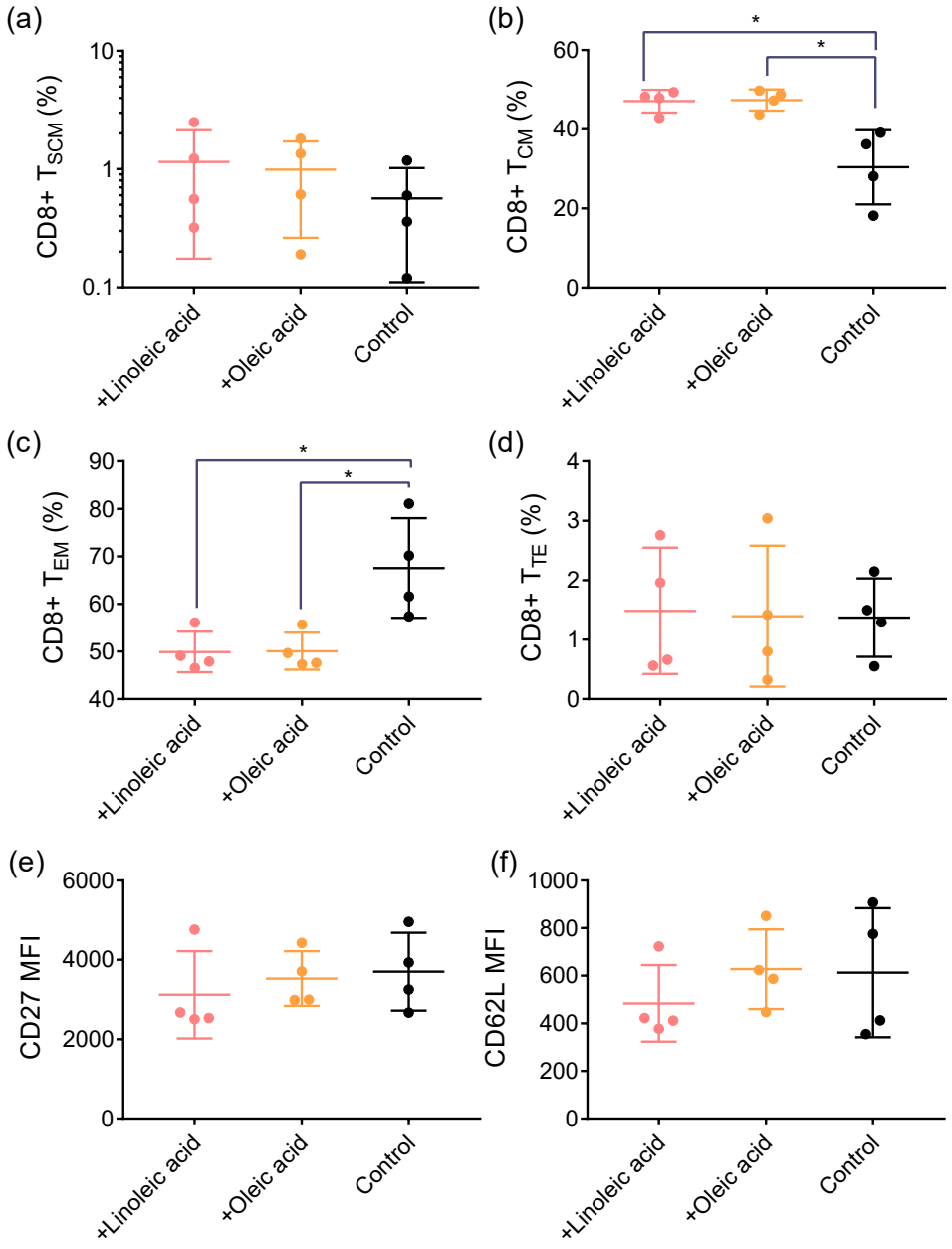

Figure 3.6: Flow cytometry characterisation of CD8+ T cells after eight days expansion in different media in presence of either linoleic acid or oleic acid or glycerol. Percentages of CD8+ a) T stem cell memory, b) T central memory, c) T effector memory and d) T terminally differentiated cells. Expression of CD27 (e) and CD62L (f) markers on CD3+ cells are indicated with MFI. Mean $\pm$ SD, 4 healthy donors are shown. Statistical comparisons were performed using one-way ANOVA followed by Tukey's multiple comparison tests.

3.4 Results: Developing a new feeding strategy

In Section 3.3.1, it was observed that expansion and activation of T cells in glucose-free medium resulted in central memory enriched T cell product. In this section, a new set of experiments was designed to: 1) verify the previous results in Section 3.3.1, where high central memory percentage was achieved in absence of glucose, 2) assess the impact of different concentrations of glucose in the medium on T cells, 3) evaluate the functionality of glucose-deprived T cells, 4) explore different feeding strategies to improve the fold expansion achieved in the glucose-free medium, while maintaining a high percentage of central memory T cells.

3.4.1 Glucose titration

Media with different glucose concentrations were prepared by varying the glucose level between 0mM and 25mM in a glucose-free RPMI 1640 (supplemented with 10% FBS, 2mM L-glutamine, 1% Antibiotic-Antimycotic solution). Negatively isolated pan T cells were then activated and expanded in different glucose concentrations. The same medium used for inoculation of each condition was used for the feeding of the T cells during eight days of expansion.

Additionally, the feeding strategy used in this section was slightly adjusted. The previous feeding strategy (1:1 dilution on day 3,5,7) was applied to both glucose-free and glucose-containing conditions. This could potentially reduce cell density (per vol-

ume and per surface area) of T cells in glucose-free media after every feeding, as the growth of T cells in glucose deprivation conditions were significantly lower than glucose-containing conditions. Therefore, a new adjusted feeding strategy was designed to minimise over-diluting slow-growing glucose deprived T cells, while maintaining enough nutrients for the fast-growing T cells. In the new adjusted feeding, on day 5 and 7, pseudo-perfusion feeding was performed, where 1 mL of supernatant was aspirated carefully from each well without disturbing the cell aggregates. The supernatant was then replaced with fresh medium.

3.4.1.1 Growth kinetics

Figure 3.7 (a,b) shows the mean fold expansion and viability achieved by three healthy donors after eight days of expansion in different glucose concentrations. Similar fold expansion was achieved in the media with 5mM, 11mM and 25mM glucose concentration (16.8 ± 7.4, 17.2 ± 2.4, 17.3 ± 2.9, respectively). On the other hand, significantly ($\mathrm{P} < 0.05$) lower fold expansion (2.9 ± 0.5) was observed in T cells expanded in glucose deprived medium. Likewise, the viability of T cell expanded in glucose-free media on day eight was significantly lower ($\mathrm{P} < 0.001$) than other conditions.

3.4.1.2 Immunophenotypic Analysis

Figure 3.7 (c) shows the CD4:CD8 ratio of the final products. Similar CD4:CD8 ratio was observed in medium supplemented with 5mM, 11mM and 25mM glucose. In the

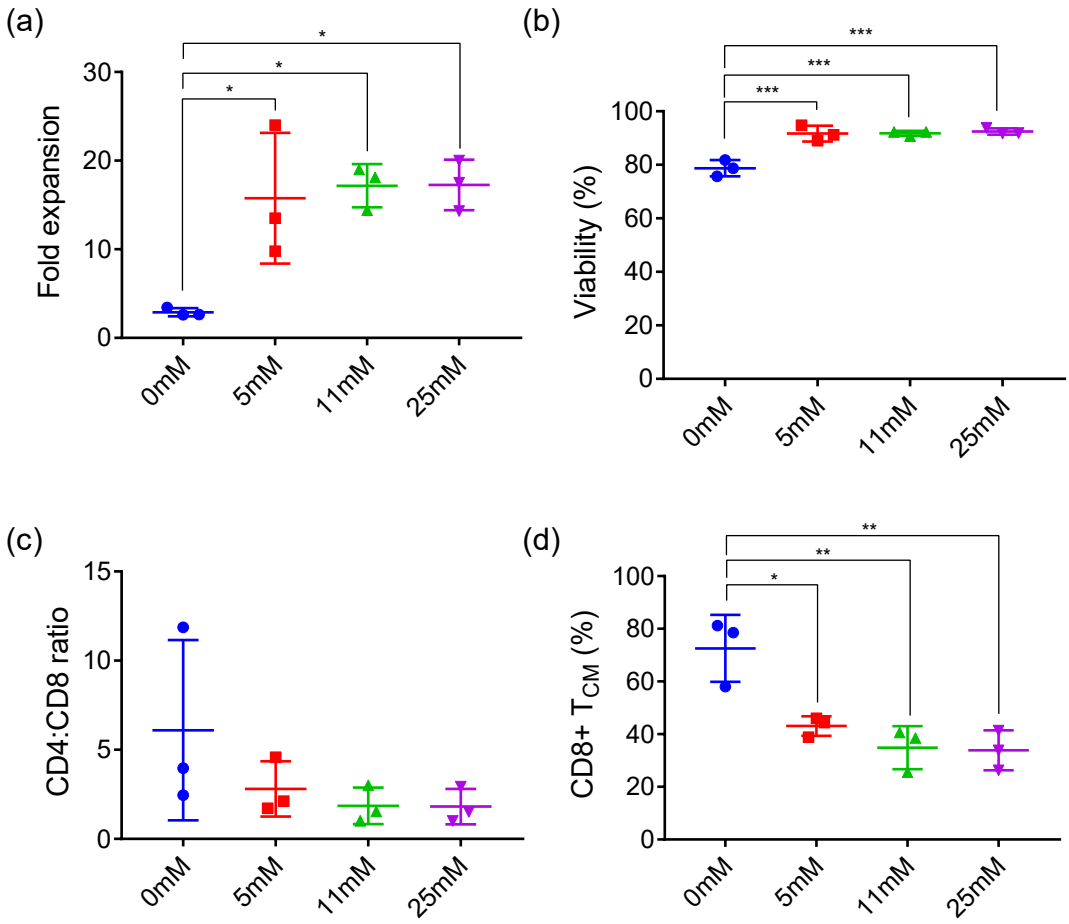

Figure 3.7: Fold expansion (a), Viability (b), CD4:CD8 ratio (c) and the percentage of CD8+ T_{CM} (d) after expansion in RPMI1640 media supplemented with different glucose concentrations (0, 4, 11, 25mM). Mean $\pm$ SD, 3 healthy donors are shown. Statistical comparisons were performed using one-way ANOVA followed by Tukey's multiple comparison tests.

glucose deprivation condition, higher CD4:CD8 ratio was observed. T_{CM} population of cytotoxic T cells is shown in Figure 3.7 (d), where significantly higher T_{CM} percentage was achieved in the final product when T cells were cultured in glucose-free medium compared to other conditions. No significant differences ($P > 0.05$) were observed between the cells grown in medium supplemented with 5mM, 11mM and 25mM glucose.

3.4.2 Non-specific stimulation of T cells

To better understand of the functional characteristics of T-cells expanded in the glucose-free medium or 11mM glucose concentration medium, the production of IL-2, IFN-γ, TNF-α and the degranulation of CD107a were measured by intracellular cytokine staining. Central memory-enriched T cells produced in glucose deprivation condition were stimulated with non-specific reagents, PMA and Ionomycin for 5 hours in the cRPMI 1640 (with 11mM of glucose). The cRPMI 1640 medium containing glucose was used to resemble the *in vivo* environment. More details on stimulation protocol and intracellular staining can be found in Section 2.5.4. The gating strategy used in this section can be found in Section A.1.

In order to compare the level of cytokines produced in each condition, MFI of IL-2, IFN-γ, TNF-α and CD107a were measured and averaged after gating on CD3+ T cells (Figure 3.8). Interestingly, T cells expanded in glucose-free media exhibited significantly higher ($P < 0.05$) IL-2 MFIs than the control medium containing 11mM glucose.

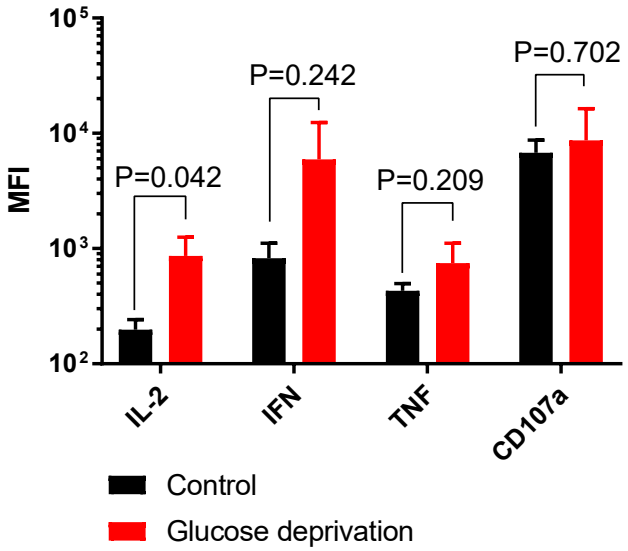

Figure 3.8: Mean fluorescence intensity of each cytokine produced by CD8+ T cells following non-specific stimulation are shown. Data representing results from 3 healthy donors are shown as Mean $\pm$ SD. Statistical comparisons were performed using multiple t-tests.

Regarding IFN-γ and TNF-α, higher MFI were observed in the glucose deprivation condition compared to the control; however, they failed to meet statistical significance ($P < 0.05$). Similar degranulation was observed in both conditions. These findings revealed that effector functions of T cells represented by the production of IL-2, IFN-γ, TNF-α and the degranulation of CD107a were not impaired as the result of expansion in glucose-free media.

3.4.3 New feeding strategy

A new feeding strategy for T cell expansion was tested. In this feeding strategy, T cells were exposed to different glucose concentrations throughout the expansion period. The objective of this experiment was to assess whether fold expansion can be improved while maintaining high T_{CM} portion in the final product by varying the glucose concentration in the medium at different stages of expansion. Activation of T cells require glucose to fuel both glycolysis and OXPHOS pathways after TCR stimulation (Chang et al., 2013). Here, it was investigated whether by providing enough glucose for activation (the first three days) and then exposing the T cells to glucose-deprivation during the expansion period (next five days), the absolute number of central memory T cells can be improved in the final product, compared to using glucose-free media for both activation and expansion periods.

Four different conditions were assessed in this experiment (Table 3.3). Control conditions used for this experiment were T cells activated and expanded for eight days in glucose-free media (Condition 1) and the RPMI 1640 medium with 11mM glucose concentration (Condition 3). In condition 2, T cells were activated and expanded in the glucose-free RPMI 1640 medium for the first three days; Then the cells were fed with the RPMI 1640 medium with 11mM glucose concentration for the next five days. In condition 4, T cells were seeded and activated in the RPMI 1640 medium with 11mM glucose concentration for the first three days; Then, T cells were fed using glucose-

Table 3.3: The table shows four conditions tested in this section. The eight days of cell culture was divided into two periods; activation period (day 0-3) and expansion period (day 3-8). The table shows whether the medium used for feeding in each period in each condition contained glucose.

	Glucose presence in the medium	
Condition	Activation period (day 0-3)	Expansion period (day 3-8)
1) 0mM	-	-
2) 0mM $\rightarrow$ 11mM	-	+
3) 11mM	+	+
4) 11mM $\rightarrow$ 0mM	+	-

free the RPMI1640 for the next five days. Similar feeding time points and strategy, as explained in 3.4.1 were used in this section.

Fold expansion and viability in the final products for the different conditions are shown in Figure 3.9 (a) and (b). The fold expansion achieved in condition 2 was 9.6 $\pm$ 3.1 which was significantly higher ($\mathrm{P} < 0.05$) than condition 1 but significantly lower ($\mathrm{P} < 0.01$) by 44% than condition 3. The fold expansion on day 8 in condition 4 was 6.8 $\pm$ 0.7 which was 135% higher than condition 1, but significantly lower ($\mathrm{P} < 0.01$) than condition 3. The final viability in condition 4 was 79.3 % $\pm$ 4.0, similar to the viability of condition 1 (78.7 % $\pm$ 3.0). Whereas, the viability of T cells in condition 2 was 84.9 % $\pm$ 1.4, relatively lower than condition 3 (91.8 $\pm$ 0.9), although not significantly ($\mathrm{P} > 0.05$).

The average of CD4:CD8 ratios achieved on day 8 were 3.6 $\pm$ 2.0 and 2.7 $\pm$ 1.5 for condition 2 and 4, respectively, which were higher than condition 3 with 11mM glucose concentration but lower than glucose deprivation condition (condition 1). Inter-

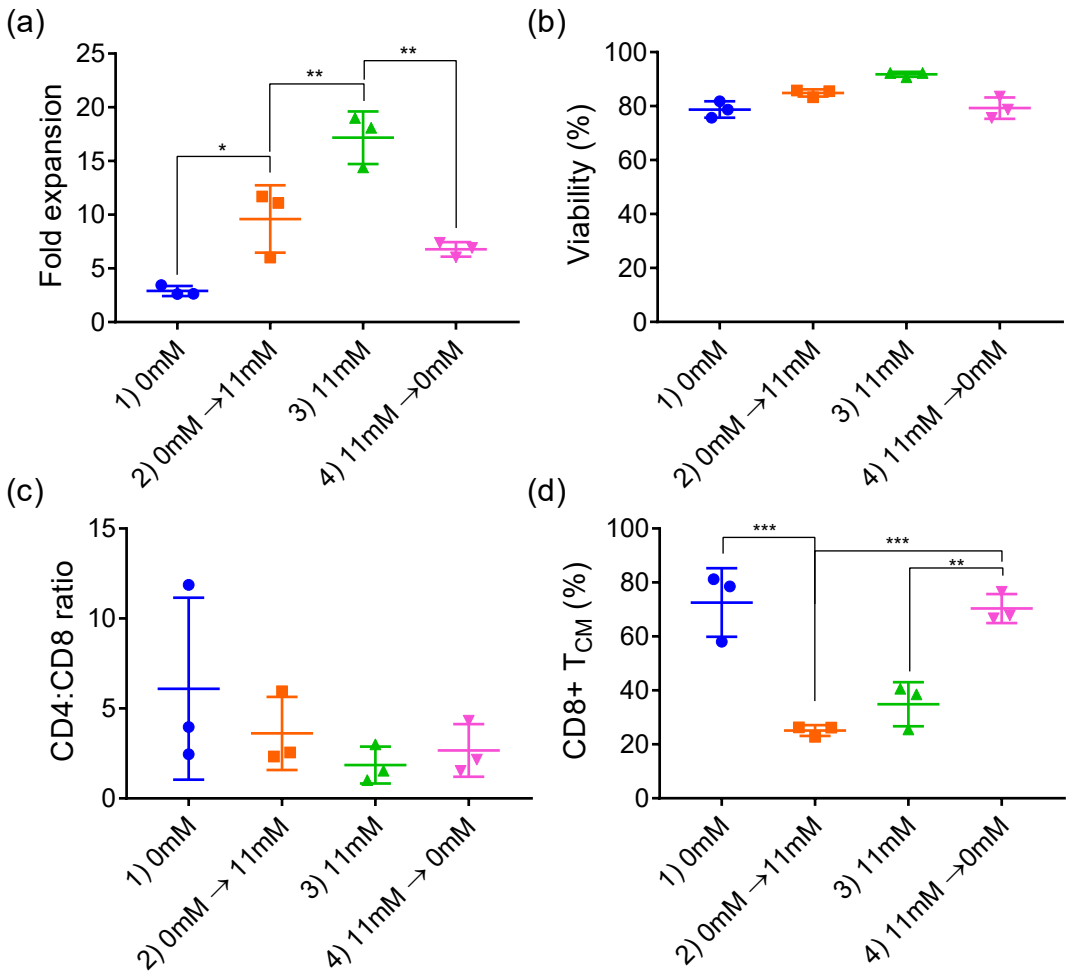

Figure 3.9: Fold expansion (a), Viability (b), CD4:CD8 ratio (c) and the percentage of CD8+ T_{CM} (d) after eight days expansion. In conditions 2 and 4, the feeding medium used was switched on day three. Data are shown as Mean $\pm$ SD for 3 healthy donors. Statistical comparisons were performed using one-way ANOVA followed by Tukey's multiple comparison tests.

estingly, similar portion of less differentiated CD8+ T_{CM} was achieved in condition 1 and condition 4 (72.6 % $\pm$ 12.7 vs 70.3 % $\pm$ 5.4). On the other hand, significantly lower ($P < 0.05$) CD8+ T_{CM} percentages of 25.1% $\pm$ 2.0 and 34.9% $\pm$ 8.2 were achieved in conditions 2 and 3, respectively.

3.5 Discussion

Metabolic reprogramming during T cell activation has been associated with T cell functionality and persistence (Cham et al., 2008; Jacobs et al., 2008; Marko et al., 2010; R. Wang et al., 2011). This metabolic reprogramming was previously reviewed in Section 1.4.1, where the importance of some of the essential metabolites for T cells was highlighted. A better understanding of how different essential nutrients in the cell culture medium affect the cell growth and phenotype can lead to the development of an optimised cell culture medium and designing of efficient feeding strategy for CAR-T therapy manufacturing with focus on improving the quality of final products. As previously explained (Section 3.1), several studies have demonstrated that one of the key contributing factors to improving the quality of CAR-T therapies is the presence of high number of memory cells in the final product (Lipp et al., 1999; Gattinoni et al., 2005; Louis et al., 2011; Kochenderfer et al., 2017; Fraietta et al., 2018). Therefore, in this chapter, a series of experiments were conducted to study whether by supplementing or restricting key nutrients in the cell culture medium, a T cell product enriched with memory cells could be produced.

3.5.1 Glucose and pyruvate

Glucose is an essential metabolite for T cells and the primary input to the glycolysis pathway. Multiple studies have observed elevated glucose metabolism and glycolysis

after stimulation of T cells in both murine and human systems (Kenneth A Frauwirth et al., 2002b; Gubser et al., 2013; Dziurla et al., 2010; Renner et al., 2015). The increased glucose uptake is channelled to increase glycolysis (Warburg effect) and to produce lactate from pyruvate, despite the presence of enough oxygen for OXPHOS to occur Warburg (1956) and MacIver et al. (2013). Following T cell activation, different T cell subsets acquire metabolic reprogramming to support specific function (MacIver et al., 2013). Effector T cells are highly glycolytic to support their pro-inflammatory cytokine production (R. Wang et al., 2011; Michalek et al., 2011). In contrast, memory cells and T_{reg} cells utilise FAO as a primary metabolic pathway to support their long-term persistence (Michalek et al., 2011; Pearce et al., 2009). Here, it was assessed whether it is possible to limit the formation and proliferation of effector T cells by glucose restriction, while allowing the memory cells development and survival.

The results in this study (Figure 3.1, 3.7) showed that growth of T cells was significantly impaired in conditions where glucose was absent in the cell culture media. Similarly, the viability of T cells cultured in the glucose-free media was lower than T cells cultured in the media containing glucose. The presence of glutamine and pyruvate did not rescue lower viability and cell growth in glucose deprivation condition by providing an input to TCA cycle and consequently mitochondrial metabolism, or potentially by fuelling glucogenesis and providing key intermediates produced during glycolysis.

Several studies have investigated the effect of glucose deprivation on mammalian

cells (Cham et al., 2005; Graham et al., 2012; Sena et al., 2013). Similar results to the ones presented in this chapter were observed in Sena et al. (2013) study, where the addition of glutamine or pyruvate failed to improve the viability and proliferation due to glucose deprivation. Interestingly, Renner et al. (2015) observed that glucose deprivation did not affect activation markers, including CD25 and CD95, whereas addition of 2-Deoxy-D-glucose (2DG) significantly reduced the activation markers expression (Renner et al., 2015). 2DG is a glucose analog, which suppresses glycolysis by inhibiting hexokinase 2, an enzyme that catalyses the first step of glycolysis. Renner et al. (2015) suggested that 2DG potentially affects mitochondrial integrity in addition to glycolysis, inhibiting T cell metabolism more compared to glucose deprivation. Therefore, it was argued that glucose deprivation could be compensated by increased OXPHOS and potentially glucogenesis, whereas the 2DG treatment blocks both glycolysis and OXPHOS pathways.

Another study showed that reduced proliferation and viability were observed in GLUT1-deficient T cells, due to lack of glucose transportation into the cells (Macintyre et al., 2014). The suggested underlying mechanisms for suppressed proliferation were the lack of essential nutrients to support biosynthesis and increased levels of phspho-AMPK (adenosine monophosphate-activated protein kinase). Increased phospho-AMPK suppresses the mammalian target of rapamycin complex 1 (mTORC1) signalling (Macintyre et al., 2014). mTORC1 activity drives T cell differentiation and

proliferation (Araki et al., 2009). Lack of G6P produced through glycolysis results in reduction of the pentose phosphate pathway activity (Wellen et al., 2010). Activated T cells use the pentose phosphate pathway to generate ribose sugar for the synthesis of nucleotides and amino acids and to reduce the cellular level of reactive oxygen species to increase cell survival (J. M. Berg et al., 2012). Therefore, the suppressed proliferation observed in glucose deprivation condition is potentially due to the lack of biosynthesis mainly supported by glycolysis pathway and the inhibition of mTORC1 activity.

The absence of glucose resulted in significantly higher CD4:CD8 ratio in the final T cell product, indicating that CD4 cells adapt better to glucose restriction compared to CD8 T cells (Figure 3.2, 3.7). The high CD4:CD8 ratio observed in glucose deprivation condition is potentially due to the difference in metabolic reprogramming between CD4+ and CD8+ T subsets. Both CD4+ and CD8+ T cells adopt aerobic glycolysis after stimulation to provide a high level of ATP in a short period to boost proliferation (Miller et al., 1994). Interestingly, CD4+ T cells have a higher proliferation rate, glycolytic activity and mitochondrial oxidative metabolism upon activation, compared to CD8+ T cells (Renner et al., 2015; Cao et al., 2014). Sena et al. (2013) showed that mitochondrial metabolism could support the activation of CD4+ T cells measured by the expression of CD25 and CD69 marker in the absence of glucose. The likely explanation for high CD4+ to CD8+ ratio observed in the results in glucose deprivation conditions is that CD4+ T cells have higher metabolic plasticity than CD8+ T cells and do not rely

on glucose metabolism as much as CD8+ T cells. Thus, helper T cells can compensate the lack of glucose metabolism by using their greater mitochondrial content and spare respiratory capacity to generate ATP (Cao et al., 2014). Our results also showed that the presence of pyruvate in the cell culture medium did not affect the CD4 to CD8 ratio in glucose deprivation condition (Figure 3.2). This suggests that CD4+ T cells are potentially using other metabolites in the cell culture medium such as glutamine to fuel their OXPHOS cycle. Higher CD4+ plasticity and adaptation to glucose-free medium was further supported from the results when the cell culture media was switched from glucose-free to the medium containing 11mM glucose after three days or vice versa (Figure 3.9), higher CD4:CD8 ratio was observed compared to T cells expanded in glucose-containing medium from the beginning.

Further analyses into CD8+ T cells subsets showed that glucose deprivation resulted in significantly higher CD8+ T_{CM} and lower CD8+ T_{EM} in the final product (Figure 3.3). Different subsets of T cells primarily use specific metabolic pathway; Effector cells highly rely on glycolysis to produce inflammatory cytokines (Chang et al., 2013). Effector T cells are highly glycolytic, but also use mitochondrial metabolism for proliferation (Sena et al., 2013; Almeida et al., 2016). On the other hand, memory cells have increased spare respiratory capacity and use OXPHOS and FAO to fuel their maintenance and survival (O'Sullivan et al., 2014b). Interestingly, as discussed in Section 1.4, memory cells primarily use Acetyl-CoA to fuel FAS and FAO rather than extracellular

fatty acids (O'Sullivan et al., 2014b). The results presented in this chapter indicated that in the absence of glucose in the medium, memory cells could still be developed. In this study, the presence of sodium pyruvate also did not impact the phenotypic composition of the memory compartment in the glucose deprivation conditions. This suggests that either not enough sodium pyruvate was supplemented in the medium to observe its effect or bypassing glycolysis to TCA cycle via uptaking extracellular pyruvate has no role in the generation of memory cells.

It is not conclusive from the results, whether glucose deprivation just inhibited the generation of effector cells or promoted the development of memory cells or both scenarios. Further studies would be required to investigate how glucose deprivation resulted in the final T cell product enriched in memory cells. Similar to the results presented, Sukumar et al. (2013) study demonstrated that augmenting the glycolytic flux by using glucose analog and glycolysis inhibitor, 2DG, throughout the activation and expansion periods resulted in inhibition of terminally differentiated T cells and preservation the of memory T cells in murine systems, characterised by CD62L and CD27 expression.

Furthermore, the results presented in Figure 3.3 (e,f) showed that the expression of CD62L was significantly reduced ($P < 0.05$) on T cells grown in glucose deprivation conditions. In contrast, (Sukumar et al., 2013) observed a high expression of CD62L marker on 2DG treated T cells. CD62L, another major lymph node homing receptor, can help to identify memory subsets. CD27, a member of the tumour necrosis factor

receptor family, is another receptor used to characterise central memory T cells. Different groups have used a different combination of CCR7, CD62L and CD27 markers to characterise central memory and effector memory CD8+ T cells. In this doctoral thesis, CCR7+ expression has been used alone to distinguish between central memory and effector memory cells. CD62L and CD27 markers were only used to identify the recently found subset of T cells, known as T_{SCM} (Gattinoni et al., 2009). Unsoeld et al. (2005) suggested that using the combination of memory markers such as CD62L and CCR7 to characterise central memory T cells may result in the exclusion of a large part of central memory T cells which express only one of the central memory markers (e,g, CD62L-CCR7+ central memory T cells). It is known that CD62L expression is variably lost with freeze-thaw cycles (Weinberg et al., 2009; Mahnke et al., 2013). However, the underlying mechanism why T cells in glucose deprivation express a significantly lower ($P < 0.05$) amount of CD62L is still unknown.

In the 2-stage feeding experiment (Figure 3.9 (d)), it was showed that by using glucose-free media to feed T cells in the second half of the cell culture period, similar percentages of CD8+ subsets but with improved fold expansion were obtained compared to using glucose-free media throughout the cell culture. Chang et al. (2013) indicated that both glycolysis and OXPHOS are required for successful stimulation of naive cells. Activating T cells initially in glucose-containing medium would allow both glycolysis and OXPHOS to fuel activation. Additionally, glucose-derived citrate can be used for

de novo FAS and lipid storage, which is also required for FAO in memory T cells (Ecker et al., 2018; O'Sullivan et al., 2014a). In the 2-stage feeding regime, the glucose-free media was used for feeding during the expansion period (day 3-8). In this period, only central memory T cells are metabolically fit to survive the glucose restriction. Therefore, using the 2-stage feeding regime would improve the fold expansion, while maintaining the memory phenotype, compared to using glucose-free medium for both activation and expansion periods.

Furthermore, the capacity of T cells to produce inflammatory cytokines was compared via intracellular cytokine staining of T cells produced either in the control media or glucose deprivation condition. T cells that were cultured in glucose deprivation condition produced a significantly higher level of IL-2, when stimulated with PMA/ionomycin (Figure 3.8). Although higher levels of IFN-γ, TNF-α were observed, both failed to achieve statistically significant differences ($\mathrm{P} > 0.05$). These results indicate that T cells generated under glucose deprivation condition retain their ability to produce inflammatory cytokine. An increased IL-2 secretion observed in the T cells grown in glucose-free media could be due to a high percentage of memory cells or different composition of CD4+ subsets available in the final product of glucose deprivation condition, compared to the control. However, Renner et al. (2015) showed IFN-γ secretion is similar between effector memory and central memory T cells, therefore it is unlikely that the secretion difference was due to different phenotypic composition of T cells. Further

investigations will be required in order to determine whether specific T cell ability to kill cancer cells is enhanced or impaired and to understand the underlying mechanism for increased inflammatory cytokine secretion.

Several studies have looked into the effect of glucose deprivation associated with solid tumour microenvironment on T cell effector function. In the murine system, Cham et al. (2005) and Cham et al. (2008) observed a significant reduction in IFN-γ but no impact on IL-2 production in glucose deprivation. In human T cells, similar IL-2, TNF-α and IFN-γ production were observed in presence or absence of glucose after T cell activation with anti-CD3/anti-CD28, suggesting that glycolytic restriction does not impact cytokine production (Renner et al., 2015). It must be noted that in these studies, T cells were stimulated in glucose-free media to simulate the *in vivo* microenvironment around solid tumours. This is indeed different from the experimental setup presented in this chapter, where T cells were cultured in glucose-free media and then stimulated them in glucose containing medium. In addition, different studies have achieved "glucose deprivation" in two different ways; one group of studies use no glucose in the medium, whereas the other group use 2DG, an analog of glucose, which blocks glucose metabolism in a media supplemented with glucose to resemble low glucose availability. This is potentially one of the reasons for contradictions in different studies findings regarding TNF-γ. Renner et al. (2015) suggested that 2DG potentially affects mitochondrial integrity in addition to glycolysis, inhabiting T cell metabolism more compared to

glucose deprivation. The activation method between different also varies; in this study, PMA in combination with ionomycin was used, whereas other mentioned studies use anti-CD3/anti-CD28 antibodies to measure the functionality of T cells. PMA/ionomycin has been commonly used in immunological research. However, it was shown that the cytokine profiles observed after stimulation with PMA/ionomycin and anti-CD3/anti-CD28 are different (Olsen et al., 2013). This factor, in addition to aforementioned differences, could also contribute to the contradictory difference observed between different studies. Overall, glucose deprivation did not cause irreversible damage to the T cells to produce cytokines, assessed by non-specific stimulation. Oppositely the glucose deprived T cells, when stimulated in normal glucose media, exhibited enhanced ability to secrete cytokines such as IL-2.

3.5.2 Fatty acids

Fatty acids are another group of essential metabolites for naive and proliferating T cells. Upon T cell activation the balance between FAO and FAS changes, where FAO decreases and FAS increases in order to maximise the availability of lipids needed for membrane synthesis during the rapid proliferation (R. Wang et al., 2011). In this section, the effect of two different unsaturated fatty acids, Linoleic and Oleic acids, on T cell growth and proliferation was assessed. Linoleic acid is a long-chain polyunsaturated omega-6 fatty acid, whereas oleic acid is a short-chain monounsaturated omega-9

fatty acid (J. M. Berg et al., 2012). The fatty acid metabolism profile of different T cell subsets is well understood; FAO plays a critical role in CD8+ memory T cells development and long-term persistence (Pearce et al., 2009; Windt et al., 2012; Windt et al., 2013). Interestingly, O'Sullivan et al. (2014a) demonstrated that effector T cells uptake extracellular FAs significantly higher than memory T cells. O'Sullivan et al. (2014a) concluded that memory T cells utilise intrinsic lipolysis of triacylglycerol (TAG) to supplies fatty acids for FAO. In contrast to O'Sullivan et al. (2014a) study, the results presented in this work showed that the presence of either linoleic acid or oleic acid in the media increased the CD8+ T_{CM} subset in the final T cell product, suggesting fatty acid presence in the medium promotes generation of memory cells during T cells expansion.

The results presented suggested a slight increase in CD4:CD8 ratio when linoleic acid was present in the medium. Angela et al. (2016) also reported that CD4+ memory cells actively acquire external fatty acids. However, no study reporting a direct comparison between the FA metabolism of CD4+ and CD8+ to explain whether the absence or presence of FAs in the media provides a favourable condition for a particular subset has been found. Further investigation will be required to directly compare CD4+ and CD8+ T cells in regards to FA consumption and oxidation to determine whether fatty acids promote the growth of CD4+ T cells over CD8+ subsets.

3.6 Conclusion

In this chapter, the effects of glucose, pyruvate and fatty acids on T cells were assessed. It was shown that by providing glucose to T cells during activation but exposing them to glucose deprivation during the expansion period, a T cell product enriched with T_{CM} subset could be produced. Supplementing the glucose-free medium with sodium pyruvate failed to improve the fold expansion. Adding other metabolites to glucose-free media such as membrane-permeable α–ketoglutarate or succinate to bypass glycolysis could be considered for further optimising the glucose deprived condition. Also, the glucose-free medium used in this chapter was supplemented with 10% FBS serum. It will be important to assess whether this approach is feasible for GMP manufacturing with the current serum-free media or with human serum.

The T cells produced in the glucose-free medium retain their functionality to produce inflammatory cytokines. However, whether the specific killing ability of glucose-deprived T cells is affected remains a question. This is particularly important for translating this feeding strategy to CAR-T therapies. Further studies are needed to understand, whether a high percentage of central memory T cells generated through this approach have improved proliferation and persistence capability upon exposure to cancer cells.

The results presented in this chapter provide a basis for further assessment of the 2-stage feeding strategy with glucose deprivation for the manufacturing of CAR-T ther-

apies. Translation of this feeding strategy to a bioreactor system also raises a question on how manufacturing conditions such as dissolved oxygen and pH affect the quality of CAR-T therapies.

Chapter 4

Glucose Deprivation Enriches For Central Memory T Cells During CAR-T Cell Expansion

4.1 Introduction

The emphasis of ACT manufacturing has been on *ex vivo* proliferation capability and producing a high number of cells. However, several pre-clinical studies and clinical trials have recently suggested that infusion of less-differentiated T cells such as T_{CM} is highly correlated with greater anti-tumour efficacy (Lipp et al., 1999; Gattinoni et al.,

2005; Louis et al., 2011; Kochenderfer et al., 2017; Fraietta et al., 2018). Therefore, the generation of a T cell product enriched with T_{CM} subset remains one of the main aims in improving CAR-T therapies.

The polyclonal expansion and differentiation of T cells are tightly linked to each other. As T cells expand and increase in cell number, a large proportion of cells becomes terminally differentiated (Gerlach et al., 2013). Currently, the clinical manufacturing primarily focuses on producing a large number of CAR-T cells in order to meet the requirements for a therapeutic dose; thus the final product normally contains a high proportion of differentiated cells (Kagoya et al., 2017).

In the previous chapter, a new feeding strategy for T cells was proposed. The 2-stage feeding approach with glucose-free media consists of feeding T cells with a glucose-containing medium during the activation stage (first 3 days) and then using glucose-free media to feed the cells during their expansion. The baseline data was produced using this approach, where it was shown that a final T cell product enriched with less-differentiated T cells could be produced.

In this chapter, the feasibility of the 2-stage feeding strategy for manufacturing CD19-specific CAR-T cells was investigated. The feeding strategy was adopted to make it suitable for clinical manufacturing of CAR-T therapies and to accommodate the presence of extra stages such as transduction and lentiviral vector washing and removal. Then proliferation capability and cytotoxicity of the T_{CM}- enriched CAR-T cells against

CD19 expressing cancer cells was assessed. Finally, potential manufacturing implications of this approach to produce CD19-specific CAR-T therapy enriched with T_{CM} in a GMP clinical setting was discussed.

4.2 Experimental procedure

CAR-T cells were generated using healthy donor pan T cells and the lentivirus encoding the CD19-specific 2nd generation CAR with the 4-1BB costimulatory domain. The CAR structure and the protocol to produce CAR-lentivirus was described in Section 2.3.1. The 2-stage approach tested in the previous chapter was used with a slight adjustment; T cells were activated and transduced at the first stage (first 4 days) in the medium containing 2 g/L (11mM) glucose and then CAR-T cells were fed with glucose-free medium for the second part of the culture period (second 4 days). The duration of initial glucose deprivation period was increased from 3 days in the previous chapter to 4 days in this chapter to accommodate for the transduction step and its wash step. The 2-stage feeding regime was tested in gas-permeable bags as they are widely used for the manufacturing of CAR-T therapies (Vormittag et al., 2018). Primary pan T cells from 6 healthy donors were thawed and rested overnight before seeding in T25 flasks at 400,000 cells/mL in 10 mL of cRPMI 1640 media containing 2 g/L (11mM) of glucose, 10% FBS, 2mM sodium pyruvate and 1% antibiotic-antimycotic supplemented with IL-7 (25 ng/mL) and IL-15 (10 ng/mL). After 24 hours co-culture of T cells with Dynabeads (3:1 bead to cell ratio), the cells were resuspended in lentiviral vector supernatant and transduced in 6-well plate as detailed in Section 2.2.5. The same batch of lentivirus was used to exclude lentiviral vector batch-to-batch variability from the experiment. Following 24 hours incubation with lentivirus, T cells from each donor were

centrifuged and resuspended in cRPMI 1640 medium (with glucose) in order to remove the viral supernatant. T cells were then transferred to a gas-permeable bag. After 48 hours of incubation on day 4, each gas-permeable bag containing CAR-T cells was split into two bags. Each bag was used for a different feeding regime, either with cRPMI 1640 medium containing no glucose (cRPMI 1640 -glucose condition) or using cRPMI 1640 media containing 2 g/L (11mM) glucose (cRPMI 1640 +glucose condition). In the first feeding on day 4, the cells in each bags were diluted at 1:1 ratio with the fresh medium. On day 5, a further dilution at 1:1 ratio for both cRPMI 1640 +glucose and cRPMI 1640 +glucose conditions was performed. On day 7, to prevent over-dilution of T cells due to slower growth in glucose-free condition, only CAR-T cells in cRPMI 1640 +glucose condition were fed (1:1 dilution). All conditions were harvested on day 8. The visual summary of the protocol used in this experiment is shown in Figure 4.1. A sample of 500 μL was taken daily from each bag and used to measure cell density and viability. The samples were then centrifuged, and the supernatant was stored in -20° to be used for medium metabolite analysis. The T cells from each sampling point were also analysed with panel 2 (Section 2.5.3) to characterise T_N, T_{CM}, T_{EM} and T_{TE} subsets of CD8+ T cells.

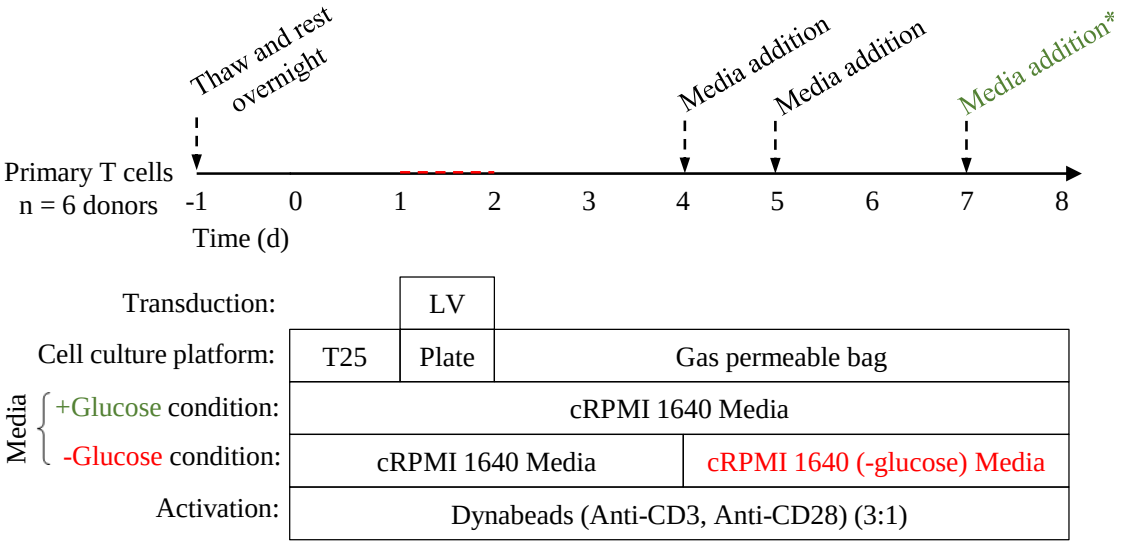

Figure 4.1: The schema shows the CAR-T cells generation protocol used for the experiments performed in this chapter. The medium used throughout the experiment for the control condition (+Glucose condition) was cRPMI 1640. The medium used for glucose deprivation (-Glucose condition) condition was cRPMI 1640 for the first 4 days, and then RPMI 1640 with no glucose was used for medium addition for the next 4 days. All media were supplemented with IL-7 (25 ng/mL) and IL-15 (10 ng/mL). The volume of cell culture medium in each bag for both conditions was doubled with the addition of fresh media on day 4 and 5. An extra medium addition (1:1 dilution) labelled as "Media addition*" was performed only for the control condition on day 7. The activation beads were added on day 0 at 3:1 beads to cells ratio. The transduction was performed on day 1 using lentiviral vector.

4.3 Results

4.3.1 Effect of glucose deprivation on T cell culture

4.3.1.1 Growth kinetics

Viable cell concentration (VCC) and viability of CAR-T cells expanded either in glucose-free medium (shown in red; -glucose condition) or with cRPMI 1640 medium containing glucose (shown in green; +glucose condition) over eight days culture period are shown in Figure 4.2 (a,b). The average viable cell density of T cells on day 1 was $(4.2 \pm 1.0) \times 10^5$ cells/mL prior to centrifuging and resuspending cells in lentiviral vector for transduction. On day 2, after removing the lentiviral vector supernatant and resuspending them in the complete fresh medium, the average viable cell density of $(4.2 \pm 1.0) \times 10^5$ cells/mL was achieved. CAR-T cells reached a cell density of $(1.4 \pm 0.4) \times 10^6$ cells/mL on day 4. At this point, the cells were split into two gas-permeable bags, each containing half of the cells. One bag was then fed (1:1 dilution) with glucose-free medium (shown in red), while the other bag was fed with standard medium (shown in green). After the first feeding (day 4), the VCC of CAR-T cells growing in medium with glucose reached $(9.7 \pm 3.2) \times 10^5$ cells/mL, whereas lower VCC of $(8.0 \pm 1.7) \times 10^5$ cells/mL was achieved in CAR-T cells fed with glucose-free medium. Two more feeding were performed on day 5 and 6. On day 7, the cell density reached $(1.2 \pm 0.3) \times 10^6$ cells/mL and $(0.5 \pm 0.1) \times 10^6$ cells/mL in +glucose and

-glucose conditions, respectively. The CAR-T cells in both conditions grew until day 8, when both conditions were harvested.

The seeding cell viability (Figure 4.2 (b)) across the 6 different healthy donors were $94.7 \pm 1.9\%$. There was a decrease in viability on day two after removing the cells from viral vector supernatant, where viability dropped to 91.6± 3.8%. During the second half of the expansion period, the average viability across four days for CAR-T cells in cRPMI 1640 medium with glucose and without glucose were 94.7% and 91.3%, respectively.

In order to compare the growth of T cells in both conditions, the total number of viable cells throughout eight days culture and the fold expansion achieved on day 8 were plotted and are shown in Figure 4.2 (c) and (d). The total number of viable cells achieved on day 8 was $(4.9 \pm 1.3) \times 10^6$ and $(2.0 \pm 0.6) \times 10^7$ for the standard condition and the glucose-deprived condition, respectively. In terms of fold expansion, significantly higher ($\mathrm{P} < 0.001$) fold expansion was achieved in the standard condition compared to the glucose-deprived CAR-T cells (12.2 ± 3.2 vs 5.0 ± 1.6).

4.3.1.2 Metabolite analysis

Figure 4.3 shows glucose, lactate, glutamine and ammonia concentrations in the cell culture supernatant throughout eight days culture period. Notably, during the transduction period, T cells were exposed to lentivirus supernatant, in which the concentrations of the metabolites were different to the cRPMI 1640 medium. The glucose concentra-

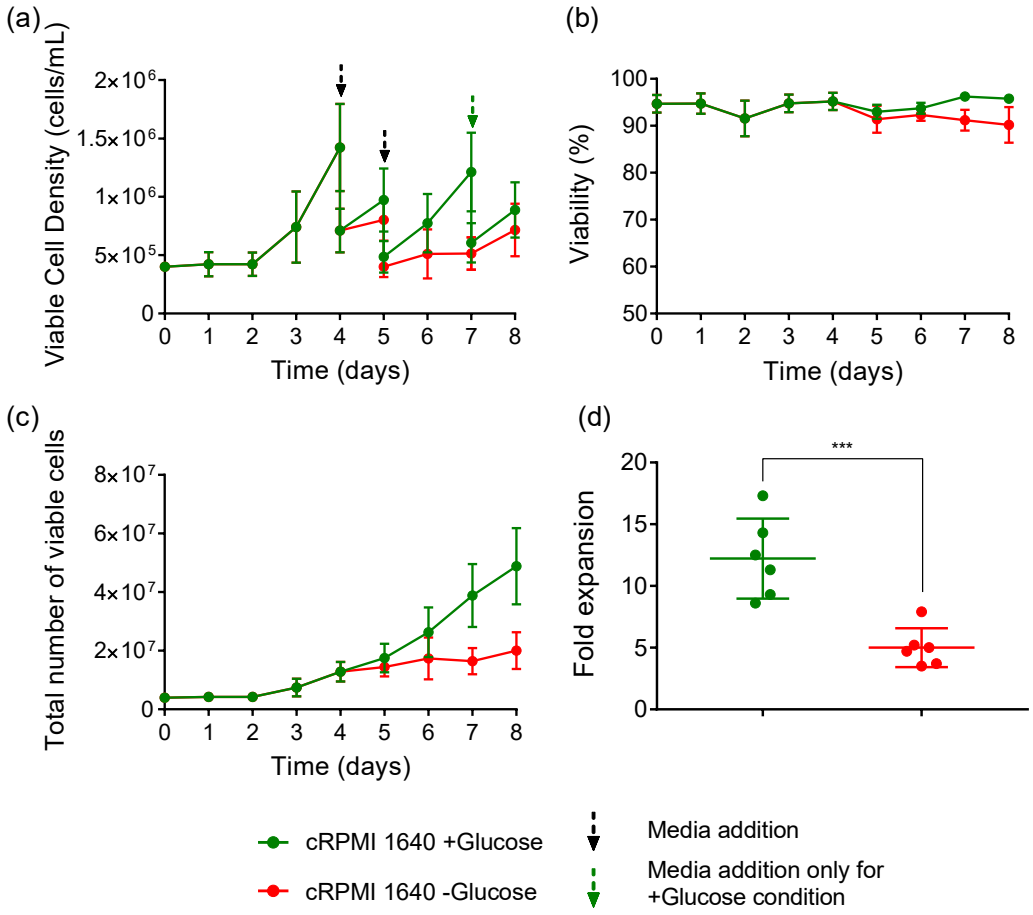

Figure 4.2: Viable cell density (a), viability (b), total number of viable cells (c) and fold expansion achieved after 8 days expansion (d) for CAR-T cells grown in complete medium with glucose (green, +glucose condition) and without glucose (red, -glucose condition) are shown. The black arrows indicate the medium addition for both conditions on day 4 and 5. The green arrow indicates the media addition only for the +glucose condition on day 7. Mean $\pm$ SD, 6 healthy donors are shown. Statistical comparison was performed using a two-tailed paired t-test.

tion of the lentivirus supernatant was 1.0 g/L, which is lower than cRPMI 1640 medium that the T cells were seeded in (1.68 g/L $\pm$ 0.01). The lactate, glutamine and ammonia levels of the lentivirus were 2.47, 0.44 and 0.024 g/L, respectively. Interestingly, during transduction period between day 1 and 2, no change in glucose, ammonia and lactate concentrations were observed. However, glutamine concentration decreased to 0.34 g/L $\pm$ 0.018 (Figure 4.3).

During the second half of the eight days culture period, the glucose concentration in the glucose deprivation condition was 0 g/L as expected. The glucose concentration in the control condition was ranging between 0.94 g/L and 0.18 g/L. This indicates that the feeding strategy was successfully providing enough glucose to prevent glucose limitation in the control condition. The lactate concentration in the glucose deprivation condition remained unchanged and was approximately 0.56 g/L between day 5 and 8, while it was ranging between 1.69 g/L to 0.65 g/L in the control condition. A decrease in glutamine concentration was observed in both conditions; however, glutamine levels were maintained between 0.1 g/L and 0.4 g/L in both control and glucose deprivation conditions. Ammonia concentration was steadily increasing in both glucose deprivation and control conditions. Ammonia levels increased to 0.021 g/L and 0.032 g/L on day 7 in the control condition and the glucose deprivation condition, respectively.

To further investigate the metabolite consumption and production per cell, metabolite concentrations were normalised to cell density throughout the post-transduction ex-

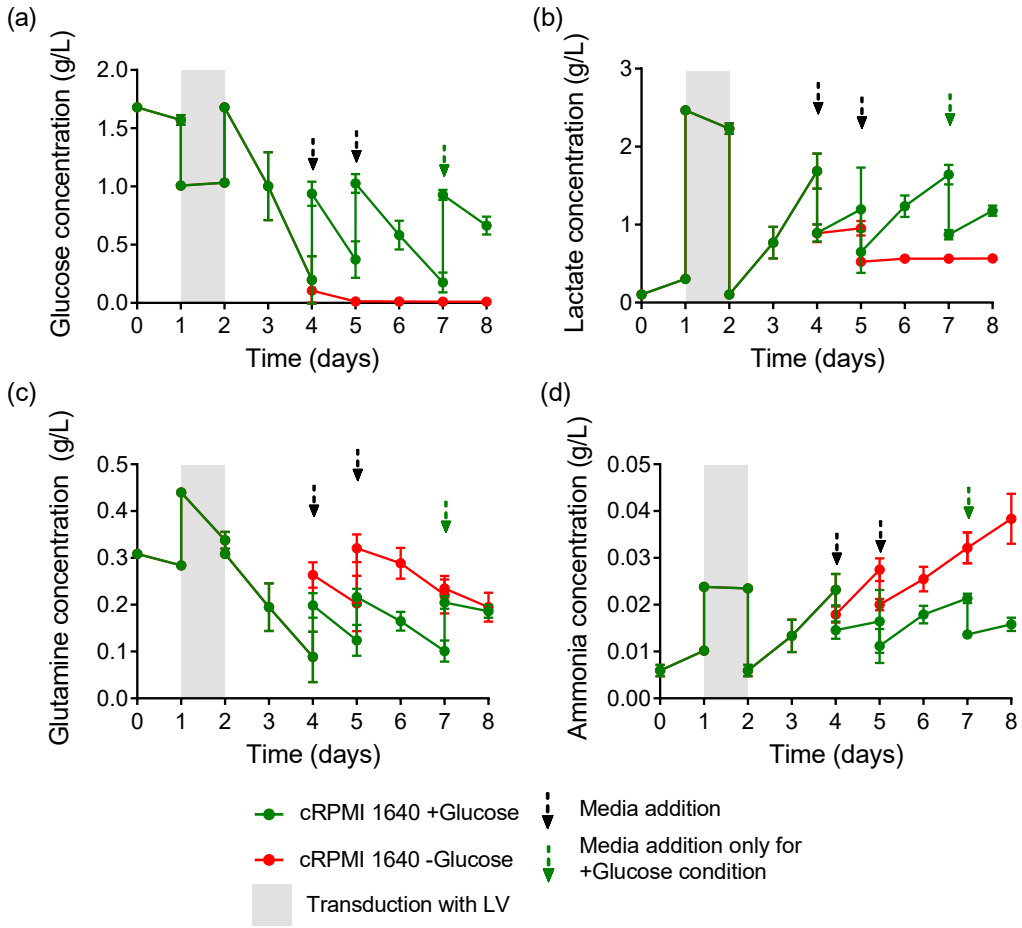

Figure 4.3: Glucose (a), lactate (b), glutamine (c) and ammonia concentrations measured in the cell culture medium throughout eight days expansion. The black arrows indicate the medium addition for both conditions on day 4 and 5. The green arrow indicates the media addition only for the +glucose condition on day 7. The grey area shows the transduction period with the lentiviral vector. Mean $\pm$ SD, 6 healthy donors are shown.

pansion period. Specific consumption and production rates during the transduction period were excluded due to loss of cells and yield in this step, mainly due to transferring and centrifuging cells multiple times.

Figure 4.4 shows glucose and glutamine specific consumption rates and lactate and ammonia specific production rates over the culture period after transduction for both conditions. The negative values indicate that the metabolites were produced by the T cells, whereas the positive values indicate the metabolites were consumed. As expected, glucose specific consumption rate in the glucose deprivation condition reached zero after feeding the cells with glucose-free medium on day 4. In the control condition, glucose consumption dropped after day 4 but remained steady around $\sim$500 pg.cell^{-1}.days^{-1} until the harvest day. Lactate specific production rates for both conditions decreased from day 3 to 5 in both conditions. The lactate specific production rate was approximately zero in glucose deprivation condition on day 5, While in the control condition, it reached to $\sim$-200 pg.cell^{-1}.days^{-1}. The control condition lactate production rate then increased on day 6 to $\sim$-700 pg.cell^{-1}.days^{-1} and then decreased to reach $\sim$-300 pg.cell^{-1}.days^{-1} on day 8 (Figure 4.4).

Glutamine consumption rate profile (Figure 4.4 (c)) shows steady decrease in glutamine consumption rate ($\sim$200 pg.cell^{-1}.days^{-1} to $\sim$60 pg.cell^{-1}.days^{-1} in average) from day 3 to 5 in both the conditions. Interestingly, glutamine specific consumption rate increased in the glucose deprivation condition to reach $\sim$120 pg.cell^{-1}.days^{-1} on

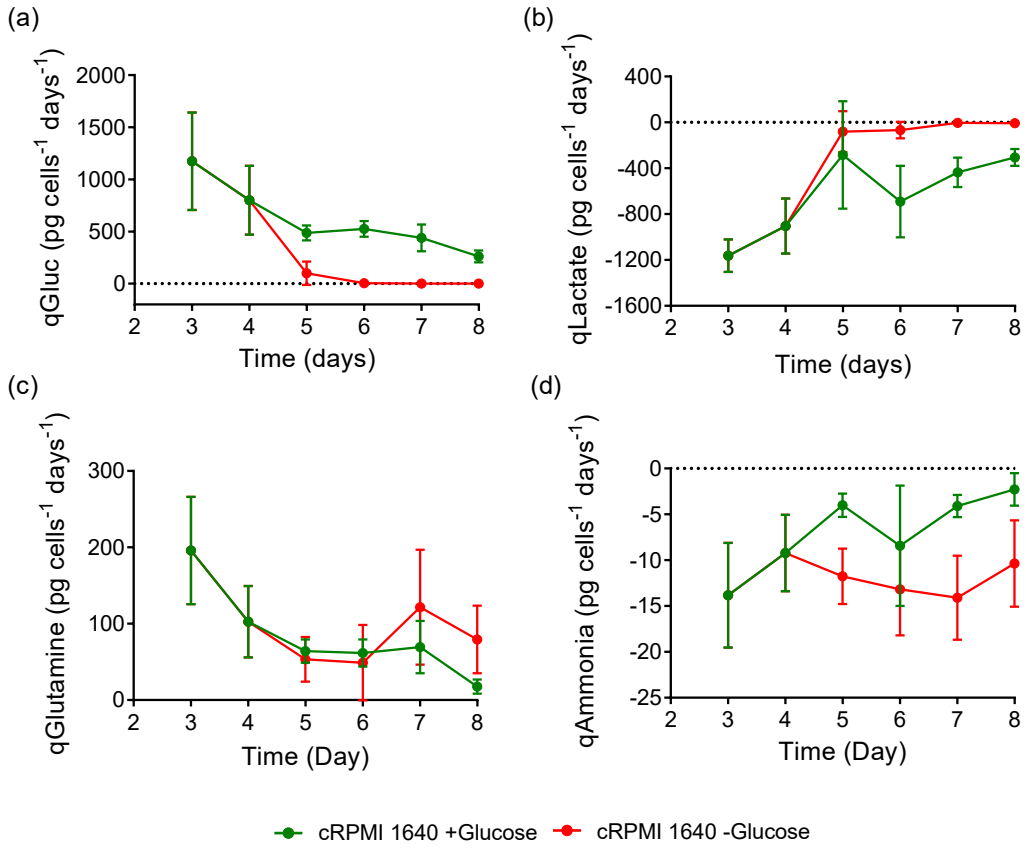

Figure 4.4: Specific glucose consumption rate (qGlucose) (a), specific lactate production rate (qLactate) (b), specific glutamine consumption rate (c) and ammonia production rate (d) in pg.cells^{-1}.days^{-1} for the control (green) and the glucose deprivation (red) conditions. Mean $\pm$ SD, 6 healthy donors are shown.

day 7 and $\sim$80 pg.cell^{-1}.days^{-1} on day 8, whereas, in the control condition, it decreased to reach $\sim$20 pg.cell^{-1}.days^{-1} on day 8. The ammonia production rate decreased for the standard condition from $\sim$-15 pg.cell^{-1}.days^{-1} on day 3 to $\sim$-5 pg.cell^{-1}.days^{-1} on day 5 and reached $\sim$-2 pg.cell^{-1}.days^{-1} on day 8. On the other hand, in the glucose deprivation condition, it remained in average around $\sim$-13 pg.cell^{-1}.days^{-1} between day 4 to 8.

To better understand the metabolite consumption and production rates during the glucose deprivation period, the average of consumption or production rates for each metabolite during the second half of expansion period (from day 4 to day 8) were calculated (Figure 4.5). The average glucose consumption and lactate production rates were significantly lower ($P < 0.001$) in the glucose deprivation condition compared to the standard condition. On the other hand, the glutamine consumption was rate was higher in the glucose deprivation condition but failed to achieve the significance difference ($P > 0.05$). The average of ammonia production rate, however, was significantly higher ($P < 0.01$) for T cells that were grown in the glucose-free medium compared to the control, indicating they were producing more ammonia per cell in the second half of the expansion period.

4.3.1.3 Immunophenotypic Analysis

In order to track phenotypic changes of CAR-T cells in both conditions, daily samples were taken and analysed by flow cytometry. Figure 4.6 (a,b) shows the change in percentages of CD4+ and CD8+ T cells. The average of CD4+ and CD8+ populations in the starting T cells were 69.2 $\pm$ 6.5 % and 22.7 $\pm$ 4.4 %, respectively. The fraction of CD4+ population slightly decreased in the first four days and reached 64.6 $\pm$ 7.6 % on day four, while the percentage of CD8+ cells increased and reached 30.0 $\pm$ 5.6 % on day four. In the second half of cell culture, a relatively higher percentage of CD4+ cells and a lower percentage of CD8+ cells were achieved in the glucose deprivation condi-

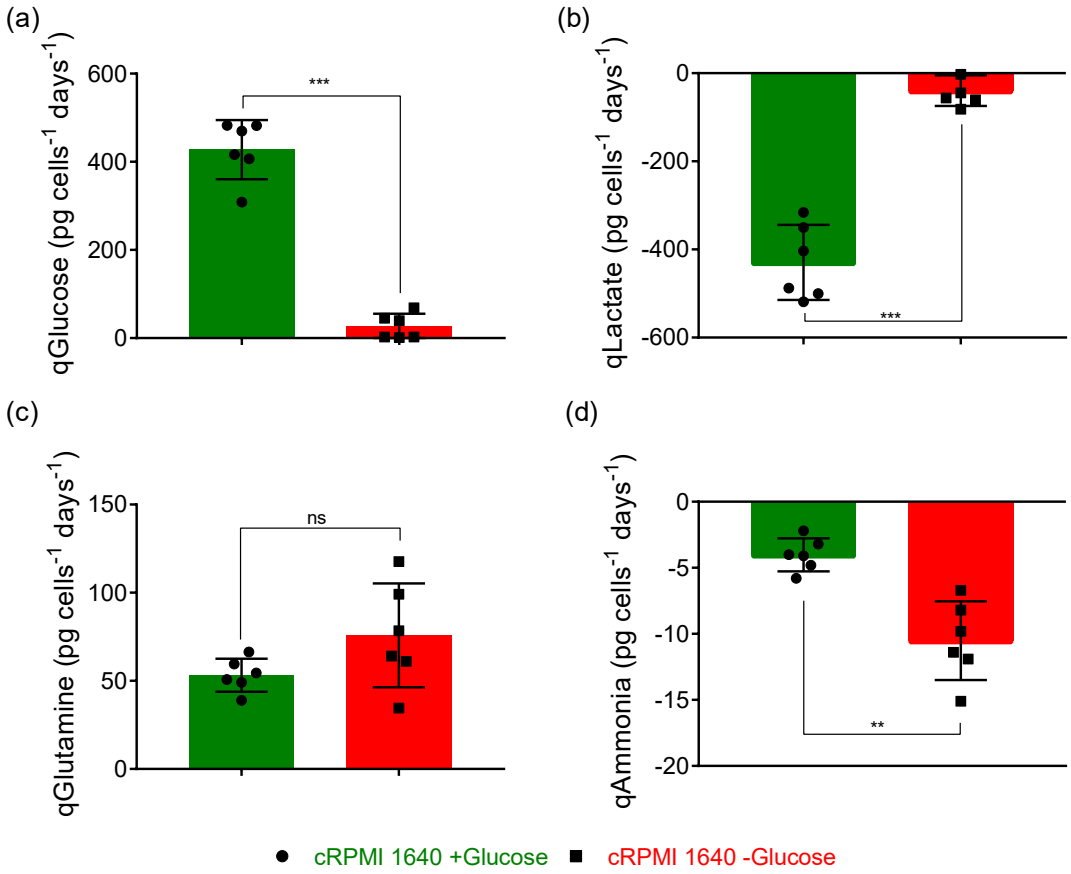

Figure 4.5: The average of specific glucose consumption rate (qGlucose) (a), specific lactate production rate (qLactate) (b), specific glutamine consumption rate (c) and ammonia production rate (d) in pg.cells^{-1}.days^{-1} for the control (green) and the glucose deprivation (red) conditions during the second half of culture period. Mean $\pm$ SD, 6 healthy donors are shown. Statistical comparisons were performed using two-tailed paired t-tests.

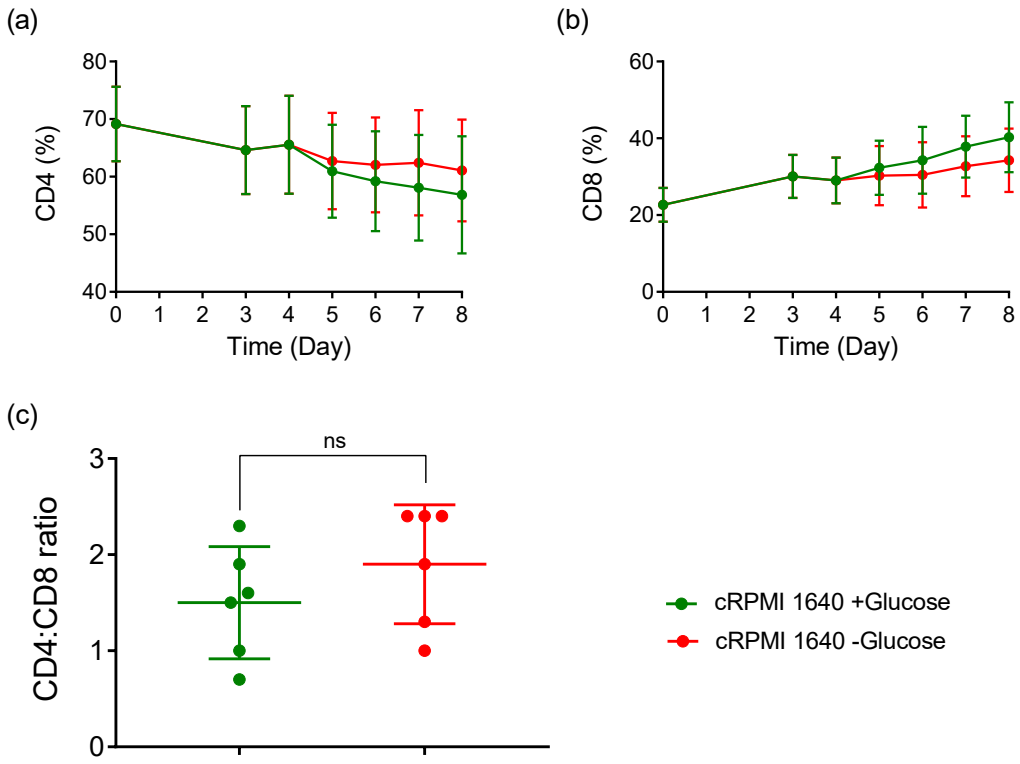

Figure 4.6: The percentages of CD4+ (a) and CD8+ (b) cells throughput the eight days expansion. CD4:CD8 ratio of T cells in the final products (c). Mean ± SD, 6 healthy donors are shown. Statistical comparisons were performed using two-tailed paired t-test.

tion, compared to the control condition. In the final T cell product grown under standard conditions, 56.9 ± 10.2 % of T cells were CD4+ cells, and 40.2 % ± 9.1 % were CD8+ cells. In comparison in the glucose deprivation condition, 61.1 ± 8.8 % of T cells were CD4+ cells, and 34.3 ± 8.3 % were CD8+ cells. This equivalent to CD4:CD8 ratio of 1.5 ± 0.6 for the control condition and 1.9 ± 0.6 for the glucose deprivation (Figure 4.6 (c)).

Figure 4.7 shows changes in percentage of each CD8+ subset throughout the expansion period. After the T cell activation, the percentage of T_N decreased from 51.2 ±

23.4% prior to the inoculation to 0.05 $\pm$ 0.04 % for the control condition and 0.11 % $\pm$ 0.01 for the glucose deprivation condition in the final product (Figure 4.8 (a) and 4.7 (a)). No significance difference was observed in the final proportion of CD8+ T_N cells in in the glucose deprivation condition compared to the control (Figure 4.8 (a)).

The proportion of CD8+ T_{CM} increased in the first half of the culture period from 16.5 $\pm$ 6.6 % in the starting material to 41.9 $\pm$ 5.6% on day three and 39.1 $\pm$ 3.8% on day four. After feeding with either standard cRPMI 1640 medium containing glucose or glucose-free medium, different trends in the proportion of CD8+ T_{CM} were observed. The proportion of CD8+ T_{CM} increased in the glucose deprivation condition to reach 90.4 $\pm$ 4.8 % on day eight. Whereas, in the control condition, the fraction of CD8+ T_{CM} cells remained unchanged in the final product compared to day 4. Statistical comparison showed that the proportion of CD8+ T_{CM} achieved in the glucose deprivation was significantly higher ($P < 0.001$) in the glucose deprivation condition (90.4 % $\pm$ 4.8 %) compared to the standard condition (45.1 $\pm$ 17.6 %) (Figure 4.8 (b)).

The fraction of CD8+ effector memory T cells (Figure 4.7 (c)) increased from 19.2 $\pm$ 12.0 % in the starting material to 54.9 $\pm$ 4.8% on day four. After feeding with glucose-free medium, the effector memory proportion of cytotoxic T cells dropped to 9.5 $\pm$ 4.8 % in the glucose deprivation condition, significantly lower ($P < 0.001$) than 54.8 $\pm$ 17.5 % achieved in the control condition (Figure 4.8 (c)).

Looking at the percentage of terminally effector T cells throughout the culture period

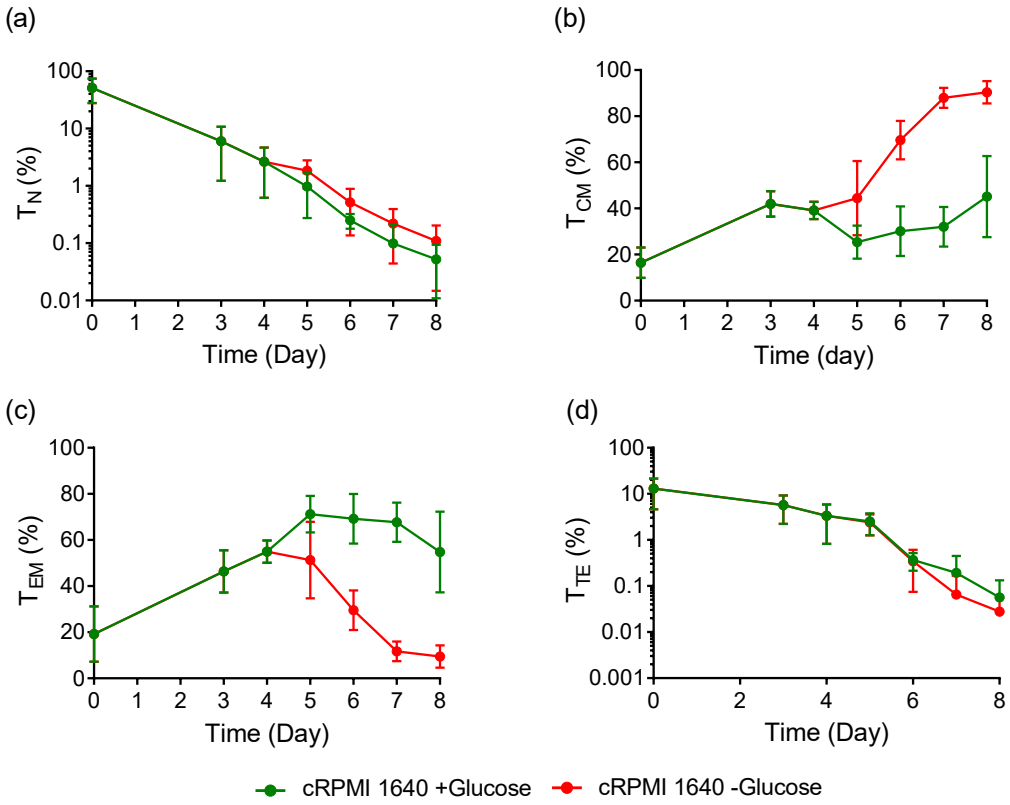

Figure 4.7: Phenotypic characterisation of CD8+ T cells in the glucose deprivation condition (red) compared with the control condition (green). a) percentage of CD8+ T naive cells, b) percentage of CD8+ T central memory cells, c) percentage of CD8+ T effector memory cells and d) percentage of CD8+ T terminally effector cells. Mean $\pm$ SD, 6 healthy donors are shown.

(Figure 4.7), a decrease in the fraction of T_{TE} was observed between day 0 to day 4. A similar trend was observed in the second half of the expansion period, where both the control and glucose deprivation conditions resulted in a decrease in the proportion of CD8+ T_{TE} cells.

Furthermore, to track how the number of each subset of cytotoxic cells has changed, the viable absolute number of each CD8+ subset was calculated throughout the culture period (Figure 4.9). A similar trend was observed in the total number of CD8+ T_N and

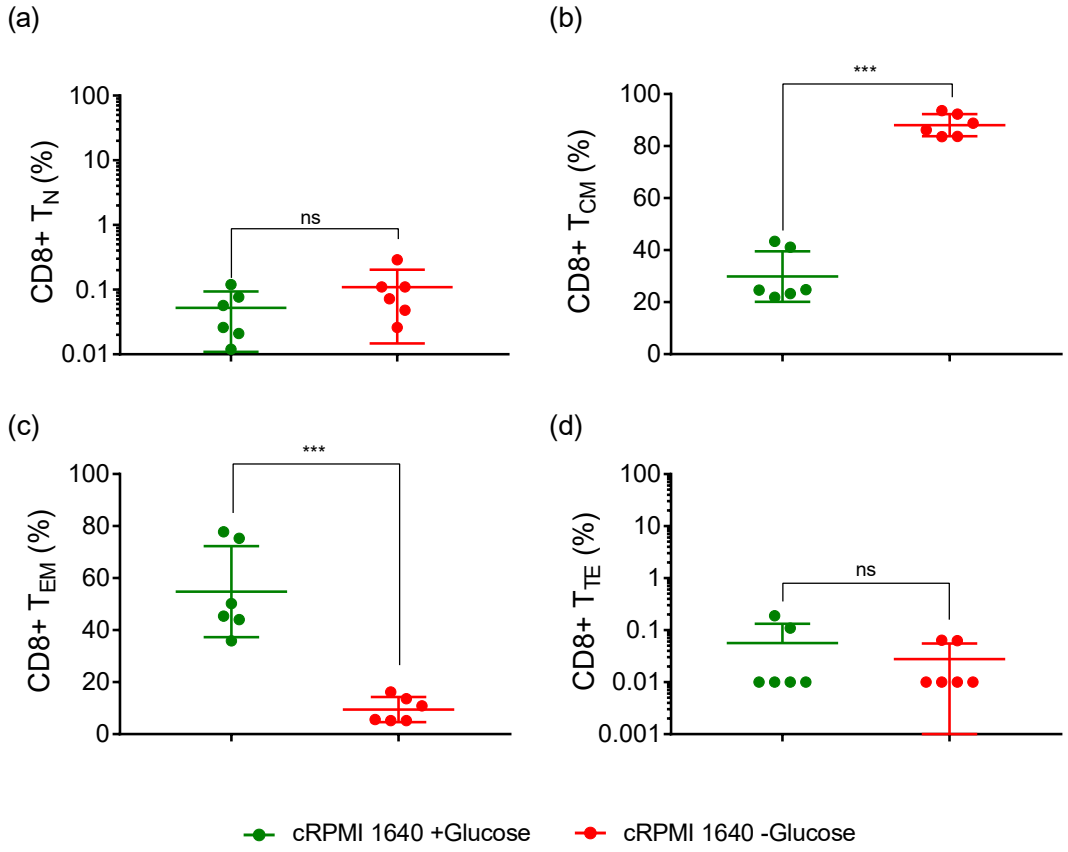

Figure 4.8: Phenotypic characterisation of CD8+ T cells on day eight in glucose deprivation condition compared with the control condition. Percentage of CD8+ subset a) T_N, b) T_{CM}, c) T_{EM} and d) T_{TE}. Mean $\pm$ SD, 6 healthy donors are shown. Statistical comparisons were performed using two-tailed paired t test.

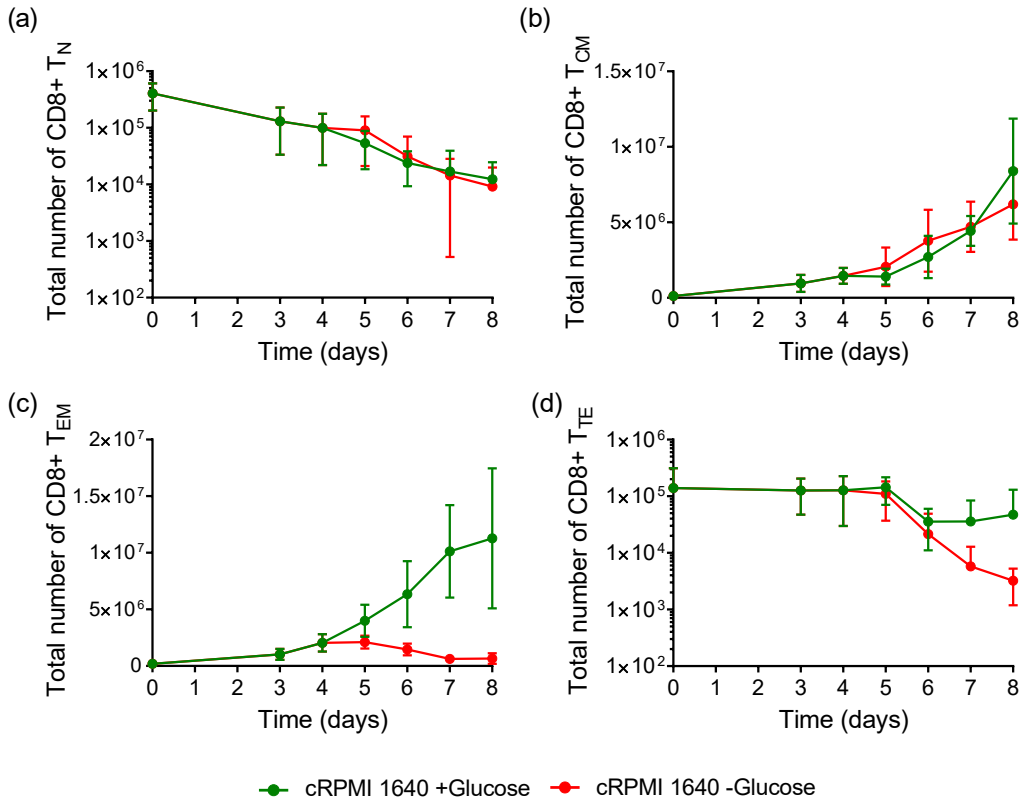

Figure 4.9: The absolute number of viable CD8+ T_N (a), T_{CM} (b), T_{EM} (c) and T_{TE} (d) throughout eight days expansion in the glucose deprivation condition (red) compared with the control (green) condition are shown. Mean $\pm$ SD, 6 healthy donors are shown.

CD8+ T_{CM} cells in both conditions. Interestingly, the total number of CD8+ T_{EM} cells (Figure 4.9 (c)) started to decline after feeding with glucose-free medium was started on day four. Whereas for the control condition, the total number of CD8+ T_{EM} continued to increase. Similarly, the total number of CD8+ T_{TE} cells started to drop after feeding with glucose-free medium. Therefore, it appears that the high percentage of CD8+ T_{CM} achieved on the last day of the culture period (Figure 4.8) was as a result of the decline in the total number of effector cells.

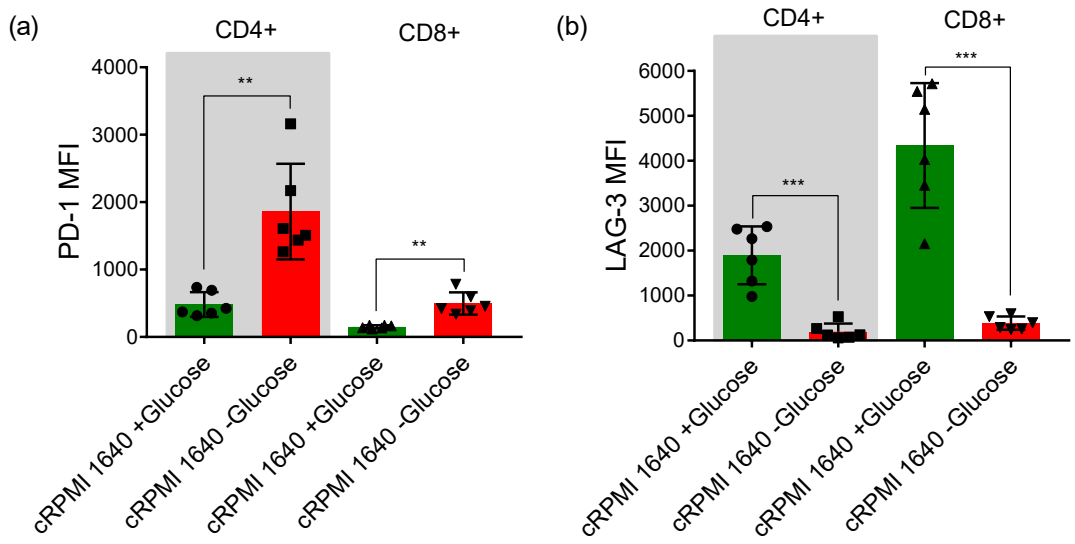

Figure 4.10: Expression of exhaustion markers PD1 (a) and LAG3 (b) on CD4+ and CD8+ T cells indicated with MFI in the glucose deprivation (red) and the control (green) conditions. Mean $\pm$ SD, 6 healthy donors are shown. Statistical comparisons were performed using two-tailed paired t-tests.

The expression of exhaustion markers, PD-1 and LAG-3, was also assessed on CD4+ ad CD8+ T cells at the end of the culture period (Figure 4.10). PD-1 expression shown as median fluorescence intensity (MFI) was significantly higher ($\mathrm{P} < 0.01$) in CD4+ T cells and CD8+ T cells in the glucose-free condition compared to the control condition. On the other hand, LAG-3 MFI was significantly higher ($\mathrm{P} < 0.001$) on CD4+ and CD8+ T cells cultured in the cRPMI 1640 medium containing glucose compared to glucose-deprived T cells.

Finally, the impact of glucose deprivation on expression of CAR was assessed. Although, during transduction period (day 1-2), the T cells from both conditions were exposed to the same level of glucose ($\sim$ 1g/L; Figure 4.3 (a)), the expression of Chimeric

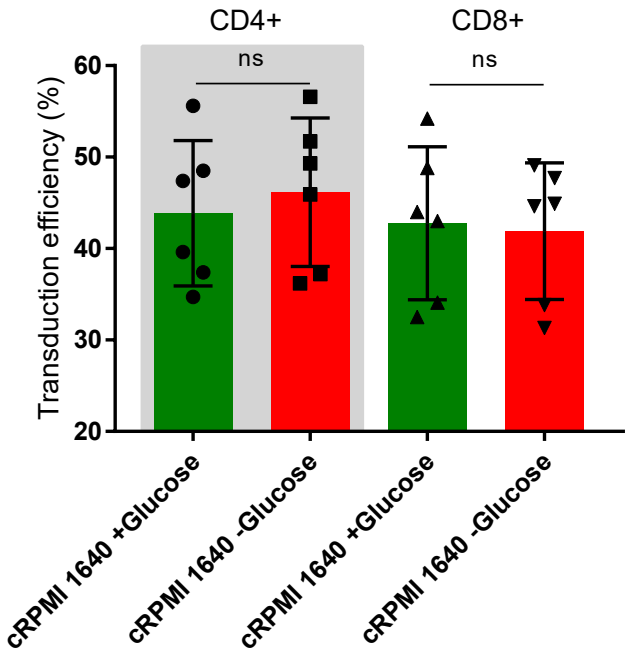

Figure 4.11: Transduction efficiency of CD4+ T cells (left) and CD8+ T cells (right) in both the control (green) and the glucose deprivation (red) conditions measured on final day of the culture period. Mean ± SD, 6 healthy donors are shown. Statistical comparisons were performed using two-tailed paired t tests.

Antigen Receptor might have been affected due to lack of glucose in the second half of the culture period. Figure 4.11 shows the transduction efficiency achieved on day eight on CD4+ and CD8+ T cells. The transduction efficiencies achieved in the control condition were 43.9 ± 7.9 % and 42.8 ± 8.4 % for CD4+ and CD8+ T cells, respectively. In the glucose deprivation condition, the transduction efficiencies were 46.2 ± 8.1 % and 41.9 ± 7.5 % for CD4+ and CD8+ T cells, respectively. The result collectively showed that glucose-free feeding does not affect the expression of CAR on T cells.

In summary, the immunophenotypic analysis in this section showed that during the glucose deprivation period in the 2-stage feeding method, CD8+ T_{EM} and T_{TE} cells stopped growing. This consequently resulted in a T_{CM}-enriched CAR-T product. Transduction and the CAR expression on T cells were unaffected in the 2-stage feeding

method. Conflicting results were observed on the effect of glucose deprivation on the level of exhaustion; a higher level of PD-1, but a lower level of LAG-3 were observed on CAR-T cells that were expanded using the 2-stage feeding regime.

4.3.2 Functionality of glucose-deprived T cells

We sought to assess functionality and persistence of the CD19-specific CAR-T cells generated in the glucose deprivation condition from different aspects; firstly, *in vitro* specific killing ability and cytokine secretion ability of the generated CAR-T cells against CD19-positive cancer cells were assessed. Then, the CAR-T cells proliferation capability upon exposure to CD19 antigen was evaluated. In this section, the CAR-T product generated with the 2-stage feeding using the glucose-free medium will be referred to as T_{CM}-enriched CAR-T product. Whereas, the CAR-T cells produced with the standard level of glucose will be referred to as the standard CAR-T product.

4.3.2.1 *In vitro* killing assay

The *in vitro* cytotoxicity of CAR-T cells against two target cell lines expressing the CD19 antigen, Raji and NALM6, were evaluated. Raji is a Burkitt's Lymphoma cell line, whereas, NALM6 is a CD19 positive acute lymphoblastic leukaemia (ALL) cell line. These two cell lines are commonly used to assess the cytotoxicity of immune cells such as Natural Killer cells (Yan et al., 1998), gamma delta T cells (Lamb et al., 2001), and currently commonly used to evaluate the anti-tumour activity of genetically

modified T cells such as CAR-T cells. There are different approaches for measuring *in vitro* cytotoxicity including, Chromium-51 release assay (Holden et al., 1977), lactate dehydrogenase (LDH) release assay (An et al., 2016) and flow cytometric based assays Zaritskaya et al., 2010; Kandarian et al., 2017. In this work, the flow cytometric bead assay was used to measure the absolute number of remaining live target cells after 48 hours co-culture with CAR-T cells at 1:1 effector to target ratio. This protocol was adapted from the protocol used in Stavrou et al. (2018) study. Further details about the protocol can be found in Section 2.4.2.

The CAR-T cells generated in the standard or glucose-free medium were composed of different percentages of transduced CAR-T cells, as shown in Figure 4.11. Therefore, in order to start with the similar percentage of transduction across different donors for the killing assay, transduced T cells were isolated after harvesting on day eight using Miltenyi CD34 magnetic beads, which select T cells expressing CAR containing the Q8/RQR8 domain. The standard cRPMI 1640 medium containing glucose was used for the killing assay to test both T_{CM}-enriched CAR-T product and the standard CAR-T product. Figure 4.12 shows the percentage of viable target cells remaining after 48 hours of the co-culture at 1:1 effector to target ratio. All data were normalised to the percentage of viable target cells remaining after co-culture with non-transduced T cells to exclude the background cytotoxicity of T cells from the results. Similar viable target cells remaining of 8.3 $\pm$ 2.9 % and 6.0 $\pm$ 0.6 % were achieved in the NALM6 killing

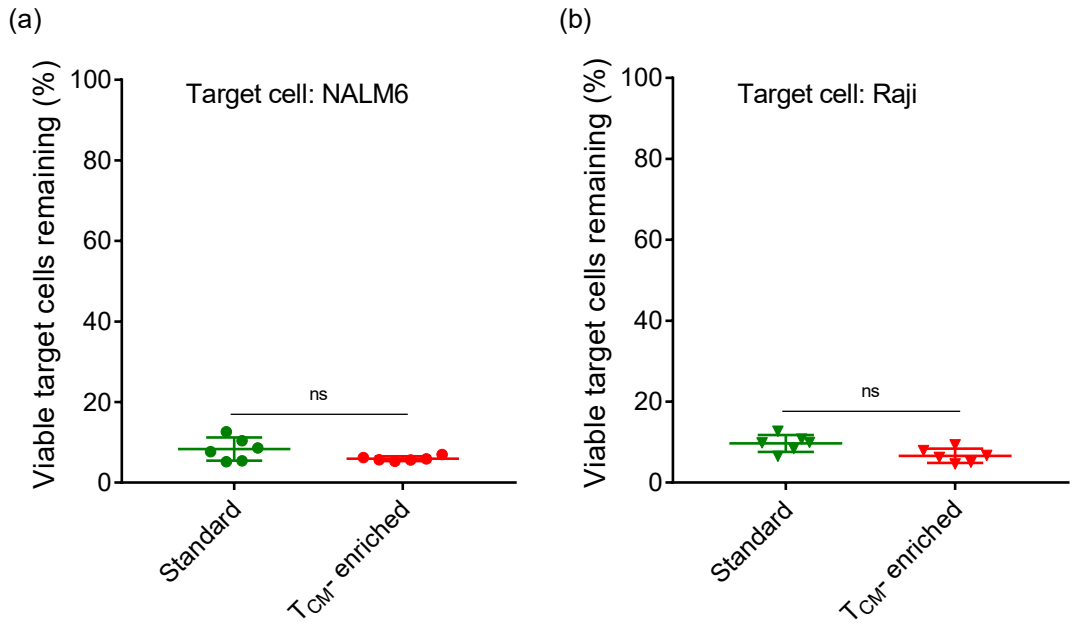

Figure 4.12: The percentages of viable remaining NALM6 (a) and Raji (b) after 48 hours co-culture with T_{CM}-enriched CAR-T product (red) or the standard CAR-T product (green). The cell killing was measured by the absolute number of live target cells remaining, identified with SYTOX™ Red staining and CountBright counting beads. Mean ± SD, 6 healthy donors are shown. The percentage calculated for each donor is an average of 3 technical replicates for *in vitro* killing assay. Statistical comparisons were performed using two-tailed paired t-tests.

assay for the standard and T_{CM}-enriched CAR-T products, respectively (Figure 4.12 (a)). Similarly, no significant difference was observed in the *in vitro* killing ability of both products against Raji cells (Figure 4.12 (b)). The results in this section suggested that the killing ability of the anti-CD19 CAR-T cells generated through the 2-stage feeding method was not impaired.

4.3.2.2 Cytokine secretion

To further analyse the potential impact of glucose deprivation on the functionality of CD4+ and CD8+ subsets, seven soluble cytokines were measured in the supernatant after 24 hours co-culture with the NALM6 target cells (Figure 4.13). The isolated CAR-T cells were co-cultured with the NALM6 cells at 1:1 effector to target ratio in the standard cRPMI 1640 media containing glucose. After 24 hours co-culture with cancer cells, the supernatant was used to measure multiple cytokines including, IFN-γ, TNF-α, and IL-2 using the Cytometric Bead Array assay(more details in Section 2.4.3 .

The seven cytokines measured in the supernatant are key cytokines produced by CD4+ subsets including T helper-1, T helper-2, T helper-17 and T_{reg} and cytotoxic T cells. The result showed that significantly lower ($P < 0.01$) level of IL-17A, a cytokine mainly produced by T helper-17 cells, was produced by T_{CM}-enriched CAR-T cells compared to the standard CAR-T product (Figure 4.13). Similar IFN-γ profile was observed in both conditions, whereas, significantly higher ($P < 0.001$) TNF-α, a cytokine associated with both T helper-1 and cytotoxic T cells, was produced by T_{CM}-enriched CAR-T cells. Comparing the level of IL-10, the main cytokine produced by regulatory T cells, between the two products showed that there was a significantly higher ($P < 0.01$) level of IL-10 in the supernatant of T_{CM}-enriched CAR-T cells. The concentration of IL-4, produced by T helper-2 cells, was also significantly lower ($P < 0.001$) in the co-culture supernatant of CAR-T cells produced in the glucose deprivation condition com-

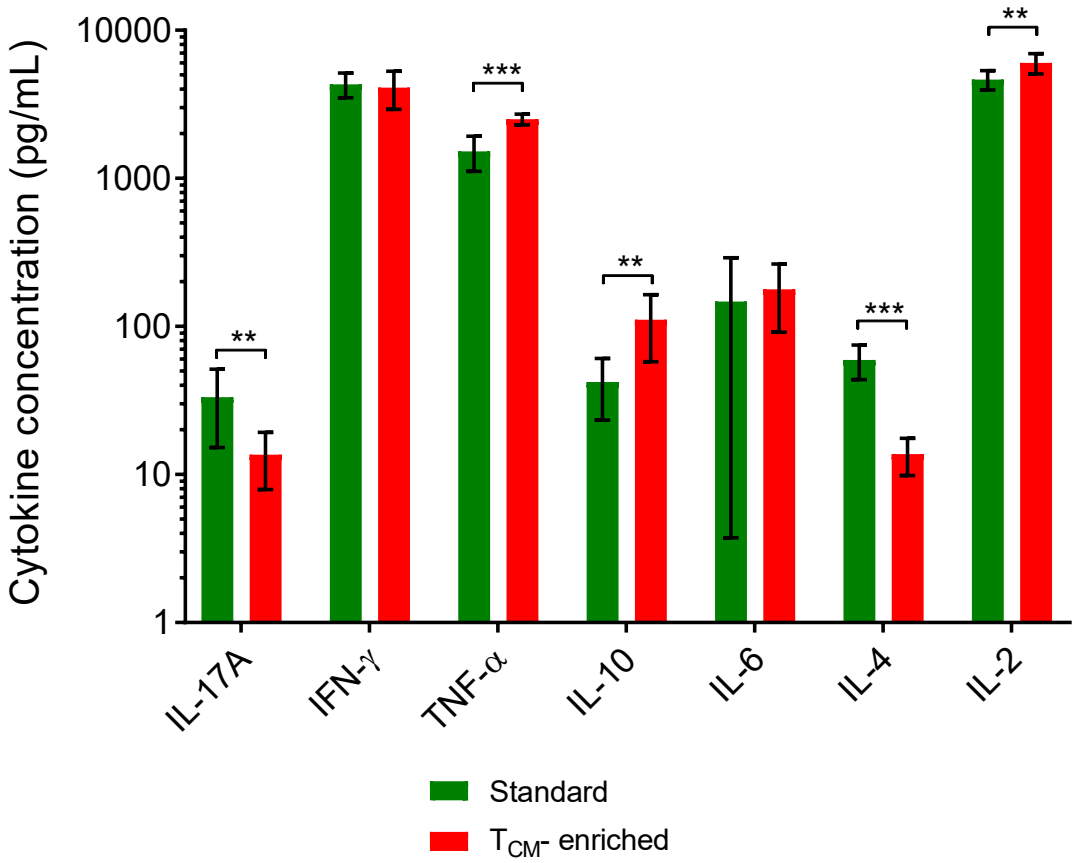

Figure 4.13: Concentration of different cytokines (IL-17A, IFN-γ, TNF-α, IL-10, IL-6, IL-4 and IL-2) in the supernatant of CAR-T cells after 24 hours co-culture with NALM6 CD19 positive cells. Mean $\pm$ SD, 4 healthy donors are shown. Statistical comparisons were performed using two-tailed paired t tests.

pared to the control. Finally, T_{CM}-enriched CAR-T cells produced significantly higher ($P < 0.01$) level of IL-2 cytokine compared to the standard CAR-T cells. To summarise, T_{CM}-enriched cells generated from glucose deprivation condition produced higher level of TNF-α, IL-10 and IL-2 than the standard CAR-T product (Figure 4.13).

4.3.2.3 Proliferation assay

In order to assess the proliferation, longevity and re-stimulation capabilities of T cells generated in different conditions, a proliferation assay was designed and performed. The isolated CAR-T cells were co-cultured at 1:1 effector to target ratio with CD19-positive NALM6 cells for six days. After three and six days of co-culture, a sample was taken and analysed via flow cytometry to identify and measure the density of CAR-T cells. More details about the proliferation assay could be found in Section 2.4.4. The visual summary of the proliferation assay is shown in Figure 4.14. After six days of co-culture, CAR-T cells were isolated with CD3+ isolation kit and the proliferation assay was repeated two more times. In the first stimulation, the fold expansion achieved for the T_{CM}-enriched CAR-T cells was 3.9 $\pm$ 1.5 for day three and 13.25 $\pm$ 5.1 for day six (Figure 4.15 (a)). These were significantly higher ($P < 0.05$) than the fold expansion achieved in the standard CAR-T products, where the 1.0 $\pm$ 0.3 fold expansion was achieved on day three, and 4.6 $\pm$ 1.9 fold expansion was achieved on day six. During the second re-stimulation assay (Figure 4.15 (b)), the T_{CM}-enriched CAR-T cells showed better proliferation capability compared to the control. On day three and six 2.8 $\pm$ 1.2 and 3.6 $\pm$ 1.4 fold expansion were achieved for the T_{CM}-enriched CAR-T cells compared to 1.6 $\pm$ 0.7 and 3.1 $\pm$ 1.5 for the standard CAR-T products. In the third re-stimulation assay (Figure 4.15 (c)), 0.3 $\pm$ 0.2 and 1.4 $\pm$ 0.9 fold expansion were achieved in the T_{CM}-enriched CAR-T cells on day three and six respectively, compared

to 0.4 $\pm$ 0.1 and 1.7 $\pm$ 1.0 fold expansion in the control condition.

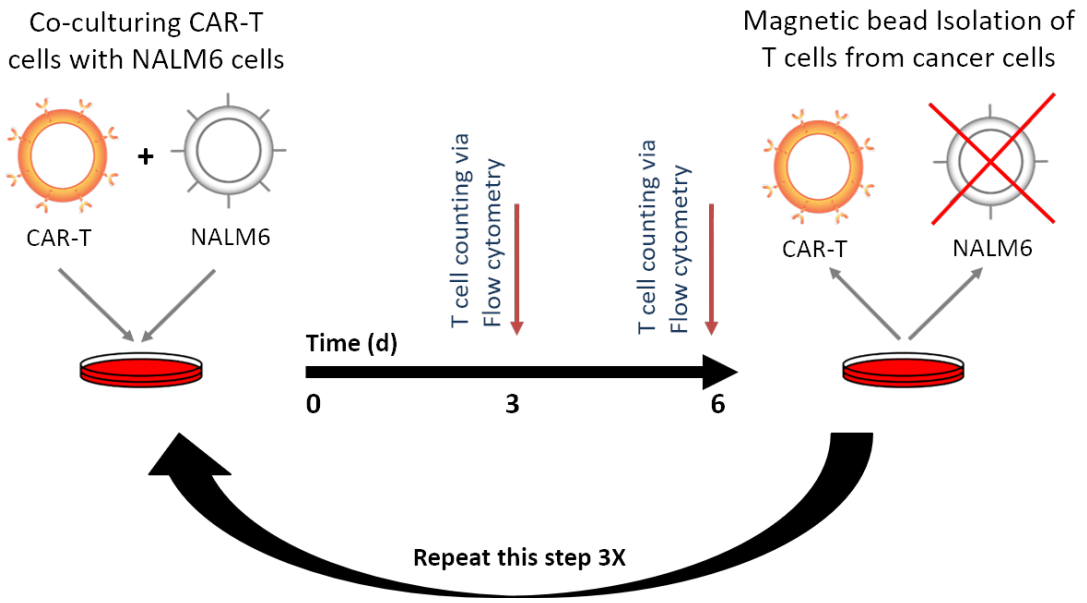

Figure 4.14: The schema shows the methodology used during the re-stimulation assay. Isolated CAR-T cells were co-cultured with CD19-positive NALM6 cells at 1:1 effector to target ratio for 6 days. The CAR-T cells fold expansion was measured on day 3 and 6, using anti-CD3 antibody and CountBright counting beads. CAR-T cells were then isolated from NALM6 cells and co-cultured again with NALM6 cells. This process was repeated three times.

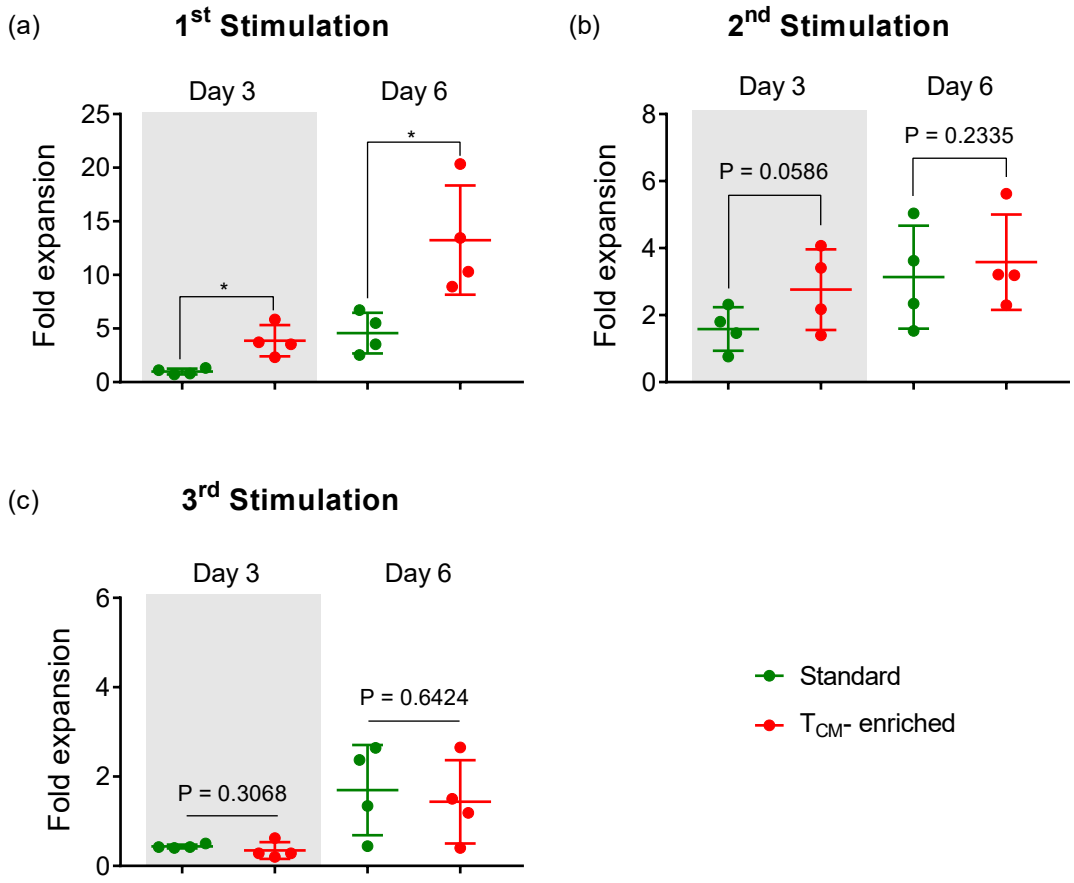

Figure 4.15: The fold expansion of CAR-T cells after the first stimulation (a), the second stimulation (b) and the third stimulation (c). Mean ± SD, 4 healthy donors are shown. The fold expansion calculated for each donor is an average of 4 technical replicates. Statistical comparisons were performed using two-tailed paired t-tests.

4.4 Discussion

Limiting the level of glucose and other metabolites such as glutamine have been used previously in the bioprocessing field to improve CHO cell culture performance (Cruz et al., 1999; Gagnon et al., 2011; Wong et al., 2005). Pre-conditioning cells before transplantation using different type environment and metabolites in various cell therapies such as with Mesenchymal Stem cells is another approach that has been used to improve the *in vivo* longevity of the cells (Moya et al., 2017; Salazar-Noratto et al., 2020). In adoptive T cell therapy, strategies such as modulating T cell metabolic balance or T cell development through chemical inhibitors such as Akt inhibitors have been suggested and successfully demonstrated (reviewed in Section 1.4.3).

4.4.1 Glucose deprivation enriches for central memory T cells

In this chapter, we adapted the 2-stage feeding strategy developed in Chapter 3 to a feeding strategy suitable for CAR-T therapy manufacturing. The new feeding regime switches from the glucose-containing medium to the glucose-free medium on day four. Therefore, early steps of the manufacturing, including, cell activation with Dynabeads and transduction with the lentiviral vector were performed in the presence of glucose. After starting glucose-free media feeding, multiple events were observed; 1) the total number of viable cells and viability declined compared the control (Figure 4.2), 2) the percentage of T_{CM} cells increased, 3) the percentage of T_{EM} cells declined. Ultimately,

these events led to similar observations as in chapter 3, where T cells generated through the 2-stage feeding approach were highly enriched with T_{CM} cells.

There were two potential explanations discussed in the previous chapter; 1) glucose deprivation resulted in increased growth and formation of T_{CM} cells, or 2) glucose deprivation limited the formation and growth of other subsets but T_{CM}. From comparing the absolute number of each subset (Figure 4.9), it was clear that CD8+ T_{EM} cells stopped growing and potentially died when glucose-free feeding started. Similarly, a drop in the absolute number of CD8+ T_{TE} was observed during the glucose deprivation period. The absolute number of CD8+ T_{CM} and T_N followed a similar trend in both control and glucose deprivation conditions. Altogether these data suggest that glucose deprivation resulted in CAR-T product enriched with memory cells by limiting the growth of effector cells, evident by the decline in the number of CD8+ T_{EM} and T_{TE} cells (Figure 4.9).

Regarding CD4:CD8 ratio, in the previous chapter, we observed an increase in CD4:CD8 ratio when T cells were cultured in glucose deprivation. However, similar CD4:CD8 ratio was observed when the 2-stage feeding regime was used. Similarly, there was no significant difference between CD4:CD8 ratio (Figure 4.6) in the final CAR-T cells produced with the 2-stage feeding strategy compared to the control. However, a change in the trend of CD4+ (%) and CD8+ (%) was observed; during glucose deprivation period, the percentage of CD4+ cells increased slightly, whereas the per-

centage of CD8+ cells decreased. Therefore, with a similar trend potentially this can result in a significant difference in CD4:CD8 ratio in CAR-T processes longer than eight days. As discussed in Section 3.5.1, the likely explanation for this trend is that CD4+ T cells have higher metabolic plasticity than CD8+ T cells and can use their greater mitochondrial content and spare respiratory capacity to generate ATP to compensate the lack of glucose in the medium (Cao et al., 2014).

The concentrations of glucose, lactate, glutamine and ammonia were also monitored during the CAR-T expansion (Figure 4.3). No glucose and glutamine exhaustion throughout the eight days expansion was observed in the control condition, indicating that the feeding strategy used in this experiment was not limiting in terms of glucose and glutamine delivery to CAR-T cells. In order to understand the metabolite intake or waste metabolites production at the cellular level, glucose, glutamine, lactate and ammonia concentrations were normalised to cell number (Figure 4.4 and 4.5). The specific glucose consumption and lactate production rates were at the highest on day 3. This is called the ”Warburg” phenomenon, in which T cells preferentially use glycolysis upon activation and channel glucose-driven pyruvate to lactate production (Warburg, 1956; MacIver et al., 2013).

The specific consumption of glucose dropped to zero during the glucose deprivation period, since no glucose was available for T cells to consume. Similarly, the specific production of lactate also dropped to zero. These data collectively suggest limited or no

glycolytic activity during the glucose-free period and limited conversion of pyruvate to lactate.

The glutamine consumption rate initially (day 4-6) followed the same downward trend in both the glucose deprivation and the control conditions. However, between day 6-8, the glutamine consumption rate increased in the glucose deprivation condition. The difference in glutamine consumption rate was also reflected in the average glutamine consumption rate between day 4-8 (Figure 4.5); however, it did not reach statistical significance. Interestingly, the ammonia specific production rate was significantly higher during the glucose deprivation period (Figure 4.5). Glutamine is an essential amino acid, and a nitrogen and energy source for proliferating T cells and its uptake and metabolism has been shown to be critical for T cell function (Newsholme et al., 1985; Kenneth A Frauwirth et al., 2002b; Carr et al., 2010). Ammonia is mainly generated by nitrogen-based molecules catabolism such as amino acids and particularly by glutamine catabolism through glutaminase pathway (DeBerardinis et al., 2008). In the previous chapter, it was discussed that in the absence of glucose, T cells could utilise pyruvate, fatty acids and glutamine to fuel OXPHOS. It is evident from the presented results that during glucose deprivation glutamine consumption and ammonia production are higher per cell, suggesting that glucose-deprived T cells were consuming glutamine and potentially supplemented sodium pyruvate to fuel OXPHOS and to generate energy. Wellen et al. (2010) reported that depleting extracellular glucose results in disruption of the

hexosamine pathway and consequently reduces the glutamine uptake in IL-3-dependent cells such as hematopoietic cells. However, this effect was not observed in this study, likely due to the fact that interleukin-3 receptor, CD123, is absent on T cells and is predominantly restricted to cells of the myeloid lineage (Sato et al., 1993; Wellen et al., 2010).

4.4.2 Functionality of central memory enriched CAR-T cells

4.4.2.1 Transduction

The transduction efficiency was assessed to determine whether the 2-stage feeding strategy with glucose-free media is feasible for CAR-T cell manufacturing. The first period (four days) of CAR-T expansion, including the transduction step, was exactly the same in both control and glucose deprivation conditions. Therefore no impact from glucose derivation on transduction efficiency was expected. The results clearly confirmed this; the glucose deprivation condition did not affect CAR expression on CD4+ and CD8+ T cells, indicating that four days of glucose deprivation did not negatively affect CAR transgene expression or resulted in CAR shedding on T cells. Further studies are required to verify this data with patient cells. However, it can be argued, that since the transduction step in both conditions was performed in the medium containing glucose, no difference should be expected in future studies using patients cells.

4.4.2.2 Exhaustion

T cell exhaustion is a term used for T cell dysfunction due to chronic infections or cancer (Zajac et al., 1998). T cell exhaustion is characterised with T cell inability to produce inflammatory cytokines such as TNF-α, IL-2, IFN-γ, reduced proliferative capability and longevity (Barber et al., 2006; Blank et al., 2007; C. Wang et al., 2017). Different regulatory markers including Programmed cell death protein 1 (PD-1), Lymphocyte activation gene-3 (LAG-3), T cell immunoglobulin mucin-3 (TIM-3) are reported to have key roles in exhaustion and are associated with T cell exhaustion. For cancer treatment, various studies reported that dysfunctional CD8+ T cells *in vivo* express these markers (Chauvin et al., 2015; C. Wang et al., 2017). Therefore, their expression is being used in various studies as an indicator of T cell exhaustion in manufacturing (Bajgain et al., 2014; Mock et al., 2016; Alnabhan et al., 2018). This is particularly evident in the Fraietta et al. (2018) study, where it was demonstrated that the CAR-T therapies that resulted in complete remission for treating Chronic Lymphocytic Leukemia (CLL) were expressing significantly lower amount of LAG-3 and PD-1 markers on their CD8+ T cells, compared to partial or no remission.

The expression of PD-1, a key negative regulator of T cells, was assessed at the end of the CAR-T expansion in this study. The data indicate that both CD4+ and CD8+ populations of T cells exposed to the glucose-free medium are exhausted based on PD-1 expression (Figure 4.10). A similar observation was shown by Chang et al. (2013)

in his study, in which it was found that PD-1 expression was directly affected by the cellular metabolism of the T cells. Chang et al. (2013) demonstrated that suppressing aerobic glycolysis by glucose deprivation increases PD-1 expression. However, PD-1 expression was relatively lowered and the ability of CD4+ T cells to produce IFN-γ was reversed, when the cells were cultured in glucose-containing medium. A similar explanation applies to the data presented in this chapter; the elevated PD-1 expression observed in glucose-deprived T cells is likely due to a change in their metabolic status, rather than exhaustion driven by chronic stimulation of T cells Barber et al. (2006). Chang et al. (2013) data suggested that the exhaustion is reversible when T cells are stimulated in normal glucose environment, similar to the *in vivo* conditions. Therefore, glucose deprivation driven exhaustion in CAR-T cells would likely be reversed when they are re-stimulated by cancer cells in the body in the presence of glucose.

To further verify the exhaustion status of T cells, LAG-3 expression was also assessed. LAG-3 is another inhibitory receptor found both on CD4+ and CD8+ T cells, which regulates IFN-γ production and cell proliferation (Workman et al., 2003; Workman et al., 2004). Contrary to PD-1 expression, LAG-3 expression was significantly lower on glucose-deprived T cells, indicating less exhaustion of glucose-deprived CAR-T cells (Figure 4.10). Macon-Lemaitre et al. (2005) demonstrated that LAG-3 signalling inhibits activation and expansion of both CD4+ and CD8+ T cells. High expression of LAG-3 on CAR-T cells cultured with glucose is potentially the inhibitory response of

T cells to activation and expansion. Whereas, in glucose-deprived CAR-T cells, lack of glucose already suppressed the activation and proliferation of T cells. Scharping et al. (2016) also reported that there is an inverse correlation between mitochondrial mass, mitochondrial activity and LAG-3 expression in tumour infiltrating T cells. This could be seen in this study, where CAR-T cells generated in glucose deprivation condition were highly enriched in central memory cells, known to have higher mitochondrial content (Windt et al., 2013). Moreover, T cells that were expressing LAG-3 had high glucose intake relative to LAG-3 negative T cells, similar to our study where glucose availability for T cells was correlated with LAG-3 expression. PD-1 and LAG-3 expression in this study was used as an indicator for the function of CAR-T cells. Further studies are required to investigate the contradictory results in PD-1 and LAG-3 expression and the underlying mechanism, which is out of the scope of this thesis. However, further investigations were performed to examine the function and proliferative capability of T_{CM}-enriched CAR-T cells generated with the 2-stage feeding regime.

4.4.2.3 *In vitro* cytotoxicity

The *in vitro* killing capability of CAR-T cells was assessed and verified with two CD19+ cell lines, NALM6 and Raji (Figure 4.12). The *in vitro* killing assay must resemble the *in vivo* condition, where the killing of cancer cells will occur, hence the medium with glucose was used for the duration of co-culture. No significant difference was observed in the short-term killing capability of the T_{CM} enriched CAR-T cells compared

to the standard CAR-T cells, indicating that killing ability was unaffected by glucose restriction.

To further characterise the functionality of CAR-T cells during *in vitro* killing assay, the soluble cytokines were measured in the supernatant after 24 hours of the co-culture with NALM6 cells (Figure 4.13). Understanding the cytokines profile of CAR-T cells also helps to understand more about the function of helper (CD4+) T cells, which compose more than 50% of the final product. IL-2, IFN-γ and TNF-α are produced by both CD4+ T helper-1 (Th-1) cells and CD8+ T cells upon activation. The Th-1 subset has been demonstrated to have superior anti-tumour efficacy compared to other CD4+ T cells (Nishimura et al., 2000). Therefore, its cytokines are commonly used to evaluate the *in vitro* efficacy of CAR-T cells. Despite having a high number of effector cells in standard CAR-T cells, and a higher level of PD-1 marker on glucose-deprived CAR-T cells, the effector cytokines IL-2, IFN-γ and TNF-α were similar or higher in T_{CM} enriched CAR-T cells . This indicates that the T_{CM} cells in the T_{CM} enriched CAR-T product were activated by the CD19 protein on the target cells and gained effector functions.

IL-17A and IL-4 were produced at a significantly higher level by standard CAR-T cells compared to T_{CM} enriched CAR-T cells. IL-4 is a cytokine produced mainly by T helper-2 (Th-2) T cells and plays a key role in the differentiation of naive T helper cells to Th-2 cells. Th-2 cells produce inhibitory cytokines such as IL-5 and IL-13 (Seder

et al., 1992; Golubovskaya et al., 2016). Activated T cells also express IL-4 receptor, allowing IL-4 to promote proliferation in both CD4+ and CD8+ T cells (Mitchell et al., 1989). There are suggestions that endogenous IL-4 produced by cancer cells or by T cells protect cancer cells from apoptosis (Conticello et al., 2004; Todaro et al., 2008; Yuzhalin et al., 2014), hence unfavourable for cancer immunotherapy. In contradiction, exogenous IL-4 has shown to have anti-tumour activity in several studies (Eguchi et al., 2005; Post et al., 2007; Wilkie et al., 2010). To our knowledge, although IL-4 secretion was observed in CD19 specific CAR-T cell activation (Xue et al., 2017), no positive anti-tumour effect has been associated with higher IL-4 secretion for CAR-T therapy.

Physiologically, IL-17A, the main cytokine produced by T helper-17 (Th-17), is thought to be a pro-inflammatory which plays an important role in immunity against infection, by engaging neutrophils and macrophages to infected tissues (Denman, 1992). Regarding cancer therapy, there are pieces of evidence that Th-7 cells and IL-17A improve anti-tumour activity against melanoma *in vivo* (Muranski et al., 2015). In contrast, IL-17A, IL-6 and IL-23 have been associated with impairing immune surveillance by CD8+ T cells (Tartour et al., 1999; Yu et al., 2007). Majchrzak et al. (2016) argued that the benefits of lymphocytes that produce IL-17A outweighs the negative impact and suggested the potential application of Th-17 cells for cellular cancer therapies. However, there is no direct correlation between the clinical efficacy of CAR-T therapies and the level of IL-17A secretion from CAR-T cells.

A significantly higher concentration of IL-10 was found in T_{CM} enriched CAR-T cells during the *in vitro* killing assay. CD4+ T_{reg} cells, the main producer of IL-10, are well characterised in terms of their immunosuppressive function on both CD4+ and CD8+ T cells (Thornton et al., 1998; Antony et al., 2005). The presence of T-reg cells showed to prevent effective immunotherapy treatment (Antony et al., 2005; Kofler et al., 2011). Although T-reg cells in the context of this study are considered immunosuppressive and potentially not favourable for cancer immunotherapies such melanoma or acute lymphoblastic leukaemia, their application for cellular therapy of autoimmune diseases are demonstrated as explained in Section 1.2.3.

In summary, the differences in concentrations of different cytokines likely reflect the difference in the frequency of CD4+ and CD8+ T cells and their subsets in standard CAR-T product compared to T_{CM} enriched CAR-T. The observation on lower concentrations of IL-4 and IL-17A were an indicator of a possibly lower number of Th-2 and Th-17 CD4+ T cells in the glucose-deprived CAR-T cells. This is potentially due to suppression of glycolysis as the result of glucose deprivation, which suppresses the differentiation and proliferation of T helper cells such as Th-1, Th-2, Th-17 (Shi et al., 2011; Wei et al., 2017). On the other hand, T-reg cells are more dependent on lipid metabolism and have a low level of glut1 (Pearce et al., 2013b); therefore, glucose deprivation provided a more suitable environment for T-reg cells and potentially resulted in selective expansion of T-reg cells compared to other helper cells.

Overall, T_{CM} enriched CAR-T cells generated through the 2-stage feeding regime surprisingly produced higher cytokines associated with the effector function of T cells and Th-1 phenotype compared to the standard CAR-T cells. Although, both standard and T_{CM} enriched CAR-T cells produced cytokines associated with T-reg, Th-2 and Th-17 cells, the concentrations of these cytokines were logarithmically lower relative to the effector cytokines and similar to other CD19-specific CAR-T studies such as Mock et al. (2016) and Sabatino et al. (2016). The results, therefore, indicated that glucose-deprived CAR-T cells are capable of producing different cytokines when stimulated in a glucose containing environment. However, the high level of IL-10 secretion from the T_{CM} enriched CAR-T requires further investigation and characterisation.

4.4.2.4 Proliferative capacity

The proliferative capacity and the persistence of generated CAR-T cells were examined (Figure 4.15). The method used in this study was *in vitro* serial re-stimulation of the CAR-T cells with the CD19-positive NALM6 cells. T_{CM} enriched CAR-T cells demonstrated improved proliferative response upon the first stimulation. The proliferative capacity continued to be higher for T_{CM} enriched CAR-T cells in the second stimulation. However, in the third stimulation, similar expansion capacity was observed in both conditions. The expansion capacity of T cells is a key contributor to the successful tumour eradication and is directly associated with their differentiation identity. Gattinoni et al. (2005) and Hinrichs et al. (2009) demonstrated that T cell products enriched in central

memory cells, characterised with high levels of lymphoid-homing molecules such as CCR7, CD62L and CD27 resulted in an improved *in vivo* anti-tumour efficacy. Furthermore, Gattinoni et al. (2011) showed in a mouse model that sorted T_{CM}, or T_{SCM} subsets have better survival and antitumour activity compared to T_{EM} cells. Interestingly, Ghassemi et al. (2018) demonstrated that early harvested CAR-T cells that have not gone through prolonged and extensive *ex vivo* expansion had enhanced proliferation, persistence and clinical efficacy *in vivo*. Similarly, in this study, the glucose-deprived CAR-T cells underwent less proliferation and differentiation during *ex vivo* culture compared to the standard CAR-T cells, hence, had enhanced proliferation and persistence *in vitro* tested with the serial re-stimulation assay.

4.4.3 Manufacturing Feasibility

4.4.3.1 CAR-T Release Criteria

In this section, the final attributes of T_{CM} enriched CAR-T cells were assessed against the common release criteria acceptance range and the control condition. Different immunotherapies, including CAR-T therapies, have different release criteria post-manufacturing. Release criteria cannot be generalised, and each clinical trial and manufacturing protocol has its own acceptance range for release criteria. However, Roddie et al. (2019) reviewed the most common release assays used for CAR-T therapy manufacturing. These release assays include viability, identity, purity, mubiological sterility, stability and po-

tency. The relevant non-GMP criteria for this study are viability, purity and potency. Regarding viability, normally above 70% viability is accepted at the end of manufacturing (Gee, 2018; Roddie et al., 2019). Although the viability in T_{CM} enriched CAR-T product was lower than the standard CAR-T cells, the viability in all the tested donors still fell within the acceptance range. It must be noted that the viability achieved in this study was with healthy donor cells; therefore, the tests must be verified with less healthy and potentially slow growing patients' cells.

The purity acceptance range is particularly important in the manufacturing processes where the starting material is the mixture of different cell types such as PBMCs. Therefore, this is less relevant in this study as the starting T cells were negatively isolated for CD3+ T cells; hence very high purity ($> 95\%$) of CD3+ T cells was achieved after expansion.

Regarding transduction efficiency, the minimum required for product release varies in different clinical trials or manufacturing processes (Kalos et al. (2011), Schuster et al. (2017), and Shannon L. Maude et al. (2014) protocols); Kalos et al. (2011) protocol set the release criteria at 20% transduction efficiency. Moreover, David L Porter et al. (2015) reported the median of 20.1% during the manufacturing with a similar CAR transgene to our study. Therefore in this study, 20% was used as a minimum requirement and benchmark for transduction. A direct comparison was not possible due to differences in concentration and functional titre of lentivirus used in different

studies and variation in protocols used for transduction step. While the results from the benchmark studies mentioned above were generated with patient cells and not the healthy donor cells as shown in this investigation, studying the transduction efficiency on healthy donor still provides a meaningful baseline for further investigations with patient cells Levine et al. (2016).

For potency assay, both IFN-γ release and cytotoxicity toward a CD19+ cancer cell lines were assessed. Comparable potency was observed in the T_{CM} enriched CAR-T product compared to the control condition. The number of CAR-T cells required per dose varies in different CAR-T therapies; The threshold to meet clinical dose is defined by the type and stage of cancer, age and weight of the patient. The contributing factors to the final number of CAR-T product in the manufacturing are transduction efficiency, the proliferation rate of CAR-T cells and manufacturing yield in each step. Sabatino et al. (2016) and Ghassemi et al. (2018) discussed that although there may be an association between the number of CAR-T cells in a dose and the clinical outcome, the quality of CAR-T cells is what determines the CD19-specific CAR-T therapy potency for treating leukaemia. Ghassemi et al. (2018) showed that CAR-T cells that were harvested early on day three rather than day 9 showed an improved tumour control and antileukemic activity in murine ALL models. This was despite having a 6-fold lower number of CAR-T cells in the CAR-T doses that were harvested earlier compared to day 9. Similarly, Sabatino et al. (2016) also showed that despite achieving 2-3 fold lower fold expansion

in T_{SCM} enriched product compared to the standard product, the antitumour response achieved in T_{SCM} enriched CAR-T cells were more long-lasting and robust.

Here, we similarly argue that T_{CM} enriched CAR-T cells generated through the 2-stage feeding regime could provide a more robust and long-lasting response compared to the standard CAR-T products. The absolute number of CD8+ T_{CM} cells was similar in the final product of both T_{CM} enriched CAR-T and the standard CAR-T product (Figure 4.9). Whether the presence of effector cells in the CAR-T therapy affects the clinical outcome or could potentially result in any adverse effect is still unknown. Christopher A. Klebanoff et al. (2016) demonstrated that antigen-experienced memory cells significantly enhance naive T cells differentiation through Fas-FasL interaction. Whether such an interaction exists between effector and memory CD8+ T-cell subsets and whether they can influence one another's differentiation status and ultimately anti-tumour function remains unknown (Linnemann et al., 2011; Christopher A. Klebanoff et al., 2012). If effector subsets have a deleterious effect the anti-tumour function of the memory cells, then the innovative feeding presented in this doctoral thesis can be used to generate a pool of enriched memory cells.

Furthermore, the main CAR-T therapies side effects, including Cytokine Release Syndrome (CRS) and Neurological toxicity, are associated with elevated inflammatory cytokines upon infusion of CAR-T cells (Bonifant et al., 2016). Here, we are arguing that by infusing a lower number of CAR-T cells, but enriched with only more potent and

long-lasting cells such as CD8+ T_{CM}, the elevated inflammatory cytokines that typically occur early (<1 week) after the infusion, could be better managed and the occurrence of side effects could be reduced. However, so far, no study has found a correlation between the purity T_{CM} cells in the final CAR-T products and the occurrence of CRS or neurological toxicity.

4.4.3.2 GMP and clinical suitability

The feasibility of the 2-stage feeding in gas-permeable bags, which are widely used for CAR-T cell activation and expansion was demonstrated (Vormittag et al., 2018). Regarding clinical-grade manufacturing, other aspects including, the difficulty of the manufacturing protocol for execution and the suitability for GMP operations must be considered. The 2-stage feeding protocol suggested includes a change of the feeding medium from glucose-containing medium to glucose-free medium half-way through the expansion period. In practice, this means cleanroom operators must use two different media throughout the manufacturing of an autologous therapy, which imposes further complexity in medium preparation and increases the risk of human error during each feeding step. Furthermore, there is limited GMP-grade medium available in the market that offers glucose-free formulation; to our knowledge, none of the widely used media such as X-VIVO15, TexMACS and AIM V has a glucose-free variety. However, many vendors such as Thermofisher and Lonza development service offer customisation of medium formulation. One remaining question is whether glucose-free feeding would

work with serum-free media. In this study, glucose-free RPMI 1640 was supplemented with 10% FBS. But in clinical manufacturing, either serum-free media or serum content (human AB serum) less than 5% are being used (Medvec et al., 2018).

The 2-stage feeding strategy poses other advantages other than enriching the final product with T_{CM} cells. The 2-stage feeding protocol as executed and explained in this chapter, required lower amount of medium and cytokine. This is because, during the glucose deprivation period, "less favourable" effector T cells stopped growing. Therefore, there is lower number of CAR-T cells to maintain and grow. This also means there is less competition for key nutrients such as amino acids for T_{CM} cells. Alternatively, this study provides the basis for other feeding strategies widely used in bioprocessing such as bolus fed-batch feeding (Kochanowski et al., 2011). For instance, CAR-T cells expansion could start with a glucose-containing medium for the first four days (batch phase), and then a bolus of concentrated glucose-free essential nutrients such as amino acids and fatty acids can be added for the second half of the expansion period. In this approach, CAR-T cells consume the glucose in the medium in the batch phase and inevitably enter the glucose deprivation condition during the second half, where bolus additions provide key nutrients for the growth of T_{CM} and T_{SCM} cells. Lowering the volume of medium and cytokines used for producing a CAR-T dose would ultimately reduce the cost of manufacturing, reduce the economic burden to healthcare systems and improve the patients' access to CAR-T therapies.

4.4.3.3 Optimisation

The work presented in this thesis was performed with RPMI 1640 medium (with/without glucose) supplemented with 10% FBS. As mentioned before, this strategy must be tested with serum-free medium in order to become suitable for clinical manufacturing of CAR-T therapies. Furthermore, the RPMI 1640 medium used in this study lacks fatty acids and other components found in other advanced media such as X-VIVO15. Therefore, a glucose-free advanced medium such as X-VIVO15 could potentially improve the fold expansion and quality of the CAR-T therapy generated through the 2-stage feeding regime.

Another possible optimisation of the glucose-free medium is by supplementing it with another carbohydrate such as galactose. Although galactose is not efficiently metabolised in the glycolysis pathway (Chang et al., 2013), could provide an alternative to glucose for T cells in the glucose-free medium. Interestingly, while this study was conducted, a patent (Publication number: WO/2018/157072) was filed by Life Technoligies corporation, a leading medium manufacturer and the vendor of AIM V serum free medium. The patent is about the formulation of a new serum free medium, in which both glucose and galactose are supplemented at 1:9 ratio in addition to one or more fatty acids. The patent claims that the medium retains the less-differentiated phenotype of T cells and enhances the expansion of CAR-T cells.

Furthermore, as mentioned in Section 3.6, adding other components to the glucose-

free medium such as membrane-permeable α–ketoglutarate or succinate could provide an alternative pathway for T cells to bypass glycolysis. Moreover, in this study, the levels of amino acids, glutamine and sodium pyruvate were not measured. Therefore, there is a possibility that the glucose-free medium was deprived of these metabolites during the culture. Therefore, an analysis of medium supernatant by High-Performance Liquid Chromatography (HPLC) for the metabolites mentioned above would provide more insight into this study. The HPLC analysis would, therefore provide a baseline to have a better understanding of other metabolites profile and how to further optimise the glucose-free medium.

Finally, translating this feeding regime from a gas-permeable bag to a bioreactor system such as the WAVE bioreactor would give the opportunity to monitor and control process parameter such (dO_2) and pH. These parameters in a gas-permeable bag used in this study were not monitored and controlled. Therefore, how controlling pH and dO_2 impact the CAR-T product quality and yield is another aspect that needs to be considered.

4.5 Conclusion

It is clear from preclinical models and clinical trials that infusion of less-differentiated T_N, T_{SCM} and T_{CM} T cell subsets in CAR-T therapy would result in an improved persistence and anti-tumour outcome (Lipp et al., 1999; Gattinoni et al., 2005; Louis et al., 2011; Kochenderfer et al., 2017; Fraietta et al., 2018). In this study, the feasibility of using the 2-stage feeding regime for generating CD19-specific CAR-T therapy enriched with T_{CM} cells was demonstrated. The generated CAR-T products through this method were then tested for their anti-tumour function and proliferation capacity. The proliferation capacity of the T_{CM} enriched product was significantly better than the standard CAR-T therapy. The CAR-T cells exposed to glucose deprivation also retained their *in vitro* killing function, and the ability to produce inflammatory cytokines. Interestingly, more effector cytokines were observed where T_{CM} enriched CAR-T cells were stimulated with CD19-positive cancer cells.

Other potential advantages of this method for manufacturing CAR-T therapies were also discussed. Fewer cells would be generated through this method; therefore, less volume of media and cytokines would be required. On the other hand, using two different media in one manufacturing process adds to the already complex and labour-intensive process. Finally, the limitations and potential future works in terms of further optimisation of CAR-T manufacturing were discussed; one of the uncharacterised aspects is the optimum dO_2 and pH for growing T cells in the bioreactor, which will be addressed

in the next chapter. Overall, this study generated a baseline data for utilising metabolites restriction such as glucose deprivation for redirecting the composition of CAR-T product to favourable, less differentiated subsets.

Chapter 5

Impacts of pH, Dissolved Oxygen and Agitation on T Cell Expansion

5.1 Introduction

The expansion of primary T cells under static conditions or rocking motion (RM) has been considered standard practice for manufacturing of T cells for immunotherapy applications (Xiuyan Wang et al., 2016). Currently, the GMP-grade clinical manufacturing of T cells is mainly being done with permeable gas membrane bags, RM bioreactors or

CliniMACS prodigy system (Miltenyi Biotec Inc.) (Somerville et al., 2012; Mock et al., 2016; Iyer et al., 2018; Vormittag et al., 2018).

In regard to in-line process control and monitoring, dissolved oxygen (dO_2) and pH readings are standard measurements in bioprocessing; dO_2 drops where oxygen transfer rate is not enough to meet cellular demand and pH drops in response to increased secretion of lactic acid (Rogatzki et al., 2015). For mammalian cells manufacturing, dO_2 and pH of the cell culture medium are usually held within a certain range. The main purpose of controlling pH and dO_2 is to avoid exposing cells to the acidic environment caused by the accumulation of waste metabolites such as lactic acid and to provide enough oxygen to support the metabolism of cells. Reportedly, dO_2 and pH readings can also be incorporated into a control system for an automated medium feeding or can be used as a measure for viable cell concentration (Pigeau et al., 2018). The effects of different pH and oxygen levels on expansion and differentiation of other cell types such as human MSCs are well studied (Lavrentieva et al., 2010). However, the impact of controlled pH and dO_2 at different levels on T cells and the interaction between them is still not fully understood.

Inside the human body, T cells are exposed to a wide range of oxygen and pH levels with oxygen tensions changing from 0.2-3% in the thymus, 0.5-4.5% in spleen and lymph nodes to 13% in arterial blood (K. A. McLaughlin et al., 1996; Caldwell et al., 2001; Braun et al., 2001; Hale et al., 2002; Carreau et al., 2011; McNamee et al., 2013;

Zenewicz, 2017). In regard to pH, T cells are exposed to pH level varying from 7.4 in healthy tissues to 6.0-6.9 in the tumour microenvironment and inflammatory tissues (Ashby, 1966; Griffiths, 1991; Gerweck et al., 1996; Corbet et al., 2017). Several studies thus far have investigated the effects of pH and dO_2 on T cells (K. R. Atkuri et al., 2005; L. M. McLaughlin et al., 2005; Berahovich et al., 2019; Carswell et al., 2000; Bosticardo et al., 2001), however, what is not yet clear is the impact of different levels of pH and dO_2 during the manufacturing on quality and growth of T cells.

In this chapter, small scale studies in deep well plates were conducted to investigate the impact of pH, dO_2, and agitation speed on the expansion and quality of primary T cells. Initially, shaken deep well plates were compared with static conditions (Section 5.2). Once the impact of agitation on T cell growth has been determined, further studies in the micro-Matrix, a high throughput microbioreactor, were conducted to investigate the impact of two levels of pH and dO_2 on the expansion and phenotypic composition of primary T cells (section 5.2.2).

5.2 Experimental procedure

5.2.1 Agitated vs. static culture conditions

The aim of the first part was to assess the feasibility of growing primary T cells in agitated (dynamic) conditions. Static and dynamic cultures were conducted using 24 deep square well plates with flat bottom (Applikon-Biotechnology, The Netherlands) without integrated sensors for pH, dO_2 and temperature on a shaker with 25mm shaking orbital diameter. T cells isolated from three healthy donors were used for each condition with three technical replicates (three wells) for each healthy donor. The medium used in this study is RPMI 1640 supplemented with 10% FBSv, 2mM L-glutamine, 1% Antibiotic-Antimycotic solution (complete RPMI 1640; cRPMI 1640) and IL-7 (25 ng/mL) and IL-15 (10 ng/mL). T cells were seeded at 400,000 cells/mL density in 2 mL of complete medium at 37°, in the 5% CO_2 incubator. Sandwich covers (CR1224a; Enzyscreen) were used to minimise evaporation while allowing gas transfer to the culture medium throughout the experiment. The sandwich cover consist of a silicone layer, a ePTFE layer and a microfiber layer held together in a rigid stainless steel cover. These layers have multiple small holes (size: 1.2 x 5mm), which allows 0.7 mL/ minute exchange of headspace air, and limits the evaporation rate to 16µL/well/day (Chaturvedi et al., 2014). The sandwich covers and the deep well plates were clamped together tightly by the cover clamps (CR1700; Enzyscreen), which was mounted onto the orbital shaker. To compensate for a small amount of evaporation observed during the cell culture pe-

riod, on day three, all wells volume were measured by a 2 mL serological pipette, and enough Deionized (DI) water was added to make up the volume of each well to 2 mL.

The first three days of the cell culture were conducted in batch. Then perfusion mimic (explained in Section 2.2.7.2) was performed 72h post-inoculation at 0.5 Vessel Volume per Day (VVD) rate to remove the waste medium and to provide fresh nutrients. This rate of feeding was increased after 120h post-inoculation to 2x 0.5 VVD to provide enough nutrients for the T cell growth at their exponential growth phase (summarised in Figure 5.1). The growth and viability of T cells were assessed by the cell counter, while, the composition of T cells was assessed by flow cytometry using panel 2 (Section 2.5.3) after eight days of expansion.

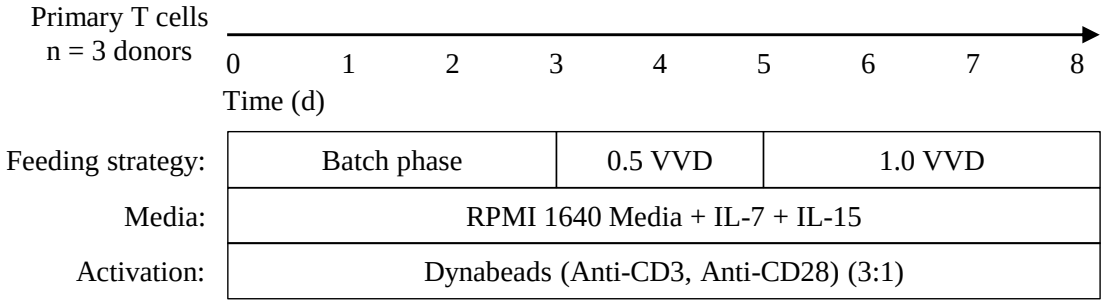

Figure 5.1: The schema shows the feeding strategy used during the 8 days experiments (day 1-3: batch phase, day 3-5: 0.5 VVD, 5-8: 1.0 VVD). The medium used throughout the experiment was cRPMI 1640 supplemented with IL-7 (25 ng/mL) and IL-15 (10 ng/mL). The activation beads were added on day 0 at 3:1 cells to beads ratio.

5.2.2 Impact of dissolved oxygen and pH on T cells

The pH and dO_2 values selected for investigation in this section were decided based on physiological and *in vitro* levels. As for low dissolved oxygen level, dO_2 25% air

saturation was decided, which is approximately the same as gas oxygen tension in lymph nodes. For high dissolved oxygen level, dO_2 90% was chosen, which is approximately similar to what cells are exposed to inside the 5% CO_2 incubators (Wenger et al., 2015). Throughout this section, the term physiological oxygen level will be used to refer to 25% dissolved oxygen, whereas atmospheric oxygen level refers to 90% dissolved oxygen level. As for pH, high level of 7.4 was chosen since it is similar to the pH found in neutral and normal tissues (Mordon et al., 1992; Erra Diaz et al., 2018). pH 6.9 was chosen as low pH, which is approximately the pH reached in uncontrolled T cell culture due to the accumulation of lactic acid (Costariol et al., 2019).

In order to control dO_2 and pH at specific levels, the micro-Matrix system (Applikon Biotechnology) was used. This microbioreactor has been successfully used with other cell types such as Chinese hamster ovary (CHO) cells (Wiegmann et al., 2018). The micro-Matrix cultivation system is a shaken high throughput screening tool (25mm orbital diameter), with a single use pre-calibrated cassette consisting of 24 independent microbioreactors (Figure 5.2) with a working volume ranging between 1-7 mL for each well. Each microbioreactor (or well) is facilitated with its own pH, temperature, dO_2 sensors (Figure 5.2d) and PID controller and is supplied with four separate gas lines with the maximum gas flow rate set to 1.4 mL/min. The aeration is achieved through overlay for each well individually; therefore, this system is capable of creating a different gas mixture in each well. The pH control was achieved through increasing CO_2 aeration to

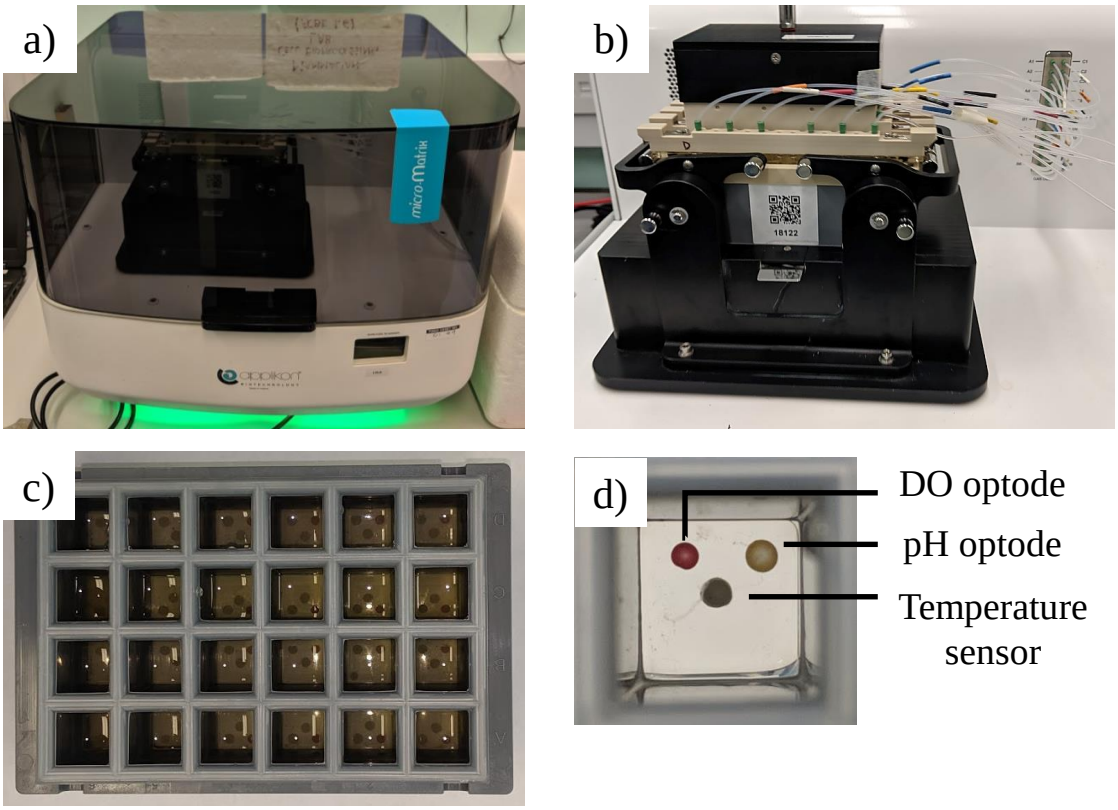

Figure 5.2: The micro-Matrix cultivation system. a) the micro-Matrix, b) the cassette attached to gas tubings inside the bioreactor, c) square deep well cassette from the top view, c) bottom of each well showing different sensors.

decrease the pH of the medium and by manual bolus additions of sodium bicarbonate buffer (250 mM $NaHCO_3$ and 250 mM Na_2CO_3) to increase the pH, when needed. The control of dO_2 was achieved via increasing overlay gassing of O_2 to increase the dO_2 and increase gassing with N_2 to decrease the dO_2. The same feeding strategy, activation method and medium were used as previously explained (Figure 5.1) with an extra manual addition of bicarbonate on day 4 for pH control. Due to the limited capacity of each cassette, the whole experiment was separated into 4 different blocks (Table 5.1). An example of the layout of one cassette is shown in Figure 5.3. In order to assess whether there is an interaction between pH and dO_2, two separate two-way ANOVA were performed between the different combination of dO_2 and pH at 100 rpm and 200 rpm.

Cassette	1	2	3	4	5	6
A	HD4 DO 90%, pH 7.4			HD4 DO 90%, pH 6.9		
B	HD6 DO 90%, pH 7.4			HD6 DO 90%, pH 6.9		
C	HD8 DO 90%, pH 7.4			HD8 DO 90%, pH 6.9		
D	X	X	X	X	X	X

Figure 5.3: An example of cassette layout used with micro-Matrix cultivation system.

pH	Dissolved Oxygen	Shaking speed	Block
6.9	25%	100	1
7.4	25%	100	1
6.9	90%	100	2
6.9	25%	200	3
7.4	90%	100	2
7.4	25%	200	3
6.9	90%	200	4
7.4	90%	200	4

Table 5.1: The experiment layout showing different pH, dO_2 and agitation speed tested in different combinations. Due to the limited size of each cassette (24 deep wells), the experiment was divided into four different blocks, where each block was performed in one cassette.

5.3 Results

5.3.1 Agitated vs. static culture conditions

5.3.1.1 Growth kinetics

Figure 5.4 (a) and (b) presents the fold expansion and viability achieved following eight days expansion in three different conditions. Fold expansion was significantly higher ($P < 0.001$) at 200 rpm than the static condition (20.3 $\pm$ 3.1 vs 9.7 $\pm$ 1.2). Fold expansion achieved at 100 rpm (6.2 $\pm$ 0.6) was significantly lower ($P < 0.001$) than the static control. The viability measurements for all conditions were above 90% , with static and 200 rpm conditions resulting in better viability than 100 rpm.

5.3.1.2 Immunophenotypic Analysis

The quality of T cells in different conditions was assessed by CD4:CD8 ratio and percentages of T_N, T_{CM}, T_{EM} and T_{TE} cells. There is no significant difference in CD4:CD8 ratios amongst different conditions (Figure 5.4 (c)). The percentages of T_{CM}, T_{EM} and T_{TE} which give a good indication of T cell differentiation are shown in Figure 5.4 (d), (e) and (f). CD8+ T_{CM} percentages across different shaking speed and the control were similar. Regarding the effector phenotypes (Figure 5.4 (e,f)), at 200 rpm CD8+ T cells were driven more toward T_{TE} compared with 100 rpm and static conditions. Finally, the amount of CD8+ T_N was lower than 2% in all conditions (data is not shown).

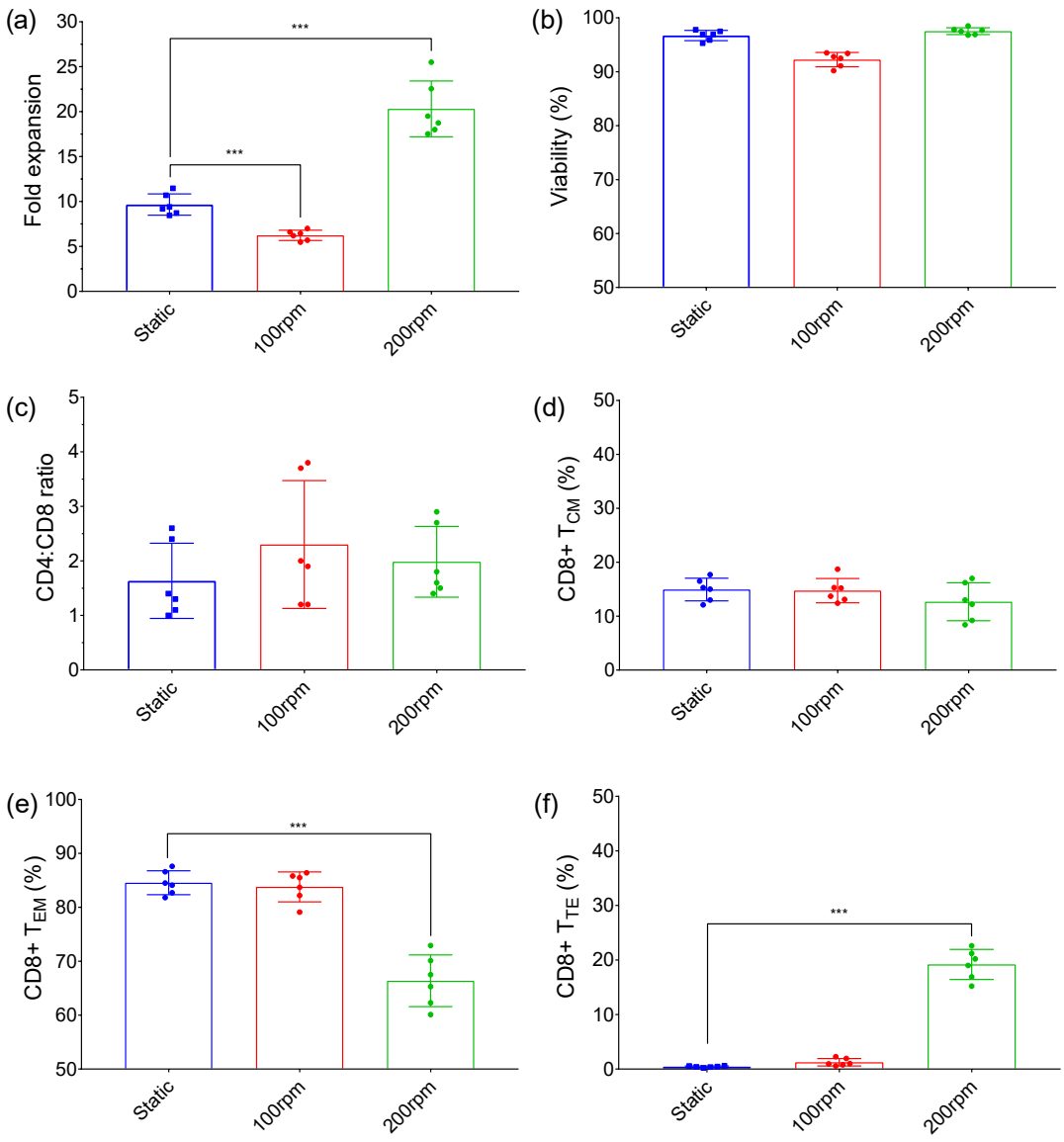

Figure 5.4: Fold expansion (a), final cell viability (b), CD4:CD8 ratio (c), CD8+ subsets (T_{CM} (d) , T_{EM} (e), T_{TE} (f)) of primary T cells after eight days expansion in static and agitated conditions. Mean $\pm$ SD, 3 healthy donors (2 technical replicates each) are shown. Statistical comparisons (a) were performed using a paired two-tailed t-test.

5.3.2 Impact of pH and Dissolved Oxygen on T cells expansion

5.3.2.1 Growth Kinetics

Cell growth and viability were monitored throughout the expansion period via daily sampling from day three (Figure 5.5). In all conditions, a three days lag phase was observed before T cells entered their exponential phase. At the end of the expansion period (Figure5.5 (a)), it was observed that at 100 rpm agitation speed, cell growth slows down, potentially suggesting reaching the plateau phase. In contrast, T cells grown at 200 rpm were still in their exponential phase on day eight, indicating that cells could possibly have grown more if perfusion and cell expansion were continued. The viability of T cells (Figure 5.5 (b)) cultured at 100 rpm in different dO_2 and pH dropped to 80-90% on day 3 and then steadily increased to $\approx$ 90% viability by the end of the expansion. T cells expanded at 200 rpm maintained their high viability until day 3. However, a slight decrease on day 4, one day after starting perfusion, was observed which was followed by a steady increase in viability to $\approx$ 95% on day 8.

Figure 5.6 presents the fold expansion results at different dO_2 (25% & 90%) and pH levels (6.9 & 7.4) at two different agitation speeds (100 and 200 rpm). As previously shown in section 5.3, cell growth is significantly affected by agitation speed. This is evident in Figure 5.6, where fold expansions achieved in all the four different combinations of dO_2 and pH at 200 rpm agitation speed were higher than fold expansion achieved in similar combinations of dO_2 and pH at 100 rpm. Furthermore, the combination of

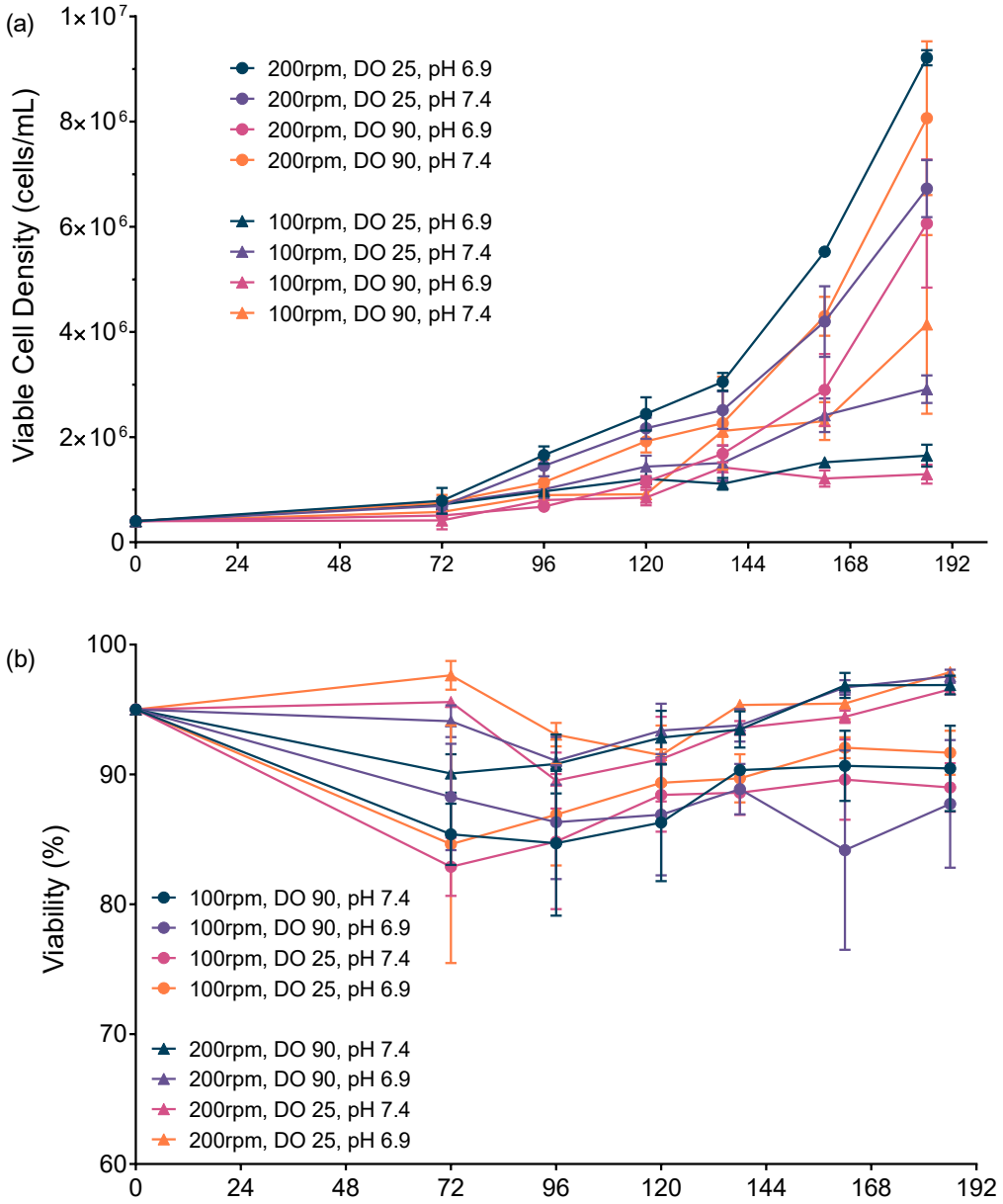

Figure 5.5: Growth (a) and viability (b) curves of of primary T cells over eight days expansion at different controlled pH and dO_2 and agitation speeds. Mean ± SD, 3 healthy donors (2-3 technical replicates for each donor) are shown.

low dO_2 and low pH at 200 rpm and high $dO_2$and high pH at 200 rpm resulted in the highest fold expansion of 22.6 ± 2.6 and 20.8 ± 3.7, respectively. Interestingly, pH 6.9 negatively affected cell proliferation, except when coupled with low dO_2 and 200 rpm agitation speed. In addition, a two-way ANOVA revealed that the interaction between dO_2 and pH is significant at 200 rpm for fold expansion with F-value = 32.34, $P<0.001$. Interestingly, the ANOVA analysis for 100 rpm agitation speed showed that pH is the most significant factor affecting fold expansion with F-value = 58.38, $P<0.001$. The presence of interaction between dO_2 and pH at higher shaking speed suggests that the way T cells react to different pH depends on the level dO_2, or vice versa.

5.3.2.2 Metabolite analysis

As explained previously, a pseudoperfusion approach was used following 72 hours of batch culture in order to replenish the cell culture medium with glucose and other nutrients, while removing waste products such as lactate. Figure 5.7 and 5.8 show the glucose and lactate concentration over an eight days expansion period for each of the conditions at 200 rpm and 100 rpm agitation speeds. The measured levels of glucose and lactate show their concentration in the medium at the associated time point before performing the medium exchange. It was observed that glucose in all conditions at 100 rpm was exhausted after 96 hours despite 0.5 vessel volume medium exchange on day 3. In contrast, glucose exhaustion was not observed at 200 rpm. The decrease in viability of 100 rpm conditions observed after 72 hours did not coincide with glucose limitation,

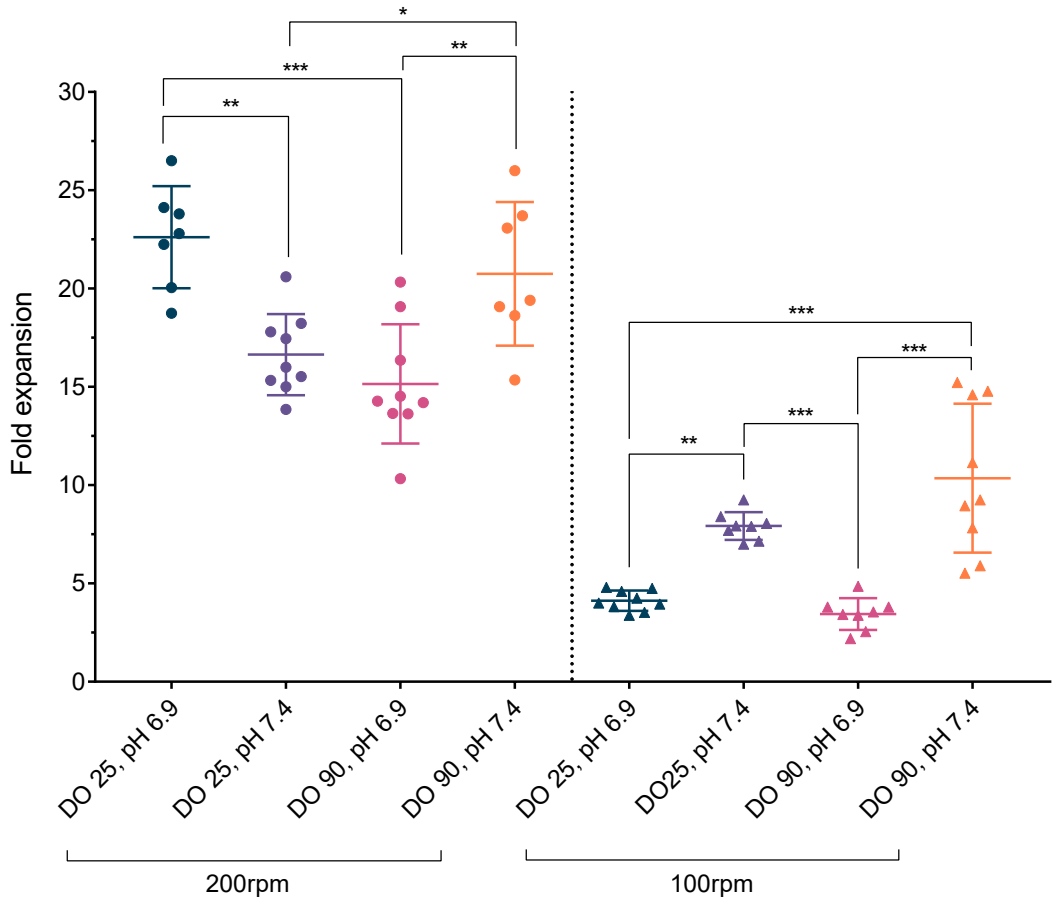

Figure 5.6: Fold expansion of primary T cells over eight days expansion at different controlled pH and dO_2 and agitation speeds. Mean $\pm$ SD, 3 healthy donors (2-3 technical replicates for each donor) are shown. Statistical comparisons were performed using two-way ANOVA followed by Tukey's multiple comparison tests.

suggesting that either the exhaustion of other nutrients or other factors as explained earlier in section 5.2 caused the drop in viability in the first 72 hours. However, a decrease in the glucose concentration, toward the later stages of T cells expansion may have contributed to the lower viability and growth in conditions at 100 rpm. Glucose exhaustion was not a limiting factor for the conditions at 200 rpm, except for dO_2 90% and pH 7.4

condition.

At 200 rpm shaking speed, the lowest glucose concentration in the first three days was observed at dO_2 25% and pH 7.4, Whereas, at dO_2 90% and pH 6.9 highest glucose concentration was observed. Consistent with glucose concentration data, T cells in dO_2 25% and pH 7.4 appeared to produce the highest amount of lactate in the first three days (Figure 5.8), whereas, T cells grown in dO_2 90% and pH 6.9 produced the least amount of lactate. Similar trends were observed for the same conditions at 100 rpm agitation speed, where T cells grown in dO_2 25% and pH 7.4 consumed and produced the highest amount of glucose and lactate, respectively.

The specific glucose consumption and lactate production were calculated for each day (shown in FigureB.1), when metabolite and cell count measurements were available. The average of glucose consumption and lactate production from day 3 to 8 were then calculated for each condition shown in Figure 5.9. Distinctly, T cells grown at 100 rpm shaking speed consumed a higher amount of glucose compared to 100 rpm conditions. At 100 rpm, higher glucose consumption was observed at pH 6.9 compare to pH 7.4. This is, in fact, interesting because glucose consumption is often correlated with the growth of mammalian cells; however, in this case, cells with better growth consumed less glucose. Regarding the lactate production, T cells cultured under controlled pH 6.9 produced less lactate compared to pH 7.4. This difference between different pH in the specific lactate production is notably higher at 100 rpm conditions.

The yield coefficient of lactate from glucose ($Y_{Lactate/Glucose}$) is shown in Figure 5.10. The $Y_{Lactate/Glucose}$ provide us with an estimate of glycolysis activity based on lactate production from glucose. The average yield of lactate from glucose in all conditions is less than the theoretical yield of 2.0. The yield of lactate per glucose achieved in pH 6.9 is lower than pH 7.4 in 100 rpm agitation speed; however, this trend does not apply to different dO_2 and pH at 200 rpm agitation speed.

5.3.2.3 Immunophenotypic Analysis

Looking at the CD4:CD8 ratio at the end of the T cell expansion (Figure 5.11), high variability between donors were observed. CD4:CD8 ratio from two donors were very similar, however, the third donor had a lower percentage of CD8+ cells, which skewed the CD4:CD8 ratio results to a higher number. By comparing different conditions at 200 rpm agitation speed, the CD4:CD8 ratios were similar in all conditions. On the other hand, at 100 rpm shaking speed, T cells at dO_2 25% had higher of CD4:CD8 ratio relative to dO_2 90%.

Flow cytometry analysis of subpopulations of CD8+ T cells is presented in Figure 5.12. CD8+ T cells were analysed in terms of the less differentiated and more desired population of T_{CM} and the more differentiated and less desired population of T_{EM} cells. The Figure 5.12 showed that the highest two T_{CM} percentages of 32.6 % ± 11.3 and 24.4 % ± 5.8 were achieved in dO_2 25% and pH 7.4 at 200 and 100 rpm shaking speeds, respectively. On the other hand, the lowest T_{CM} percentages were achieved where high

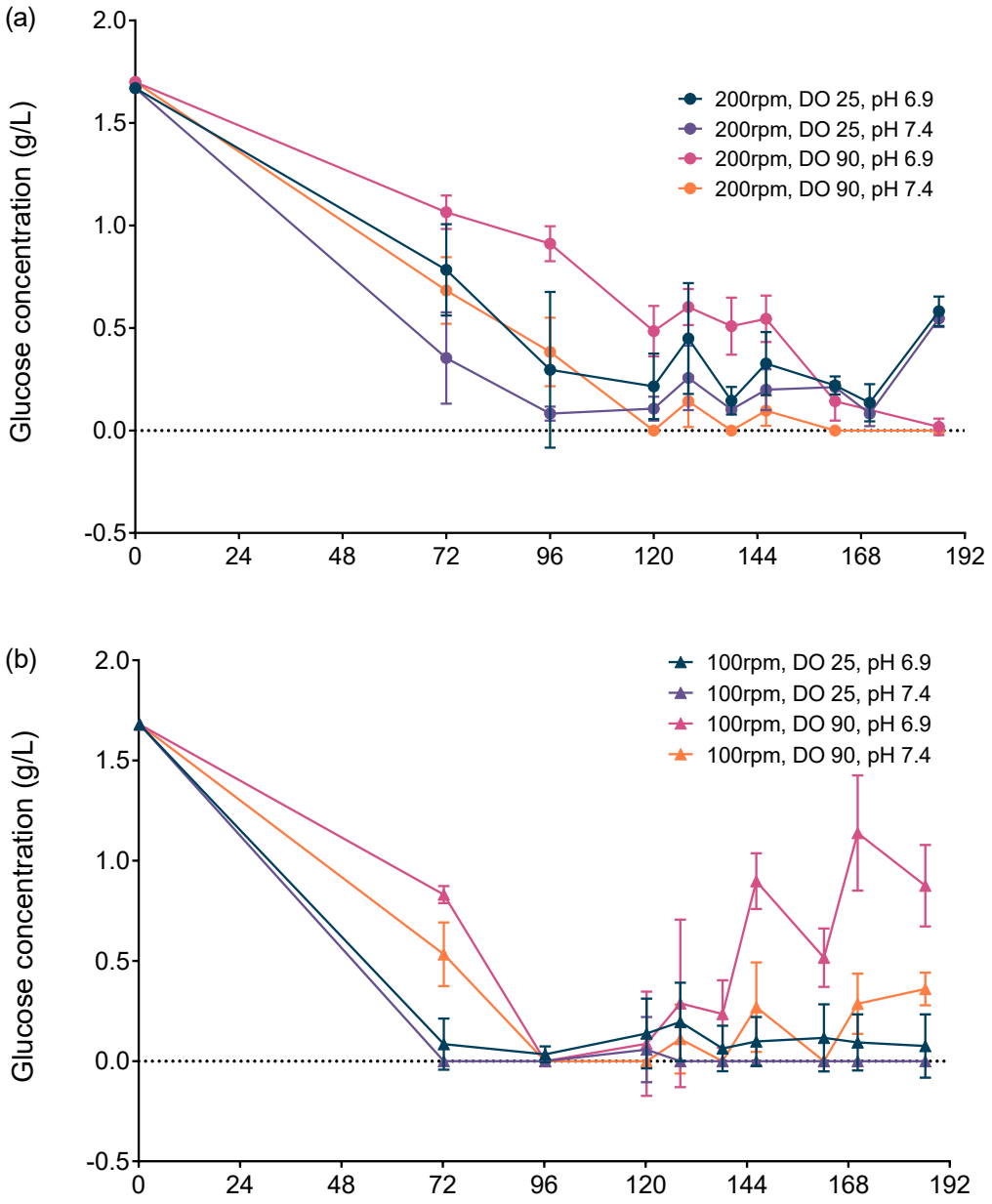

Figure 5.7: Glucose concentration of primary T cells medium over eight days expansion at different controlled pH and dO_2 at 200 rpm (a) and 100 rpm (b) agitation speeds. Mean $\pm$ SD, 3 healthy donors (2-3 technical replicates for each donor) are shown.

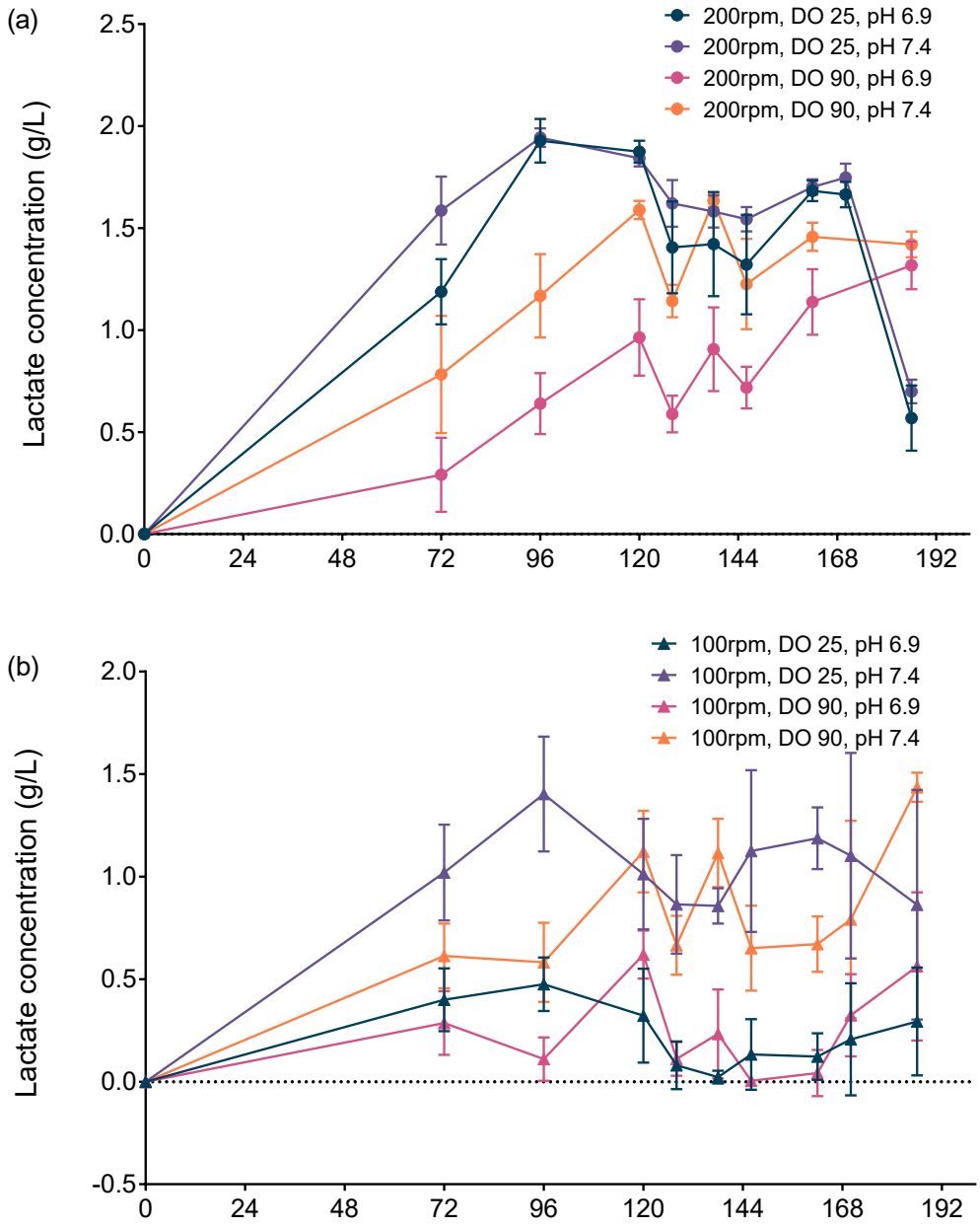

Figure 5.8: Lactate concentration of primary T cells medium over eight days expansion at different controlled pH and dO_2 at 200 rpm (a) and 100 rpm (b) agitation speeds. Mean $\pm$ SD, 3 healthy donors (2-3 technical replicates for each donor) are shown.

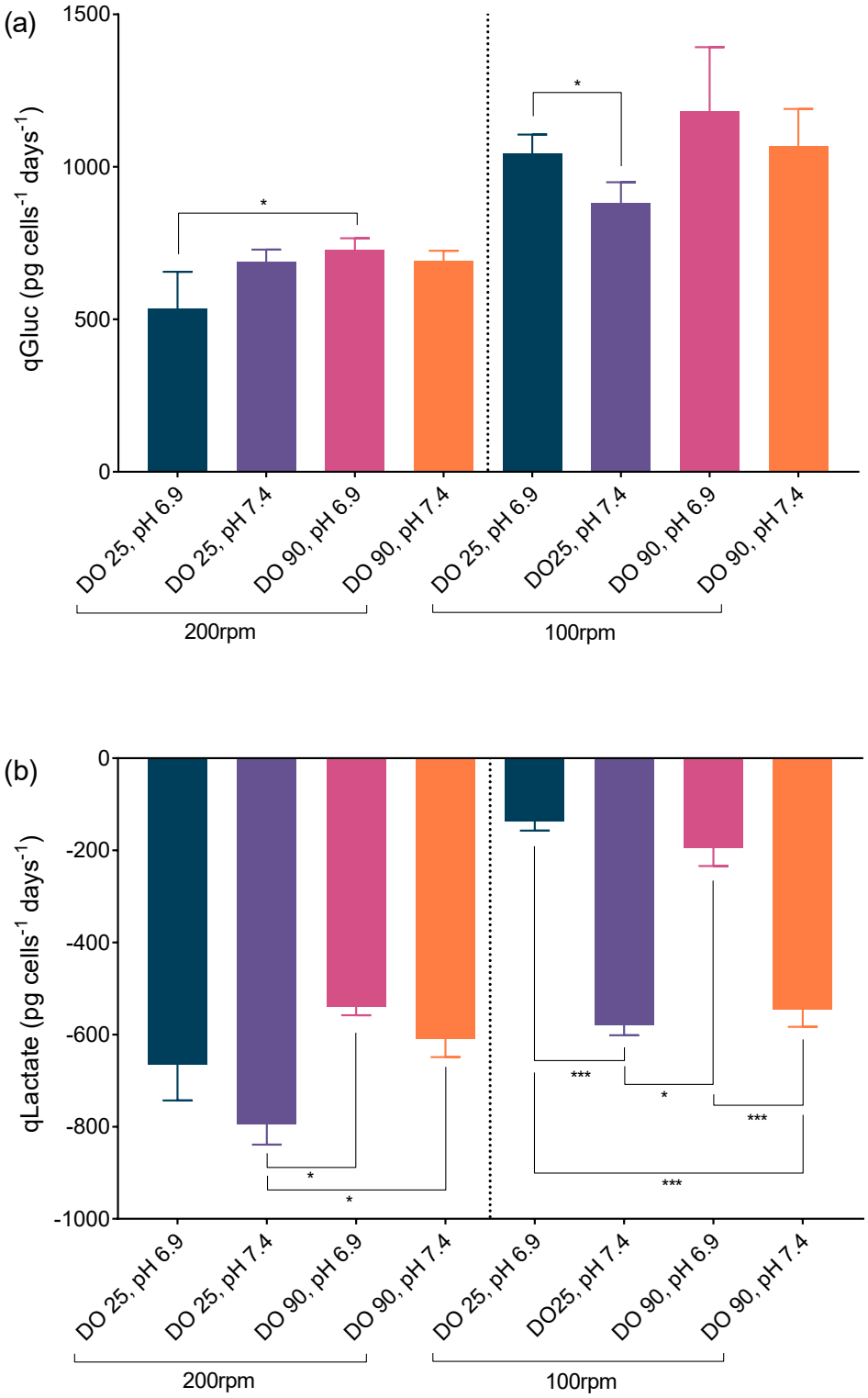

Figure 5.9: Specific glucose consumption rate (qGlucose) (a) and specific lactate production rate (qLactate) (b) in $\mathrm{pgcells^{-1}days^{-1}}$ unit for two agitation speeds and different combinations of pH and dO_2. Mean $\pm$ SD, 3 healthy donors are shown. Statistical comparisons were performed using Tukey's multiple comparison tests.

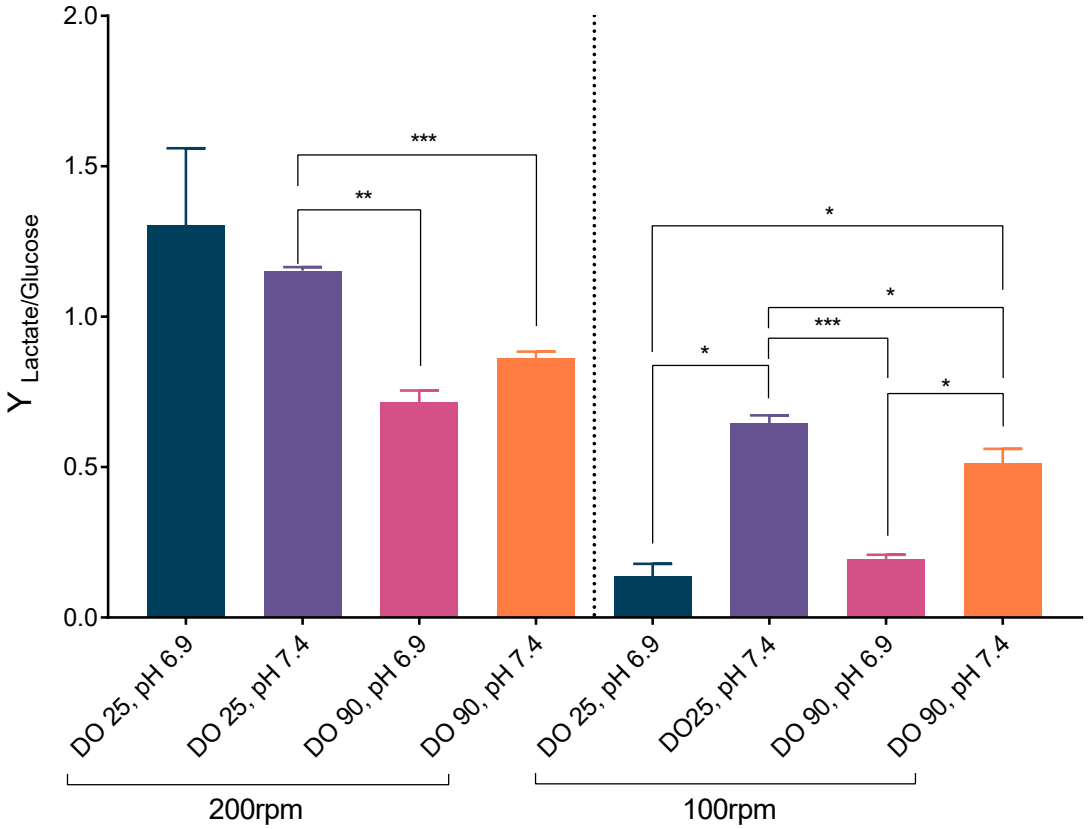

Figure 5.10: Lactate yield from glucose ($Y_{Lactate/Glucose}$) for two different levels of pH, dO_2 and agitation speeds. Mean $\pm$ SD, 3 healthy donors are shown. Statistical comparisons were performed using Tukey's multiple comparison tests.

dO_2 was combined with high pH and when low pH was combined with low dO_2 at both shaking speeds. As expected, T_{EM} percentage was lowest in conditions where the highest percentage of T_{CM} cells were observed and vice versa. A two-way ANOVA revealed that the interaction between dO_2 and pH is the most significant factor with regard to T central memory (%) with F-value = 17.53, $P<0.001$ and F-value = 13.03, P = 0.001 for 200 and 100 rpm, respectively. This interaction suggests that strong interaction exists between dO_2 and pH as previously observed for growth of T cells.

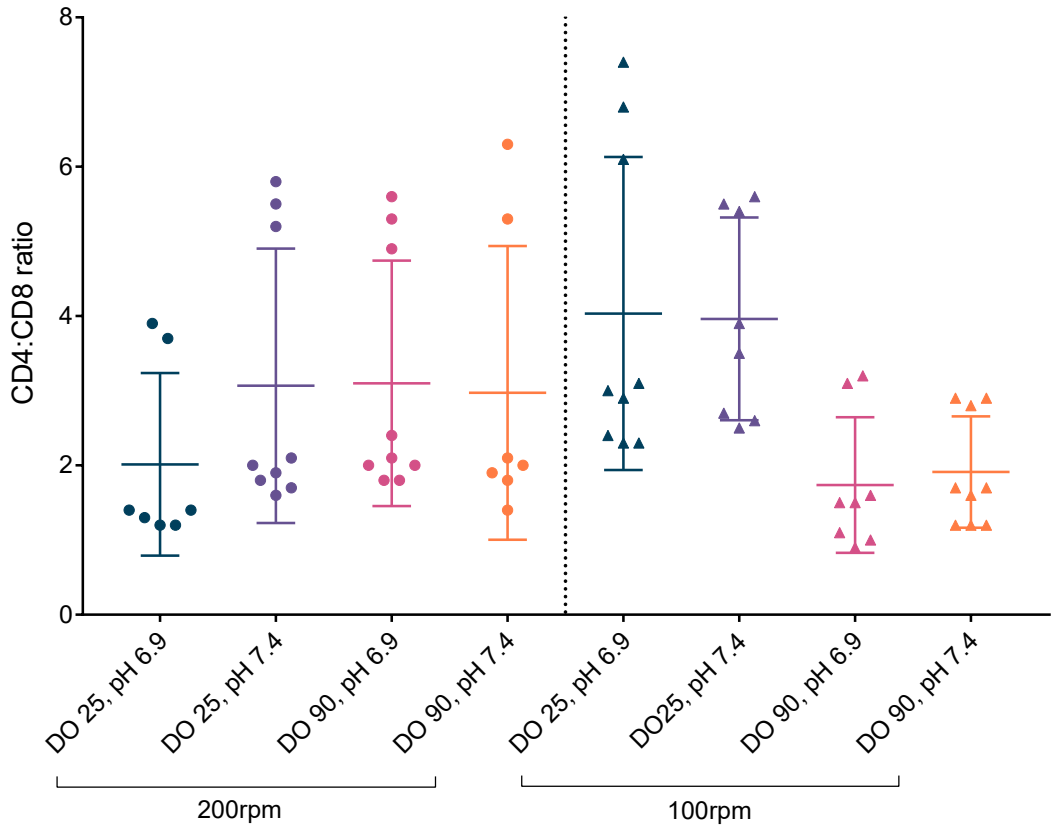

Figure 5.11: CD4:CD8 ratios of T cell products at the end of 8 days expansion at different pH, dO_2 and agitation speeds. Mean $\pm$ SD, 3 healthy donors (2-3 technical replicates for each donor) are shown.

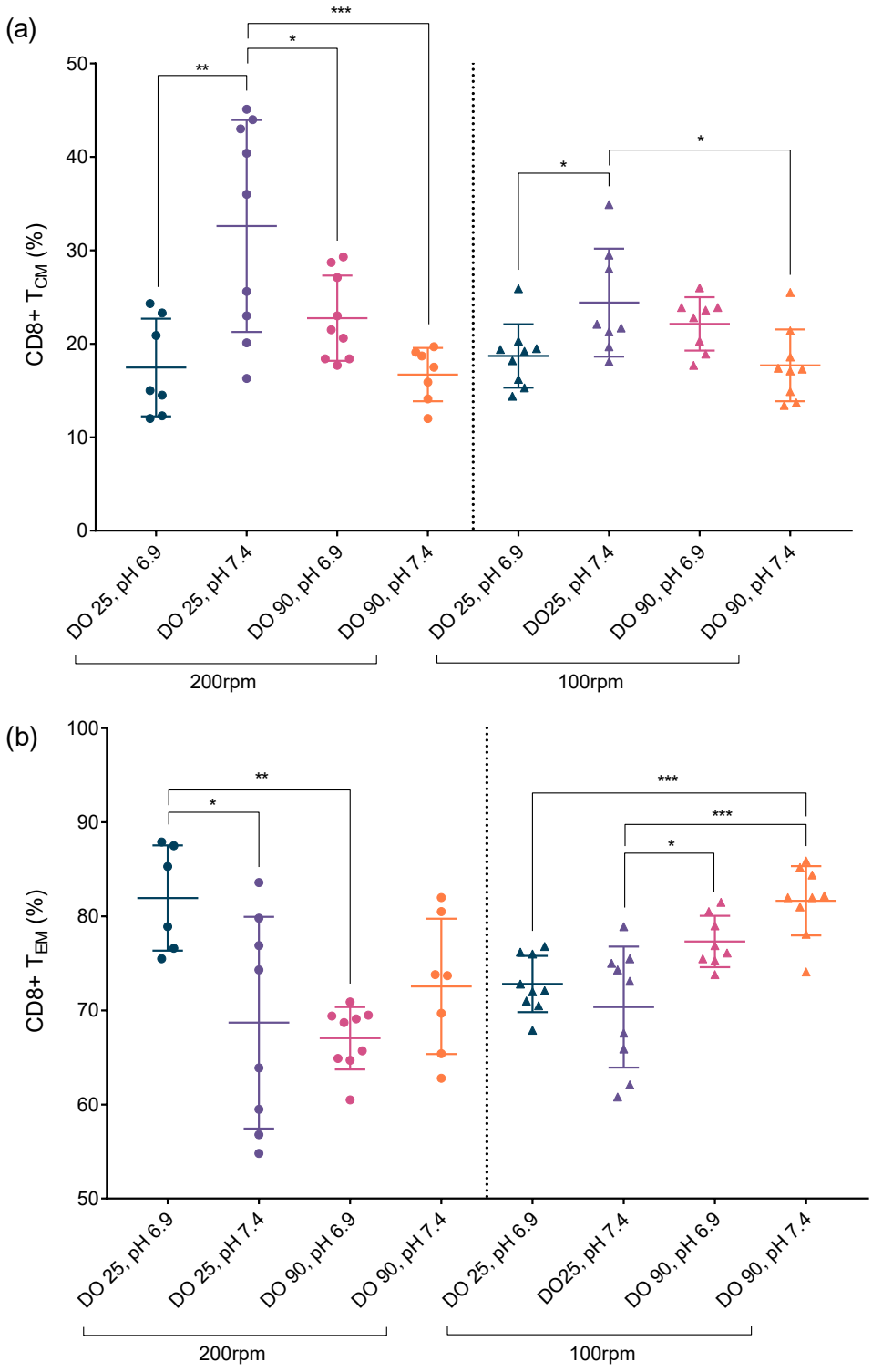

Figure 5.12: Phenotypic characterisation of CD8+ T cells after eight days expansion at different controlled pH, dO_2 and agitation speeds. a) Percentage of CD8+ T central memory cells, b) percentage of CD8+ T effector memory cells. Mean $\pm$ SD, 3 healthy donors (2-3 technical replicates for each donor) are shown. Statistical comparisons were performed using two-way ANOVA followed by Tukey's multiple comparison tests.

5.4 Discussion

With the adoptive cell therapy industry moving from expansion in gas-permeable bags, flasks and non-controlled bioreactor in clinical trials to commercial manufacturing with either scale-out for autologous therapies or scale-up for allogeneic therapies, there is a need to characterise the design of space for manufacturing of T cell therapies, and to assess how different operating parameters such as dO_2 and pH affect growth, quality and functionality of T immunotherapy products. The aims of this study were to show that micro scale systems such as micro-Matrix could be used as a process development tool for T cell therapies manufacturing and to assess the impact of dO_2, pH, agitation and their respective interactions on T cells. The importance of assessing the interaction between process parameters rather than individual parameters separately has been reported in the biotechnology field for other cell types (Trummer et al., 2006; Brunner et al., 2017). A comprehensive understanding of T cell metabolism and interaction with process parameters is of significant importance for process optimisation and scale-up, as the field is moving more toward large scale manufacturing of T cells through scaling up or scaling out for immunotherapy application.

5.4.1 Effects of agitation on T cell expansion

Shaking speed impacts cell growth in multiple ways; Increased agitation improves the rate of oxygen transfer and provides better medium homogenisation. In the case of T

cells activation with Dynabeads, the interaction between T cells and Dynabeads is also likely to be another key factor. T cell activation and proliferation *in vitro* requires multiple signals including TCR stimulation signal, costimulatory signal, and cytokine signal (Kershaw et al., 2013). In this experiment, T cells activation via beads provides TCR and costimulatory signals via anti-CD3 and anti-CD28 antibodies. Increasing agitation results in a higher rate of cells encounter with beads coated with anti-CD3 and anti-CD28, hence higher probability and rate of primary and costimulatory signals received by T cells. The bead-cell interaction has also been previously explained by Costariol et al. (2019), where it was argued that the higher energy dissipation per unit volume results in a higher frequency of interactions between beads and T cells, hence improved proliferation. Furthermore, the culture medium supplemented with IL-7 and IL-15 cytokines, which was routinely fed into the culture medium from day three, provides the stimulatory cytokine signal. The high rate of bead-to-cell interaction in high shaking speed of 200 rpm in addition to continuous prolonged exposure of cells to the beads and cytokines drives T cells from their naive state to effector phenotypes, which explain the generation of highly differentiated effector cells at 200 rpm (Figure 5.4f). Interestingly, at 100 rpm, fold expansion achieved was significantly lower ($\mathrm{P} < 0.001$) than static control. Visually it was seen that under 100 rpm agitation speed, the T cells were concentrating at the centre of the well, forming large aggregates which could be seen through visual observation. It is evident that at low shaking speed, energy dissipation is

not enough to mix the cells thoroughly and to suspend them homogeneously inside the culture medium. Potential reasons for lower viability and growth at 100 rpm are lack of sufficient bead-cell interaction, insufficient oxygen transfer to the cells at the centre of aggregates, inadequate supply of nutrients and removal of toxic metabolites resulted from non-homogeneous mixing and therefore build up of high gradient metabolic waste around and within the cell aggregates.

5.4.2 Lag phase

Comparing the T cell growth in all the conditions (Figure 5.5a), a three days lag phase was observed in all conditions at both agitation speeds. This initial growth lag phase also have been seen for other cell types such as MSCs, where the initial attachment of cells to microcarriers is considered to be the main issue (Rafiq et al., 2017), hence the lag phase was reduced by intermittent agitation at the beginning of the expansion, which allows the cells to attach better to microcarriers. A similar approach of intermittent stirring at the beginning of cell expansion was used by Klarer et al. (2018) when expanding T cells using a stirred ambr 15 bioreactor (Klarer et al., 2018), which relatively reduced the lag phase. One potential explanation for the lag phase is that cells were adopting to the culture environment post-thawing. Also, part of this lag duration could be the time needed by T cells to reach the signalling threshold for T cell proliferation; these times for clonal expansion upon TCR stimulation are between 2 h to 24 h for CD4+ and

CD8+ T cells (Au-Yeung et al., 2014). Furthermore, the balance between differentiation of naive cells and death of effector cells is another potential reason for this lag phase. T cells composition in starting material is composed of mainly naive, effector memory and terminally effector T cells. Upon activation, naive cells undergo spontaneous proliferation, which generates memory and effector cells, thus increasing cell number, Whereas some of short-lived terminally differentiated T cells die through apoptosis or programmed cell death to maintains homoeostasis similar to what occurs after *in vivo* immune response (Hand et al., 2009; W. Cui et al., 2010). This balance between the generation of memory and effect cells from naive cells and death of terminally effector cells would create a constant viable cell number initially until exponential growth of T cells overtake the death of a limited number of terminally effector cells. The death of terminally effector cells could therefore be a potential justification for the drop in the viability within the first three days. However, to prove this hypothesis, further studies on the first three days upon activation are required.

5.4.3 Impact of dissolved oxygen on T cell expansion

In the bioprocessing of mammalian cells, the level of oxygen plays a critical role (J. Wang et al., 1994). Therefore, it is often monitored and controlled in manufacturing of mammalian cells. For T cells, the need to deliver enough oxygen to the cells has led to the development of new cell expansion technologies such as G-Rex and gas permeable

bags, where highly gas permeable materials are used to maximise gas transfer to T cells, showing the importance of oxygen transfer to T cells. In this study, the effect of atmospheric (dO_2 90% air saturation) and physiological oxygen (dO_2 25% air saturation) levels on the expansion of T cells at different agitation speeds were compared. Interestingly, different oxygen level did not impair T cell expansion at 100 rpm. However, expansion of T cells cultured at 200 rpm was impaired when dO_2 25% was coupled with pH 7.4 or dO_2 90% was coupled with pH 6.9.

Several studies have investigated the effect of oxygen on T cell expansion; Bohnenkamp et al. (2002) showed that 25% dO_2 resulted in the highest fold expansion for T cells expanded in stirred bioreactor, where pH was controlled at 7.2. Atkuri et al. (2005, 2007) reported that the fold expansion of T cells stimulated by anti-CD3/CD28 antibodies was 50% higher at atmospheric oxygen level than physiological oxygen level (Kondala R Atkuri et al., 2007; K. R. Atkuri et al., 2005). This was likely due to an accumulation of naturally produced intracellular Nitric Oxide and Reactive Oxygen Species in T cells cultured at 5% oxygen tension (L. M. McLaughlin et al., 2005). Furthermore, Larbi et al. (2010) showed that T cells divide more rapidly in atmospheric oxygen level than the physiological level. This was likely due to an accumulation of cyclic adenosine monophosphate (cAMP) at low oxygen level and consequently reduced T cell activation via lymphocyte-specific protein tyrosine kinase (Lck) inhibition (Millen et al., 2006; Larbi et al., 2010). These studies are comparable to the results presented in this chapter;

T cells that were cultured in pH 7.4 and dO_2 90% had approximately 50% higher fold expansion compared to pH 7.4 and dO_2 25%. In contrast to our results, another study by Berahovich et al. (2019) showed that physiological oxygen level of 5% compared to atmospheric oxygen level of 18% did not impair either T cell nor CD19 CAR-T cell expansion.

Upon activation, T cells switch their metabolism from the mainly oxidative phosphorylation (OXPHOS) and fatty acid metabolism associated with naive cells to an increased rate of glycolysis, glucose consumption and lactate production in activated T cells (MacIver et al., 2013). This phenomenon of cells using a high rate of aerobic glycolysis despite the presence of sufficient oxygen for OXPHOS was first described by Warburg (1956) for cancer cells. The results presented in this chapter demonstrated that $Y_{Lactate/Glucose}$ is higher in low dO_2 than high dO_2 at 200 rpm. However, the difference of $Y_{Lactate/Glucose}$ between dO_2 25% and dO_2 90% was less significant at 100 rpm than 200 rpm. The high yield of lactate from glucose suggests that the majority of pyruvate produced by glucose consumption is channelled toward lactate conversion rather than acetyl-CoA. Reduction of pyruvate to lactate by lactate dehydrogenase (LDH) produce NAD+ from NADH, which is needed for a high rate of glycolysis in fast-dividing cells (Schurich et al., 2019). This is similar to Larbi et al. (2010) study, in which it was found that T cells activated under physiological oxygen tension shift their metabolism more toward glycolysis (Larbi et al., 2010). Larbi et al. (2010) also reported induc-

tion of Hypoxia-inducible factors-1α (HIF-1α) in T cells activated at 2% oxygen level (equivalent to dO_2 10% air saturation). HIF-1α induction leads to phosphorylation of Akt, which consequently induces LDH kinases and overexpression of glucose receptor, GLUT-1, which ultimately leads to an increased rate of glycolysis (Lukashev et al., 2006; Jacobs et al., 2008; Larbi et al., 2010). However, whether HIF-1α induction occurs at a higher oxygen level of 5% (equivalent to dO_2 25% air saturation), similar to what was used in this experiment, is unknown.

By comparing the quality of T cells at the end of eight days expansion, it can be seen that a higher percentage of less differentiated CD8+ T_{CM} cells were produced at physiological oxygen level compared to dO_2 90% at both 100 and 200 rpm, when pH was maintained at 7.4. In contrast to our results, Berahovich et al. (2019) reported that the differentiation status of T cells assessed based on CD27+ marker expression does not change between physiological and atmospheric oxygen level. Similarly, Kondala R Atkuri et al. (2007) showed that subsets of T cells were largely unaffected when culturing T cells in different oxygen levels. However, the physiological oxygen level delayed activation of T cells assessed by CD69 marker expression (Kondala R Atkuri et al., 2007). In summary, the results presented in this study suggests that high level of interaction between dO_2 and pH exists at 200 rpm agitation speed, which requires further comprehensive analysis to understand the underlying mechanism.

5.4.4 Impact of pH on T cell expansion

pH is another important physical parameter for the cultivation of mammalian cells. From a bioprocessing point of view, low pH is normally caused by the production of lactic acid as a byproduct to cell growth. In the life sciences, studying the impact of low pH on T cells is very important, because low pH is one of the main characteristics of the immune-suppressive solid tumour microenvironment. T cells are able to sense the extracellular pH and accumulation of protons by Proton-sensing G protein-coupled receptors (Erra Diaz et al., 2018). However, how extracellular acidosis affects or triggers different signalling pathways is poorly characterised. In this study, it was shown that pH 7.4 resulted in higher fold expansion at 100 rpm. As for 200 rpm, high pH results in improved fold expansion only when dO_2 was maintained at 90%. These results indicate that pH as low as 6.9 has an inhibitory effect on T cell growth when combined with dO_2 90%. There are limited studies available investigating the effect of pH on *in vitro* expansion of T cells; Carswell et al. (2000) investigated the effect of pH on T cells stimulated with phytohemagglutinin (PHA) and reported significantly higher proliferation capacity for pH 7.0 and 7.2 compared to pH 7.4. Other studies (Bohnenkamp et al., 2002; Calcinotto et al., 2012; Fischer et al., 2007; Pilon-Thomas et al., 2016) suggest that pH as low as 6.5-6.7 inhibits T cell activation and growth. These studies suggest that an optimal pH for T cell expansion exist within the range of 7.0-7.3.

The metabolic data based on the consumption of glucose and lactate showed that in

all conditions lowering pH to 6.9 had an inhibitory effect on lactate production. This inhibitory effect of pH on the specific lactic acid production rate was significantly higher at 100 rpm agitation speed. This could be due to the fact that T cells expanded at 100 rpm were not uniformly suspended in the medium and were concentrated in large aggregates at the centre of the well, which potentially exposed T cells to lower pH than pH 6.9 and nutrient gradients. The effect of pH on the rate of glycolysis has been investigated for other cell types such as skeletal cells or fibroblasts; In agreement with our findings, there are reports that an increase in extracellular H^+ (or low pH) suppressed the rate of lactate generation (Iistry, 1966; Halperin et al., 1969; Dobson et al., 1986; Erecifska et al., 1995). Reduced lactate production was potentially due to inhibition of phosphofructokinase, a key enzyme in the glycolysis pathway, by protons (Iistry, 1966; Halperin et al., 1969; Dobson et al., 1986; Erecifska et al., 1995).

Comparing the phenotypes of CD8+ T cells, no correlation between pH and percentage of T_{CM} or T_{EM} was observed. In the literature, it was demonstrated that T cells activated with PHA, a non-specific stimulus, at pH 7.4 have significantly higher expression of activation marker CD25, and produce a higher amount of IL-2 and IFN-γ, compared to T cells activated at pH 6.6 (Bosticardo et al., 2001). However, the addition of Anti-CD28 mAb, which resembles our activation method more closely, restored the proliferation capacity, activation markers expression and different cytokines secretion of T cells (Bosticardo et al., 2001). Other studies demonstrated the suppressive effect

of lactic acid on T cells (Fischer et al., 2007; Erra Diaz et al., 2018), in the tumour microenvironment, which is reversible when T cells are exposed to the lactic-acid free and neutral pH environment. Therefore, suggesting that T cells lose their *in vivo* and therapeutic functionality due to *in vitro* expansion in low pH is not justified.

5.4.5 Potential role of dissolved carbon dioxide

The dissolved CO_2 level in the culture medium is another important physical parameter in bioprocessing of mammalian cells. Controlling partial pressure of carbon dioxide (pCO_2) level is very important, particularly in large scale manufacturing where it becomes more challenging to remove excess CO_2 produced by cells due to mixing limitations and higher solubility due to the increased hydrostatic pressure (Feng et al., 2006). Higher pCO_2 in the cell culture is also associated with increased osmolality due to the equilibrium between bicarbonate and dissolved CO_2, which could independently affect the cell culture performance (Kimura et al., 1999). Lowering pH in the presented study in this chapter was via increasing CO_2 concentration in the head space of each well (done via micro-Matrix control loop). Whereas, in the above-mentioned studies, lowering pH in the cell culture medium was achieved through other methods; some studies use lactic acid to study low pH (Fischer et al., 2007; Nakagawa et al., 2015), where decoupling the effect of lactic acid or low pH on T cells would be impossible. Other studies use diluted hydrochloric acid (Bosticardo et al., 2001; Carswell et al., 2000) to

study the impact of low pH level on cells. In our study, to maintain a pH of 6.9 at the beginning of the experiment, the bioreactor needed to inject a higher amount of CO_2 to keep the pH at the specified set point of 6.9 before cells start growing and producing lactic acid. Therefore, it is argued here that T cells in pH 6.9 conditions were exposed to a higher concentration of dissolved CO_2. Several studies investigating the impact of CO_2 on different cell types have been carried out; Kimura et al. (1999), Goyal et al. (2005), and Meghrous et al. (2015) found that elevated pCO_2 and osmolality has an inhibitory effect on the growth and production kinetics of CHO, hybridoma cells and insect cell, respectively, while Bohnenkamp et al. (2002) demonstrated negative impact of osmolality higher than 0.302 Osmol/kg on T cell viability. Metabolic profile of the cells exposed to elevated pCO_2 also showed lower glycolysis activity at 140 mm Hg pCO_2 (DeZengotita et al., 2011). Furthermore, Vohwinkel et al. (2011) examined the effect of elevated CO_2 on fibroblasts and provided evidence that increased CO_2 impairs mitochondrial function, which decreases O_2 consumption and ATP production. Despite the described negative impacts of increased pCO_2 in the cell culture medium, effective pH control using CO_2 in bioreactor setup has been demonstrated for CHO cells (Hoshan et al., 2019). It is beyond the scope of this study to examine the effect of CO_2 on T cells. However, as increasing the CO_2 injection was the only way that the bioreactor could reduce the pH, T cells in all conditions with controlled pH of 6.9 might have been exposed to elevated CO_2 compared to pH 7.4 in the first three days. It must be noted that due

to the software limitation, it was not possible to record the amount of CO_2 that was injected into each well.

5.4.6 Optimal manufacturing condition for T cell therapies

The focus of this study was how agitation, dO_2 and pH affect the expansion and final product quality of T cells. In the first part of this experiment, it was demonstrated that proliferation rate of T cells can be improved significantly at 200 rpm agitation speed without adversely affecting the phenotype. This means adopting stirred bioreactor for clinical manufacturing of T cell therapies could potentially reduce the manufacturing time and costs mainly associated with the expansion stage and would allow for an increased number of batches per year in a manufacturing facility. Regarding the T cell phenotypes, as discussed in the previous chapters, there are several studies suggesting that T cell subsets with high *in vivo* proliferative capacity such as T_{CM} cells are preferred for immunotherapy applications due to their *in vivo* longevity and good cytotoxic function (Gattinoni et al., 2011; Scarselli et al., 2015; Xiuli Wang et al., 2016). The ”optimum” composition of CAR-T cells for cancer immunotherapy is subjective to each clinical trial or study, but a recent clinical study by Cameron J Turtle et al. (2016) has suggested that defined 1:1 ratio of CD4+ to CD8+ CAR-T cells, highly enriched with T_{CM} cells has clinical advantages in patients with Acute Lymphoblastic Leukemia. The combination of pH 7.4 and dO_2 25% at 200 rpm between the tested conditions was

the best combination for the expansion of T cells while generating a high proportion of central memory cells. Although lower fold expansion was achieved in dO_2 25% and pH 7.4 and 200 rpm shaking speed compared to other conditions such dO_2 25% and pH 6.9 at 200 rpm, the average of the percentage of CD8+ T_{CM} was higher than in other tested conditions. Therefore, changing physical operating parameters such as pH and dO_2 could be used as a strategy to further increase the percentage of CD8+ T_{CM} cells in the final product.

These preliminary results show the impact of pH, dO_2 and agitation speed during on the expansion of T cells, however, a series of different experiments is needed to further validate our data for immunotherapy application. Although, phenotypic analysis based on the expression of CCR7 and CD45RO markers give us a good indication of the differentiation status of T cells, the *in vivo* performance of T cells cannot be predicted solely based on these results. To have a better overview of how the CAR-T cells produced in different pH and oxygen levels perform *in vivo*, validation of these results with T cells transduced with CAR transgene and then animal model study or *in vitro* killing assay would be at least required.

5.5 Conclusion

The present study was designed to determine the effect of agitation, controlled pH and dO_2 on T cells. All the assessed parameters are scale-dependent process parameters and have significant importance in large scale manufacturing of T cells for both autologous and allogenic purposes. In the first part of this investigation, it was demonstrated that culturing T cells in the stirred platform compared to static condition enhanced the growth without adversely affecting their phenotypes. However, the shaking speed or energy dissipation rate must be high enough to suspend T cells and Dynabeads thoroughly in the medium. Furthermore, this study showed the importance of studying interactions between multiple parameters, rather than studying each parameter individually while optimising T cell manufacturing processes. For instance, it was demonstrated that there is a significant interaction between pH and dO_2 and how changing the combination of these parameters could significantly affect the final product.

Screening multiple parameters using micro-Matrix system revealed the potential application of this system for process research and development. The working volume of each bioreactor (1-7 mL) is large enough to provide enough cells for multiple assays and small enough to make it suitable for research and development with reduced cost and to be used where limited number of cells are available (e.g. when working with patient cells). Individual gas and medium supply to each bioreactor enable us to test a variety of culture conditions such as different gas mixture or different feeding strategies.

Chapter 6

Conclusions and Future Work

6.1 Conclusions

CAR-T cell therapies have emerged as a successful therapy for treating blood cancers. However, the application of CAR-T is not limited to blood malignancies and the application of CAR-T therapies is currently being investigated for treating different diseases (Section 1.2.3). Despite ongoing advance in CAR-T therapy, *ex vivo* manufacturing of T cells is still not fully characterised, and there are still gaps in understanding how CAR-T manufacturing processes could affect the quality and ultimately efficiency of CAR-T therapies. The main focus of this doctoral thesis was to assess how to improve the quality of CAR-T cell therapies by altering the manufacturing process parameters such as the feeding regime and bioreactor parameters such as dissolved oxygen and pH.

To achieve the aims of this doctoral thesis described in Section 1.5, the following studies were done.

Firstly, in chapter 3, the impact of different medium metabolites including glucose, sodium pyruvate, and fatty acids on T cell quality and proliferation were assessed. Interestingly, it was demonstrated that glucose deprivation reduces the proliferation rate of T cells but enriches for T_{CM} subset during T cell activation and expansion. Secondly, a novel feeding regime, called 2-stage feeding, was designed, in which T cells were fed with glucose-containing medium in the first three days and then with the glucose-free medium for the next five days. This feeding regime successfully improved the low fold expansion observed in glucose deprivation condition, but produced a T product enriched with T_{CM} subset.

In chapter 4, it was shown that that the 2-stage feeding strategy can be used to generate a CAR-T product enriched with T_{CM} cells.The potential underlying mechanism behind the generation of high purity T_{CM} was suppressing the growth of CD8+ effector subsets. The *in vitro* functionality and persistence of the T_{CM} enriched CAR-T therapy was then assessed, where comparable killing ability was shown. However, the proliferation capacity of T_{CM} enriched CAR-T product after co-culture with CD19 positive cancer cell line, NALM6, was significantly higher than the standard CAR-T product. Collectively, the data suggested that metabolite restriction approach could be used to selectively expand only one subset of T cells.

The 2-stage feeding strategy was tested in a gas-permeable bags in Chapter 4. However, the current trend in the ACT field is manufacturing T cell therapies in more advanced systems with improved process monitoring and control such as WAVE or stirred bioreactors. There has been suggestions that stirred bioreactors such as ambr system could be used to expand T cells (Costariol et al., 2019). Therefore, in Chapter 5, it was evaluated how T cell phenotypic composition and growth would be affected in a agitated system and what is the best operating condition for expanding T cells to achieve high percentage of CD8+ T_{CM} cells. It was initially demonstrated the feasibility of growing T cells in an agitated system such as micro-Matrix and how expanding and producing T cell therapies in an agitated platform could improve T cell growth. Different combinations of two levels of dO_2 and pH in an agitated system was then assessed to characterise the design space of these process parameters. Based on this study, the optimal condition that yielded the highest T_{CM} in the final product were pH 7.4 and dO_2 25%. The work presented in this chapter also demonstrated that there is a strong interaction between dO_2 and pH for the expansion of T cells. It is conclusive that the interaction between multiple process parameters must be considered when optimising a CAR-T manufacturing process. Hence, the importance of systemic statistical approaches such Design of Experiment (DOE) approach, where interaction between multiple different parameters can be assessed. Furthermore, the importance of small-scale high throughput systems such as micro-Matrix bioreactor for high throughput screening of different parameters

for CAR-T therapy manufacturing was demonstrated. Ultimately, the results in this chapter provided a basis for further characterisation of the design space for operating stirred bioreactors.

6.2 Future Work

There are other outstanding questions that must be addressed prior to integrating the 2-stage feeding approach or the controlled pH and dO_2 into the CAR-T therapy manufacturing process.

- In this doctoral thesis, all tests were done using healthy donor isolated T cells. The feasibility of this feeding strategy must therefore be tested with patients' cells that have undergone different chemotherapy regimes and treatments.
- The feasibility of this approach in the absence of serum in the glucose-free medium must be tested. This requires customising an already available advanced media such as X-VIVO15 or TexMACS to create a glucose-free type.
- All the tests performed in this thesis were *in vitro*, therefore the *in vivo* efficacy and anti-leukemic activity of the generated CAR-T cells must also be assessed in animal models. This would be critical to see the longer term positive effect or potential adverse effects of the T_{CM} enriched CAR-T cells. Ultimately, after the following tests, the approach could be considered to be used in a clinical trial.

- The results in Chapter 5 were generated using non-transduced T cells. Therefore, the results must be verified with transduced CAR-T cells and their *in vitro* and *in vivo* functionality must be assessed.

- The combination of the 2-stage feeding regime and controlled pH 7.4 and dO_2 25% in an a stirred platform could potentially provide the high number of T cells enriched in central memory cells. However, as demonstrated in Chapter 5, there could be high level of interaction between different parameters. Hence, it is suggested that the combination of pH 7.4 and dO_2 25% and the 2-stage medium feeding to be tested to assess whether there is a interaction and whether combining these two strategies could further improve the quality of the CAR-T cells.

Appendix A

Non-specific Stimulation

Figure A.1 and A.2 show inflammatory cytokine profiles of more differentiated CCR7- and less differentiated CCR7+ T cells generated under the deprivation condition compared to T cells generated in the standard glucose concentration medium (control) in two representing donors. In the control condition, T cells comprising mainly of CCR7- drove the majority of the effector function, whereas both CCR7+ and CCR7- T cells generated under glucose deprivation produced inflammatory cytokines. The combination of non-stained and on-stimulated controls were used for gating (Figure A.3).

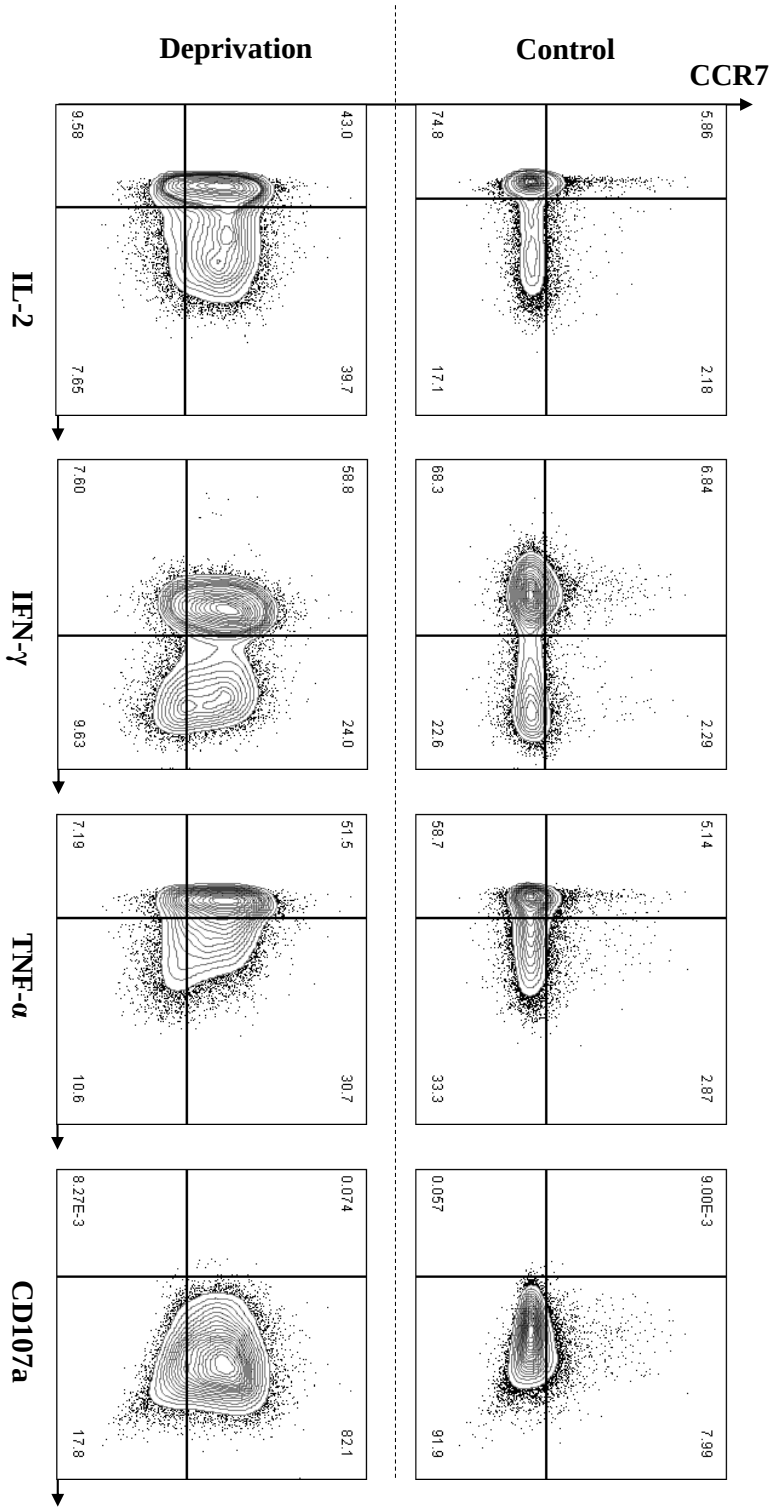

Figure A.1: Intracellular cytokine staining of IL-2, IFN-γ, TNF-α and CD107a of final T cell product after expansion in glucose deprivation condition and control condition are shown from a representative healthy donor after stimulation with PMA and Ionomycin. Data are shown after gating on single CD3+CD8+ cells. Numbers indicate the percentage of cells in each quadrant. The quadrant gating was done based on FMO and non-stimulated controls.

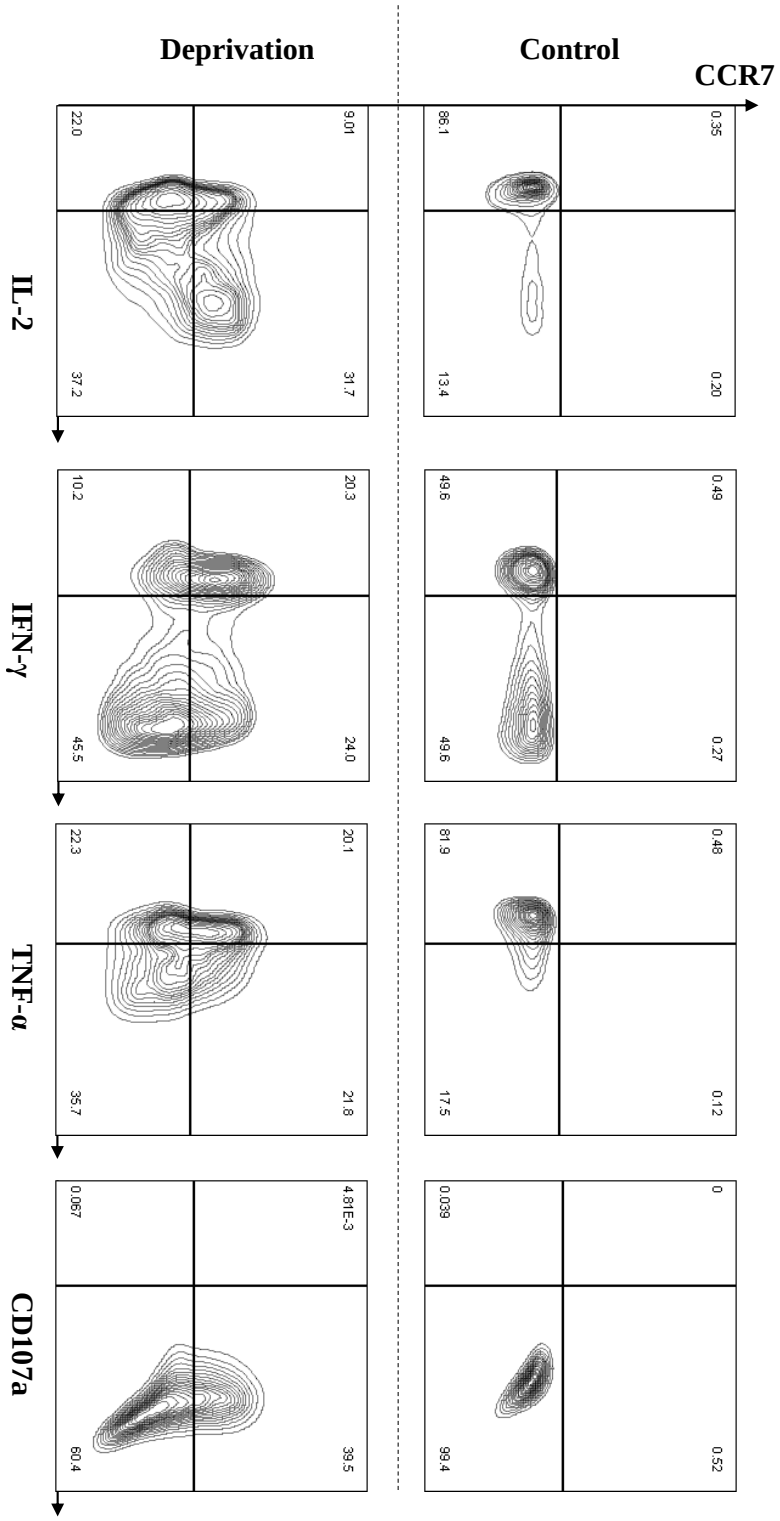

Figure A.2: Intracellular cytokine staining of IL-2, IFN-γ, TNF-α and CD107a of final T cell product after expansion in glucose deprivation condition and control condition are shown from a representative healthy donor after stimulation with PMA and Ionomycin. Data are shown after gating on single CD3+CD8+ cells. Numbers indicate the percentage of cells in each quadrant. The quadrant gating was done based on FMO and non-stimulated controls.

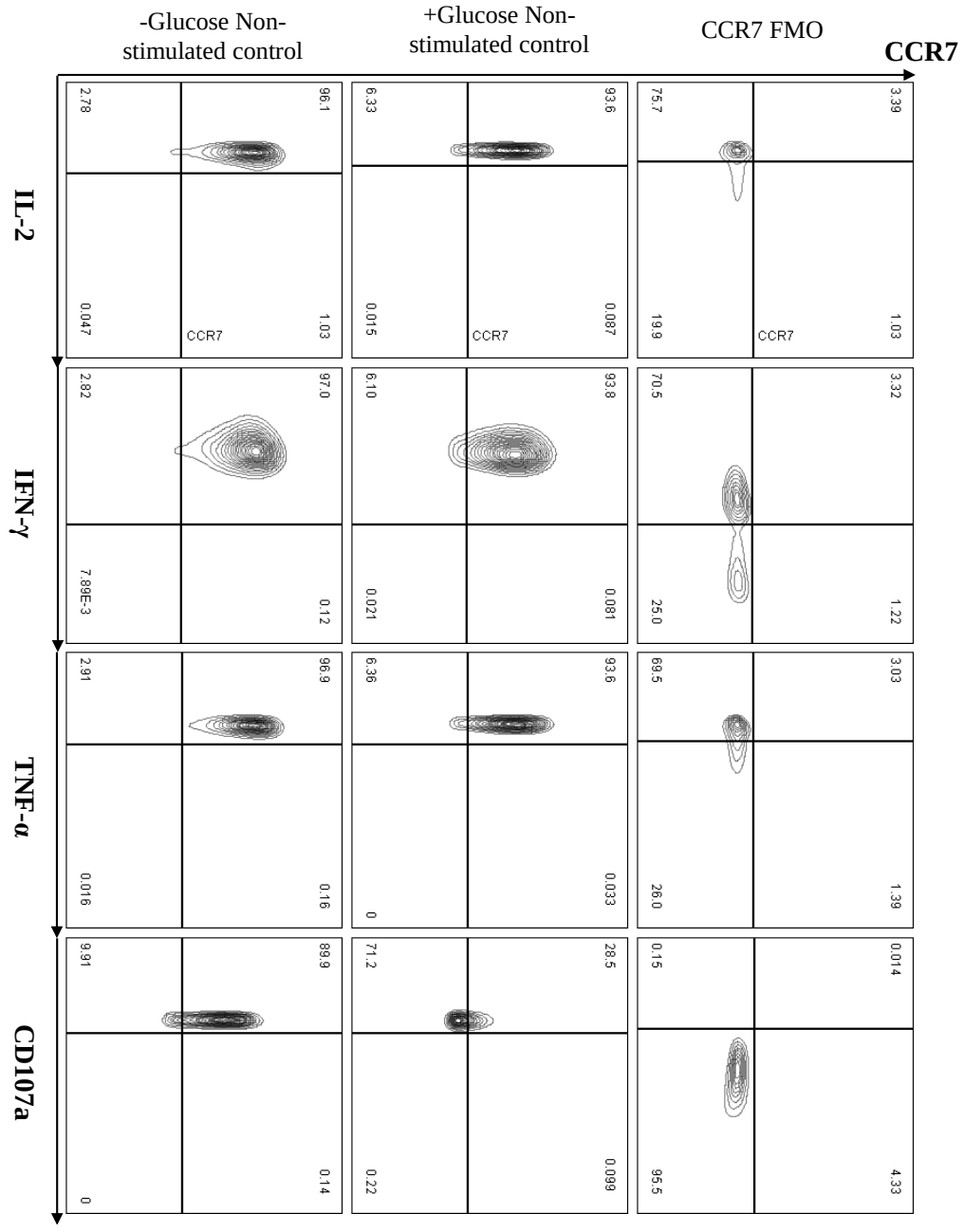

Figure A.3: Intracellular cytokine staining controls for IL-2, IFN-γ, TNF-α and CD107a.

Appendix B

Specific Consumption and Production Rates

The specific glucose consumption and lactate production rates throughout the 8 days expansion period are shown in Figure B.1.

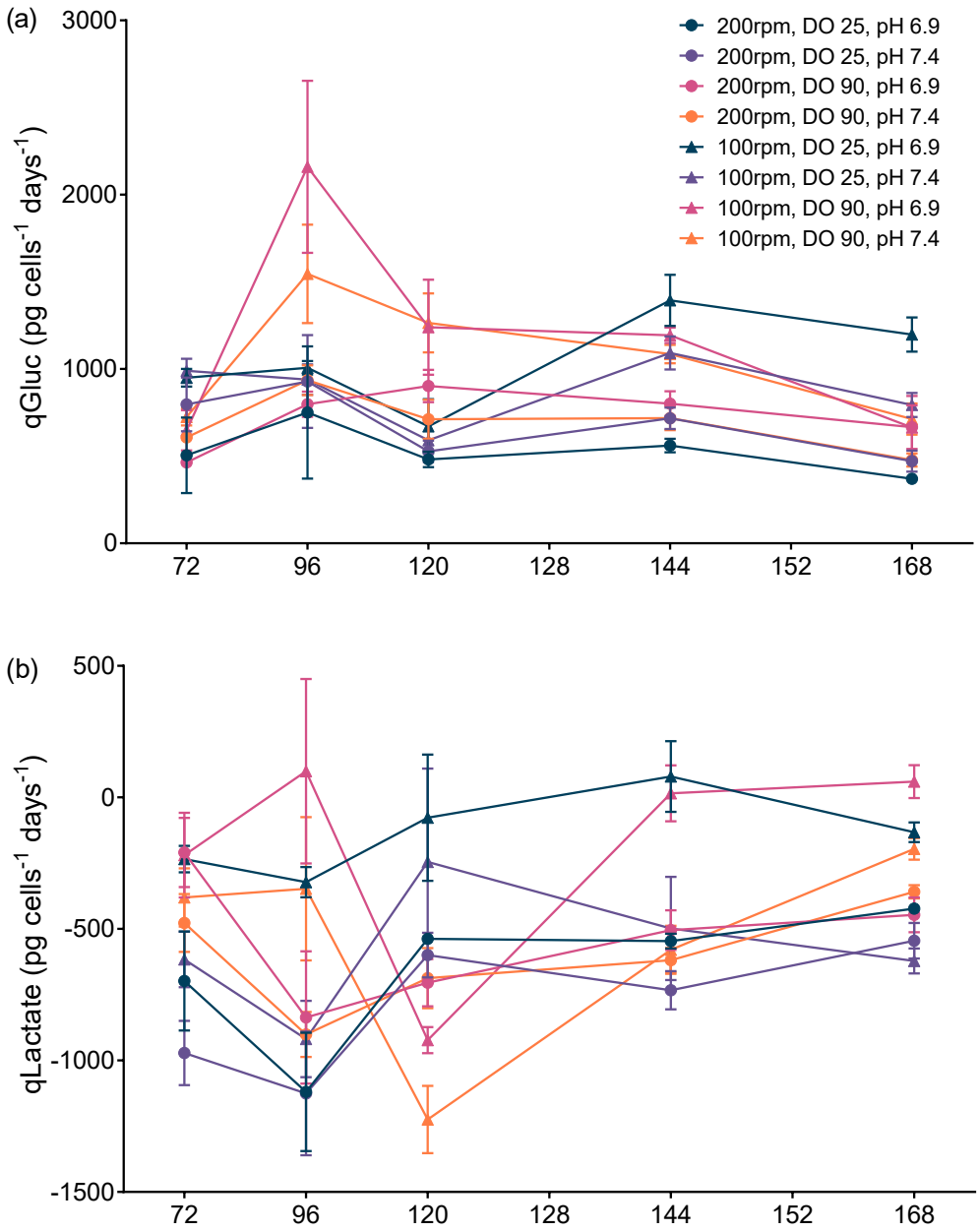

Figure B.1: Specific glucose consumption (a) and specific lactate production (b) of T cells expanded in different controlled pH and DO conditions at 100 rpm and 200 rpm agitation speeds (mean ± SD, 3 healthy donors)

References

Ali, Syed Abbas, Victoria Shi, Irina Maric, Michael Wang, David F. Stroncek, Jeremy J. Rose, Jennifer N. Brudno, Maryalice Stetler-Stevenson, Steven A. Feldman, Brenna G. Hansen, Vicki S. Fellowes, Frances T. Hakim, Ronald E. Gress, and James N. Kochenderfer (2016). "T cells expressing an anti-B-cell maturation antigen chimeric antigen receptor cause remissions of multiple myeloma". In: *Blood*. ISSN: 15280020. DOI: 10.1182/blood-2016-04-711903.

Almeida, Luis, Matthias Lochner, Luciana Berod, and Tim Sparwasser (2016). "Metabolic pathways in T cell activation and lineage differentiation". In: *Seminars in Immunology* 28.5, pp. 1–11. ISSN: 10445323. DOI: 10.1016/j.smim.2016.10.009. URL: http://linkinghub.elsevier.com/retrieve/pii/S1044532316301063.

Alnabhan, Rehab, Ahmed Gaballa, Lisa Mari Mörk, Jonas Mattsson, Michael Uhlin, and Isabelle Magalhaes (2018). "Media evaluation for production and expansion of anti-CD19 chimeric antigen receptor T cells". In: *Cytotherapy* 20.7, pp. 941–951.

ISSN: 14772566. DOI: 10.1016/j.jcyt.2018.04.007. URL: https://doi.org/10.1016/j.jcyt.2018.04.007.

An, Na, Zhongfei Tao, Saisai Li, Haiyan Xing, Kejing Tang, Zheng Tian, Qing Rao, Min Wang, and Jianxiang Wang (2016). "Construction of a new anti-CD19 chimeric antigen receptor and the anti-leukemia function study of the transduced T cells". In: *Oncotarget* 7.9, pp. 10638–10649. ISSN: 19492553. DOI: 10.18632/oncotarget.7079.

Angela, Mulki, Yusuke Endo, Hikari K. Asou, Takeshi Yamamoto, Damon J. Tumes, Hirotake Tokuyama, Koutaro Yokote, and Toshinori Nakayama (2016). "Fatty acid metabolic reprogramming via mTOR-mediated inductions of PPARγ directs early activation of T cells". In: *Nature Communications* 7, p. 13683. ISSN: 2041-1723. DOI: 10.1038/ncomms13683. URL: http://www.nature.com/doifinder/10.1038/ncomms13683.

Anthony-Gonda, Kim, Ariola Bardhi, Alex Ray, Nina Flerin, Mengyan Li, Weizao Chen, Christina Ochsenbauer, John C. Kappes, Winfried Krueger, Andrew Worden, Dina Schneider, Zhongyu Zhu, Rimas Orentas, Dimiter S. Dimitrov, Harris Goldstein, and Boro Dropulic (2019). "Multispecific anti-HIV duoCAR-T cells display broad in vitro antiviral activity and potent in vivo elimination of HIV-infected cells in a humanized mouse model". In: *Science Translational Medicine*. ISSN: 19466242. DOI: 10.1126/scitranslmed.aav5685.

Antony, Paul A., Ciriaco A. Piccirillo, Akgül Akpinarli, Steven E. Finkelstein, Paul J. Speiss, Deborah R. Surman, Douglas C. Palmer, Chi-Chao Chan, Christopher A. Klebanoff, Willem W. Overwijk, Steven A. Rosenberg, and Nicholas P. Restifo (2005). "CD8 + T Cell Immunity Against a Tumor/Self-Antigen Is Augmented by CD4 + T Helper Cells and Hindered by Naturally Occurring T Regulatory Cells". In: *The Journal of Immunology* 174.5, pp. 2591–2601. ISSN: 0022-1767. DOI: 10.4049/jimmunol.174.5.2591.

Araki, Koichi, Alexandra P. Turner, Virginia Oliva Shaffer, Shivaprakash Gangappa, Susanne A. Keller, Martin F. Bachmann, Christian P. Larsen, and Rafi Ahmed (2009). "mTOR regulates memory CD8 T-cell differentiation". In: *Nature* 460.7251, pp. 108–112. ISSN: 00280836. DOI: 10.1038/nature08155.

Ashby, B.Sterry (1966). "pH STUDIES IN HUMAN MALIGNANT TUMOURS". In: *The Lancet* 288.7458, pp. 312–315. ISSN: 01406736. DOI: 10.1016/s0140-6736(66)92598-0.

Atkuri, K. R., L. A. Herzenberg, and L. A. Herzenberg (2005). "Culturing at atmospheric oxygen levels impacts lymphocyte function". In: *Proceedings of the National Academy of Sciences* 102.10, pp. 3756–3759. ISSN: 0027-8424. DOI: 10.1073/pnas.0409910102.

Atkuri, Kondala R, Leonard A Herzenberg, Anna-Kaisa Niemi, Tina Cowan, and Leonore A Herzenberg (2007). "Importance of culturing primary lymphocytes at physiolog-

ical oxygen levels." In: *Proceedings of the National Academy of Sciences of the United States of America* 104.11, pp. 4547–52. ISSN: 0027-8424. DOI: 10.1073/pnas.0611732104. URL: http://www.pnas.org/content/104/11/4547.full.

Bajgain, Pradip, Roopa Mucharla, John Wilson, Dan Welch, Usanarat Anurathapan, Bitao Liang, Xiaohua Lu, Kyle Ripple, John M Centanni, Christine Hall, David Hsu, Larry a Couture, Shubhranshu Gupta, Adrian P Gee, Helen E Heslop, Ann M Leen, Cliona M Rooney, and Juan F Vera (2014). "Optimizing the production of suspension cells using the G-Rex "M" series." In: *Molecular therapy. Methods & clinical development* 1.January, p. 14015. ISSN: 2329-0501. DOI: 10.1038/mtm.2014.15. URL: http://www.pubmedcentral.nih.gov/articlerender.fcgi?artid=4362380%7B%5C&%7Dtool=pmcentrez%7B%5C&%7Drendertype=abstract.

Barber, Daniel L., E. John Wherry, David Masopust, Baogong Zhu, James P. Allison, Arlene H. Sharpe, Gordon J. Freeman, and Rafi Ahmed (2006). "Restoring function in exhausted CD8 T cells during chronic viral infection". In: *Nature* 439.7077, pp. 682–687. ISSN: 00280836. DOI: 10.1038/nature04444.

Barrett, David M., Nathan Singh, Xiaojun Liu, Shuguang Jiang, Carl H. June, Stephan A. Grupp, and Yangbing Zhao (2014). "Relation of clinical culture method to T-cell memory status and efficacy in xenograft models of adoptive immunotherapy". In: *Cytotherapy* 16.5, pp. 619–630. ISSN: 14772566. DOI: 10.1016/j.jcyt.2013.10.013. URL: http://dx.doi.org/10.1016/j.jcyt.2013.10.013.

Bauer, Daniel E, Georgia Hatzivassiliou, Fangping Zhao, Charalambos Andreadis, and Craig B Thompson (Sept. 2005). "ATP citrate lyase is an important component of cell growth and transformation". In: *Oncogene* 24.41, pp. 6314–6322. ISSN: 0950-9232. DOI: 10.1038/sj.onc.1208773. URL: http://www.ncbi.nlm.nih.gov/pubmed/16007201%20http://www.nature.com/doifinder/10.1038/sj.onc.1208773.

Bellone, Matteo and Arianna Calcinotto (2013). *Ways to enhance lymphocyte trafficking into tumors and fitness of tumor infiltrating lymphocytes*. DOI: 10.3389/fonc.2013.00231.

Berahovich, Robert, Xianghong Liu, Hua Zhou, Elias Tsadik, Shirley Xu, Vita Golubovskaya, and Lijun Wu (2019). "Hypoxia Selectively Impairs CAR-T Cells In Vitro". In: *Cancers* 11.5, p. 602. DOI: 10.3390/cancers11050602.

Berg, J M, J L Tymoczko, and L Stryer (2012). "Biochemistry, 7th Edition". In: *W H Freeman*.

Berg, J, J Tymoczko, and L Stryer (2002). *Biochemistry, 5th edition*. ISBN: 0-7167-3051-0.

Berod, Luciana, Christin Friedrich, Amrita Nandan, Jenny Freitag, Stefanie Hagemann, Kirsten Harmrolfs, Aline Sandouk, Christina Hesse, Carla N. Castro, Heike BaHre, Sarah K. Tschirner, Nataliya Gorinski, Melanie Gohmert, Christian T. Mayer, Jochen Huehn, Evgeni Ponimaskin, Wolf Rainer Abraham, Rolf MüLler, Matthias Lochner,

and Tim Sparwasser (2014). “De novo fatty acid synthesis controls the fate between regulatory T and T helper 17 cells”. In: *Nature Medicine* 20.11. ISSN: 1546170X. DOI: 10.1038/nm.3704.

Bestor, Timothy H. (2000). *Gene silencing as a threat to the success of gene therapy*. DOI: 10.1172/JCI9459.

Blank, Christian and Andreas Mackensen (2007). “Contribution of the PD-L1/PD-1 pathway to T-cell exhaustion: An update on implications for chronic infections and tumor evasion”. In: *Cancer Immunology, Immunotherapy* 56.5, pp. 739–745. ISSN: 03407004. DOI: 10.1007/s00262-006-0272-1.

Blat, Dan, Ehud Zigmond, Zoya Alteber, Tova Waks, and Zelig Eshhar (2014). “Suppression of murine colitis and its associated cancer by carcinoembryonic antigen-specific regulatory T cells”. In: *Molecular Therapy*. ISSN: 15250024. DOI: 10.1038/mt.2014.41.

Boardman, D. A., C. Philippeos, G. O. Fruhwirth, M. A.A. Ibrahim, R. F. Hannen, D. Cooper, F. M. Marelli-Berg, F. M. Watt, R. I. Lechler, J. Maher, L. A. Smyth, and G. Lombardi (2017). “Expression of a Chimeric Antigen Receptor Specific for Donor HLA Class I Enhances the Potency of Human Regulatory T Cells in Preventing Human Skin Transplant Rejection”. In: *American Journal of Transplantation*. ISSN: 16006143. DOI: 10.1111/ajt.14185.

Bohnenkamp, H., U. Hilbert, and T. Noll (2002). "Bioprocess development for the cultivation of human T-lymphocytes in a clinical scale". In: *Cytotechnology* 38.1-3, pp. 135–145. ISSN: 09209069. DOI: 10.1023/A:1021174619613.

Bonifant, Challice L., Hollie J. Jackson, Renier J. Brentjens, and Kevin J. Curran (2016). "Toxicity and management in CAR T-cell therapy". In: *Molecular Therapy - Oncolytics* 3.January, p. 16011. ISSN: 23727705. DOI: 10.1038/mto.2016.11. URL: http://dx.doi.org/10.1038/mto.2016.11.

Bosticardo, Marita, Silvia Ariotti, Giuliana Losana, Paola Bernabei, and Francesco Novelli (2001). "Biased activation of human T lymphocytes due to low extracellular pH is antagonized by B7 / CD28 costimulation". In: pp. 2829–2838.

Braun, Rod D., Jennifer L. Lanzen, Stacey A. Snyder, and Mark W. Dewhirst (2001). "Comparison of tumor and normal tissue oxygen tension measurements using OxyLite or microelectrodes in rodents". In: *American Journal of Physiology-Heart and Circulatory Physiology* 280.6, H2533–H2544. ISSN: 0363-6135. DOI: 10.1152/ajpheart.2001.280.6.h2533.

Brentjens, Renier J, Marco L Davila, Isabelle Riviere, Jae Park, Xiuyan Wang, Lindsay G Cowell, Shirley Bartido, Jolanta Stefanski, Clare Taylor, Malgorzata Olszewska, Oriana Borquez-Ojeda, Jinrong Qu, Teresa Wasielewska, Qing He, Yvette Bernal, Ivelise V Rijo, Cyrus Hedvat, Rachel Kobos, Kevin Curran, Peter Steinherz, Joseph Jurcic, Todd Rosenblat, Peter Maslak, Mark Frattini, and Michel Sadelain (n.d.[a]).

"CD19-Targeted T Cells Rapidly Induce Molecular Remissions in Adults with Chemotherapy-Refractory Acute Lymphoblastic Leukemia". In: (). URL: http://stm.sciencemag.org/content/scitransmed/5/177/177ra38.full.pdf.

Brentjens, Renier J, Isabelle Rivie, Jae H Park, Marco L Davila, Xiuyan Wang, Jolanta Stefanski, Clare Taylor, Raymond Yeh, Shirley Bartido, Oriana Borquez-Ojeda, Malgorzata Olszewska, Yvette Bernal, Hollie Pegram, Mark Przybylowski, Daniel Hollyman, Yelena Usachenko, Domenick Pirraglia, James Hosey, Elmer Santos, Elizabeth Halton, Peter Maslak, David Scheinberg, Joseph Jurcic, Mark Heaney, Glenn Heller, Mark Frattini, and Michel Sadelain (n.d.[b]). "Safety and persistence of adoptively transferred autologous CD19-targeted T cells in patients with relapsed or chemotherapy refractory B-cell leukemias". In: (). DOI: 10.1182/blood-2011-04-348540. URL: http://www.bloodjournal.org/content/bloodjournal/118/18/4817.full.pdf.

Brindley, David A., Natasha L. Davie, Emily J. Culme-Seymour, Chris Mason, David W. Smith, and Jon A. Rowley (2012). *Peak serum: Implications of serum supply for cell therapy manufacturing*. DOI: 10.2217/rme.11.112.

Brocker, Thomas (2000). *Chimeric Fv-zeta or Fv-epsilon receptors are not sufficient to induce activation or cytokine production in peripheral T cells. - PubMed - NCBI*. URL: https://www.ncbi.nlm.nih.gov/pubmed/10961908 (visited on 11/04/2019).

Brocker, Thomas and Klaus Karjalainen (May 1995). “Signals through T cell receptor-ζ chain alone are insufficient to prime resting T lymphocytes”. In: *Journal of Experimental Medicine* 181.5, pp. 1653–1659. ISSN: 15409538. DOI: 10.1084/jem.181.5.1653.

Brudno, Jennifer N., Irina Maric, Steven D. Hartman, Jeremy J. Rose, Michael Wang, Norris Lam, Maryalice Stetler-Stevenson, Dalia Salem, Constance Yuan, Steven Pavletic, Jennifer A. Kanakry, Syed Abbas Ali, Lekha Mikkilineni, Steven A. Feldman, David F. Stroncek, Brenna G. Hansen, Judith Lawrence, Rashmika Patel, Frances Hakim, Ronald E. Gress, and James N. Kochenderfer (2018). “T cells genetically modified to express an anti -B-Cell maturation antigen chimeric antigen receptor cause remissions of poor-prognosis relapsed multiple myeloma”. In: *Journal of Clinical Oncology*. ISSN: 15277755. DOI: 10.1200/JCO.2018.77.8084.

Brunner, Matthias, Jens Fricke, Paul Kroll, and Christoph Herwig (2017). “Investigation of the interactions of critical scale-up parameters (pH, pO2 and pCO2) on CHO batch performance and critical quality attributes”. In: *Bioprocess and Biosystems Engineering* 40.2, pp. 251–263. ISSN: 16157605. DOI: 10.1007/s00449-016-1693-7.

Busch, Dirk H., Simon P. Frassle, Daniel Sommermeyer, Veit R. Buchholz, and Stanley R. Riddell (2016). “Role of memory T cell subsets for adoptive immunotherapy”. In:

Seminars in Immunology 28.1, pp. 28–34. ISSN: 10963618. DOI: 10.1016/j.smim.2016.02.001. URL: http://dx.doi.org/10.1016/j.smim.2016.02.001.

Byersdorfer, Craig A., Victor Tkachev, Anthony W. Opipari, Stefanie Goodell, Jacob Swanson, Stacy Sandquist, Gary D. Glick, and James L.M. Ferrara (2013). "Effector T cells require fatty acid metabolism during murine graft-versus-host disease". In: *Blood* 122.18, pp. 3230–3237. ISSN: 15280020. DOI: 10.1182/blood-2013-04-495515.

Calcinotto, Arianna, Paola Filipazzi, Matteo Grioni, Manuela Iero, Angelo De Milito, Alessia Ricupito, Agata Cova, Rossella Canese, Elena Jachetti, Monica Rossetti, Veronica Huber, Giorgio Parmiani, Luca Generoso, Mario Santinami, Martina Borghi, Stefano Fais, Matteo Bellone, and Licia Rivoltini (2012). "Modulation of microenvironment acidity reverses anergy in human and murine tumor-infiltrating T lymphocytes". In: *Cancer Research* 72.11, pp. 2746–2756. ISSN: 00085472. DOI: 10.1158/0008-5472.CAN-11-1272.

Caldwell, Charles C., Hidefumi Kojima, Dmitriy Lukashev, John Armstrong, Mark Farber, Sergey G. Apasov, and Michail V. Sitkovsky (2001). "Differential Effects of Physiologically Relevant Hypoxic Conditions on T Lymphocyte Development and Effector Functions". In: *The Journal of Immunology* 167.11, pp. 6140–6149. ISSN: 0022-1767. DOI: 10.4049/jimmunol.167.11.6140.

Canestrari, Emanuele, Hayley R. Steidinger, Brianna McSwain, Steven J. Charlebois, and Christina Tenenhaus Dann (2019). "Human platelet lysate media supplement supports lentiviral transduction and expansion of human T lymphocytes while maintaining memory phenotype". In: *Journal of Immunology Research*. ISSN: 23147156. DOI: 10.1155/2019/3616120.

Cao, Yilin, Jeffrey C. Rathmell, and Andrew N. Macintyre (2014). "Metabolic reprogramming towards aerobic glycolysis correlates with greater proliferative ability and resistance to metabolic inhibition in CD8 versus CD4 T cells". In: *PLoS ONE* 9.8, pp. 1–15. ISSN: 19326203. DOI: 10.1371/journal.pone.0104104.

Carr, Erikka L., Alina Kelman, Glendon S. Wu, Ravindra Gopaul, Emilee Senkevitch, Anahit Aghvanyan, Achmed M. Turay, and Kenneth A. Frauwirth (2010). "Glutamine Uptake and Metabolism Are Coordinately Regulated by ERK/MAPK during T Lymphocyte Activation". In: *The Journal of Immunology* 185.2, pp. 1037–1044. ISSN: 0022-1767. DOI: 10.4049/jimmunol.0903586.

Carreau, Aude, Bouchra El Hafny-Rahbi, Agata Matejuk, Catherine Grillon, and Claudine Kieda (2011). "Why is the partial oxygen pressure of human tissues a crucial parameter? Small molecules and hypoxia". In: *Journal of Cellular and Molecular Medicine* 15.6, pp. 1239–1253. ISSN: 15821838. DOI: 10.1111/j.1582-4934.2011.01258.x.

Carswell, K S and E T Papoutsakis (2000). “Extracellular pH affects the proliferation of cultured human T cells and their expression of the interleukin-2 receptor.” In: *Journal of immunotherapy (Hagerstown, Md. : 1997)* 23.6, pp. 669–74. ISSN: 1524-9557. URL: http://www.ncbi.nlm.nih.gov/pubmed/11186155.

Cha, Esther, Laura Graham, Masoud H Manjili, and Harry D Bear (July 2010). “IL-7 + IL-15 are superior to IL-2 for the ex vivo expansion of 4T1 mammary carcinoma-specific T cells with greater efficacy against tumors in vivo.” In: *Breast cancer research and treatment* 122.2, pp. 359–69. ISSN: 1573-7217. DOI: 10.1007/s10549-009-0573-0. URL: http://www.ncbi.nlm.nih.gov/pubmed/19826947%20http://www.pubmedcentral.nih.gov/articlerender.fcgi?artid=PMC4033304.

Cham, Candace M., Gregory Driessens, James P. O’Keefe, and Thomas F. Gajewski (2008). “Glucose deprivation inhibits multiple key gene expression events and effector functions in CD8+ T cells”. In: *European Journal of Immunology* 38.9, pp. 2438–2450. ISSN: 00142980. DOI: 10.1002/eji.200838289.

Cham, Candace M. and Thomas F. Gajewski (2005). “ Glucose Availability Regulates IFN-γ Production and p70S6 Kinase Activation in CD8 + Effector T Cells ”. In: *The Journal of Immunology* 174.8, pp. 4670–4677. ISSN: 0022-1767. DOI: 10.4049/jimmunol.174.8.4670.

Chang, Chih Hao, Jonathan D. Curtis, Leonard B. Maggi, Brandon Faubert, Alejandro V. Villarino, David O'Sullivan, Stanley Ching Cheng Huang, Gerritje J.W. Van Der Windt, Julianna Blagih, Jing Qiu, Jason D. Weber, Edward J. Pearce, Russell G. Jones, and Erika L. Pearce (2013). "XPosttranscriptional control of T cell effector function by aerobic glycolysis". In: *Cell* 153.6, p. 1239. ISSN: 10974172. DOI: 10.1016/j.cell.2013.05.016. URL: http://dx.doi.org/10.1016/j.cell.2013.05.016.

Chaoul, Nada, Catherine Fayolle, Belinda Desrues, Marine Oberkampf, Alexandre Tang, Daniel Ladant, and Claude Leclerc (2015). "Rapamycin impairs antitumor CD8p T-cell responses and vaccine-induced tumor eradication". In: *Cancer Research*. ISSN: 15387445. DOI: 10.1158/0008-5472.CAN-15-0454.

Chaturvedi, Kirti, Susan Y. Sun, Thomas O'Brien, Yan J. Liu, and James W. Brooks (2014). "Comparison of the behavior of CHO cells during cultivation in 24-square deep well microplates and conventional shake flask systems". In: *Biotechnology Reports* 1-2, pp. 22–26. ISSN: 2215017X. DOI: 10.1016/j.btre.2014.04.001. URL: http://dx.doi.org/10.1016/j.btre.2014.04.001.

Chauvin, Joe-marc, Alan J Korman, Hassane M Zarour, Joe-marc Chauvin, Ornella Pagliano, Julien Fourcade, Zhaojun Sun, Hong Wang, Cindy Sander, John M Kirkwood, Tseng-hui Timothy Chen, Mark Maurer, Alan J Korman, and Hassane M Zarour (2015). "TIGIT and PD-1 impair tumor antigen - specific CD8 + T cells

in melanoma patients". In: *Journal of Clinical Investigation* 125.5, pp. 2046–2058. DOI: 10.1172/JCI80445.and.

Chiao, J. W., M. Heil, Z. Arlin, J. D. Lutton, Y. S. Choi, and K. Leung (1986). "Suppression of lymphocyte activation and functions by a leukemia cell-derived inhibitor". In: *Proceedings of the National Academy of Sciences of the United States of America* 83.10, pp. 3432–3436. ISSN: 00278424. DOI: 10.1073/pnas.83.10.3432.

Cieri, Nicoletta, Barbara Camisa, Fabienne Cocchiarella, Mattia Forcato, Giacomo Oliveira, Elena Provasi, Attilio Bondanza, Claudio Bordignon, Jacopo Peccatori, Fabio Ciceri, Maria Teresa Lupo-Stanghellini, Fulvio Mavilio, Anna Mondino, Silvio Bicciato, Alessandra Recchia, and Chiara Bonini (Jan. 2013). "IL-7 and IL-15 instruct the generation of human memory stem T cells from naive precursors." In: *Blood* 121.4, pp. 573–84. ISSN: 1528-0020. DOI: 10.1182/blood-2012-05-431718. URL: http://www.ncbi.nlm.nih.gov/pubmed/23160470.

Conticello, Concetta, Francesca Pedini, Ann Zeuner, Mariella Patti, Monica Zerilli, Giorgio Stassi, Angelo Messina, Cesare Peschle, and Ruggero De Maria (2004). "IL-4 Protects Tumor Cells from Anti-CD95 and Chemotherapeutic Agents via Up-Regulation of Antiapoptotic Proteins". In: *The Journal of Immunology* 172.9, pp. 5467–5477. ISSN: 0022-1767. DOI: 10.4049/jimmunol.172.9.5467.

Corbet, Cyril and Olivier Feron (2017). "Tumour acidosis: From the passenger to the driver's seat". In: *Nature Reviews Cancer* 17.10, pp. 577–593. ISSN: 14741768. DOI: 10.1038/nrc.2017.77.

Costariol, Elena, Marco Rotondi, Arman Amini, Christopher J. Hewitt, Alvin W. Nienow, Thomas R.J. Heathman, Martina Micheletti, and Qasim A. Rafiq (2019). "Establishing the scalable manufacture of primary human T cells in an automated stirred tank bioreactor". In: *Biotechnology and Bioengineering*, bit.27088. ISSN: 0006-3592. DOI: 10.1002/bit.27088. URL: https://onlinelibrary.wiley.com/doi/abs/10.1002/bit.27088.

Cruz, Helder J, L Moreira, and Manuel J T Carrondo (1999). "Metabolic Shifts by Nutrient". In: *Biotechnology*.

Cui, Guoliang, Matthew M. Staron, Simon M. Gray, Ping Chih Ho, Robert A. Amezquita, Jingxia Wu, and Susan M. Kaech (2015). "IL-7-induced glycerol transport and TAG synthesis promotes memory CD8+ T cell longevity". In: *Cell* 161.4, pp. 750–761. ISSN: 10974172. DOI: 10.1016/j.cell.2015.03.021. arXiv: 15334406. URL: http://dx.doi.org/10.1016/j.cell.2015.03.021.

Cui, Weiguo and Susan M. Kaech (2010). "Generation of effector CD8+ T cells and their conversion to memory T cells". In: *Immunological Reviews* 236.1, pp. 151–166. ISSN: 01052896. DOI: 10.1111/j.1600-065X.2010.00926.x.

Davila, Marco L, Isabelle Riviere, Xiuyan Wang, Shirley Bartido, Jae Park, Kevin Curran, Stephen S Chung, Jolanta Stefanski, Oriana Borquez-Ojeda, Malgorzata Olszewska, Jinrong Qu, Teresa Wasielewska, Qing He, Mitsu Fink, Himaly Shinglot, Maher Youssif, Mark Satter, Yongzeng Wang, James Hosey, Hilda Quintanilla, Elizabeth Halton, Yvette Bernal, Diana C G Bouhassira, Maria E Arcila, Mithat Gonen, Gail J Roboz, Peter Maslak, Dan Douer, Mark G Frattini, Sergio Giralt, Michel Sadelain, and Renier Brentjens (2014). "No Title". In: *Sci. Transl. Med* 6, pp. 224–25. DOI: 10.1126/scitranslmed.3008226. URL: http://stm.sciencemag.org/content/scitransmed/6/224/224ra25.full.pdf%20www.sciencetranslationalmedicine.org/cgi/content/full/6/224/224ra25/DC1.

DeBerardinis, Ralph J., Nabil Sayed, Dara Ditsworth, and Craig B. Thompson (2008). "Brick by brick: metabolism and tumor cell growth". In: *Current Opinion in Genetics and Development* 18.1, pp. 54–61. ISSN: 0959437X. DOI: 10.1016/j.gde.2008.02.003.

Denman, A.M. (1992). "Cellular and Molecular Immunology". In: *Postgraduate Medical Journal*. ISSN: 0032-5473. DOI: 10.1136/pgmj.68.798.305.

DeRenzo, Christopher and Stephen Gottschalk (2019). "Genetic modification strategies to enhance CAR T cell persistence for patients with solid tumors". In: *Frontiers*

in Immunology 10.FEB, pp. 1–8. ISSN: 16643224. DOI: 10.3389/fimmu.2019.00218.

DeZengotita, Vivian M., Roy Kimura, and William M. Miller (2011). "Effects of CO2 and osmolality on hybridoma cells: growth, metabolism and monoclonal antibody production". In: 1, pp. 213–227. DOI: 10.1007/978-94-011-4786-622.

Dobson, G. P., E. Yamamoto, and P. W. Hochachka (1986). "Phosphofructokinase control in muscle: nature and reversal of pH-dependent ATP inhibition". In: *American Journal of Physiology-Regulatory, Integrative and Comparative Physiology* 250.1, R71–R76. ISSN: 0363-6119. DOI: 10.1152/ajpregu.1986.250.1.r71.

Driessens, Gregory, Justin Kline, and Thomas F Gajewski (May 2009). "Costimulatory and coinhibitory receptors in anti-tumor immunity." In: *Immunological reviews* 229.1, pp. 126–44. ISSN: 1600-065X. DOI: 10.1111/j.1600-065X.2009.00771.x. URL: http://www.ncbi.nlm.nih.gov/pubmed/19426219%20http://www.pubmedcentral.nih.gov/articlerender.fcgi?artid=PMC3278040.

Dudley, Mark E., John R. Wunderlich, Thomas E. Shelton, Jos Even, and Steven A. Rosenberg (2003). "Generation of Tumor-Infiltrating Lymphocyte Cultures for Use in Adoptive Transfer Therapy for Melanoma Patients". In: *Journal of Immunotherapy* 26.4, pp. 332–342. ISSN: 15374513. DOI: 10.1097/00002371-200307000-00005.

Dziurla, R., T. Gaber, M. Fangradt, M. Hahne, R. Tripmacher, P. Kolar, C. M. Spies, G. R. Burmester, and F. Buttgereit (2010). "Effects of hypoxia and/or lack of glucose on cellular energy metabolism and cytokine production in stimulated human CD4+ T lymphocytes". In: *Immunology Letters* 131.1, pp. 97–105. ISSN: 01652478. DOI: 10.1016/j.imlet.2010.02.008. URL: http://dx.doi.org/10.1016/j.imlet.2010.02.008.

Ecker, Christopher, Lili Guo, Stefana Voicu, Luis Gil-de-Gómez, Andrew Medvec, Luis Cortina, Jackie Pajda, Melanie Andolina, Maria Torres-Castillo, Jennifer L. Donato, Sarya Mansour, Evan R. Zynda, Pei Yi Lin, Angel Varela-Rohena, Ian A. Blair, and James L. Riley (2018). "Differential Reliance on Lipid Metabolism as a Salvage Pathway Underlies Functional Differences of T Cell Subsets in Poor Nutrient Environments". In: *Cell Reports* 23.3, pp. 741–755. ISSN: 22111247. DOI: 10.1016/j.celrep.2018.03.084.

Eguchi, J., K. Hiroishi, S. Ishii, T. Baba, T. Matsumura, A. Hiraide, H. Okada, and M. Imawari (2005). "Interleukin-4 gene transduced tumor cells promote a potent tumor-specific Th1-type response in cooperation with interferon-α transduction". In: *Gene Therapy* 12.9, pp. 733–741. ISSN: 09697128. DOI: 10.1038/sj.gt.3302401.

Erdogan, Beril, Esra Uzaslan, Ferah Budak, Mehmet Karadag, Dane Ediger, Barbaros Oral, Güher Göral, Ercüment Ege, and Oktay Gözü (2005). "The evaluation of solu-

ble Fas and soluble Fas ligand levels of bronchoalveolar lavage fluid in lung cancer patients." In: *Tüberküloz ve toraks*. ISSN: 04941373.

Erecifska, M, J Deas, and I. A Silver (1995). "The Effect of pH on Glycolysis and Phosphofructokinase Activity in Cultured Cells and Synaptosomes". In: *Journal of Neurochemistry* 65.6, pp. 2765–2772. ISSN: 1471-4159. DOI: 10.1046/j.1471-4159.1995.65062765.x.

Erra Diaz, Fernando, Ezequiel Dantas, and Jorge Geffner (2018). "Unravelling the interplay between extracellular acidosis and immune cells". In: *Mediators of Inflammation* 2018. ISSN: 14661861. DOI: 10.1155/2018/1218297.

Eshhar, Z., T. Waks, G. Gross, and D. G. Schindler (1993). "Specific activation and targeting of cytotoxic lymphocytes through chimeric single chains consisting of antibody-binding domains and the γ or ζ subunits of the immunoglobulin and T-cell receptors". In: *Proceedings of the National Academy of Sciences of the United States of America* 90.2, pp. 720–724. ISSN: 00278424. DOI: 10.1073/pnas.90.2.720.

Fabbri, M, R Ridolfi, R Maltoni, L Ridolfi, A Riccobon, E Flamini, F De Paola, G M Verdecchia, and D Amadori (n.d.). "Tumor infiltrating lymphocytes and continuous infusion interleukin-2 after metastasectomy in 61 patients with melanoma, colorectal and renal carcinoma." In: *Tumori* 86.1 (), pp. 46–52. ISSN: 0300-8916. URL: http://www.ncbi.nlm.nih.gov/pubmed/10778766.

Fauci, Anthony S., Domenico Mavilio, and Shyam Kottilil (2005). "Erratum: NK cells in hiv infection: Paradigm for protection or targets for ambush (Nature Reviews Immunology (2005) 5 (835-843))". In: *Nature Reviews Immunology* 5.11, p. 844. ISSN: 14741733. DOI: 10.1038/nri1710.

Fedorov, Victor D., Maria Themeli, and Michel Sadelain (2013). "PD-1- and CTLA-4-based inhibitory chimeric antigen receptors (iCARs) divert off-target immunotherapy responses". In: *Science Translational Medicine*. ISSN: 19466234. DOI: 10.1126/scitranslmed.3006597.

Feng, Li, Hashimura Yasunori, Pendleton Robert, Harms Jean, Collins Erin, and Lee Brian (2006). "A Systematic Approach for Scale-Down Model Development and Characterization of Commercial Cell Culture Processes". In: *Biotechnology Progress* 22.3, pp. 696–703. URL: http://ejournals.ebsco.com/direct.asp?ArticleID=40A19AAB0AEA2F993FC7.

Festag, Marvin M., Julia Festag, Simon P. Fraßle, Theresa Asen, Julia Sacherl, Sophia Schreiber, Martin A. Mück-Hausl, Dirk H. Busch, Karin Wisskirchen, and Ulrike Protzer (2019). "Evaluation of a Fully Human, Hepatitis B Virus-Specific Chimeric Antigen Receptor in an Immunocompetent Mouse Model". In: *Molecular Therapy*. ISSN: 15250024. DOI: 10.1016/j.ymthe.2019.02.001.

Fischer, Karin, Simon Voelkl, Norbert Meidenbauer, Julia Ammer, Eva Gottfried, Sabine Schwarz, Gregor Rothe, Sabine Hoves, Kathrin Renner, Birgit Timischl, Andreas

Mackensen, Leoni Kunz-Schughart, Reinhard Andreesen, Stefan W Krause, and Marina Kreutz (2007). "Inhibitory effect of tumor cell-derived lactic acid on human T cells." In: *Blood* 109.9, pp. 3812–3819. DOI: 10.1182/blood-2006-07-035972. URL: http://eutils.ncbi.nlm.nih.gov/entrez/eutils/elink.fcgi?dbfrom=pubmed%7B%5C&%7Did=17255361%7B%5C&%7Dretmode=ref%7B%5C&%7Dcmd=prlinks.

Fletcher, Matthew, Maria E. Ramirez, Rosa A. Sierra, Patrick Raber, Paul Thevenot, Amir A. Al-Khami, Dulfary Sanchez-Pino, Claudia Hernez, Dorota D. Wyczechowska, Augusto C. Ochoa, and Paulo C. Rodriguez (2015). "L-Arginine depletion blunts antitumor T-cell responses by inducing myeloid-derived suppressor cells". In: *Cancer Research* 75.2, pp. 275–283. ISSN: 15387445. DOI: 10.1158/0008-5472.CAN-14-1491.

Fraietta, Joseph A, Simon F Lacey, Elena J Orlando, Iulian Pruteanu-malinici, Mercy Gohil, Stefan Lundh, Alina C Boesteanu, Yan Wang, Roddy S O Connor, Wei-ting Hwang, Edward Pequignot, David E Ambrose, Changfeng Zhang, Nicholas Wilcox, Felipe Bedoya, Corin Dorfmeier, Fang Chen, Lifeng Tian, Harit Parakandi, Minal Gupta, Regina M Young, F Brad Johnson, Irina Kulikovskaya, Li Liu, Jun Xu, Sadik H Kassim, Megan M Davis, Bruce L Levine, Noelle V Frey, Donald L Siegel, Alexander C Huang, E John Wherry, Hans Bitter, Jennifer L Brogdon, David L Porter, Carl H June, and J Joseph Melenhorst (2018). "Determinants of response

and resistance to CD19 chimeric antigen receptor (CAR) T cell therapy of chronic lymphocytic leukemia". In: ISSN: 1078-8956. DOI: 10.1038/s41591-018-0010-1.

Frauwirth, Kenneth A. and Craig B. Thompson (2002a). "Activation and inhibition of lymphocytes by costimulation". In: *The Journal of Clinical Investigation* 109.3. DOI: 10.1172/JCI200214941.

Frauwirth, Kenneth A, James L Riley, Marian H Harris, Richard V Parry, Jeffrey C Rathmell, David R Plas, Rebecca L Elstrom, Carl H June, and Craig B Thompson (2002b). "The CD28 Signaling Pathway Regulates Glucose Metabolism of metabolism in response to changes in cellular condi- tions. However, it has recently been shown that signals from cell surface receptors are required to control the ability of resting cells to tak". In: *Immunity* 16, pp. 769–777. ISSN: 10747613. DOI: 10.1016/S1074-7613(02)00323-0.

Fujita, K, H Ikarashi, K Takakuwa, S Kodama, A Tokunaga, T Takahashi, and K Tanaka (May 1995). "Prolonged disease-free period in patients with advanced epithelial ovarian cancer after adoptive transfer of tumor-infiltrating lymphocytes." In: *Clinical cancer research : an official journal of the American Association for Cancer Research* 1.5, pp. 501–7. ISSN: 1078-0432. URL: http://www.ncbi.nlm.nih.gov/pubmed/9816009.

Gabrilovich, Dmitry, Tadao Ishida, Tsunehiro Oyama, Sophia Ran, Vladimir Kravtsov, Sorena Nadaf, and David P. Carbone (1998). "Vascular endothelial growth factor inhibits the development of dendritic cells and dramatically affects the differentiation of multiple hematopoietic lineages in vivo". In: *Blood*. ISSN: 00064971. DOI: 10.1182/blood.v92.11.4150.

Gagnon, Matthew, Gregory Hiller, Yen Tung Luan, Amy Kittredge, Jordy Defelice, and Denis Drapeau (2011). "High-End pH-controlled delivery of glucose effectively suppresses lactate accumulation in CHO Fed-batch cultures". In: *Biotechnology and Bioengineering* 108.6, pp. 1328–1337. ISSN: 00063592. DOI: 10.1002/bit.23072.

Gardner, Rebecca A, Olivia Finney, Colleen Annesley, Hannah Brakke, Corinne Summers, Kasey Leger, Marie Bleakley, Christopher Brown, Stephanie Mgebroff, Karen S Kelly-Spratt, Virginia Hoglund, Catherine Lindgren, Assaf P Oron, Daniel Li, Stanley R Riddell, Julie R Park, and Michael C Jensen (2017). "Intent-to-treat leukemia remission by CD19 CAR T cells of defined formulation and dose in children and young adults". In: *Blood* 129.25. DOI: 10.1182/blood-2017-02-769208. URL: http://www.bloodjournal.org/content/bloodjournal/129/25/3322.full.pdf.

Gattinoni, L, Christopher A. Klebanoff, Douglas C. Palmer, Claudia Wrzesinski, Keith Kerstann, Zhiya Yu, Steven E. Finkelstein, Marc R. Theoret, Steven A. Rosenberg, and Nicholas P. Restifo (2005). "Acquisition of full effector function in vitro para-

doxically impairs the in vivo antitumor efficacy of adoptively transferred CD8+ T cells". In: *Journal of Clinical Investigation* 115.6, pp. 1616–1626. ISSN: 00219738. DOI: 10.1172/JCI24480.

Gattinoni, L, Enrico Lugli, Yun Ji, Zoltan Pos, Chrystal M Paulos, Maire F Quigley, Jorge R Almeida, Emma Gostick, Zhiya Yu, Carmine Carpenito, Ena Wang, Daniel C Douek, David A Price, Carl H June, Francesco M Marincola, Mario Roederer, and Nicholas P Restifo (Sept. 2011). "A human memory T cell subset with stem cell -like properties". In: *Nature Medicine* 17.10, pp. 1290–1297. ISSN: 1078-8956. DOI: 10.1038/nm.2446. URL: http://www.ncbi.nlm.nih.gov/pubmed/21926977%20http://www.pubmedcentral.nih.gov/articlerender.fcgi?artid=PMC3192229%20http://www.nature.com/doifinder/10.1038/nm.2446.

Gattinoni, L, X S Zhong, D C Palmer, Y Ji, C S Hinrichs, Z Yu, C Wrzesinski, A Boni, L Cassard, L M Garvin, C M Paulos, P Muranski, and N P Restifo (2009). "Wnt signaling arrests effector T cell differentiation and generates CD8+ memory stem cells". In: *Nat Med* 15.7, pp. 808–813. ISSN: 1078-8956. DOI: 10.1038/nm.1982. URL: http://www.ncbi.nlm.nih.gov/pubmed/19525962.

Gattinoni, Luca, Christopher A Klebanoff, and Nicholas P Restifo (2012). "Paths to stemness: building the ultimate antitumour T cell." In: *Nature reviews. Cancer* 12.10, pp. 671–84. ISSN: 1474-1768. DOI: 10.1038/nrc3322. URL: http://www.

nature.com/doifinder/10.1038/nrc3204%7B%5C%%7D5Cnhttp://www.ncbi.nlm.nih.gov/pubmed/22996603.

Gee, Adrian P. (2018). "GMP CAR-T cell production". In: *Best Practice and Research: Clinical Haematology* 31.2, pp. 126–134. ISSN: 15321924. DOI: 10.1016/j.beha.2018.01.002. URL: https://doi.org/10.1016/j.beha.2018.01.002.

Gerlach, Carmen, Jan C. Rohr, Leila Perie, Nienke Van Rooij, Jeroen W.J. Van Heijst, Arno Velds, Jos Urbanus, Shalin H. Naik, Heinz Jacobs, Joost B. Beltman, Rob J. De Boer, and Ton N.M. Schumacher (2013). "Heterogeneous differentiation patterns of individual CD8+ T cells". In: *Science* 340.6132, pp. 635–639. ISSN: 10959203. DOI: 10.1126/science.1235487.

Gerweck, Leo E. and Kala Seetharaman (1996). "Cellular pH gradient in tumor versus normal tissue: Potential exploitation for the treatment of cancer". In: *Cancer Research* 56.6, pp. 1194–1198. ISSN: 00085472.

Geyer, Mark B., Isabelle Riviere, Brigitte Senechal, Xiuyan Wang, Yongzeng Wang, Terence J. Purdon, Meier Hsu, Sean M. Devlin, Elizabeth Halton, Nicole Lamanna, Jurgen Rademaker, Michel Sadelain, Renier J. Brentjens, and Jae H. Park (2018). "Autologous CD19-Targeted CAR T Cells in Patients with Residual CLL following Initial Purine Analog-Based Therapy". In: *Molecular Therapy*. ISSN: 15250024. DOI: 10.1016/j.ymthe.2018.05.018.

Ghassemi, Saba, Felipe Bedoya, Selene Nunez-Cruz, Carl June, Jos Melenhorst, and Michael Milone (2016). "203. Shortened T Cell Culture with IL-7 and IL-15 Provides the Most Potent Chimeric Antigen Receptor (CAR)-Modified T Cells for Adoptive Immunotherapy". In: *Molecular Therapy*. ISSN: 15250016. DOI: 10.1016/s1525-0016(16)33012-x.

Ghassemi, Saba, Francisco J. Martinez-Becerra, Alyssa M. Master, Sarah A. Richman, David Heo, John Leferovich, Yitao Tu, Juan Carlos Garcia-Ca≈naveras, Asma Ayari, Yinan Lu, Ai Wang, Joshua D. Rabinowitz, Michael C. Milone, Carl H. June, and Roddy S. O'Connor (2020). "Enhancing Chimeric Antigen Receptor T Cell Anti-tumor Function through Advanced Media Design". In: *Molecular Therapy - Methods and Clinical Development* 18.September, pp. 595–606. ISSN: 23290501. DOI: 10.1016/j.omtm.2020.07.008. URL: https://doi.org/10.1016/j.omtm.2020.07.008.

Ghassemi, Saba, Selene Nunez-Cruz, Roddy S. O'Connor, Joseph A. Fraietta, Prachi R. Patel, John Scholler, David M. Barrett, Stefan M. Lundh, Megan M. Davis, Felipe Bedoya, John Leferovich, Simon F. Lacey, Bruce L. Levine, Stephan A. Grupp, Carl H. June, J. Joseph Melenhorst, and Michael C. Milone (2018). "Reducing Ex Vivo Culture Improves the Anti-leukemic Activity of Chimeric Antigen Receptor (CAR)-T Cells". In: *Cancer Immunology Research* 6.September, canimm.0405.2017. ISSN: 2326-6066. DOI: 10.1158/2326-6066.CIR-17-0405.

URL: http://cancerimmunolres.aacrjournals.org/lookup/doi/10.1158/2326-6066.CIR-17-0405.

Gilham, David E. and John Maher (Aug. 2017). *'Atypical' CAR T cells: NKG2D and Erb-B as examples of natural receptor/ligands to target recalcitrant solid tumors*. DOI: 10.2217/imt-2017-0045.

Giri, J G, S Kumaki, M Ahdieh, D J Friend, A Loomis, K Shanebeck, R DuBose, D Cosman, L S Park, and D M Anderson (Aug. 1995). "Identification and cloning of a novel IL-15 binding protein that is structurally related to the alpha chain of the IL-2 receptor." In: *The EMBO journal* 14.15, pp. 3654–63. ISSN: 0261-4189. URL: http://www.ncbi.nlm.nih.gov/pubmed/7641685%20http://www.pubmedcentral.nih.gov/articlerender.fcgi?artid=PMC394440.

Gohil, M., A. Dai, S. Mackey, D. Negorev, N.A. Hennesy, M. O'Rourke, A. Lamontagne, D. Holland, R.M. Leskowitz, J. Xu, M. Ozerova, J.S. McKee, E. Pequignot, D. Siegel, S. Schuster, J. Svoboda, A. Garfall, A. Cohen, E. Stadtmauer, W. Gladney, B.L. Levine, J.A. Fraietta, and M.M. Davis (May 2019). "Myeloid derived suppressor cells (MDSCS) reduce the manufacturing feasibilty of gene modified T cells." In: *Cytotherapy* 21.5, S19. ISSN: 14653249. DOI: 10.1016/j.jcyt.2019.03.315.

Golubovskaya, Vita and Lijun Wu (2016). "Different subsets of T cells, memory, effector functions, and CAR-T immunotherapy". In: *Cancers* 8.3. ISSN: 20726694. DOI: 10.3390/cancers8030036.

Goyal, Asti, Sunil K. Gupta, Thomas Vanden Boom, Marie M. Zhu, Steven S. Lee, and Douglas L. Rank (2005). "Effects of elevated pCO2 and osmolality on growth of CHO cells and production of antibody-fusion protein B1: A case study". In: *Biotechnology Progress* 21, pp. 70–77. DOI: 10.1021/bp049815s.

Graham, Nicholas A., Martik Tahmasian, Bitika Kohli, Evangelia Komisopoulou, Maggie Zhu, Igor Vivanco, Michael A. Teitell, Hong Wu, Antoni Ribas, Roger S. Lo, Ingo K. Mellinghoff, Paul S. Mischel, and Thomas G. Graeber (2012). "Glucose deprivation activates a metabolic and signaling amplification loop leading to cell death". In: *Molecular Systems Biology* 8.589, pp. 1–16. ISSN: 17444292. DOI: 10.1038/msb.2012.20. URL: http://dx.doi.org/10.1038/msb.2012.20.

Griffiths, J. R. (1991). "Are cancer cells acidic?" In: *British Journal of Cancer* 64.3, pp. 425–427. ISSN: 15321827. DOI: 10.1038/bjc.1991.326.

Grupp, Stephan A, Michael Kalos, David Barrett, Richard Aplenc, David L Porter, Susan R Rheingold, David T Teachey, Anne Chew, Bernd Hauck, J Fraser Wright, Michael C Milone, Bruce L Levine, and Carl H June (2013). "Chimeric Antigen Receptor -Modified T Cells for Acute Lymphoid Leukemia". In: 16.18. DOI: 10.1056/NEJMoa1215134. URL: http://www.nejm.org/doi/pdf/10.1056/NEJMoa1215134.

Gubser, Patrick M., Glenn R. Bantug, Leyla Razik, Marco Fischer, Sarah Dimeloe, Gideon Hoenger, Bojana Durovic, Annaise Jauch, and Christoph Hess (2013). "Rapid

effector function of memory CD8+ T cells requires an immediate-early glycolytic switch". In: *Nature Immunology* 14.10, pp. 1064–1072. ISSN: 15292908. DOI: 10.1038/ni.2687.

Hale, Laura P., Rod D. Braun, William M. Gwinn, Paula K. Greer, and Mark W. Dewhirst (2002). "Hypoxia in the thymus: role of oxygen tension in thymocyte survival". In: *American Journal of Physiology-Heart and Circulatory Physiology* 282.4, H1467–H1477. ISSN: 0363-6135. DOI: 10.1152/ajpheart.00682.2001.

Halperin, Mitchell L., Helen Connors, Arnold Relman, and Manfred Karnovsky (1969). "of pH on". In: 244.2, pp. 384–391.

Hand, Timothy W. and Susan M. Kaech (2009). "Intrinsic and extrinsic control of effector T cell survival and memory T cell development". In: *Immunologic Research* 45.1, pp. 46–61. ISSN: 0257277X. DOI: 10.1007/s12026-008-8027-z.

Heiden, Matthew G Vander, Lewis C. Cantley, and Craig B. Thompson (2009). "Understanding the warburg effect: The metabolic requirements of cell proliferation". In: *Science* 324.5930, pp. 1029–1033. ISSN: 00368075. DOI: 10.1126/science.1160809.

Hinrichs, Christian S., Zachary A. Borman, Lydie Cassard, Luca Gattinoni, Rosanne Spolski, Yu Zhiya, Luis Sanchez-Perez, Pawel Muranski, Steven J. Kern, Carol Logun, Douglas C. Palmer, Ji Yun, Robert N. Reger, Warren J. Leonard, Robert L. Danner, Steven A. Rosenberg, and Nicholas P. Restifo (2009). "Adoptively trans-

ferred effector cells derived from naive rather than central memory CD8+ T cells mediate superior antitumor immunity". In: *Proceedings of the National Academy of Sciences of the United States of America* 106.41, pp. 17469–17474. ISSN: 00278424. DOI: 10.1073/pnas.0907448106.

Hinrichs, Christian S., Rosanne Spolski, Chrystal M. Paulos, Luca Gattinoni, Keith W. Kerstann, Douglas C. Palmer, Christopher A. Klebanoff, Steven A. Rosenberg, Warren J. Leonard, and Nicholas P. Restifo (2008). "IL-2 and IL-21 confer opposing differentiation programs to CD8+ T cells for adoptive immunotherapy". In: *Blood* 111.11, pp. 5326–5333. ISSN: 00064971. DOI: 10.1182/blood-2007-09-113050.

Holden, Howard T., Robert K. Oldham, John R. Ortaldo, and Ronald B. Herberman (Mar. 1977). "Standardization of the Chromium-51 Release, Cell-Mediated Cytotoxicity Assay: Cryopreservation of Mouse Effector and Target Cells2". In: *JNCI: Journal of the National Cancer Institute* 58.3, pp. 611–622. ISSN: 1460-2105. DOI: 10.1093/jnci/58.3.611. URL: https://academic.oup.com/jnci/article-lookup/doi/10.1093/jnci/58.3.611.

Hollyman, Daniel, Jolanta Stefanski, Mark Przybylowski, Shirley Bartido, Oriana Borquez-Ojeda, Clare Taylor, Raymond Yeh, Vanessa Capacio, Malgorzata Olszewska, James Hosey, Michel Sadelain, Renier J. Brentjens, and Isabelle Riviere (2009). "Manufacturing validation of biologically functional T cells targeted to CD19 antigen for

autologous adoptive cell therapy". In: *Journal of Immunotherapy* 32.2, pp. 169–180. ISSN: 15249557. DOI: 10.1097/CJI.0b013e318194a6e8.

Hombach, Andreas, Anja Wieczarkowiecz, Thomas Marquardt, Claudia Heuser, Loretta Usai, Christoph Pohl, Barbara Seliger, and Hinrich Abken (July 2001). "Tumor-Specific T Cell Activation by Recombinant Immunoreceptors: CD3ζ Signaling and CD28 Costimulation Are Simultaneously Required for Efficient IL-2 Secretion and Can Be Integrated into One Combined CD28/CD3ζ Signaling Receptor Molecule". In: *The Journal of Immunology* 173.1, pp. 695.1–695. ISSN: 0022-1767. DOI: 10.4049/jimmunol.173.1.695.

Hoshan, Linda, Rubin Jiang, Joseph Moroney, Ashley Bui, Xiaolin Zhang, Ta Chun Hang, and Sen Xu (2019). "Effective bioreactor pH control using only sparging gases". In: *Biotechnology Progress* 35.1, pp. 1–7. ISSN: 15206033. DOI: 10.1002/btpr.2743.

Iistry, C H E (1966). "1 Communications". In: *Communications* 17, pp. 4110–4112.

Irving, B.A. and A. Weiss (1991). "The Cytoplasmic Domain of the T Cell Receptor Zeta Chain". In: *Cell* 64.5, pp. 891–901. URL: http://www.sciencedirect.com/science/article/pii/009286749190314O.

Iyer, Rohin K., Paul A. Bowles, Howard Kim, and Aaron Dulgar-Tulloch (2018). "Industrializing Autologous Adoptive Immunotherapies: Manufacturing Advances and

Challenges". In: *Frontiers in Medicine* 5.May, pp. 1–9. DOI: 10.3389/fmed.2018.00150.

Jacobs, Sarah R., Catherine E. Herman, Nancie J. MacIver, Jessica A. Wofford, Heather L. Wieman, Jeremy J. Hammen, and Jeffrey C. Rathmell (2008). "Glucose Uptake Is Limiting in T Cell Activation and Requires CD28-Mediated Akt-Dependent and Independent Pathways". In: *The Journal of Immunology* 180.7, pp. 4476–4486. ISSN: 0022-1767. DOI: 10.4049/jimmunol.180.7.4476.

Jacoby, Elad, Bella Bielorai, Abraham Avigdor, Orit Itzhaki, Daphna Hutt, Vered Nussboim, Amilia Meir, Adva Kubi, Michal Levy, Dragoslav Zikich, Li at Zeltzer, Karin Brezinger, Jacob Schachter, Arnon Nagler, Michal J. Besser, and Amos Toren (2018). "Locally produced CD19 CAR T cells leading to clinical remissions in medullary and extramedullary relapsed acute lymphoblastic leukemia". In: *American Journal of Hematology*. ISSN: 10968652. DOI: 10.1002/ajh.25274.

Jameson, Stephen C. and David Masopust (2018). "Understanding Subset Diversity in T Cell Memory". In: *Immunity* 48.2, pp. 214–226. ISSN: 10974180. DOI: 10.1016/j.immuni.2018.02.010. URL: https://doi.org/10.1016/j.immuni.2018.02.010.

Johnson, Laura A., Richard A. Morgan, Mark E. Dudley, Lydie Cassard, James C. Yang, Marybeth S. Hughes, Udai S. Kammula, Richard E. Royal, Richard M. Sherry, John R. Wunderlich, Chyi Chia R. Lee, Nicholas P. Restifo, Susan L. Schwarz, Alexandria

P. Cogdill, Rachel J. Bishop, Hung Kim, Carmen C. Brewer, Susan F. Rudy, Carter VanWaes, Jeremy L. Davis, Aarti Mathur, Robert T. Ripley, Debbie A. Nathan, Carolyn M. Laurencot, and Steven A. Rosenberg (2009). "Gene therapy with human and mouse T-cell receptors mediates cancer regression and targets normal tissues expressing cognate antigen". In: *Blood* 114.3, pp. 535–546. ISSN: 00064971. DOI: 10.1182/blood-2009-03-211714.

Kagoya, Yuki, Munehide Nakatsugawa, Toshiki Ochi, Yuchen Cen, Tingxi Guo, Mark Anczurowski, Kayoko Saso, Marcus O. Butler, and Naoto Hirano (2017). "Transient stimulation expands superior antitumor T cells for adoptive therapy". In: *JCI Insight* 2.2, pp. 1–13. DOI: 10.1172/jci.insight.89580.

Kalos, Michael, Michael Kalos, Bruce L Levine, David L Porter, Sharyn Katz, and Stephan A Grupp (2011). "T Cells with Chimeric Antigen Receptors Have Potent Antitumor Effects and Can Establish Memory in Patients with Advanced Leukemia". In: 73.95. DOI: 10.1126/scitranslmed.3002842.

Kandarian, Fadi, Gemalene M. Sunga, Diana Arango-Saenz, and Maura Rossetti (Aug. 2017). "A flow cytometry-based cytotoxicity assay for the assessment of human NK cell activity". In: *Journal of Visualized Experiments* 2017.126. ISSN: 1940087X. DOI: 10.3791/56191. URL: http://www.ncbi.nlm.nih.gov/pubmed/28829424%20http://www.pubmedcentral.nih.gov/articlerender.fcgi?artid=PMC5614136.

Kershaw, Michael H., Jennifer A. Westwood, and Phillip K. Darcy (Aug. 2013). "Gene-engineered T cells for cancer therapy". In: *Nature Reviews Cancer* 13.8, pp. 525–541. ISSN: 1474-175X. DOI: 10.1038/nrc3565. URL: http://www.nature.com/articles/nrc3565.

Kim, Ryungsa, Manabu Emi, and Kazuaki Tanabe (May 2007). "Cancer immunoediting from immune surveillance to immune escape". In: *Immunology* 121.1, pp. 1–14. ISSN: 0019-2805. DOI: 10.1111/j.1365-2567.2007.02587.x. URL: http://doi.wiley.com/10.1111/j.1365-2567.2007.02587.x.

Kimura, Roy and William Miller (1999). "Erratum: Effects of elevated pCO2 and/or osmolality on the growth and recombinant tPA production of CHO cells". In: *Biotechnology and Bioengineering* 63.2, pp. 253–253. ISSN: 1097-0290. DOI: 10.1002/(SICI)1097-0290(19990420)63:23.0.CO;2-D.

Klarer, Alex, David Smith, Ryan Cassidy, Thomas Heathman, and Qasim Rafiq (2018). "IN". In: *Bioprocess International*.

Klebanoff, Christopher A., Luca Gattinoni, and Nicholas P. Restifo (2012). "Sorting through subsets: Which T-cell populations mediate highly effective adoptive immunotherapy?" In: *Journal of Immunotherapy* 35.9, pp. 651–660. ISSN: 15249557. DOI: 10.1097/CJI.0b013e31827806e6.

Klebanoff, Christopher A., Christopher D. Scott, Anthony J. Leonardi, Tori N. Yamamoto, Anthony C. Cruz, Claudia Ouyang, Madhu Ramaswamy, Rahul Roychoud-

huri, Yun Ji, Robert L. Eil, Madhusudhanan Sukumar, Joseph G. Crompton, Douglas C. Palmer, Zachary A. Borman, David Clever, Stacy K. Thomas, Shashankkumar Patel, Zhiya Yu, Pawel Muranski, Hui Liu, Ena Wang, Francesco M. Marincola, Alena Gros, Luca Gattinoni, Steven A. Rosenberg, Richard M. Siegel, and Nicholas P. Restifo (2016). "Memory T cell-driven differentiation of naive cells impairs adoptive immunotherapy". In: *Journal of Clinical Investigation* 126.1, pp. 318–334. ISSN: 15588238. DOI: 10.1172/JCI81217.

Klebanoff, Christopher A, Joseph G Crompton, Anthony J Leonardi, Tori N Yamamoto, Smita S Chandran, Robert L Eil, Madhusudhanan Sukumar, Suman K Vodnala, Jinhui Hu, Yun Ji, David Clever, Mary A Black, Devikala Gurusamy, Michael J Kruhlak, Ping Jin, David F Stroncek, Luca Gattinoni, Steven A Feldman, and Nicholas P Restifo (2017). "Inhibition of AKT signaling uncouples T cell differentiation from expansion for receptor-engineered adoptive immunotherapy". In: *JCI Insight* 2.23, pp. 1–17. ISSN: 0021-9738. DOI: 10.1172/JCI.INSIGHT.95103. URL: https://doi.org/10.1172/jci.insight.95103:e95103.%7B%5C%%7D0Ahttps://doi.org/10.1172/jci.%7B%5C%%7D0Ahttp://insight.jci.org%7B%5C%%7D0Ahttps://doi.org/10.1172/jci.insight.95103%7B%5C%%7D0Ahttps://insight.jci.org/articles/view/95103.

Klebanoff, Christopher A, Steven E Finkelstein, Deborah R Surman, Michael K Lichtman, Luca Gattinoni, Marc R Theoret, Navrose Grewal, Paul J Spiess, Paul A Antony,

Douglas C Palmer, Yutaka Tagaya, Steven A Rosenberg, Thomas A Waldmann, and Nicholas P Restifo (2003). "IL-15 enhances the in vivo antitumor activity of tumor-reactive CD8". In: URL: http://www.pnas.org/content/pnas/101/7/1969.full.pdf.

Kochanowski, Nadine, Gaetan Siriez, Sarah Roosens, and Laetitia Malphettes (2011). "Medium and feed optimization for fed-batch production of a monoclonal antibody in CHO cells". In: *BMC Proceedings* 5.S8, P75. ISSN: 1753-6561. DOI: 10.1186/1753-6561-5-s8-p75. URL: http://www.biomedcentral.com/1753-6561/5/S8/P75.

Kochenderfer, James N, Mark E Dudley, Robert O Carpenter, Sadik H Kassim, Jeremy J Rose, William Telford, Frances T Hakim, David Halverson, Daniel H Fowler, Nancy M Hardy, Anthony Mato, Dennis D Hickstein, Juan Gea-Banacloche, Steven Z Pavletic, Claude Sportes, Irina Maric, Steven Feldman, Brenna G Hansen, Jennifer Wilder, Bazetta Blacklock-Schuver, Bipulendu Jena, Michael Bishop, Steven a Rosenberg, and Ronald E Gress (2013). "Donor-Derived Anti-CD19 Chimeric-Antigen-Receptor-Expressing T Cells Cause Regression Of Malignancy Persisting After Allogeneic Hematopoietic Stem Cell Transplantation". In: *Blood* 122.21, p. 151. ISSN: 0006-4971. DOI: 10.1182/blood-2013-08-519413.R.E.G.. URL: http://bloodjournal.hematologylibrary.org/content/122/21/151.abstract.

Kochenderfer, James N, Robert P T Somerville, Tangying Lu, Victoria Shi, Adrian Bot, John Rossi, Allen Xue, Stephanie L Goff, James C Yang, Richard M Sherry, Christopher A Klebanoff, Udai S Kammula, Marika Sherman, Arianne Perez, Constance M Yuan, Tatyana Feldman, Jonathan W Friedberg, Mark J Roschewski, Steven A Feldman, Lori Mcintyre, Mary Ann Toomey, and Steven A Rosenberg (2017). "Lymphoma Remissions Caused by Anti-CD19 Chimeric Antigen Receptor T Cells Are Associated With High Serum Interleukin-15 Levels". In: *J Clin Oncol* 35. DOI: 10.1200/JCO.2016.71.3024. URL: http://clf1.medpagetoday.com/content/pdf/reading-room/asco/JCO%20HM%20Kochenderfer040317.pdf.

Kochenderfer, James N, Wyndham H Wilson, John E Janik, Mark E Dudley, Steven a Feldman, Irina Maric, Mark Raffeld, Debbie-ann N Nathan, J Brock, Richard a Morgan, Steven a Rosenberg, Maryalice Stetler-stevenson, and Brock J Lanier (2010). "Eradication of B-lineage cells and regression of lymphoma in a patient treated with autologous T cells genetically engineered to recognize Brief report Eradication of B-lineage cells and regression of lymphoma in a patient treated with autologous T cells". In: 116.20, pp. 4099–4102. DOI: 10.1182/blood-2010-04-281931.

Kofler, David M., Markus Chmielewski, Gunter Rappl, Anja Hombach, Tobias Riet, Annette Schmidt, Andreas A. Hombach, Clemens Martin Wendtner, and Hinrich Abken (2011). "CD28 costimulation impairs the efficacy of a redirected T-cell antitumor attack in the presence of regulatory T cells which can be overcome by pre-

venting lck activation". In: *Molecular Therapy* 19.4, pp. 760–767. ISSN: 15250024. DOI: 10.1038/mt.2011.9. URL: http://dx.doi.org/10.1038/mt.2011.9.

Krause, Anja, Hong Fen Guo, Jean Baptiste Latouche, Cuiwen Tan, Nai Kong V Cheung, and Michel Sadelain (Aug. 1998). "Antigen-dependent CD28 signaling selectively enhances survival and proliferation in genetically modified activated human primary T lymphocytes". In: *Journal of Experimental Medicine* 188.4, pp. 619–626. ISSN: 00221007. DOI: 10.1084/jem.188.4.619.

Krebs, Karin, Nina Böttinger, Li Rung Huang, Markus Chmielewski, Silke Arzberger, Georg Gasteiger, Clemens Jager, Edgar Schmitt, Felix Bohne, Michaela Aichler, Wolfgang Uckert, Hinrich Abken, Mathias Heikenwalder, Percy Knolle, and Ulrike Protzer (2013). "T Cells Expressing a Chimeric Antigen Receptor That Binds Hepatitis B Virus Envelope Proteins Control Virus Replication in Mice". In: *Gastroenterology*. ISSN: 15280012. DOI: 10.1053/j.gastro.2013.04.047.

Kuwana, Yoshihisa, Yoshihiro Asakura, Naoko Utsunomiya, Mamoru Nakanishi, Yohji Arata, Seiga Itoh, Fumihiko Nagase, and Yoshikazu Kurosawa (Dec. 1987). "Expression of chimeric receptor composed of immunoglobulin-derived V resions and T-cell receptor-derived C regions". In: *Biochemical and Biophysical Research Communications* 149.3, pp. 960–968. ISSN: 10902104. DOI: 10.1016/0006-291X(87)90502-X.

Lamb, L. S., P. Musk, Z. Ye, F. Van Rhee, S. S. Geier, J. J. Tong, K. M. King, and P. J. Henslee-Downey (Mar. 2001). "Human γ δ+ T lymphocytes have in vitro graft vs leukemia activity in the absence of an allogeneic response". In: *Bone Marrow Transplantation* 27.6, pp. 601–606. ISSN: 02683369. DOI: 10.1038/sj.bmt.1702830. URL: http://www.ncbi.nlm.nih.gov/pubmed/11319589.

Larbi, Anis, Henning Zelba, David Goldeck, and Graham Pawelec (2010). "Induction of HIF-1α and the glycolytic pathway alters apoptotic and differentiation profiles of activated human T cells". In: *Journal of Leukocyte Biology* 87.2, pp. 265–273. DOI: 10.1189/jlb.0509304.

Lavrentieva, Antonina, Ingrida Majore, Cornelia Kasper, and Ralf Hass (2010). "Effects of hypoxic culture conditions on umbilical cord-derived human mesenchymal stem cells". In: *Cell Communication and Signaling* 8, pp. 1–9. ISSN: 1478811X. DOI: 10.1186/1478-811X-8-18.

Lee, Daniel W, James N Kochenderfer, Maryalice Stetler-Stevenson, Yongzhi K Cui, Cindy Delbrook, Steven A Feldman, Terry J Fry, Rimas Orentas, Marianna Sabatino, Nirali N Shah, Seth M Steinberg, Dave Stroncek, Nick Tschernia, Constance Yuan, Hua Zhang, Ling Zhang, Steven A Rosenberg, Alan S Wayne, and Crystal L Mackall (2015). "T cells expressing CD19 chimeric antigen receptors for acute lymphoblastic leukaemia in children and young adults: a phase 1 dose-escalation trial". In: *The Lancet* 385.9967, pp. 517–528. DOI: 10.1016/S0140-6736(14)61403-3. URL:

http://ac.els-cdn.com/S0140673614614033/1-s2.0-S0140673614614033-main.pdf?%20tid=99440826-08d0-11e7-9580-00000aacb35f%7B%5C&%7Dacdnat=1489507947%208fecbf8b2c7a92df87e4d7138e499c5f.

Lee, JangEun, Matthew C. Walsh, Kyle L. Hoehn, David E. James, E. John Wherry, and Yongwon Choi (2014). "Regulator of Fatty Acid Metabolism, Acetyl Coenzyme A Carboxylase 1, Controls T Cell Immunity". In: *The Journal of Immunology* 192.7, pp. 3190–3199. ISSN: 0022-1767. DOI: 10.4049/jimmunol.1302985.

Levine, Bruce L., James Miskin, Keith Wonnacott, and Christopher Keir (2016). "Global Manufacturing of CAR T-Cell Therapy". In: *Molecular Therapy - Methods & Clinical Development* 4.March, pp. 92–101. ISSN: 23290501. DOI: 10.1016/j.omtm.2016.12.006. URL: http://linkinghub.elsevier.com/retrieve/pii/S2329050116302029.

Levine, Bruce L., Joseph D. Mosca, James L. Riley, Richard G. Carroll, Maryanne T. Vahey, Linda L. Jagodzinski, Kenneth F. Wagner, Douglas L. Mayers, Donald S. Burke, Owen S. Weislow, Daniel C. St. Louis, and Carl H. June (1996). "Antiviral effect and ex vivo CD4+ T cell proliferation in HIV-positive patients as a result of CD28 costimulation". In: *Science* 272.5270, pp. 1939–1943. ISSN: 00368075. DOI: 10.1126/science.272.5270.1939.

Levring, Trine Boegh, Ann Kathrine Hansen, Bodil Lisbeth Nielsen, Martin Kongsbak, Marina Rode Von Essen, Anders Woetmann, Niels Ødum, Charlotte Menne

Bonefeld, and Carsten Geisler (2012). "Activated human CD4 + T cells express transporters for both cysteine and cystine". In: *Scientific Reports* 2, pp. 2–7. ISSN: 20452322. DOI: 10.1038/srep00266.

Linnemann, Carsten, Ton N.M. Schumacher, and Gavin M. Bendle (2011). "T-cell receptor gene therapy: Critical parameters for clinical success". In: *Journal of Investigative Dermatology* 131.9, pp. 1806–1816. ISSN: 15231747. DOI: 10.1038/jid.2011.160. URL: http://dx.doi.org/10.1038/jid.2011.160.

Lipp, Martin, Federica Sallusto, Danielle Lenig, Reinhold Fo, and Antonio Lanzavecchia (1999). "Two subsets of memory T lymphocyteswith distinct homing potentials and effector functions Federica". In: 401.October. URL: www.nature.com.

Lock, Dominik, Nadine Mockel-Tenbrinck, Katharina Drechsel, Carola Barth, Daniela Mauer, Thomas Schaser, Carolin Kolbe, Wael Al Rawashdeh, Janina Brauner, Olaf Hardt, Natali Pflug, Udo Holtick, Peter Borchmann, Mario Assenmacher, and Andrew Kaiser (2017). "Automated Manufacturing of Potent CD20-Directed Chimeric Antigen Receptor T Cells for Clinical Use". In: *Human Gene Therapy* 28.10, pp. 914–925. ISSN: 15577422. DOI: 10.1089/hum.2017.111.

Louis, Chrystal U., Barbara Savoldo, Gianpietro Dotti, Martin Pule, Eric Yvon, G. Doug Myers, Claudia Rossig, Heidi V. Russell, Oumar Diouf, Enli Liu, Hao Liu, Meng Fen Wu, Adrian P. Gee, Zhuyong Mei, Cliona M. Rooney, Helen E. Heslop, and Malcolm K. Brenner (2011). "Antitumor activity and long-term fate of chimeric

antigen receptor-positive T cells in patients with neuroblastoma". In: *Blood* 118.23, pp. 6050–6056. ISSN: 00064971. DOI: 10.1182/blood-2011-05-354449.

Lu, Tangying Lily, Omar Pugach, Robert Somerville, Steven A. Rosenberg, James N. Kochenderfer, Marc Better, and Steven A. Feldman (2016). "A Rapid Cell Expansion Process for Production of Engineered Autologous CAR-T Cell Therapies". In: *Human Gene Therapy Methods* 27.6, pp. 209–218. ISSN: 19466544. DOI: 10.1089/hgtb.2016.120.

Ludwig, Josh and Mark Hirschel (2020). "Methods and Process Optimization for Large-Scale CAR T Expansion Using the G-Rex Cell Culture Platform". In: *Methods in Molecular Biology* 2086, pp. 165–177. ISSN: 19406029. DOI: 10.1007/978-1-0716-0146-412.

Lukashev, Dmitriy, Boris Klebanov, Hidefumi Kojima, Alex Grinberg, Akiko Ohta, Ludmilla Berenfeld, Roland H. Wenger, Akio Ohta, and Michail Sitkovsky (2006). " Cutting Edge: Hypoxia-Inducible Factor 1α and Its Activation-Inducible Short Isoform I.1 Negatively Regulate Functions of CD4 + and CD8 + T Lymphocytes ". In: *The Journal of Immunology* 177.8, pp. 4962–4965. ISSN: 0022-1767. DOI: 10.4049/jimmunol.177.8.4962.

Ma, Ruihua, Tiantian Ji, Huafeng Zhang, Wenqian Dong, Xinfeng Chen, Pingwei Xu, Degao Chen, Xiaoyu Liang, Xiaonan Yin, Yuying Liu, Jingwei Ma, Ke Tang, Yi Zhang, Yue'E Peng, Jinzhi Lu, Xiaofeng Qin, Xuetao Cao, Yonghong Wan, and Bo

Huang (2018). “A Pck1-directed glycogen metabolic program regulates formation and maintenance of memory CD8 + T cells”. In: *Nature Cell Biology* 20.1, pp. 21–27. ISSN: 14764679. DOI: 10.1038/s41556-017-0002-2. URL: http://dx.doi.org/10.1038/s41556-017-0002-2.

Macintyre, Andrew N., Valerie A. Gerriets, Amanda G. Nichols, Ryan D. Michalek, Michael C. Rudolph, Divino Deoliveira, Steven M. Anderson, E. Dale Abel, Benny J. Chen, Laura P. Hale, and Jeffrey C. Rathmell (2014). “The glucose transporter Glut1 is selectively essential for CD4 T cell activation and effector function”. In: *Cell Metabolism* 20.1, pp. 61–72. ISSN: 19327420. DOI: 10.1016/j.cmet.2014.05.004. URL: http://dx.doi.org/10.1016/j.cmet.2014.05.004.

MacIver, N J, R D Michalek, and J C Rathmell (2013). “Metabolic regulation of T lymphocytes”. In: *Annu Rev Immunol* 31, pp. 259–283. ISSN: 1545-3278. DOI: 10.1146/annurev-immunol-032712-095956. arXiv: NIHMS150003. URL: http://www.ncbi.nlm.nih.gov/pubmed/23298210.

Macon-Lemaitre, Laetitia and Frederic Triebel (2005). “The negative regulatory function of the lymphocyte-activation gene-3 co-receptor (CD223) on human T cells”. In: *Immunology* 115.2, pp. 170–178. ISSN: 00192805. DOI: 10.1111/j.1365-2567.2005.02145.x.

Maher, John, Renier J. Brentjens, Gertrude Gunset, Isabelle Riviere, and Michel Sadelain (2002). “Human T-lymphocyte cytotoxicity and proliferation directed by a sin-

gle chimeric TCRζ/CD28 receptor". In: *Nature Biotechnology* 20.1, pp. 70–75. ISSN: 10870156. DOI: 10.1038/nbt0102-70.

Mahnke, Yolanda D., Tess M. Brodie, Federica Sallusto, Mario Roederer, and Enrico Lugli (2013). "The who's who of T-cell differentiation: Human memory T-cell subsets". In: *European Journal of Immunology* 43.11, pp. 2797–2809. ISSN: 00142980. DOI: 10.1002/eji.201343751.

Majchrzak, Kinga, Michelle H. Nelson, Stefanie R. Bailey, Jacob S. Bowers, Xue Zhong Yu, Mark P. Rubinstein, Richard A. Himes, and Chrystal M. Paulos (2016). "Exploiting IL-17-producing CD4+ and CD8+ T cells to improve cancer immunotherapy in the clinic". In: *Cancer Immunology, Immunotherapy* 65.3, pp. 247–259. ISSN: 14320851. DOI: 10.1007/s00262-016-1797-6.

Majzner, Robbie G and Crystal L Mackall (2019). "Clinical lessons learned from the first leg of the CAR T cell journey." In: *Nature medicine* 25.9, pp. 1341–1355. ISSN: 1546-170X. DOI: 10.1038/s41591-019-0564-6. URL: http://www.ncbi.nlm.nih.gov/pubmed/31501612.

Makkouk, Amani and George Weiner (2015). "Cancer Immunotherapy and Breaking Immune Tolerance-New Approaches to an Old Challenge". In: DOI: 10.1158/0008-5472.CAN-14-2538.

Mardiana, Sherly and Saar Gill (2020). “CAR T Cells for Acute Myeloid Leukemia: State of the Art and Future Directions”. In: *Frontiers in Oncology* 10.May, pp. 1–12. ISSN: 2234943X. DOI: 10.3389/fonc.2020.00697.

Marko, Aimee J, Rebecca A Miller, Alina Kelman, and Kenneth A Frauwirth (2010). “Induction of Glucose Metabolism in Stimulated T Lymphocytes Is Regulated by Mitogen-Activated Protein Kinase Signaling”. In: DOI: 10.1371/journal.pone.0015425. URL: www.cancer.gov.

Maude, S. L., T. W. Laetsch, J. Buechner, S. Rives, M. Boyer, H. Bittencourt, P. Bader, M. R. Verneris, H. E. Stefanski, G. D. Myers, M. Qayed, B. De Moerloose, H. Hiramatsu, K. Schlis, K. L. Davis, P. L. Martin, E. R. Nemecek, G. A. Yanik, C. Peters, A. Baruchel, N. Boissel, F. Mechinaud, A. Balduzzi, J. Krueger, C. H. June, B. L. Levine, P. Wood, T. Taran, M. Leung, K. T. Mueller, Y. Zhang, K. Sen, D. Lebwohl, M. A. Pulsipher, and S. A. Grupp (2018). “Tisagenlecleucel in children and young adults with B-cell lymphoblastic leukemia”. In: *New England Journal of Medicine*. ISSN: 15334406. DOI: 10.1056/NEJMoa1709866.

Maude, Shannon L., Noelle Frey, Pamela A. Shaw, Richard Aplenc, David M. Barrett, Nancy J. Bunin, Anne Chew, Vanessa E. Gonzalez, Zhaohui Zheng, Simon F. Lacey, Yolanda D. Mahnke, Jan J. Melenhorst, Susan R. Rheingold, Angela Shen, David T. Teachey, Bruce L. Levine, Carl H. June, David L. Porter, and Stephan A. Grupp (Oct. 2014). “Chimeric Antigen Receptor T Cells for Sustained Remissions

in Leukemia". In: 371.16, pp. 1507–17. DOI: 10.1056/NEJMoa1407222. arXiv: NIHMS150003. URL: http://www.nejm.org/doi/10.1056/NEJMoa1407222%20http://www.ncbi.nlm.nih.gov/pubmed/25317870%20http://www.pubmedcentral.nih.gov/articlerender.fcgi?artid=PMC4267531.

McGowan, Eileen, Qimou Lin, Guocai Ma, Haibin Yin, Size Chen, and Yiguang Lin (2020). "PD-1 disrupted CAR-T cells in the treatment of solid tumors: Promises and challenges". In: *Biomedicine and Pharmacotherapy* 121.October 2019, p. 109625. ISSN: 19506007. DOI: 10.1016/j.biopha.2019.109625. URL: https://doi.org/10.1016/j.biopha.2019.109625.

McLaughlin, Kelly A., Barbara A. Osborne, and Richard A. Goldsby (1996). "The role of oxygen in thymocyte apoptosis". In: *European Journal of Immunology* 26.5, pp. 1170–1174. ISSN: 00142980. DOI: 10.1002/eji.1830260531.

McLaughlin, Laura M. and Bruce Demple (2005). "Nitric oxide-induced apoptosis in lymphoblastoid and fibroblast cells dependent on the phosphorylation and activation of p53". In: *Cancer Research* 65.14, pp. 6097–6104. ISSN: 00085472. DOI: 10.1158/0008-5472.CAN-04-4254.

McNamee, Eóin N., Darlynn Korns Johnson, Dirk Homann, and Eric T. Clambey (2013). "Hypoxia and hypoxia-inducible factors as regulators of T cell development, differentiation, and function". In: *Immunologic Research* 55.1-3, pp. 58–70. ISSN: 0257277X. DOI: 10.1007/s12026-012-8349-8.

Medvec, Andrew R., Christopher Ecker, Hong Kong, Emily A. Winters, Joshua Glover, Angel Varela-Rohena, and James L. Riley (2018). "Improved Expansion and In Vivo Function of Patient T Cells by a Serum-free Medium". In: *Molecular Therapy - Methods & Clinical Development* 8.March, pp. 65–74. ISSN: 23290501. DOI: 10.1016/j.omtm.2017.11.001. URL: http://linkinghub.elsevier.com/retrieve/pii/S2329050117301171.

Meghrous, Jamal, Nikolai Khramtsov, Barry C. Buckland, Manon M.J. Cox, Laura A. Palomares, and Indresh K. Srivastava (2015). "Dissolved carbon dioxide determines the productivity of a recombinant hemagglutinin component of an influenza vaccine produced by insect cells". In: *Biotechnology and Bioengineering* 112.11, pp. 2267–2275. ISSN: 10970290. DOI: 10.1002/bit.25634.

Mellman, Ira, George Coukos, and Glenn Dranoff (Dec. 2011). "Cancer immunotherapy comes of age". In: *Nature* 480.7378, pp. 480–489. ISSN: 0028-0836. DOI: 10.1038/nature10673. URL: http://www.nature.com/articles/nature10673.

Merten, Otto Wilhelm, Matthias Hebben, and Chiara Bovolenta (2016). "Production of lentiviral vectors". In: *Molecular Therapy - Methods and Clinical Development* 3.September 2015, p. 16017. ISSN: 23290501. DOI: 10.1038/mtm.2016.17. URL: http://dx.doi.org/10.1038/mtm.2016.17.

Michalek, Ryan D., Valerie A. Gerriets, Sarah R. Jacobs, Andrew N. Macintyre, Nancie J. MacIver, Emily F. Mason, Sarah A. Sullivan, Amanda G. Nichols, and Jeffrey C.

Rathmell (2011). " Cutting Edge: Distinct Glycolytic and Lipid Oxidative Metabolic Programs Are Essential for Effector and Regulatory CD4 + T Cell Subsets ". In: *The Journal of Immunology* 186.6, pp. 3299–3303. ISSN: 0022-1767. DOI: 10.4049/jimmunol.1003613.

Millen, Jennifer, Margaret R. MacLean, and Miles D. Houslay (2006). "Hypoxia-induced remodelling of PDE4 isoform expression and cAMP handling in human pulmonary artery smooth muscle cells". In: *European Journal of Cell Biology* 85.7, pp. 679–691. ISSN: 01719335. DOI: 10.1016/j.ejcb.2006.01.006.

Miller, Edwin S., Julio C. Klinger, Cem Akin, D. Anne Koebel, and Gerald Sonnenfeld (1994). "Inhibition of murine splenic T lymphocyte proliferation by 2-deoxy-D-glucose-induced metabolic stress". In: *Journal of Neuroimmunology* 52.2, pp. 165–173. ISSN: 01655728. DOI: 10.1016/0165-5728(94)90110-4.

Milone, Michael C. and Una O'Doherty (2018). "Clinical use of lentiviral vectors". In: *Leukemia* 32.7, pp. 1529–1541. ISSN: 14765551. DOI: 10.1038/s41375-018-0106-0. URL: http://dx.doi.org/10.1038/s41375-018-0106-0.

Mitchell, L. C., L. S. Davis, and P. E. Lipsky (1989). "Promotion of human T lymphocyte proliferation by IL-4". In: *Journal of Immunology*. ISSN: 0022-1767.

Mock, Ulrike, Lauren Nickolay, Brian Philip, Gordon Weng Kit Cheung, Hong Zhan, Ian C.D. Johnston, Andrew D. Kaiser, Karl Peggs, Martin Pule, Adrian J. Thrasher, and Waseem Qasim (2016). "Automated manufacturing of chimeric antigen receptor

T cells for adoptive immunotherapy using CliniMACS prodigy". In: *Cytotherapy* 18.8, pp. 1002–1011. ISSN: 14772566. DOI: 10.1016/j.jcyt.2016.05.009. URL: http://dx.doi.org/10.1016/j.jcyt.2016.05.009.

Mordon, S., V. Maunoury, J. M. Devoisselle, Y. Abbas, and D. Coustaud (1992). "Characterization of tumorous and normal tissue using a pH-sensitive fluorescence indicator (5,6-carboxyfluorescein) in vivo". In: *Journal of Photochemistry and Photobiology, B: Biology* 13.3-4, pp. 307–314. ISSN: 10111344. DOI: 10.1016/1011-1344(92)85070-B.

Moya, Adrien, Nathanael Larochette, Joseph Paquet, Mickael Deschepper, Morad Bensidhoum, Valentina Izzo, Guido Kroemer, Herve Petite, and Delphine Logeart-Avramoglou (2017). "Quiescence Preconditioned Human Multipotent Stromal Cells Adopt a Metabolic Profile Favorable for Enhanced Survival under Ischemia". In: *Stem Cells* 35.1, pp. 181–196. ISSN: 15494918. DOI: 10.1002/stem.2493.

Munder, Markus, Henriette Schneider, Claudia Luckner, Thomas Giese, Claus Dieter Langhans, Jose M. Fuentes, Pascale Kropf, Ingrid Mueller, Armin Kolb, Manuel Modolell, and Anthony D. Ho (2006). "Suppression of T-cell functions by human granulocyte arginase". In: *Blood* 108.5, pp. 1627–1634. ISSN: 00064971. DOI: 10.1182/blood-2006-11-010389.

Munn, David H., Joseph Pressey, Arthur C. Beall, Richard Hudes, and Mark R. Alderson (1996). "Selective activation-induced apoptosis of peripheral T cells imposed

by macrophages: A potential mechanism of antigen-specific peripheral lymphocyte deletion". In: *Journal of Immunology* 156.2, pp. 523–532. ISSN: 0022-1767.

Muranski, Pawel, Andrea Boni, Paul A Antony, Lydie Cassard, Kari R Irvine, Andrew Kaiser, Chrystal M Paulos, Douglas C Palmer, Christopher E Touloukian, Krzysztof Ptak, Luca Gattinoni, Claudia Wrzesinski, Christian S Hinrichs, Keith W Kerstann, Lionel Feigenbaum, Chi-chao Chan, and Nicholas P Restifo (2015). "Tumor-specific Th17-polarized cells eradicate large established melanoma". In: *Immunobiology* 112.2, pp. 362–374. DOI: 10.1182/blood-2007-11-120998. An. URL: https://www.statista.com/statistics/263794/number-of-downloads-from-the-apple-app-store/.

Nakagawa, Yohko, Yasuyuki Negishi, Masumi Shimizu, Megumi Takahashi, Masao Ichikawa, and Hidemi Takahashi (2015). "Effects of extracellular pH and hypoxia on the function and development of antigen-specific cytotoxic T lymphocytes". In: *Immunology Letters* 167.2, pp. 72–86. ISSN: 18790542. DOI: 10.1016/j.imlet.2015.07.003. URL: http://dx.doi.org/10.1016/j.imlet.2015.07.003.

Nakaya, Mako, Yichuan Xiao, Xiaofei Zhou, Jae Hoon Chang, Mikyoung Chang, Xuhong Cheng, Marzenna Blonska, Xin Lin, and Shao Cong Sun (2014). "Inflammatory T cell responses rely on amino acid transporter ASCT2 facilitation of glutamine uptake and mTORC1 kinase activation". In: *Immunity* 40.5, pp. 692–705. ISSN: 10974180.

DOI: 10.1016/j.immuni.2014.04.007. URL: http://dx.doi.org/10.1016/j.immuni.2014.04.007.

Neal, Lillian R, Stefanie R Bailey, Megan M Wyatt, Jacob S Bowers, Kinga Majchrzak, Michelle H Nelson, Carl Haupt, Chrystal M Paulos, and Juan C Varela (2017). "The Basics of Artificial Antigen Presenting Cells in T Cell-Based Cancer Immunotherapies." In: *Journal of immunology research and therapy* 2.1, pp. 68–79. ISSN: 2472-727X. URL: http://www.ncbi.nlm.nih.gov/pubmed/28825053%20http://www.pubmedcentral.nih.gov/articlerender.fcgi?artid=PMC5560309.

Neelapu, S. S., F. L. Locke, N. L. Bartlett, L. J. Lekakis, D. B. Miklos, C. A. Jacobson, I. Braunschweig, O. O. Oluwole, T. Siddiqi, Y. Lin, J. M. Timmerman, P. J. Stiff, J. W. Friedberg, I. W. Flinn, A. Goy, B. T. Hill, M. R. Smith, A. Deol, U. Farooq, P. McSweeney, J. Munoz, I. Avivi, J. E. Castro, J. R. Westin, J. C. Chavez, A. Ghobadi, K. V. Komanduri, R. Levy, E. D. Jacobsen, T. E. Witzig, P. Reagan, A. Bot, J. Rossi, L. Navale, Y. Jiang, J. Aycock, M. Elias, D. Chang, J. Wiezorek, and W. Y. Go (2017). "Axicabtagene ciloleucel CAR T-cell therapy in refractory large B-Cell lymphoma". In: *New England Journal of Medicine*. ISSN: 15334406. DOI: 10.1056/NEJMoa1707447.

Newsholme, Eric A., Bernard Crabtree, and M. Salleh M. Ardawi (1985). "Glutamine Metabolism in Lymphocytes: Its Biochemical, Physiological and Clinical Impor-

tance". In: *Quarterly Journal of Experimental Physiology* 70.4, pp. 473–489. ISSN: 1469445X. DOI: 10.1113/expphysiol.1985.sp002935.

Nicklin, Paul, Philip Bergman, Bailin Zhang, Ellen Triantafellow, Henry Wang, Beat Nyfeler, Haidi Yang, Marc Hild, Charles Kung, Christopher Wilson, Vic E. Myer, Jeffrey P. MacKeigan, Jeffrey A. Porter, Y. Karen Wang, Lewis C. Cantley, Peter M. Finan, and Leon O. Murphy (2009). "Bidirectional Transport of Amino Acids Regulates mTOR and Autophagy". In: *Cell* 136.3, pp. 521–534. ISSN: 00928674. DOI: 10.1016/j.cell.2008.11.044. URL: http://dx.doi.org/10.1016/j.cell.2008.11.044.

Nishimura, Takashi, Minoru Nakui, Marimo Sato, Kenji Iwakabe, Hidemitsu Kitamura, Masashi Sekimoto, Akio Ohta, Toshiaki Koda, and Shinichiro Nishimura (2000). "The critical role of Th1-dominant immunity in tumor immunology". In: *Cancer Chemotherapy and Pharmacology* 46.SUPPL. Pp. 52–61. ISSN: 03445704. DOI: 10.1007/pl00014051.

O'Sullivan, David, Gerritje W.J. VanderWindt, Stanley Ching Cheng Huang, Jonathan D. Curtis, Chih Hao Chang, Michae D.L. Buck, Jing Qiu, Amber M. Smith, Wing Y. Lam, Lisa M. DiPlato, Fong Fu Hsu, Morris J. Birnbaum, Edward J. Pearce, and Erika L. Pearce (2014a). "Memory CD8+ T Cells Use Cell-Intrinsic Lipolysis to Support the Metabolic Programming Necessary for Development". In: *Immunity*

41.1, pp. 75–88. ISSN: 10974180. DOI: 10.1016/j.immuni.2014.06.005. URL: http://dx.doi.org/10.1016/j.immuni.2014.06.005.

O'Sullivan, David, Gerritje W.J. VanderWindt, Stanley Ching Cheng Huang, Jonathan D. Curtis, Chih Hao Chang, Michae D.L. Buck, Jing Qiu, Amber M. Smith, Wing Y. Lam, Lisa M. DiPlato, Fong Fu Hsu, Morris J. Birnbaum, Edward J. Pearce, and Erika L. Pearce (2014b). "Memory CD8+ T Cells Use Cell-Intrinsic Lipolysis to Support the Metabolic Programming Necessary for Development". In: *Immunity* 41.1, pp. 75–88. ISSN: 10974180. DOI: 10.1016/j.immuni.2014.06.005. URL: http://dx.doi.org/10.1016/j.immuni.2014.06.005.

Olsen, Ingrid and Ludvig M. Sollid (2013). "Pitfalls in determining the cytokine profile of human T cells". In: *Journal of Immunological Methods* 390.1-2, pp. 106–112. ISSN: 00221759. DOI: 10.1016/j.jim.2013.01.015. URL: http://dx.doi.org/10.1016/j.jim.2013.01.015.

Park, Jae H., Isabelle Riviere, Mithat Gonen, Xiuyan Wang, Brigitte Senechal, Kevin J. Curran, Craig Sauter, Yongzeng Wang, Bianca Santomasso, Elena Mead, Mikhail Roshal, Peter Maslak, Marco Davila, Renier J. Brentjens, and Michel Sadelain (2018). "Long-Term Follow-up of CD19 CAR Therapy in Acute Lymphoblastic Leukemia". In: *New England Journal of Medicine*. ISSN: 0028-4793. DOI: 10.1056/NEJMoa1709919.

Patsoukis, Nikolaos, Kankana Bardhan, Pranam Chatterjee, Duygu Sari, Bianling Liu, Lauren N. Bell, Edward D. Karoly, Gordon J. Freeman, Victoria Petkova, Pankaj

Seth, Lequn Li, and Vassiliki A. Boussiotis (Mar. 2015). "PD-1 alters T-cell metabolic reprogramming by inhibiting glycolysis and promoting lipolysis and fatty acid oxidation". In: *Nature Communications* 6, p. 6692. ISSN: 2041-1723. DOI: 10.1038/ncomms7692. URL: http://www.nature.com/doifinder/10.1038/ncomms7692.

Pearce, Erika L. and Edward J. Pearce (2013a). "Metabolic pathways in immune cell activation and quiescence". In: *Immunity* 38.4, pp. 633–643. ISSN: 10747613. DOI: 10.1016/j.immuni.2013.04.005. URL: http://dx.doi.org/10.1016/j.immuni.2013.04.005.

Pearce, Erika L., Maya C. Poffenberger, Chih Hao Chang, and Russell G. Jones (2013b). "Fueling immunity: Insights into metabolism and lymphocyte function". In: *Science* 342.6155. ISSN: 10959203. DOI: 10.1126/science.1242454.

Pearce, Erika L., Matthew C. Walsh, Pedro J. Cejas, Gretchen M. Harms, Hao Shen, Li San Wang, Russell G. Jones, and Yongwon Choi (2009). "Enhancing CD8 T-cell memory by modulating fatty acid metabolism". In: *Nature* 460.7251, pp. 103–107. ISSN: 00280836. DOI: 10.1038/nature08097.

Peggs, K., S. Verfuerth, and S. Mackinnon (Feb. 2001). "Induction of cytomegalovirus (CMV)-specific T-cell responses using dendritic cells pulsed with CMV antigen: A novel culture system free of live CMV virions". In: *Blood* 97.4, pp. 994–1000. ISSN: 00064971. DOI: 10.1182/blood.V97.4.994.

Philip, B, E Kokalaki, L Mekkaoui, S Thomas, K Straathof, B Flutter, V Marin, T Marafioti, R Chakraverty, D Linch, SA Quezada, KS Peggs, and M Pule (2014). "A Highly Compact Epitope-Based Marker Suicide Gene for Safer and Easier Adoptive T-cell Gene Therapy". In: *Blood* 124.8, pp. 1277–1287. ISSN: 1528-0020. DOI: https://doi.org/10.1182/blood-2014-01-545020. URL: http://www.bloodjournal.org/content/124/8/1277.

Pigeau, Gary M., Elizabeth Csaszar, and Aaron Dulgar-Tulloch (2018). "Commercial Scale Manufacturing of Allogeneic Cell Therapy". In: *Frontiers in Medicine* 5.August, pp. 1–8. DOI: 10.3389/fmed.2018.00233.

Pilon-Thomas, Shari, Krithika N. Kodumudi, Asmaa E. El-Kenawi, Shonagh Russell, Amy M. Weber, Kimberly Luddy, Mehdi Damaghi, Jonathan W. Wojtkowiak, James J. Mule, Arig Ibrahim-Hashim, and Robert J. Gillies (2016). "Neutralization of tumor acidity improves antitumor responses to immunotherapy". In: *Cancer Research* 76.6, pp. 1381–1390. ISSN: 15387445. DOI: 10.1158/0008-5472.CAN-15-1743.

Plouffe, Brian D., Shashi K. Murthy, and Laura H. Lewis (2015). "Fundamentals and Application of Magnetic Particles in Cell Isolation and Enrichment". In: *Bone* 23.1, pp. 1–7. ISSN: 15378276. DOI: 10.1088/0034-4885/78/1/016601. arXiv: NIHMS150003.

Porter, David L., Bruce L. Levine, Michael Kalos, Adam Bagg, and Carl H. June (Aug. 2011). "Chimeric Antigen Receptor -Modified T Cells in Chronic Lymphoid Leukemia".

In: *New England Journal of Medicine* 365.8, pp. 725–733. ISSN: 0028-4793. DOI: 10.1056/NEJMoa1103849. URL: http://www.nejm.org/doi/abs/10.1056/NEJMoa1103849.

Porter, David L, Wei-Ting Hwang, Noelle V Frey, Simon F Lacey, Pamela A Shaw, Alison W Loren, Adam Bagg, Katherine T Marcucci, Angela Shen, Vanessa Gonzalez, David Ambrose, Stephan A Grupp, Anne Chew, Zhaohui Zheng, Michael C Milone, Bruce L Levine, Jan J Melenhorst, and Carl H June (2015). "Chimeric antigen receptor T cells persist and induce sustained remissions in relapsed refractory chronic lymphocytic leukemia". In: *Science Translational Medicine*. URL: http://stm.sciencemag.org/content/scitransmed/7/303/303ra139.full.pdf.

Porter, David L, Bruce L Levine, Nancy Bunin, Edward A Stadtmauer, Selina M Luger, Steven Goldstein, Alison Loren, Julie Phillips, Sunita Nasta, Alexander Perl, Steven Schuster, Donald Tsai, Ambika Sohal, Elizabeth Veloso, Stephen Emerson, and Carl H June (2006). "A phase 1 trial of donor lymphocyte infusions expanded and activated ex vivo via CD3 / CD28 costimulation". In: *Blood* 107.4, pp. 1325–1331. DOI: 10.1182/blood-2005-08-3373.Supported.

Post, Dawn E., Eric M. Sandberg, Michele M. Kyle, Narra Sarojini Devi, Daniel J. Brat, Zhiheng Xu, Mourad Tighiouart, and Erwin G. Van Meir (2007). "Targeted cancer gene therapy using a hypoxia inducible factor-dependent oncolytic aden-

ovirus armed with interleukin-4". In: *Cancer Research* 67.14, pp. 6872–6881. ISSN: 00085472. DOI: 10.1158/0008-5472.CAN-06-3244.

Qualls, Joseph E., Chitra Subramanian, Wasiulla Rafi, Amber M. Smith, Liza Balouzian, Ashley A. Defreitas, Kari Ann Shirey, Benjamin Reutterer, Elisabeth Kernbauer, Silvia Stockinger, Thomas Decker, Isao Miyairi, Stefanie N. Vogel, Padmini Salgame, Charles O. Rock, and Peter J. Murray (2012). "Sustained generation of nitric oxide and control of mycobacterial infection requires argininosuccinate synthase 1". In: *Cell Host and Microbe* 12.3, pp. 313–323. ISSN: 19313128. DOI: 10.1016/j.chom.2012.07.012. URL: http://dx.doi.org/10.1016/j.chom.2012.07.012.

Rabinovich, Gabriel A, Dmitry Gabrilovich, and Eduardo M Sotomayor (2007). "Immunosuppressive strategies that are mediated by tumor cells." In: *Annual review of immunology* 25, pp. 267–96. ISSN: 0732-0582. DOI: 10.1146/annurev.immunol.25.022106.141609. URL: http://www.ncbi.nlm.nih.gov/pubmed/17134371%20http://www.pubmedcentral.nih.gov/articlerender.fcgi?artid=PMC2895922.

Rafiq, Qasim A., Mariana P. Hanga, Thomas R.J. Heathman, Karen Coopman, Alvin W. Nienow, David J. Williams, and Christopher J. Hewitt (2017). "Process development of human multipotent stromal cell microcarrier culture using an automated high-throughput microbioreactor". In: *Biotechnology and Bioengineering* 114.10, pp. 2253–2266. ISSN: 10970290. DOI: 10.1002/bit.26359.

Raje, Noopur, Jesus Berdeja, Yi Lin, David Siegel, Sundar Jagannath, Deepu Madduri, Michaela Liedtke, Jacalyn Rosenblatt, Marcela V. Maus, Ashley Turka, Lyh Ping Lam, Richard A. Morgan, Kevin Friedman, Monica Massaro, Julie Wang, Greg Russotti, Zhihong Yang, Timothy Campbell, Kristen Hege, Fabio Petrocca, M. Travis Quigley, Nikhil Munshi, and James N. Kochenderfer (2019). "Anti-BCMA CAR T-cell therapy bb2121 in relapsed or refractory multiple myeloma". In: *New England Journal of Medicine*. ISSN: 15334406. DOI: 10.1056/NEJMoa1817226.

Raman, Marine C.C., Pierre J. Rizkallah, Ruth Simmons, Zoe Donnellan, Joseph Dukes, Giovanna Bossi, Gabrielle S. Le Provost, Penio Todorov, Emma Baston, Emma Hickman, Tara Mahon, Namir Hassan, Annelise Vuidepot, Malkit Sami, David K. Cole, and Bent K. Jakobsen (Jan. 2016). "Direct molecular mimicry enables off-target cardiovascular toxicity by an enhanced affinity TCR designed for cancer immunotherapy". In: *Scientific Reports* 6. ISSN: 20452322. DOI: 10.1038/srep18851.

Renner, Kathrin, Anna Lena Geiselhöringer, Matthias Fante, Christina Bruss, Stephanie Farber, Gabriele Schönhammer, Katrin Peter, Katrin Singer, Reinhard Andreesen, Petra Hoffmann, Peter Oefner, Wolfgang Herr, and Marina Kreutz (2015). "Metabolic plasticity of human T cells: Preserved cytokine production under glucose deprivation or mitochondrial restriction, but 2-deoxy-glucose affects effector functions". In: *European Journal of Immunology* 45.9, pp. 2504–2516. ISSN: 15214141. DOI: 10.1002/eji.201545473.

Roddie, Claire, Maeve O'Reilly, Juliana Dias Alves Pinto, Ketki Vispute, and Mark Lowdell (2019). "Manufacturing chimeric antigen receptor T cells: issues and challenges". In: *Cytotherapy* 21.3, pp. 327–340. ISSN: 14772566. DOI: 10.1016/j.jcyt.2018.11.009. URL: https://doi.org/10.1016/j.jcyt.2018.11.009.

Rogatzki, Matthew J., Brian S. Ferguson, Matthew L. Goodwin, and L. Bruce Gladden (2015). "Lactate is always the end product of glycolysis". In: *Frontiers in Neuroscience* 9.FEB, pp. 1–7. ISSN: 1662453X. DOI: 10.3389/fnins.2015.00022.

Romero, Jose Maria, Pilar Jimenez, Teresa Cabrera, Jose Manuel Cózar, Susana Pedrinaci, Miguel Tallada, Federico Garrido, and Francisco Ruiz-Cabello (Feb. 2005). "Coordinated downregulation of the antigen presentation machinery and HLA class I/β2-microglobulin complex is responsible for HLA-ABC loss in bladder cancer". In: *International Journal of Cancer* 113.4, pp. 605–610. ISSN: 00207136. DOI: 10.1002/ijc.20499.

Rosenberg, S A, B S Packard, P M Aebersold, D Solomon, S L Topalian, S T Toy, P Simon, M T Lotze, J C Yang, and C A Seipp (Dec. 1988). "Use of tumor-infiltrating lymphocytes and interleukin-2 in the immunotherapy of patients with metastatic melanoma. A preliminary report." In: *The New England journal of medicine* 319.25, pp. 1676–80. ISSN: 0028-4793. DOI: 10.1056/NEJM198812223192527. URL: http://www.ncbi.nlm.nih.gov/pubmed/3264384.

Rosenberg, Steven A. and Nicholas P. Restifo (Apr. 2015). "Adoptive cell transfer as personalized immunotherapy for human cancer". In: *Science* 348.6230, pp. 62–68. ISSN: 10959203. DOI: 10.1126/science.aaa4967.

Rosenberg, Steven A., Paul Spiess, and Rene Lafreniere (1986). "A new approach to the adoptive immunotherapy of cancer with tumor-infiltrating lymphocytes". In: *Science* 233.4770, pp. 1318–1321. ISSN: 00368075. DOI: 10.1126/science.3489291.

Rosenberg, Steven A., James C. Yang, Richard M. Sherry, Udai S. Kammula, Marybeth S. Hughes, Giao Q. Phan, Deborah E. Citrin, Nicholas P. Restifo, Paul F. Robbins, John R. Wunderlich, Kathleen E. Morton, Carolyn M. Laurencot, Seth M. Steinberg, Donald E. White, and Mark E. Dudley (2011). "Durable complete responses in heavily pretreated patients with metastatic melanoma using T-cell transfer immunotherapy". In: *Clinical Cancer Research* 17.13, pp. 4550–4557. ISSN: 10780432. DOI: 10.1158/1078-0432.CCR-11-0116.

Roybal, Kole T., Levi J. Rupp, Leonardo Morsut, Whitney J. Walker, Krista A. McNally, Jason S. Park, and Wendell A. Lim (2016). "Precision Tumor Recognition by T Cells with Combinatorial Antigen-Sensing Circuits". In: *Cell*. ISSN: 10974172. DOI: 10.1016/j.cell.2016.01.011.

Sabatino, Marianna, Jinhui Hu, Michele Sommariva, Sanjivan Gautam, Vicki Fellowes, James D. Hocker, Sean Dougherty, Haiying Qin, Christopher A. Klebanoff, Terry J. Fry, Ronald E. Gress, James N. Kochenderfer, David F. Stroncek, Yun Ji, and

Luca Gattinoni (2016). “Generation of clinical-grade CD19-specific CAR-modified CD8+ memory stem cells for the treatment of human B-cell malignancies.” In: *Blood* 128.4, pp. 519–28. ISSN: 1528-0020. DOI: 10.1182/blood-2015-11-683847. URL: http://www.bloodjournal.org/cgi/doi/10.1182/blood-2015-11-683847%7B%5C%%7D5Cnhttp://www.ncbi.nlm.nih.gov/pubmed/27226436%7B%5C%%7D5Cnhttp://www.pubmedcentral.nih.gov/articlerender.fcgi?artid=PMC4965906.

Sadelain, Michel, Renier Brentjens, and Isabelle Riviere (2013). “The basic principles of chimeric antigen receptor design”. In: *Cancer Discovery* 3.4, pp. 388–398. ISSN: 21598274. DOI: 10.1158/2159-8290.CD-12-0548. arXiv: NIHMS150003.

Sadelain, Michel, Isabelle Riviere, and Stanley Riddell (2017). “Therapeutic T cell engineering”. In: *Nature Publishing Group* 545. DOI: 10.1038/nature22395. URL: https://www.nature.com/articles/nature22395.pdf.

Salazar-Noratto, Giuliana E., Guotian Luo, Cyprien Denoeud, Mathilde Padrona, Adrien Moya, Morad Bensidhoum, Rena Bizios, Esther Potier, Delphine Logeart-Avramoglou, and Herve Petite (2020). “Understanding and leveraging cell metabolism to enhance mesenchymal stem cell transplantation survival in tissue engineering and regenerative medicine applications”. In: *Stem Cells* 38.1, pp. 22–33. ISSN: 15494918. DOI: 10.1002/stem.3079.

Sanber, Khaled S., Sean B. Knight, Sam L. Stephen, Ranbir Bailey, David Escors, Jeremy Minshull, Giorgia Santilli, Adrian J. Thrasher, Mary K. Collins, and Yasuhiro Takeuchi (2015). "Construction of stable packaging cell lines for clinical lentiviral vector production". In: *Scientific Reports* 5. ISSN: 20452322. DOI: 10.1038/srep09021.

Sato, N., C. Caux, T. Kitamura, Y. Watanabe, K. I. Arai, J. Banchereau, and A. Miyajima (1993). "Expression and factor-dependent modulation of the interleukin-3 receptor subunits on human hematopoietic cells". In: *Blood*. ISSN: 00064971. DOI: 10.1182/blood.v82.3.752.bloodjournal823752.

Scarselli, Alessia, Luca Basso Ricci, Federica Barzaghi, Eugenio Montini, Serena Scala, Andrea Calabria, Chiara Bonini, Nicoletta Cieri, Alessandro Aiuti, Cristina Baricordi, Maria Grazia Roncarolo, Hamoud Al-Mousa, Claudio Bordignon, Luca Biasco, Caterina Cancrini, Francesca Dionisio, Stefania Giannelli, and Roberta Pajno (2015). "In vivo tracking of T cells in humans unveils decade-long survival and activity of genetically modified T memory stem cells". In: *Science Translational Medicine* 7.273, pp. 30–33. ISSN: 1946-6234. DOI: 10.1126/scitranslmed.3010314.

Scharping, Nicole E., Ashley V. Menk, Rebecca S. Moreci, Ryan D. Whetstone, Rebekah E. Dadey, Simon C. Watkins, Robert L. Ferris, and Greg M. Delgoffe (2016). "The Tumor Microenvironment Represses T Cell Mitochondrial Biogenesis to Drive

Intratumoral T Cell Metabolic Insufficiency and Dysfunction". In: *Immunity* 45.2, pp. 374–388. ISSN: 10974180. DOI: 10.1016/j.immuni.2016.07.009. URL: http://dx.doi.org/10.1016/j.immuni.2016.07.009.

Schurich, Anna, Isabelle Magalhaes, and Jonas Mattsson (2019). "Metabolic regulation of CAR T cell function by the hypoxic microenvironment in solid tumors". In: *Immunotherapy* 11.4, pp. 335–345. ISSN: 17507448. DOI: 10.2217/imt-2018-0141.

Schuster, Stephen J., Michael R. Bishop, Constantine S. Tam, Edmund K. Waller, Peter Borchmann, Joseph P. McGuirk, Ulrich Jager, Samantha Jaglowski, Charalambos Andreadis, Jason R. Westin, Isabelle Fleury, Veronika Bachanova, S. Ronan Foley, P. Joy Ho, Stephan Mielke, John M. Magenau, Harald Holte, Serafino Pantano, Lida B. Pacaud, Rakesh Awasthi, Jufen Chu, Özlem Anak, Gilles Salles, and Richard T. Maziarz (2019). "Tisagenlecleucel in adult relapsed or refractory diffuse large B-cell lymphoma". In: *New England Journal of Medicine*. ISSN: 15334406. DOI: 10.1056/NEJMoa1804980.

Schuster, Stephen J., Jakub Svoboda, Elise A. Chong, Sunita D. Nasta, Anthony R. Mato, Özlem Anak, Jennifer L. Brogdon, Iulian Pruteanu-Malinici, Vijay Bhoj, Daniel Landsburg, Mariusz Wasik, Bruce L. Levine, Simon F. Lacey, Jan J. Melenhorst, David L. Porter, and Carl H. June (2017). "Chimeric Antigen Receptor T Cells in Refractory B-Cell Lymphomas". In: *New England Journal of Medicine*,

NEJMoa1708566. ISSN: 0028-4793. DOI: 10.1056/NEJMoa1708566. URL: http://www.nejm.org/doi/10.1056/NEJMoa1708566.

Seder, R A, J L Boulay, F Finkelman, S Barbier, S Z Ben-Sasson, G Le Gros, and W E Paul (1992). "CD8+ T cells can be primed in vitro to produce IL-4." In: *Journal of immunology (Baltimore, Md. : 1950)*. ISSN: 0022-1767.

Seif, Michelle, Hermann Einsele, and Jürgen Löffler (2019). "CAR T Cells Beyond Cancer: Hope for Immunomodulatory Therapy of Infectious Diseases". In: *Frontiers in Immunology* 10.November. ISSN: 16643224. DOI: 10.3389/fimmu.2019.02711.

Sena, Laura A., Sha Li, Amit Jairaman, Murali Prakriya, Teresa Ezponda, David A. Hildeman, Chyung Ru Wang, Paul T. Schumacker, Jonathan D. Licht, Harris Perlman, Paul J. Bryce, and Navdeep S. Chandel (2013). "Mitochondria Are Required for Antigen-Specific T Cell Activation through Reactive Oxygen Species Signaling". In: *Immunity* 38.2, pp. 225–236. ISSN: 10747613. DOI: 10.1016/j.immuni.2012.10.020. URL: http://dx.doi.org/10.1016/j.immuni.2012.10.020.

Shi, Lewis Z., Ruoning Wang, Gonghua Huang, Peter Vogel, Geoffrey Neale, Douglas R. Green, and Hongbo Chi (2011). "HIF1α-dependent glycolytic pathway orchestrates a metabolic checkpoint for the differentiation of TH17 and Treg cells". In: *Journal of Experimental Medicine* 208.7, pp. 1367–1376. ISSN: 00221007. DOI: 10.1084/jem.20110278.

Shibuya, Terry Y., Wei Zen Wei, Michelle Zormeier, John Ensley, Wael Sakr, Robert H. Mathog, Robert J. Meleca, George H. Yoo, Carl H. June, Bruce L. Levine, and Lawrence G. Lum (2000). "Anti-CD3/anti-CD28 bead stimulation overcomes CD3 unresponsiveness in patients with head and neck squamous cell carcinoma". In: *Archives of Otolaryngology - Head and Neck Surgery* 126.4, pp. 473–479. ISSN: 08864470. DOI: 10.1001/archotol.126.4.473.

Sinclair, Linda V., Julia Rolf, Elizabeth Emslie, Yun Bo Shi, Peter M. Taylor, and Doreen A. Cantrell (2013). "Control of amino-acid transport by antigen receptors coordinates the metabolic reprogramming essential for T cell differentiation". In: *Nature Immunology* 14.5, pp. 500–508. ISSN: 15292908. DOI: 10.1038/ni.2556.

Singh, Harjeet, Matthew J. Figliola, Margaret J. Dawson, Helen Huls, Simon Olivares, Kirsten Switzer, Tiejuan Mi, Sourindra Maiti, Partow Kebriaei, Dean A. Lee, Richard E. Champlin, and Laurence J.N. Cooper (May 2011). "Reprogramming CD19-specific T cells with IL-21 signaling can improve adoptive immunotherapy of B-lineage malignancies". In: *Cancer Research* 71.10, pp. 3516–3527. ISSN: 00085472. DOI: 10.1158/0008-5472.CAN-10-3843.

Singh, Harjeet, Matthew J. Figliola, Margaret J. Dawson, Simon Olivares, Ling Zhang, Ge Yang, Sourindra Maiti, Pallavi Manuri, Vladimir Senyukov, Bipulendu Jena, Partow Kebriaei, Richard E. Champlin, Helen Huls, and Laurence J. N. Cooper (May 2013). "Manufacture of Clinical-Grade CD19-Specific T Cells Stably Expressing

Chimeric Antigen Receptor Using Sleeping Beauty System and Artificial Antigen Presenting Cells". In: *PLoS ONE* 8.5. Ed. by Hossam M. Ashour, e64138. ISSN: 1932-6203. DOI: 10.1371/journal.pone.0064138. URL: https://dx.plos.org/10.1371/journal.pone.0064138.

Singh, Harjeet, Helen Huls, Partow Kebriaei, and Laurence J.N. Cooper (2014). "A new approach to gene therapy using Sleeping Beauty to genetically modify clinical-grade T cells to target CD19". In: *Immunological Reviews* 257.1, pp. 181–190. ISSN: 01052896. DOI: 10.1111/imr.12137.

Singh, Nathan, Jessica Perazzelli, Stephan A. Grupp, and David M. Barrett (2016). "Early memory phenotypes drive T cell proliferation in patients with pediatric malignancies". In: *Science Translational Medicine* 8.320, pp. 1–10. ISSN: 19466242. DOI: 10.1126/scitranslmed.aad5222.

Singh, Vijay (1999). "Disposable bioreactor for cell culture using wave-induced agitation". In: *Cytotechnology* 30.1-3, pp. 149–158. ISSN: 09209069. DOI: 10.1007/0-306-46860-374.

Somerville, Robert PT et al. (2012). "Clinical scale rapid expansion of lymphocytes for adoptive cell transfer therapy in the WAVE® bioreactor". In: *Journal of Translational Medicine* 10.1, p. 69. ISSN: 1479-5876. DOI: 10.1186/1479-5876-10-69. URL: http://translational-medicine.biomedcentral.com/articles/10.1186/1479-5876-10-69.

Spolski, Rosanne and Warren J. Leonard (Apr. 2008). “Interleukin-21: Basic Biology and Implications for Cancer and Autoimmunity”. In: *Annual Review of Immunology* 26.1, pp. 57–79. ISSN: 0732-0582. DOI: 10.1146/annurev.immunol.26.021607.090316.

Sprent, Jonathan and Charles D. Surh (2011). “Normal T cell homeostasis: The conversion of naive cells into memory-phenotype cells”. In: *Nature Immunology* 12.6, pp. 478–484. ISSN: 15292908. DOI: 10.1038/ni.2018.

Stavrou, Maria, Brian Philip, Charlotte Traynor-White, Christopher G. Davis, Shimobi Onuoha, Shaun Cordoba, Simon Thomas, and Martin Pule (2018). “A Rapamycin-Activated Caspase 9-Based Suicide Gene”. In: *Molecular Therapy* 26.5, pp. 1266–1276. ISSN: 15250024. DOI: 10.1016/j.ymthe.2018.03.001. URL: https://doi.org/10.1016/j.ymthe.2018.03.001.

Stroncek, D.F, Fellowes V., Pham C., Khuu H., Fowler D.H., Wood L.V., and Sabatino M. (2014). “Counter-flow elutriation of clinical peripheral blood mononuclear cell concentrates for the production of dendritic and T cell therapies”. In: *Journal of Translational Medicine* 12.1, p. 241. ISSN: 1479-5876. URL: http://www.embase.com/search/results?subaction=viewrecord%7B%5C&%7Dfrom=export%7B%5C&%7Did=L600193392%7B%5C%%7D5Cnhttp://dx.doi.org/10.1186/s12967-014-0241-y%7B%5C%%7D5Cnhttp://sfx.aub.aau.dk/sfxaub?sid=

EMBASE%7B%5C&%7Dissn=14795876%7B%5C&%7Did=doi:10.1186%7B%5C%%7D2Fs12967-014-0241-y%7B%5C&%7Datitle=Counter-flow+elutriation+.

Sukumar, Madhusudhanan, Jie Liu, Yun Ji, Murugan Subramanian, Joseph G. Crompton, Zhiya Yu, Rahul Roychoudhuri, Douglas C. Palmer, Pawel Muranski, Edward D. Karoly, Robert P. Mohney, Christopher A. Klebanoff, Ashish Lal, Toren Finkel, Nicholas P. Restifo, and Luca Gattinoni (2013). "Inhibiting glycolytic metabolism enhances CD8+ T cell memory and antitumor function". In: *Journal of Clinical Investigation* 123.10, pp. 4479–4488. ISSN: 00219738. DOI: 10.1172/JCI69589.

Szmania, Susann, Amanda Galloway, Mary Bruorton, Philip Musk, Geraldine Aubert, Andrew Arthur, Haywood Pyle, Nancy Hensel, Ta Nga, Lawrence Lamb, Toni Dodi, Alejandro Madrigal, John Barrett, Jean Henslee-Downey, and Frits Van Rhee (Aug. 2001). "Isolation and expansion of cytomegalovirus-specific cytotoxic T lymphocytes to clinical scale from a single blood draw using dendritic cells and HLA-tetramers". In: *Blood* 98.3, pp. 505–512. ISSN: 00064971. DOI: 10.1182/blood.V98.3.505.

Tartour, Eric, François Fossiez, Isabelle Joyeux, Annie Galinha, Alain Gey, Emmanuel Claret, Xavier Sastre-Garau, Jérôme Couturier, Veronique Mosseri, Virginie Vives, Jacques Banchereau, Wolf H. Fridman, John Wijdenes, Serge Lebecque, and Catherine Sautès-Fridman (1999). "Interleukin 17, a T-cell-derived cytokine, promotes tu-

morigenicity of human cervical tumors in nude mice". In: *Cancer Research* 59.15, pp. 3698–3704. ISSN: 00085472.

Thieme, Daniel, Lynn Reuland, Toni Lindl, Friedrich Kruse, and Thomas Fuchsluger (2018). "Optimized human platelet lysate as novel basis for a serum-, xeno-, and additive-free corneal endothelial cell and tissue culture". In: *Journal of Tissue Engineering and Regenerative Medicine*. ISSN: 19327005. DOI: 10.1002/term.2574.

Thornton, Angela M. and Ethan M. Shevach (1998). "CD4+ CD25+ Immunoregulatory T Cells Suppress Polyclonal T Cell Activation In Vitro by Inhibiting Interleukin 2 Production". In: *The journal of experiment* 188.2, pp. 287–296.

Todaro, M., Y. Lombardo, M. G. Francipane, M. Perez Alea, P. Cammareri, F. Iovino, A. B. Di Stefano, C. Di Bernardo, A. Agrusa, G. Condorelli, H. Walczak, and G. Stassi (2008). "Apoptosis resistance in epithelial tumors is mediated by tumor-cell-derived interleukin-4". In: *Cell Death and Differentiation* 15.4, pp. 762–772. ISSN: 14765403. DOI: 10.1038/sj.cdd.4402305.

Topalian, Suzanne L., F. Stephen Hodi, Julie R. Brahmer, Scott N. Gettinger, David C. Smith, David F. McDermott, John D. Powderly, Richard D. Carvajal, Jeffrey A. Sosman, Michael B. Atkins, Philip D. Leming, David R. Spigel, Scott J. Antonia, Leora Horn, Charles G. Drake, Drew M. Pardoll, Lieping Chen, William H. Sharfman, Robert A. Anders, Janis M. Taube, Tracee L. McMiller, Haiying Xu, Alan J. Korman, Maria Jure-Kunkel, Shruti Agrawal, Daniel McDonald, Georgia D. Kol-

lia, Ashok Gupta, Jon M. Wigginton, and Mario Sznol (2012). “Safety, activity, and immune correlates of anti-PD-1 antibody in cancer”. In: *New England Journal of Medicine*. ISSN: 15334406. DOI: 10.1056/NEJMoa1200690.

Trummer, Evelyn, Katharina Fauland, Silke Seidinger, Kornelia Schriebl, Christine Lattenmayer, Renate Kunert, Karola Vorauer-Uhl, Robert Weik, Nicole Borth, Hermann Katinger, and Dethardt Müller (2006). “Process parameter shifting: Part I. Effect of DOT, pH, and temperature on the performance of Epo-Fc expressing CHO cells cultivated in controlled batch bioreactors”. In: *Biotechnology and Bioengineering* 94.6, pp. 1033–1044. ISSN: 00063592. DOI: 10.1002/bit.21013.

Tumaini, Barbara, Daniel W. Lee, Tasha Lin, Luciano Castiello, David F. Stroncek, Crystal Mackall, Alan Wayne, and Marianna Sabatino (2013a). “Simplified process for the production of anti-CD19-CAR-engineered Tcells”. In: *Cytotherapy* 15.11, pp. 1406–1415. ISSN: 14653249. DOI: 10.1016/j.jcyt.2013.06.003.

— (2013b). “Simplified process for the production of anti-CD19-CAR-engineered T cells”. In: *Journal of Cytotherapy* 15, pp. 1406–1415. DOI: 10.1016/j.jcyt.2013.06.003. URL: https://ac.els-cdn.com/S1465324913005872/1-s2.0-S1465324913005872-main.pdf?%20tid=bade6b5f-022f-4375-b1ce-94de67c98910%7B%5C&%7Dacdnat=1520360010%20df396200c8c1bb59af56a0adb6dd210d.

Turtle, C. J., L.-A. Hanafi, C. Berger, M. Hudecek, B. Pender, E. Robinson, R. Hawkins, C. Chaney, S. Cherian, X. Chen, L. Soma, B. Wood, D. Li, S. Heimfeld, S. R.

Riddell, and D. G. Maloney (2016). “Immunotherapy of non-Hodgkins lymphoma with a defined ratio of CD8+ and CD4+ CD19-specific chimeric antigen receptor-modified T cells”. In: *Science Translational Medicine* 8.355, 355ra116–355ra116. ISSN: 1946-6234. DOI: 10.1126/scitranslmed.aaf8621. URL: http://stm.sciencemag.org/cgi/doi/10.1126/scitranslmed.aaf8621.

Turtle, Cameron J., Kevin A. Hay, Laila Aicha Hanafi, Daniel Li, Sindhu Cherian, Xueyan Chen, Brent Wood, Arletta Lozanski, John C. Byrd, Shelly Heimfeld, Stanley R. Riddell, and David G. Maloney (2017). “Durable molecular remissions in chronic lymphocytic leukemia treated with CD19-Specific chimeric antigen Receptor-modified T cells after failure of ibrutinib”. In: *Journal of Clinical Oncology*. ISSN: 15277755. DOI: 10.1200/JCO.2017.72.8519.

Turtle, Cameron J, Laila-aicha Hanafi, Carolina Berger, Theodore A Gooley, Sindhu Cherian, Michael Hudecek, Daniel Sommermeyer, Katherine Melville, Barbara Pender, Tanya M Budiarto, Emily Robinson, Natalia N Steevens, Colette Chaney, Lorinda Soma, Xueyan Chen, Cecilia Yeung, Brent Wood, Daniel Li, Jianhong Cao, Shelly Heimfeld, Michael C Jensen, Stanley R Riddell, and David G Maloney (June 2016). “CD19 CAR - T cells of defined CD4 + : CD8 + composition in adult B cell ALL patients”. In: *J Clin Invest* 1.6, pp. 1–16. ISSN: 1558-8238. DOI: 10.1172/JCI85309DS1. URL: https://www.jci.org/articles/view/85309.

Unsoeld, H. and H. Pircher (2005). “Complex Memory T-Cell Phenotypes Revealed by Coexpression of CD62L and CCR7”. In: *Journal of Virology* 79.7, pp. 4510–4513. ISSN: 0022-538X. DOI: 10.1128/jvi.79.7.4510-4513.2005.

Urak, Ryan, Miriam Walter, Laura Lim, Ching Lam W. Wong, Lihua E. Budde, Sandra Thomas, Stephen J. Forman, and Xiuli Wang (2017). “Ex vivo Akt inhibition promotes the generation of potent CD19CAR T cells for adoptive immunotherapy”. In: *Journal for ImmunoTherapy of Cancer* 5.1, pp. 1–13. ISSN: 20511426. DOI: 10.1186/s40425-017-0227-4.

Vedvyas, Yogindra, Jaclyn E. McCloskey, Yanping Yang, Irene M. Min, Thomas J. Fahey, Rasa Zarnegar, Yen Michael S. Hsu, Jing Mei Hsu, Koen Van Besien, Ian Gaudet, Ping Law, Nak Joon Kim, Eric von Hofe, and Moonsoo M. Jin (2019). “Manufacturing and preclinical validation of CAR T cells targeting ICAM-1 for advanced thyroid cancer therapy”. In: *Scientific Reports* 9.1, pp. 1–15. ISSN: 20452322. DOI: 10.1038/s41598-019-46938-7.

Vohwinkel, Christine U., Emilia Lecuona, Haying Sun, Natascha Sommer, Istvan Vadasz, Navdeep S. Chandel, and Jacob I. Sznajder (2011). “Elevated CO2 levels cause mitochondrial dysfunction and impair cell proliferation”. In: *Journal of Biological Chemistry* 286.43, pp. 37067–37076. ISSN: 00219258. DOI: 10.1074/jbc.M111.290056.

Vormittag, Philipp, Rebecca Gunn, Sara Ghorashian, and Farlan S. Veraitch (2018). "A guide to manufacturing CAR T cell therapies". In: *Current Opinion in Biotechnology* 53, pp. 164–181. ISSN: 18790429. DOI: 10.1016/j.copbio.2018.01.025. URL: http://dx.doi.org/10.1016/j.copbio.2018.01.025.

Walker, Christoph, Florence Bettens, and Werner J. Pichler (1987). "Activation of T cells by cross-linking an anti-CD3 antibody with a second anti-T cell antibody: mechanism and subset-specific activation". In: *European Journal of Immunology* 17.6, pp. 873–880. ISSN: 15214141. DOI: 10.1002/eji.1830170622.

Wang, Chao, Meromit Singer, and Ana C. Anderson (2017). "Molecular Dissection of CD8+ T-Cell Dysfunction". In: *Trends in Immunology* 38.8, pp. 567–576. ISSN: 14714981. DOI: 10.1016/j.it.2017.05.008. URL: http://dx.doi.org/10.1016/j.it.2017.05.008.

Wang, Jin, Hiroyuki Honda, Yong Soo Park, Shinji Iijima, and Takeshi Kobayashi (1994). "Effect of Dissolved Oxygen Concentration on Growth and Production of Biomaterials by Animal Cell Culture". In: *Animal Cell Technology: Basic & Applied Aspects*. Dordrecht: Springer Netherlands, pp. 191–195. DOI: 10.1007/978-94-011-0848-528. URL: http://www.springerlink.com/index/10.1007/978-94-011-0848-5%2028.

Wang, Ruoning, Christopher P. Dillon, Lewis Zhichang Shi, Sandra Milasta, Robert Carter, David Finkelstein, Laura L. McCormick, Patrick Fitzgerald, Hongbo Chi,

Joshua Munger, and Douglas R. Green (2011). "The Transcription Factor Myc Controls Metabolic Reprogramming upon T Lymphocyte Activation". In: *Immunity* 35.6, pp. 871–882. ISSN: 10747613. DOI: 10.1016/j.immuni.2011.09.021. arXiv: NIHMS150003. URL: http://dx.doi.org/10.1016/j.immuni.2011.09.021.

Wang, Xiuli, Leslie L. Popplewell, Jamie R. Wagner, Araceli Naranjo, M. Suzette Blanchard, Michelle R. Mott, Adam P. Norris, Ching Lam W. Wong, Ryan Z. Urak, Wen Chung Chang, Samer K. Khaled, Tanya Siddiqi, Lihua E. Budde, Jingying Xu, Brenda Chang, Nikita Gidwaney, Sandra H. Thomas, Laurence J.N. Cooper, Stanley R. Riddell, Christine E. Brown, Michael C. Jensen, and Stephen J. Forman (2016). "Phase 1 studies of central memory-derived CD19 CAR T-cell therapy following autologous HSCT in patients with B-cell NHL". In: *Blood* 127.24, pp. 2980–2990. ISSN: 15280020. DOI: 10.1182/blood-2015-12-686725.

Wang, Xiuyan and Isabelle Riviere (2016). "Clinical manufacturing of CAR T cells: foundation of a promising therapy." In: *Molecular therapy oncolytics* 3.February, p. 16015. ISSN: 2372-7705. DOI: 10.1038/mto.2016.15. URL: http://www.ncbi.nlm.nih.gov/pubmed/27347557%7B%5C%%7D5Cnhttp://www.pubmedcentral.nih.gov/articlerender.fcgi?artid=PMC4909095.

Wang, Y., X. Y. Wang, J. R. Subjeck, P. A. Shrikant, and H. L. Kim (2011). "Temsirolimus, an mTOR inhibitor, enhances anti-tumour effects of heat shock protein

cancer vaccines". In: *British Journal of Cancer*. ISSN: 00070920. DOI: 10.1038/bjc.2011.15.

Warburg, O (Aug. 1956). "On respiratory impairment in cancer cells." eng. In: *Science (New York, N.Y.)* 124.3215, pp. 269–270. ISSN: 0036-8075 (Print).

Wei, Jun, Jana Raynor, Thanh Long M. Nguyen, and Hongbo Chi (2017). "Nutrient and metabolic sensing in T cell responses". In: *Frontiers in Immunology* 8.MAR, pp. 1–14. ISSN: 16643224. DOI: 10.3389/fimmu.2017.00247.

Weinberg, Adriana, Lin Ye Song, Cynthia Wilkening, Anne Sevin, Bruce Blais, Raul Louzao, Dana Stein, Patricia Defechereux, Deborah Durand, Eric Riedel, Nancy Raftery, Renee Jesser, Betty Brown, M. Fran Keller, Ruth Dickover, Elizabeth McFarland, and Terence Fenton (2009). "Optimization and limitations of use of cryopreserved peripheral blood mononuclear cells for functional and phenotypic T-cell characterization". In: *Clinical and Vaccine Immunology* 16.8, pp. 1176–1186. ISSN: 15566811. DOI: 10.1128/CVI.00342-08.

Weinkove, Robert, Philip George, Nathaniel Dasyam, and Alexander D. McLellan (2019). "Selecting costimulatory domains for chimeric antigen receptors: functional and clinical considerations". In: *Clinical and Translational Immunology* 8.5, pp. 1–14. ISSN: 20500068. DOI: 10.1002/cti2.1049.

Wellen, Kathryn E., Chao Lu, Anthony Mancuso, Johanna M.S. Lemons, Michael Ryczko, James W. Dennis, Joshua D. Rabinowitz, Hilary A. Coller, and Craig B. Thompson

(2010). “The hexosamine biosynthetic pathway couples growth factor-induced glutamine uptake to glucose metabolism”. In: *Genes and Development* 24.24, pp. 2784–2799. ISSN: 08909369. DOI: 10.1101/gad.1985910.

Wenger, Roland, Vartan Kurtcuoglu, Carsten Scholz, Hugo Marti, and David Hoogewijs (2015). “Frequently asked questions in hypoxia research”. In: *Hypoxia*, p. 35. DOI: 10.2147/hp.s92198.

Wiegmann, Vincent, Cristina Bernal Martinez, and Frank Baganz (July 2018). “A simple method to determine evaporation and compensate for liquid losses in small-scale cell culture systems”. In: *Biotechnology Letters* 40.7, pp. 1029–1036. ISSN: 0141-5492. DOI: 10.1007/s10529-018-2556-x. URL: http://www.ncbi.nlm.nih.gov/pubmed/29693210%20http://www.pubmedcentral.nih.gov/articlerender.fcgi?artid=PMC5990580%20http://link.springer.com/10.1007/s10529-018-2556-x.

Wieman, Heather L., Jessica A. Wofford, and Jeffrey C. Rathmell (2007). “Cytokine Stimulation Promotes Glucose Uptake via Phosphatidylinositol-3 Kinase/Akt Regulation of Glut1 Activity and Traffickin”. In: *Molecular Biology of the Cell* 18.March, pp. 976–985. DOI: 10.1091/mbc.E06.

Wilkie, Scott, Sophie E. Burbridge, Laura Chiapero-Stanke, Ana C.P. Pereira, Siobhan Cleary, Sjoukje J.C. Van Der Stegen, James F. Spicer, David M. Davies, and John Maher (2010). “Selective expansion of chimeric antigen receptor-targeted T-

cells with potent effector function using interleukin-4". In: *Journal of Biological Chemistry* 285.33, pp. 25538–25544. ISSN: 00219258. DOI: 10.1074/jbc.M110.127951.

Willinger, Tim, Tom Freeman, Mark Herbert, Hitoshi Hasegawa, Andrew J. McMichael, and Margaret F. C. Callan (Feb. 2006). "Human Naive CD8 T Cells Down-Regulate Expression of the WNT Pathway Transcription Factors Lymphoid Enhancer Binding Factor 1 and Transcription Factor 7 (T Cell Factor-1) following Antigen Encounter In Vitro and In Vivo". In: *The Journal of Immunology* 176.3, pp. 1439–1446. ISSN: 0022-1767. DOI: 10.4049/jimmunol.176.3.1439.

Windt, Gerritje J W van der, David O'Sullivan, Bart Everts, Stanley Ching-Cheng Huang, Michael D Buck, Jonathan D Curtis, Chih-Hao Chang, Amber M Smith, Teresa Ai, Brandon Faubert, Russell G Jones, Edward J Pearce, and Erika L Pearce (2013). "CD8 memory T cells have a bioenergetic advantage that underlies their rapid recall ability." In: *Proceedings of the National Academy of Sciences of the United States of America* 110.35, pp. 14336–41. ISSN: 1091-6490. DOI: 10.1073/pnas.1221740110. URL: http://www.pubmedcentral.nih.gov/articlerender.fcgi?artid=3761631%7B%5C&%7Dtool=pmcentrez%7B%5C&%7Drendertype=abstract.

Windt, Gerritje J W van der and Erika L. Pearce (2012). "Metabolic switching and fuel choice during T-cell differentiation and memory development". In: *Immunological*

Reviews 249.1, pp. 27–42. ISSN: 01052896. DOI: 10.1111/j.1600-065X.2012.01150.x. arXiv: NIHMS150003.

Wolf, Benita, Stefan Zimmermann, Caroline Arber, Melita Irving, Lionel Trueb, and George Coukos (2019). "Safety and Tolerability of Adoptive Cell Therapy in Cancer". In: *Drug Safety* 42.2, pp. 315–334. ISSN: 11791942. DOI: 10.1007/s40264-018-0779-3. URL: https://doi.org/10.1007/s40264-018-0779-3.

Wong, Danny Chee Furng, Kathy Tin Kam Wong, Lin Tang Goh, Chew Kiat Heng, and Miranda Gek Sim Yap (2005). "Impact of dynamic online fed-batch strategies on metabolism, productivity and N-glycosylation quality in CHO cell cultures". In: *Biotechnology and Bioengineering* 89.2, pp. 164–177. ISSN: 00063592. DOI: 10.1002/bit.20317.

Workman, Creg J., Linda S. Cauley, In-Jeong Kim, Marcia A. Blackman, David L. Woodland, and Dario A. A. Vignali (2004). "Lymphocyte Activation Gene-3 (CD223) Regulates the Size of the Expanding T Cell Population Following Antigen Activation In Vivo". In: *The Journal of Immunology* 172.9, pp. 5450–5455. ISSN: 0022-1767. DOI: 10.4049/jimmunol.172.9.5450.

Workman, Creg J. and Dario A.A. Vignali (2003). "The CD4-related molecule, LAG-3 (CD223), regulates the expansion of activated T cells". In: *European Journal of Immunology* 33.4, pp. 970–979. ISSN: 00142980. DOI: 10.1002/eji.200323382.

Xu, Yang, Ming Zhang, Aruna Mahendravada, Barbara Savoldo, and Gianpietro Dotti (2013). "γc Cytokines IL7 and IL15 Expanded Chimeric Antigen Receptor-Redirected T Cells (CAR-T) with Superior Antitumor Activity In Vivo". In: *Molecular Therapy*. ISSN: 15250016. DOI: 10.1016/s1525-0016(16)34384-2.

Xu, Yang, Ming Zhang, Carlos A Ramos, April Durett, Enli Liu, Olga Dakhova, Hao Liu, Chad J Creighton, Adrian P Gee, Helen E Heslop, Cliona M Rooney, Barbara Savoldo, and Gianpietro Dotti (2014). "Closely related T-memory stem cells correlate with in vivo expansion of CAR.CD19-T cells and are preserved by IL-7 and IL-15". In: DOI: 10.1182/blood-2014-01-552174. URL: http://www.bloodjournal.org/content/bloodjournal/123/24/3750.full.pdf.

Xue, Qiong, Emily Bettini, Patrick Paczkowski, Colin Ng, Alaina Kaiser, Timothy McConnell, Olja Kodrasi, Maire F. Quigley, James Heath, Rong Fan, Sean Mackay, Mark E. Dudley, Sadik H. Kassim, and Jing Zhou (2017). "Single-cell multiplexed cytokine profiling of CD19 CAR-T cells reveals a diverse landscape of polyfunctional antigen-specific response". In: *Journal for ImmunoTherapy of Cancer* 5.1, pp. 1–16. ISSN: 20511426. DOI: 10.1186/s40425-017-0293-7.

Yan, Ying, Peter Steinherz, Hans Georg Klingemann, Dieter Dennig, Barrett H. Childs, Joseph McGuirk, and Richard J. O'Reilly (1998). "Antileukemia activity of a natural killer cell line against human leukemias". In: *Clinical Cancer Research* 4.11, pp. 2859–2868. ISSN: 10780432.

Au-Yeung, B. B., J. Zikherman, J. L. Mueller, J. F. Ashouri, M. Matloubian, D. A. Cheng, Y. Chen, K. M. Shokat, and A. Weiss (2014). "A sharp T-cell antigen receptor signaling threshold for T-cell proliferation". In: *Proceedings of the National Academy of Sciences* 111.35, E3679–E3688. ISSN: 0027-8424. DOI: 10.1073/pnas.1413726111.

Ying, Zhitao, Ting He, Xiaopei Wang, Wen Zheng, Ningjing Lin, Meifeng Tu, Yan Xie, Lingyan Ping, Chen Zhang, Weiping Liu, Lijuan Deng, Feifei Qi, Yanping Ding, Xin an Lu, Yuqin Song, and Jun Zhu (2019). "Parallel Comparison of 4-1BB or CD28 Co-stimulated CD19-Targeted CAR-T Cells for B Cell Non-Hodgkin's Lymphoma". In: *Molecular Therapy - Oncolytics*. ISSN: 23727705. DOI: 10.1016/j.omto.2019.08.002.

Yu, Hua, Marcin Kortylewski, and Drew Pardoll (2007). "Crosstalk between cancer and immune cells: Role of STAT3 in the tumour microenvironment". In: *Nature Reviews Immunology* 7.1, pp. 41–51. ISSN: 14741733. DOI: 10.1038/nri1995.

Yuzhalin, Arseniy and Anton Kutikhin (2014). *Interleukins in Cancer Biology: Their Heterogeneous Role*. ISBN: 9780128013335. DOI: 10.1016/C2013-0-15174-4.

Zajac, Allan J., Joseph N. Blattman, Kaja Murali-Krishna, David J.D. Sourdive, M. Suresh, John D. Altman, and Rafi Ahmed (1998). "Viral immune evasion due to persistence of activated T cells without effector function". In: *Journal of Experi-*

mental Medicine 188.12, pp. 2205–2213. ISSN: 00221007. DOI: 10.1084/jem.188.12.2205.

Zaritskaya, Liubov, Michael R. Shurin, Thomas J. Sayers, and Anatoli M. Malyguine (June 2010). *New flow cytometric assays for monitoring cell-mediated cytotoxicity*. DOI: 10.1586/erv.10.49.

Zenewicz, Lauren A (2017). "Oxygen Levels and Immunological Studies." In: *Frontiers in immunology* 8, p. 324. ISSN: 1664-3224. DOI: 10.3389/fimmu.2017.00324. URL: http://www.ncbi.nlm.nih.gov/pubmed/28377771%20http://www.pubmedcentral.nih.gov/articlerender.fcgi?artid=PMC5359232.

Zhang, Hua, Kevin S. Chua, Martin Guimond, Veena Kapoor, Margaret V. Brown, Thomas A. Fleisher, Lauren M. Long, Donna Bernstein, Brenna J. Hill, Daniel C. Douek, Jay A. Berzofsky, Charles S. Carter, E. J. Read, Lee J. Helman, and Crystal L. Mackall (Nov. 2005). "Lymphopenia and interleukin-2 therapy alter homeostasis of CD4 +CD25+ regulatory T cells". In: *Nature Medicine* 11.11, pp. 1238–1243. ISSN: 10788956. DOI: 10.1038/nm1312.

Zhang, Hua, Kristen M. Snyder, Megan M. Suhoski, Marcela V. Maus, Veena Kapoor, Carl H. June, and Crystal L. Mackall (2007). "4-1BB Is Superior to CD28 Costimulation for Generating CD8 + Cytotoxic Lymphocytes for Adoptive Immunotherapy". In: *The Journal of Immunology* 179.7, pp. 4910–4918. ISSN: 0022-1767. DOI: 10.4049/jimmunol.179.7.4910.

Zhang, Qunfang, Weihui Lu, Chun Ling Liang, Yuchao Chen, Huazhen Liu, Feifei Qiu, and Zhenhua Dai (2018). “Chimeric antigen receptor (CAR) Treg: A promising approach to inducing immunological tolerance”. In: *Frontiers in Immunology* 9.OCT, pp. 1–8. ISSN: 16643224. DOI: 10.3389/fimmu.2018.02359.